Clinical Application of Mitochondrial Oxygen Tension Measurement

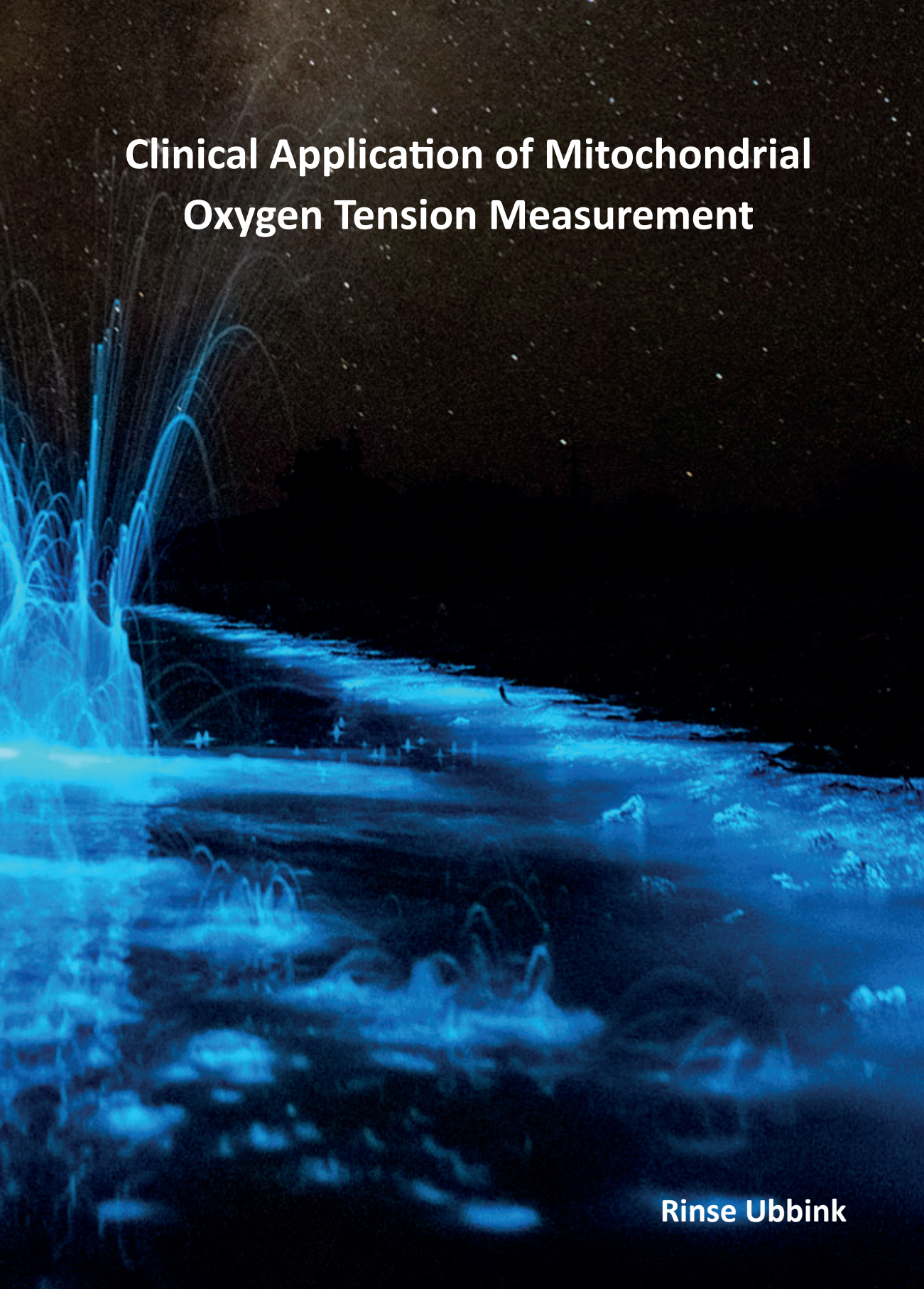

Rinse Ubbink

Clinical Application of Mitochondrial Oxygen Tension Measurement

Rinse Ubbink

Cover Noctiluca Scintillans, Storm Bay, Tasmania. Sea Sparkle photo used after approval of Jo Malcomson, Blackpaw Photography

Lay-out: Publiss I www.publiss.nl

Print: Ridderprint I www.ridderprint.nl

Clinical Application of Mitochondrial Oxygen Tension Measurement

Klinische toepassing van mitochondriaal zuurstofspanning meten

Thesis

to obtain the degree of Doctor from the

Erasmus University Rotterdam

by command of the

rector magnificus

Prof.dr. A.L. Bredenoord

and in accordance with the decision of the Doctorate Board.

The public defence shall be held on

Thursday 3 November 2022 at 15.30hrs

by

Rinse Ubbink

born in Dongeradeel, Netherlands.

Erasmus University Rotterdam

Doctoral Committee:

Promotor:	Prof.dr. R.J. Stolker
Other members:	Prof.dr. I.K.M. Reiss
	Prof.dr. M.J. Bruno
	Prof.dr. N.P. Juffermans
Copromotor:	dr. E.G. Mik

Contents

Chapter 1

Introduction

Probing Tissue Oxygenation by Delayed Fluorescence of Protoporphyrin IX

Book chapter:
Ubbink R, and Mik EG.

Published in:
CHAPTER 13. Probing Tissue Oxygenation by Delayed Fluorescence of Protoporphyrin IX. In *RSC Detection Science* (Vols. 2018-Janua, Issue 11, pp. 259–277).

Introduction

The adequate supply of oxygen to organs and tissues is of pivotal importance to sustain mammalian life. Aerobic metabolism is maintained through inhalation of air in the lungs and subsequent transport of the absorbed oxygen to tissues *via* the circulating blood. Flow of hemoglobin-bound oxygen through the macro- and microcirculation and diffusion of molecular oxygen into the tissue cells brings oxygen to its ultimate destination, the mitochondria. In the mitochondria oxygen is used in oxidative phosphorylation in order to efficiently produce adenosine triphosphate (ATP) that acts as the energy source for many cellular processes. Oxygen also plays a role in many other biochemical processes and mammalian tissue contains a large number of oxygen consuming enzymes [1], for example for reactive oxygen species generation in signal transduction [2, 3] Accurate measurements of oxygen at various levels, *e.g.* in blood, organ, tissue and (intra)cellular compartments, is of importance in both research and clinical situations. Over the last decades many techniques have been developed for oxygen measurements *in vivo* [4, 5]. These techniques gain insight into the mechanisms of oxygen delivery but to some extent also for diagnosis and treatment in patients at the bedside. In the late 1980s the phosphorescence quenching for measurement of oxygen in biological samples was introduced [6]. The possibility to use this technique *in vivo* in experimental animal studies provided researchers with a powerful and scalable tool for quantitative oxygen measurements. Although phosphorescence quenching of injectable phosphorescent dyes allowed measurement of oxygen at the microvascular and interstitial levels, [7] the ultimate goal of measuring intracellular oxygen at the level of the mitochondria remained elusive. Furthermore, because it is depended on injection of metalloporphyrin derivatives the technique in its original form has not been used in clinical applications. In 2006 we introduced quenching of delayed fluorescence of protoporphyrin IX as a means for measuring oxygen tension (PO_2) in mitochondria [8]. This technique uses the optical properties of 5-aminolevulinic acid (ALA)–induced mitochondrial PpIX.

Oxygen-dependent quenching of delayed fluorescence of PpIX can be used in cultured cells, tissues, isolated organs and in vivo. Since the technique does not rely on the injection of potentially toxic metalloporphyrin complexes it is also applicable in humans. In this chapter, we will discuss the background of the technology, its technical implementation in a laboratory setting, and the implementation of the technique in a clinical measuring device. Furthermore, we will discuss its use for measuring cellular respiration in vivo in addition to mitochondrial oxygen tension (mitoPO_2).

Background

Oxygen

Molecular oxygen is a diatomic gas that constitutes approximately 21% of the volume of air. The electron configuration of the oxygen molecule has two unpaired electrons with the same spin in degenerate orbitals. Therefore, oxygen is paramagnetic and the ground state of oxygen is a triplet state, which is very unusual compared to many other biochemically relevant molecules. The ground state being a triplet state has the important implication that molecular oxygen does not react directly with many other molecules, in contrast to the highly reactive oxygen radical singlet oxygen. The amount of oxygen dissolved in a liquid depends on the solubility coefficient of oxygen in the solvent and the partial oxygen pressure (PO_2) above the solution. Since the solubility coefficients in biological compartments are not well known, it is common to measure and report oxygen levels as PO_2 value in kPa, mmHg, or Torr (1 kPa = 7.5 mmHg = 7.5 Torr).

Porphyrins

Porphyrins belong to the most abundant molecules on earth and are essential for aerobic life because of their key role in processes related to oxygen production, oxygen transport, and oxygen use [9]. Porphyrins are cyclic macromolecules composed of four modified pyrrole subunits. Porphyrins easily form complexes with metal ions like iron and magnesium and the metal ion defines much of the specific photochemical properties of a porphyrin. Porphyrins are very good absorbers of light in the visible range. The absorption of a photon leads to photoexcitation of the porphyrin-metal complex. Photoexcitation can lead to population of an excited triplet state. Oxygen, having a triplet state as ground state, is a very effective quencher of this excited triplet state. In the process of quenching, energy is transferred to oxygen. This energy transfer leads to the formation of singlet oxygen, the basic mechanism in porphyrin-based photodynamic therapy [10]. Since the amount of oxygen is inversely related to the triplet state lifetime, the quenching properties can also be used to quantitatively measure the amount of oxygen.

For use in biological samples and *in vivo* it is mandatory that the triplet state lifetime can be easily measured, for example by phosphorescence. The method of measuring PO_2 in biological systems by means of oxygen dependent quenching of phosphorescence was introduced by Vanderkooi *et al.* at the end of the 1980s. Complexes of porphyrins with certain heavy metals show high phosphorescence yield and are very efficient oxygen probes [6]. Palladium-meso-tetra(4-carboxyphenyl) porphine (Pd-porphyrin), bound to albumin before injection, has become a standard phosphorescent dye for microvascular PO_2 measurements *in vivo* [11, 12].

Protoporphyrin IX

Oxygen-dependent quenching of phosphorescence has proven itself to be a very useful technology for biological oxygen measurements. The technique is very scalable and applications range from single cell microscopy [13] to intravitalmicroscopy [14, 15] to fiber-based measurements on organs like the heart [16] and kidney [17]. In our laboratory we use phosphorescence quenching to measure microvascular oxygen tension in various animal models for studying pathophysiological mechanisms and experimental therapies in perioperative and intensive care [18–21]. In order to improve performance of the oxygen-sensitive phosphors, for example to reduce pH-dependency or improve the two-photon absorption cross-section, new porphyrin-based oxygen- sensitive dyes have been developed over recent years [22–24].

The direct and quantitative measurement of microvascular PO_2 clearly has potential clinical applications. However, due to the need for injection of the phosphors and concerns about potential toxicity of the metalloporphyrin complexes the technique did not make the clinical step.

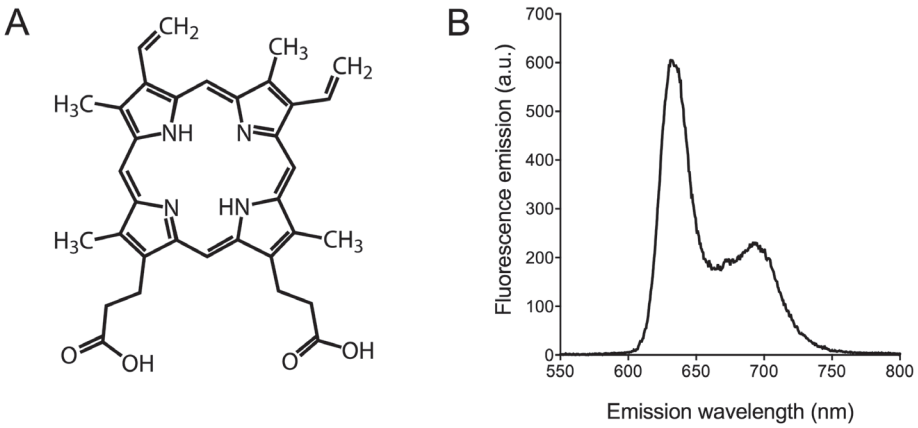

Figure 1.1 A. Structure of protoporphyrin IX. B. Fluorescence emission spectrum of protoporphyrin IX, excited at 405 nm. The two-peaked emission spectrum is typical for this porphyrin.

This latter limitation could potentially be overcome by using an endogenously synthesized porphyrin. But this porphyrin should meet the following requirements: it should have oxygen-sensitive optical properties, which are easy to measure, and which can be calibrated so the amount of oxygen can be measured as an absolute value. For this reason, we started the search for an endogenous porphyrin as oxygen-sensitive dye several years ago and found protoporphyrin IX (PpIX) to have the right properties. The structure formula of PpIX and its fluorescence emission spectrum are shown in Figure 1.1. PpIX is endogenously present and is synthesized inside the mitochondria

[25]. PpIX is the final precursor of heme in the heme biosynthetic pathway, and the conversion of PpIX to heme is a rate-limiting step. Administration of the porphyrin precursor 5-aminolevulinic acid (ALA) to cells, tissues, and animals substantially enhances the PpIX concentration [26]. Furthermore, PpIX possesses a triplet state that reacts strongly with oxygen [27]. While PpIX shows no detectable phosphorescence [28] it does emit a weak oxygen- sensitive delayed fluorescence [8], with the same emission spectrum as the prompt fluorescence and of which the lifetime relates quantitatively to the oxygen tension. Since ALA-enhanced PpIX is located in the mitochondria, PpIX acts as an intramitochondrial oxygen-sensitive dye.

Delayed Fluorescence Quenching

Figure 1.2 shows the Jablonski diagram describing interactions between protoporphyrin IX and oxygen. Excitation of PpIX to the first singlet state (S1) can lead to population of the triplet state (T1) by a process called intersystem crossing. During intersystem crossing the electron is relaxed to the triplet state by changing its spin orientation without emission of a photon. The probability that a porphyrin molecule in the T1 state relaxes to the S0 state by spontaneous relaxation is denoted by rate constant k_s. Relaxation to S0 can also occur by "triple-state quenching",

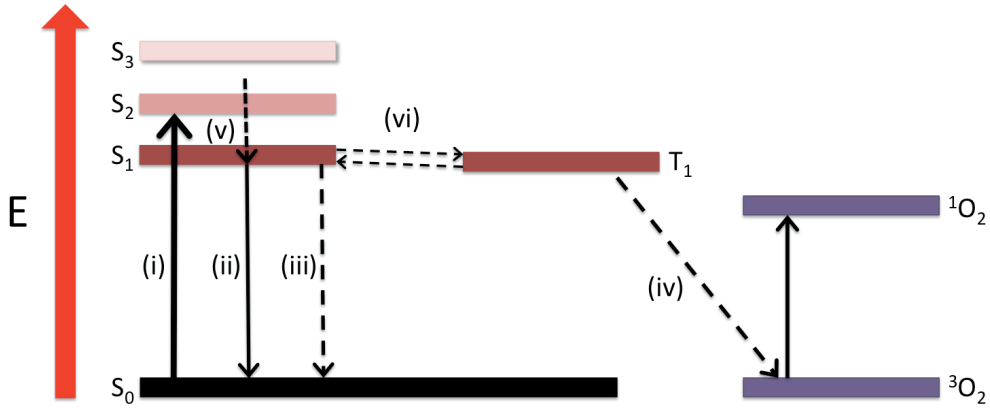

Figure 1.2 Jablonski diagram of steady and transition states of protoporphyrin IX and molecular oxygen. Absorption (i), and (delayed) fluorescence (ii), radiationless transitions (iii), energy transfer (iv), internal conversion (v), bidirectional intersystem crossing (vi), and S0, S1, S2, and S3 denote the ground state and the first three excited singlet states of protoporphyrin IX, respectively. T1 denotes the first excited triplet state. $3O_2$ and $1O_2$ denote the triplet ground state of oxygen and excited singlet oxygen, respectively.

a process in which a colliding oxygen molecule absorbs the energy from the porphyrin. Triplet-state quenching results in relaxation of the porphyrin without emission of a photon and causes the triplet-state lifetime to be dependent on the collision frequency. The collision frequency is

determined by the amount of oxygen and the chance that a single oxygen molecule causes a quenching event. The latter is defined by the Smoluochowski equation:

$$k_q = 4\pi N\gamma\left(D_o + D_f\right)\left(R_o + R_f\right) \quad (1)$$

in which k_q is known as the quenching constant, N is Avogadro's number, γ the quenching efficiency, D_o and D_f are the diffusion coefficients of oxygen and the porphyrin, respectively, and R_o and R_f are the quenching radius of oxygen and the porphyrin, respectively. The rate of relaxation of T1 to S0 is thus determined by both the transition probability by spontaneous relaxation (k_s) and the quenching probability (k_q). The decay rate of PpIX molecules in the excited triplet state after excitation with a pulse of light is given by the following differential equation:

$$\frac{d[T_1](t)}{dt} = -k_s[T_1](t) - k_q PO_2[T_1] \quad (2)$$

where [T1] denotes the amount of PpIX molecules in the excited triplet state, and PO_2 is the oxygen tension in the surrounding medium. Under ideal circumstances, *i.e.*, when the excitation pulse duration is much shorter than the triplet decay time, the solution of this differential equation yields:

$$[T_1](t) = [T_1]_0 e^{-\left(k_s + k_q PO_2\right)t} \quad (3)$$

where $[T1]_0$ denotes the amount of PpIX molecules in the excited triplet state at $t = 0$, *i.e.* immediately after the excitation pulse. Since the delayed fluorescence intensity ($I(t)$) is proportional to the number of molecules in the excited triplet state eqn (1.3) can be rewritten in the form:

$$I(t) = [I]_0 e^{\left(-\frac{t}{\tau}\right)} \quad (4)$$

in which

$$\frac{1}{\tau} = \frac{1}{\tau_0} + k_q PO_2 \quad (5)$$

This last equation is known as the Stern–Volmer relationship, in which τ is the delayed fluorescence lifetime and $\tau_0 = 1/k_s$ is the time constant of the decay of the delayed fluorescence in the absence of oxygen, *i.e.*, the decay time of spontaneous relaxation. Since the measured PO_2 in the case of aminolevulinic acid-induced mitochondrial PpIX is the oxygen tension in the mitochondria ($mitoPO_2$) the latter can be calculated from the delayed fluorescence lifetime as follows:

$$mitoPO_2 = \frac{\frac{1}{\tau} - \frac{1}{\tau_0}}{k_q} \quad (6)$$

Methods to retrieve the delayed fluorescence lifetime(s) in case of nonhomogenous $mitoPO_2$ (the situation that is normally present due to respiring mitochondria causing oxygen gradients) are explained later in this chapter.

Quenching Constants

To be able to calculate mitoPO$_2$ from the measured delayed fluorescence lifetime one has to know the calibration constants, *i.e.* the quenching constant (k_q) and the lifetime in the absence of oxygen (τ_0), from *in situ* mitochondrial protoporphyrin IX. MitoPO$_2$ reflects the local balance between oxygen supply and consumption [29]. Due to mitochondrial respiration and the presence of diffusion gradient from a higher extracellular to lower intracellular oxygen tension one can only perform calibrations in non-respiring cells and tissues. Only under such circumstances one can assume the mitoPO$_2$ to equal an applied extracellular PO$_2$. We have performed calibration experiments in which we clamped the extracellular PO$_2$ to a fixed and known value in either cell culture medium or perfusate while mitochondrial respiration was blocked by cyanide and rotenone in various models. Our first calibrations were performed in cultured cells [8] and these were quickly followed by calibrations in isolated rat hepatocytes, cardiomyocytes, isolated perfused livers and earts [30, 31]. Recently we also performed calibrations in rat skin *in vivo* [32]. At a temperature of 37 °C, the values for the quenching constants have been found to be approximately k_q = 830 mmHg s^{-1} and τ_0 = 0.8 milliseconds. No important differences have been found between the various tissues.

Measuring Mitochondrial PO$_2$

Aminolevulinic Acid

Protoporphyrin IX is endogenously present in mammalian tissues but due to a negative feedback mechanism on its synthesis the normal levels are very low. In practice this means that delayed fluorescence of PpIX can only be detected after enhancement of its levels by administration of the porphyrin precursor 5-aminolevulinic acid (ALA). ALA is the first compound in the porphyrin synthesis pathway and is produced by the enzyme ALA synthase from glycine and succinyl-CoA. For research and clinical purposes ALA is available in various forms, for example as an easily water-soluble powder for cell culture, injection and oral administration, or as plasters for administration of ALA to the skin. In the cytosol ALA is converted to coproporphyrinogen III (CPIII) *via* two intermediate steps. CPIII is transported into the mitochondria and converted to protoporphyrinogen IX and subsequently protoporphyrin IX. The conversion of PpIX to heme, by incorporation of an iron atom in the porphyrin structure, is a rate-limiting step. Therefore, administration of ALA leads to accumulation of PpIX in the mitochondria (Figure 1.3) and effectively induces an oxygen-measuring probe in these organelles. ALA itself is very hydrophilic and dissolves easily in water, making it easy to administer to biological samples such as cell cultures. Furthermore, ALA can be dissolved in a buffer and injected in the blood stream of an experimental animal to allow mitoPO$_2$ measurements in various organs. Alternatively, local

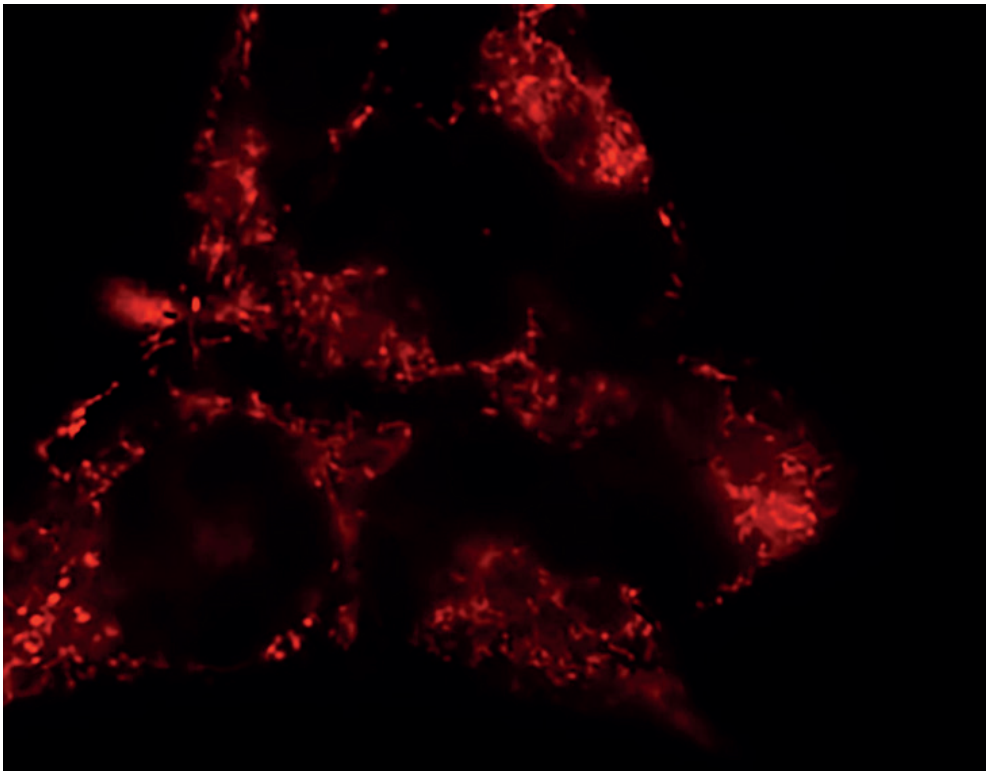

Figure 1.3 Fluorescence microscopy picture of cultured neuroblastoma cells 4 hours after addition of 5-aminolevulinic acid (ALA) to the culture medium, using a Cy3 bandpass filter. The red spots are the mitochondria that became fluorescent due to ALA-induced accumulation of protoporphyrin IX. In previous work we showed that the red fluorescence co-localizes with the mitochondria-specific probe MitoTracker Green [8].

application of ALA to tissues in the form of an ALA cream or ALA plaster is also possible. We used the latter in our first measurements of mitochondrial oxygen tension in humans [33] and for our first implementation of mitochondrial oxygen measurements in a clinical device [34]. Depending on the application, type of cells or tissues and ALA administration method the optimal timing for delayed fluorescence measurements after ALA administration is typically 2–4 hours.

Laboratory Setup

The basic principle of the delayed fluorescence measurements is straightforward and very similar to phosphorescence lifetime measurements. A complicating factor is that the relatively weak delayed fluorescence signal is easily overwhelmed by intense prompt fluorescence. Because prompt and delayed fluorescence share the same emission spectrum optical filtering is not possible. Therefore, the prompt fluorescence potentially leads to distortion

of the signal through a temporary saturation of the sensitive photodetector and electronics. Pulsed excitation with a q-switched laser in combination with time-gated detection is used to overcome such problems.

Excitation Source

Various and extensive descriptions of setups that have been used for mitoPO$_2$ measurements have been published previously [8, 31, 35, 36]. Currently, we use a compact computer-controlled tunable laser (Opolette 355-I, Opotek, Carlsbad, CA) as excitation source. This laser provides pulses with a specified duration of 4–10 nanoseconds and typically 2–4 mJ per pulse over the tunable range of 410–670 nm. The Opolette is coupled into a multimode fiber optic with a core diameter of 1000 μm by a Fiber Delivery System (Opotek), which acts as interconnect between excitation light source and the actual measuring fiber (varies with specific task). For example, for measuring mitoPO$_2$ at the surface of organs, we use a bifurcated reflection probe (FCR-7IR400-2-ME, Avantes b.v., Eerbeek, the Netherlands). Excitation light levels at the output of the excitation branch are typically in the order of 50–200 μJ per pulse.

Gated Detector

The PpIX signal is detected by a gated microchannel plate photomultiplier tube (MCP-PMT R5916U series, Hamamatsu Photonics, Hamamatsu, Japan), having a quantum efficiency of 24% at 650 nm. The MCP-PMT is mounted on a gated socket assembly (E3059-501, Hamamatsu Photonics) and cooled to −30 °C by a thermoelectric cooler (C10373, Hamamatsu Photonics). The MCP-PMT is operated at a voltage in the range of 2300–3000V by a regulated high-voltage DC power supply (C4848-02, Hamamatsu Photonics). The emission branch of the reflection probe is coupled to the detector by in-house built optics. The MCP-PMT is configured for the “normally on” mode, and the PpIX emission light is filtered by a combination of a 590 nm longpass filter (OG590, Newport, Irvine, CA) and a broadband (675 ± 25 nm) bandpass filter (Omega Optical, Brattleboro, VT).

Data-acquisition System

The output current of the photomultiplier is voltage-converted by an amplifier with an input impedance of 50 Ω, 500 times voltage amplification, and a bandwidth around 50 MHz. Data acquisition is performed by a PC-based data-acquisition system containing a 10 megasamples per second (MS s−1) simultaneous sampling data acquisition board (NI–PCI-6115, National Instruments, Austin, TX). The data acquisition runs at a rate of 10 MS s^{-1}, and typically, a number of laser pulses (repetition rate 20 Hz) are averaged before analysis to increase signal-

to-noise ratio. Control of the setup and analysis of the data are performed with software written in LabView (National Instruments, Austin, TX, USA). Examples of typical delayed fluorescence signals obtained from *in vivo* experiments are shown in Figure 1.4.

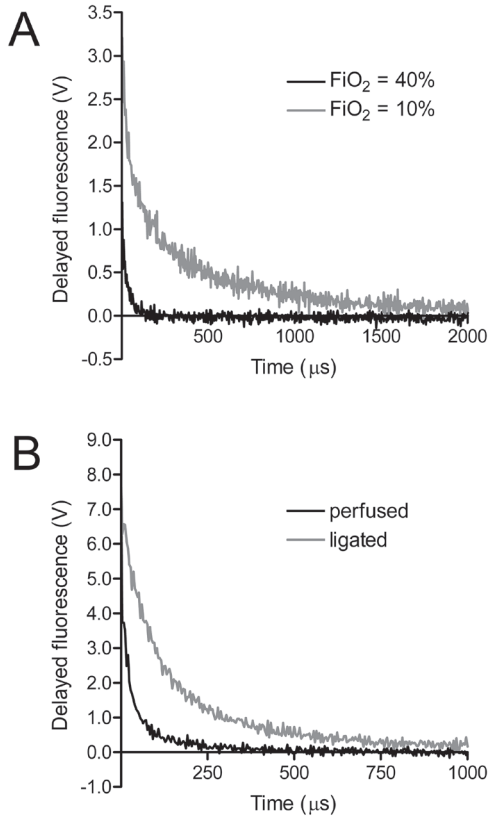

Figure 1.4 Examples of delayed fluorescence signals obtained *in vivo* in an anesthetized and mechanically ventilated rat after intravenous administration of 5-aminolevulinic acid. A. Protoporphyrin IX delayed fluorescence measured in skin from the hind limb before and after ligation of the limb and cessation of blood flow. B. Protoporphyrin IX delayed fluorescence measured in the rectus abdominis muscle during mechanical ventilation with two different inhaled oxygen concentrations [31].

Signal Analysis

The delayed fluorescence lifetime in case of a homogenous oxygen concentration and in the absence of self-quenching (*i.e.* at sufficiently low PpIX concentration) will decay monoexponentially according to eqn (1.4). However, the oxygen distribution in cells and tissues is in general not homogenous, due to the presence of oxygen gradients. In such cases, the delayed fluorescence signal can be described by an integral over an exponential kernel:

$$y(t) = \int_0^t \exp(-\lambda t)\, f(\lambda) d\lambda \tag{7}$$

where $f(\lambda)$ denotes the spectrum of reciprocal lifetimes that should be determined from the finite data set $y(t)$. The underlying distribution of oxygen tensions can be recovered by assuming that the delayed fluorescence signal can be described by a sum of rectangular distributions with adequately small chosen width (2δ), resulting in the following fit equation: [37]

$$Y^*(t) = Y(t)\exp(k_0 t)\frac{k_q \delta t}{\sinh(k_q \delta t)} = \sum w_i \exp\left(-k_q Q_i t\right) \tag{8}$$

where $Y(t)$ is the normalized phosphorescence data, k_0 is the first-order rate constant for delayed fluorescence decay in the absence of oxygen, k_q is the quenching constant, and w_i is the weight factor for the according bin with central PO_2 Q_i and width 2δ ($w_i >= 0$ and $\Sigma w_i = 1$). We have used this approach for the recovery of mitoPO_2 [30, 31] histograms.

Deconvolution of detailed lifetime distributions in the time domain is relatively slow and especially for fast real-time signal analysis it is more convenient to determine mean mitoPO_2 and an estimate of its variance directly from the photometric signal. This can be achieved by fitting distributions of quencher concentration to the delayed luminescence data [15]. The fitting function for a simple rectangular distribution with a mean PO_2 Q_m and a PO_2 range from

$$Y_R(t) = exp\left(-\left(k_0 + k_q Q_m\right)t\right)\frac{\sinh\left(k_q \delta t\right)}{k_q \delta t} \tag{9}$$

where $Y_R(t)$ is the normalized delayed fluorescence data, k_0 is the first-order rate constant for delayed fluorescence decay in the absence of oxygen, k_q is the quenching constant, and δ is half the width of the rectangular distribution. In terms of quenching constants and the Stern–Volmer relationship, eqn (1.9) can be rewritten as:

$$Y_R(t) = exp\left(-\left(\frac{1}{\tau_0} + k_q\langle PO_2\rangle\right)t\right)\frac{\sinh\left(k_q \delta t\right)}{k_q \delta t} \tag{10}$$

where $<PO_2>$ is the mean PO_2 within the sample volume and τ_0 the lifetime in the absence of oxygen. The second moment of the assumed rectangular (or uniform) distribution, the variance ($\sigma 2$), can be calculated from δ as:

$$\sigma^2 = \frac{\delta^2}{3} \tag{11}$$

Fitting eqn (1.10) to the photometric signal directly provides mean mitoPO_2 and an estimation of the heterogeneity of mitoPO_2 within the sample volume. A rectangular distribution is only a rough first approximation to many heterogeneous systems. Although the retrieval of mean mitoPO_2 has been proven reliable and robust, changes in variance should be interpreted with care. Variance should not be used for interpretation if it is uncertain whether a simple rectangular distribution is a feasible model for fitting of the data.

Multi Compartment Measurements

For *in vivo* oxygen measurements so-called near-infrared phosphors have been developed which emit phosphorescence in the near-infrared region of the optical spectrum, while being exited with visible light [38]. Since the emission spectrum (with a peak typically above 800 nm) does not overlap with the emission from PpIX, an additional detector allows a near-infrared oxygen- sensing dye to be used simultaneously with PpIX delayed fluorescence measurements. Using Oxyphor G2 (Oxygen Enterprises Ltd., Philadelphia, PA, USA), a Pd-meso- tetra-(4-carboxyphenyl)-tetrabenzoporphyrin, we have been able to simultaneously measure mitoPO_2 and extracellular PO_2 in suspensions of isolated cells [8]. Also, Oxyphor G2 can be injected in the blood stream of experimental animals for microvascular oxygen measurements. This principle (see Figure 1.5) allowed us to measure simultaneously mitochondrial and microvascular oxygen tension in various animal models [32, 35, 39].

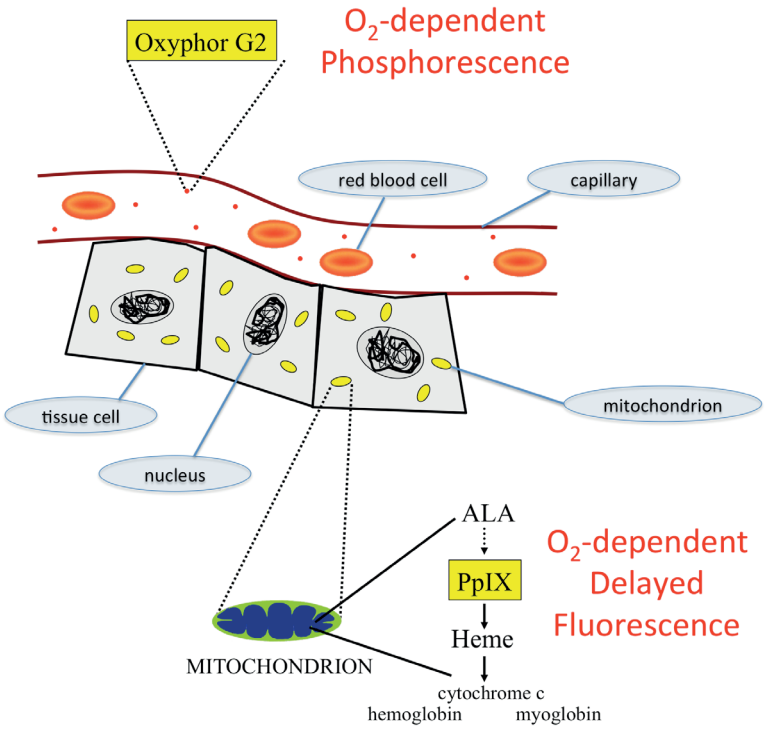

Figure 1.5 Scheme of the measuring concept for simultaneous microvascular and mitochondrial oxygen measurements. Oxyphor G2 (a near-infrared emitting oxygen-sensing phosphorescent probe) is directly injected into the bloodstream and is used as microvascular oxygen probe by means of oxygen-dependent quenching of phosphorescence. PpIX is induced in the mitochondria by administration of its precursor ALA and is used as mitochondrial oxygen probe by means of oxygendependent quenching of delayed fluorescence [35].

In vivo Cellular Respirometry

Mitochondrial oxygen tension reflects the balance between local oxygen supply and oxygen consumption. Therefore, assumed measurements are performed *in vivo*, a change in mitoPO$_2$ can be caused by an extracellular event (*e.g.* a change in blood flow or hematocrit), by an intracellular event (*e.g.* mitochondrial damage or metabolic adaptation) or by a combination of both. Under certain complex pathophysiological circumstances, for example during sepsis, it is often unclear whether the metabolic derailment is caused by insufficient oxygen supply (due to circulatory failure and shock) or cellular dysfunction [40]. Therefore, methods that probe tissue oxygenation and are able to distinguish between deviations caused by supply or demand are most welcome in both the research and clinical setting alike. In addition to mitoPO$_2$ the PpIX delayed fluorescence technique can be used to gain insight into local mitochondrial oxygen consumption (mitoVO$_2$) by directly assessing the oxygen disappearance rate (ODR) under the measuring probe while occluding the microcirculation by applying pressure with the probe. The oxygen disappearance curve, *i.e.* the kinetics of mitoPO$_2$ after cessation of local blood flow, can be analyzed by an adapted Michaelis–Menten approach. In contrast to *in vitro* respirometry in oxygen-closed reaction vessels, oxygen can diffuse back into the measuring volume. This factor has to be taken in account when performing analysis *in vivo*. We have previously shown that in skin the following formula can be used if auto-consumption of oxygen by the measuring technique is negligible [41]:

$$dP_n/d_n = -\left(V_0 \cdot P_n\right)/\left(P_{50} + P_n\right) + Z\left(P_0 - P_n\right) \tag{12}$$

In this equation, P_n is the measured PO$_2$ after excitation flash number n, P_0 is the mean PO$_2$ before stop-flow, Z is the inflow coefficient of oxygen, P_{50} is the PO$_2$ at which cellular oxygen consumption is reduced to 1/2 V_0, and dP_n/d_n is the rate of oxygen disappearance. An organ in which both mitoPO$_2$and the mitochondrial ODR can be easily measured is the skin. Using this approach, we recently demonstrated that endotoxemia causes changed cellular respiration despite tissue oxygenation being restored to normal values by resuscitation [42, 43].

Clinical Implementation

The Skin as a "Canary" of the Body

For delayed fluorescence measurements the human skin is an easily accessible and non-invasive location allowing assessment of mitochondrial oxygenation and oxygen consumption in a clinically relevant organ. The fact that ALA can be applied topically by means of a cream or plaster eases the adoption of the technique because of the lack of need for systemic administration of the compound and the associated concerns about generalized (photo) toxicity. Furthermore, optical probes can be attached to the skin without being invasive in

contrast to, for example, measurements in muscle or internal organs that would require some kind of percutaneous procedure.

Measurements in the skin are clinically meaningful because of the fact that, like the gut, the skin acts as a “canary” of the body. This means that, for example, in certain pathophysiological circumstances like hemodilution [44] cutaneous mitoPO$_2$ changes foretell changes in systemic parameters and other organs. In addition, changes in cutaneous oxygen disappearance rate correlate with ODR changes in other organs and tissues [43]. Clinical studies to further evaluate the “canary” hypothesis are needed [45] and several clinical studies in various institutions are currently underway.

Priming of the Skin

Preparation of the skin for mitochondrial oxygen measurements is needed in order to induce enough mitochondrial PpIX for delayed fluorescence detection. We use a self-adhesive patch containing 8 mg ALA (Alacare®; Photonamic GmbH & Co, Wedel, Germany) for induction of PpIX. Our preferred place to measure is the skin on the anterior chest wall above or just next to the sternum. Some skin preparation enhances ALA penetration and shortens the time until adequate signal is obtained [33]. To this end, hair (if present) is shaved and the skin is rubbed with a fine abrasive pad, *e.g.* as present on a standard electrocardiogram (ECG) sticker, to remove the top parts of the stratum corneum. After approximately 4 hours an adequate delayed fluorescence signal can be expected at the site of the patch. To prevent photobleaching of the PpIX the skin is protected from ambient light after removal of the ALA patch.

The COMET Measuring System

The oxygen-dependent quenching of delayed fluorescence of PpIX technique for measuring mitoPO$_2$ in cells, tissues and *in vivo* has shown to be robust and applicable in the laboratory setting. The next step was to bring this technology to the patient’s bedside. New requirements needed to be fulfilled including ease of transport, applicability to a patient in bed, protection against spilled water, laser safety and protection against ambient light entering the optical system, since the photo multiplier tube will be damaged immediately if it is exposed to direct sunlight or intense surgical lighting in the operating room. After successful fulfillment of all requirements a new monitor was engineered called “COMET”, an acronym for Cellular Oxygen METabolism. The COMET measuring system enables physicians to measure oxygen tension and oxygen consumption at the subcellular level in the mitochondria. Since April 2016 the COMET is a CE-marked device made by Photonics Healthcare, Utrecht, The Netherlands.

The laser used for this measuring system is a delicate device and especially the size was a real challenge. The laboratory setup is fixed and fills a wall and the first attempt to build a transportable device for clinical use was still refrigerator sized [43]. Although it allowed the first study in humans, [33] this first prototype device was not useable in the clinical setting. The COMET can be used in a clinical environment without restrictions. Without the cradle, it is 22 × 33 × 29 cm in size, weighs around 10 kg (see Figure 1.6). The use of an ALA-containing self-adhesive patch A specially developed optical Skin Sensor makes it applicable at the bedside. The light source in the COMET is a 515 nm pulsed laser with pulse duration of 60 ns and a 10 Hz repetition rate. The fluorescent signal is projected on a gated red-sensitive photomultiplier tube. A 12-inch TFT-LCD screen enables users to interact and start a single, multiple or dynamic measurements. Apart from the main switch to turn on the device, the COMET has no physical buttons.

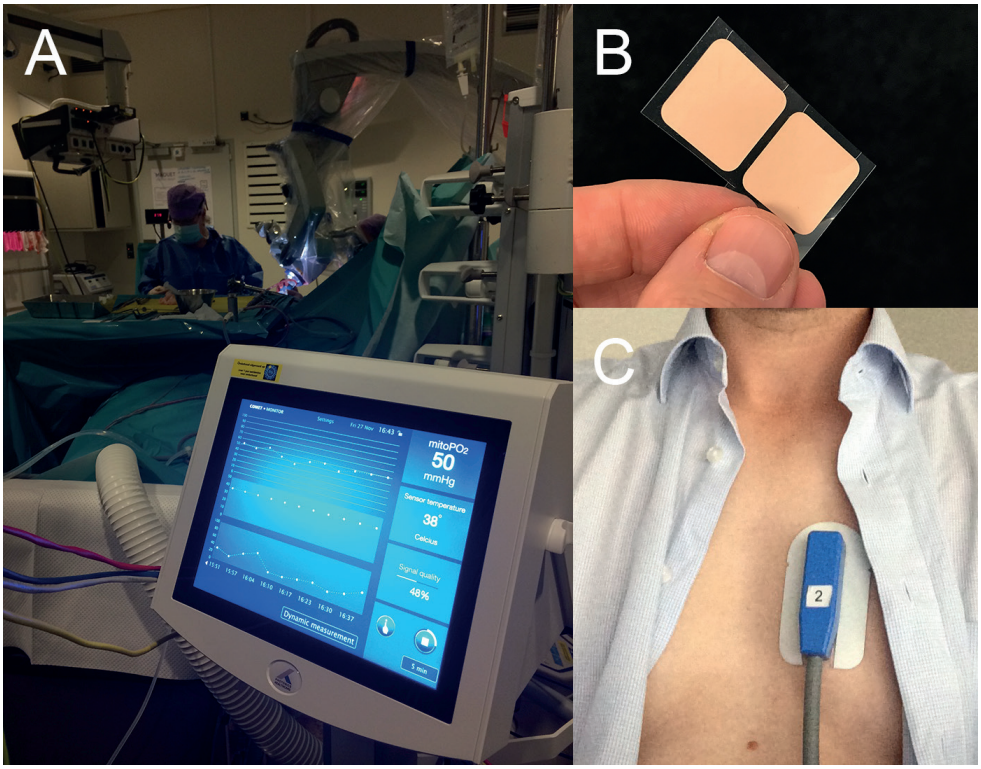

Figure 1.6 The COMET measuring system, the first clinical device for mitochondrial oxygen measurements based on delayed fluorescence of protoporphyrin IX. A. Picture of a COMET monitor during measurements for a clinical study in the operating room. B. Impression of the used ALA-containing plasters for priming of the skin. C. The Skin Sensor positioned on the chest of a healthy volunteer.

If a USB storage device is inserted in the USB-port on the rear panel the data is exported in a comma separated file format. An extensive description of the COMET device can be found elsewhere [34].

Example Measurements

To demonstrate the usability of the COMET monitor we provide two examples from actual measurements with the device. The first example is a measurement of cutaneous mitoPO$_2$ in laboratory experiment in a pig. The animal was anesthetized, mechanically ventilated under hemodynamic monitoring and control. After reaching a stable baseline situation, a protocol of progressive continuous normovolemic hemodilution was started. This means that from an arterial access blood was continuously removed at a constant rate, while at the same rate intravenous fluid was simultaneously administered *via* venous access. The effect of this intervention is that the hematocrit value continually decreased, while the circulation and blood pressure remained largely intact. The effect on cutaneous mitoPO$_2$ is shown in Figure 1.7.

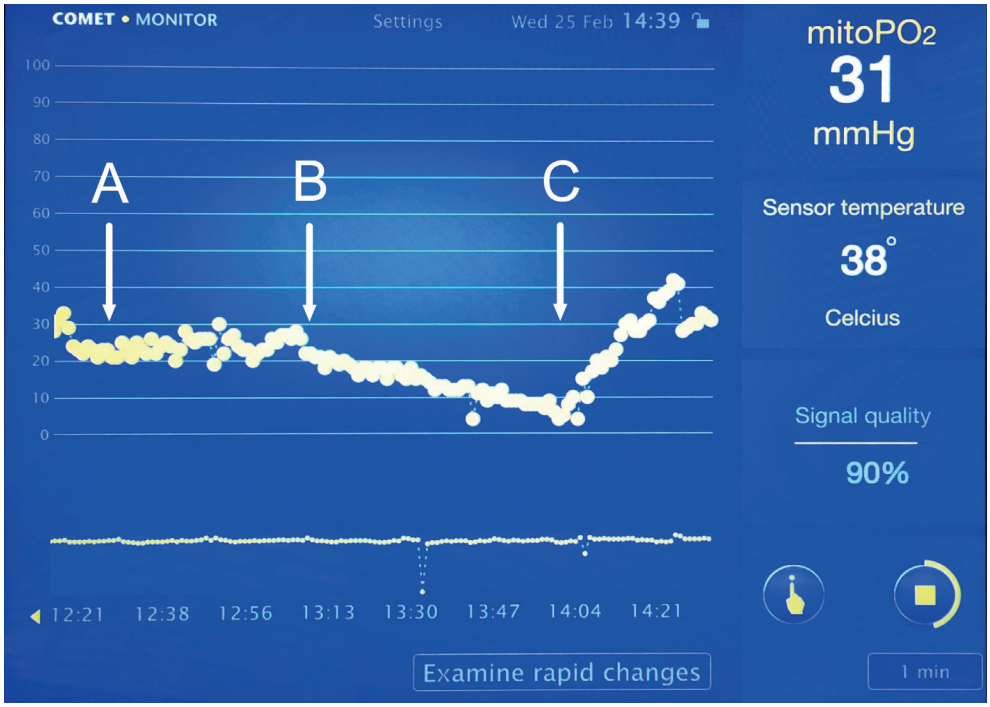

Figure 1.7 An interval measurement of cutaneous mitochondrial oxygen tension (mitoPO$_2$) performed in a pig during progressive hemodilution and subsequent blood transfusion. In this example, which is a photograph of the screen of a COMET device, mitoPO$_2$ is measured at an interval of 1 minute. At time point A the hemodilution starts, at time point B a critical hematocrit is reached and mitoPO$_2$ becomes dependent on the hemoglobin level, at time point C the animal receives a blood Transfusion

At time point A the hemodilution protocol starts. Initially compensatory mechanisms, *i.e.* increase in cardiac output and blood flow to the tissues, keep up with the decrease in hematocrit and mitoPO$_2$ remains stable. At time point B a critical hematocrit is reached in which the compensatory mechanisms start to fail. From here mitoPO$_2$ becomes dependent on the hematocrit and starts to decline with ongoing hemodilution. At time point C a blood transfusion is given which restores the hematocrit above the critical value and mitoPO$_2$ restores to values above baseline. The second example shows a dynamic mitoPO$_2$ measurement in a healthy volunteer (Figure 1.8).

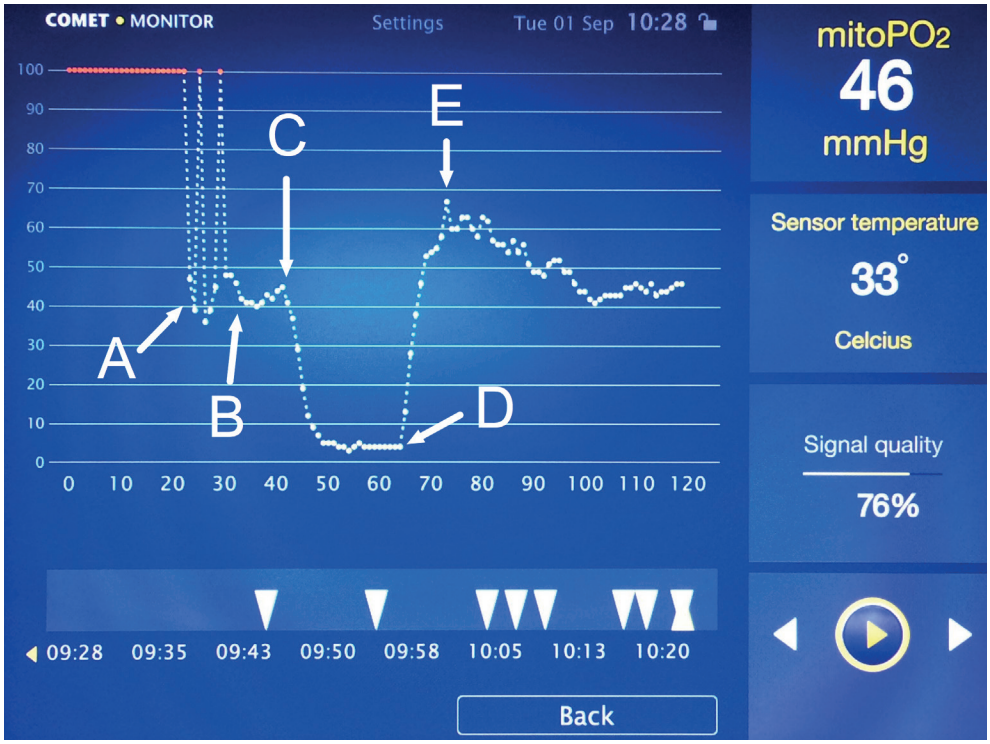

Figure 1.8 A dynamic measurement of cutaneous mitochondrial oxygen tension (mitoPO$_2$) performed in a healthy volunteer. In this example, which is a photograph of the screen of a COMET device, mitoPO$_2$ is measured at an interval of 1 second. At time point A the measuring probe is positioned, at time point B a baseline is measured, at time point C pressure is applied on the measuring probe to occlude the local microvessels and cease oxygen supply to the skin, at time point D the pressure is released and at time point E one sees the physiological hyperemic reaction resulting in a temporary overshoot of mitoPO$_2$ compared to baseline. In one screenshot one gets information about tissue oxygenation (baseline level), cellular oxygen consumption (during application of pressure) and microvascular function (*i.e.* the normal physiological hyperemic reaction).

At time point A the Skin Sensor is positioned without causing pressure on the skin. At time point B a steady signal was obtained and a number of baseline measurements were done. At

time point C pressure was applied on the Skin Sensor and the local microcirculation in the skin under the sensor was occluded. Because oxygen supply was stopped while cellular oxygen consumption went on, mitoPO$_2$ immediately decreased. The rate of this decrease could be analyzed according to eqn (1.12) in order to quantify the ODR. At time point D the pressure was released. In a healthy microcirculation the blood flow will immediately restore and show a temporarily physiological overshoot. Such overcompensation caused mitoPO$_2$ to temporarily rise above baseline values (time point E).

Clinical application of mitochondrial oxygen tension measurement

Oxygen-dependent quenching of delayed fluorescence of ALA-enhanced mitochondrial PpIX can be used to measure tissue oxygenation on the mitochondrial level. The technique is scalable from isolated cells to *in vivo* measurements and is safe and robust enough for bedside measurements in clinical applications.

With this introduction of COMET, we could start with mitoPO$_2$ measurement at the patient bedside. This opportunity let to start this thesis, investigating the clinical application of mitochondrial oxygen tension measurement. The aim and outline of this thesis can be found in **chapter 2**.

References

1. Vanderkooi JM, Erecińska M, Silver IA, et al (1991) Oxygen in mammalian tissue - methods of measurement and affinities of various reactions. Am J Physiol 260:C1131–C1150
2. Dröge W (2002) Free radicals in the physiological control of cell function. Physiol Rev 82:47–95
3. Xi Q, Cheranov SY, Jaggar JH (2005) Mitochondria-derived reactive oxygen species dilate cerebral arteries by activating Ca2+ sparks. Circ Res 97:354–62
4. Springett R, Swartz HM (2007) Measurements of Oxygen In Vivo : Overview and Perspectives on Methods to Measure Oxygen Within Cells and Tissues. Antioxid Redox Signal 9:1295–1302.
5. Swartz HM, Dunn JF (2003) Measurements of oxygen in tissues: overview and perspectives on methods. Adv Exp Med Biol 530:1–12
6. Vanderkooi JM, Maniara G, Green TJ, Wilson DF (1987) An optical method for measurement of dioxygen concentration based upon quenching of phosphorescence. J Biol Chem.
7. Wilson DF, Finikova OS, Lebedev AY, et al (2011) Measuring oxygen in living tissue: Intravascular, interstitial, and “tissue” oxygen measurements. In: Advances in Experimental Medicine and Biology
8. Mik EG, Stap J, Sinaasappel M, et al (2006) Mitochondrial PO2 measured by delayed fluorescence of endogenous protoporphyrin IX. Nat Methods 3:939–45. https://doi.org/10.1038/nmeth940
9. Layer G, Reichelt J, Jahn D, Heinz DW (2010) Structure and function of enzymes in heme biosynthesis. Protein Sci.
10. O’Connor AE, Gallagher WM, Byrne AT (2009) Porphyrin and nonporphyrin photosensitizers in oncology: Preclinical and clinical advances in photodynamic therapy. Photochem. Photobiol.
11. Lo LW, Koch CJ, Wilson DF (1996) Calibration of oxygen-dependent quenching of the phosphorescence of Pd-meso-tetra (4-carboxyphenyl) porphine: A phosphor with general application for measuring oxygen concentration in biological systems. Anal Biochem. https://doi.org/10.1006/abio.1996.0144
12. Sinaasappel M, Ince C (1996) Calibration of Pd-porphyrin phosphorescence for oxygen concentration measurements in vivo. J Appl Physiol.
13. Hogan MC (2001) Fall in intracellular PO2 at the onset of contractions in Xenopus single skeletal muscle fibers. J Appl Physiol.
14. Sinaasappel M, Donkersloot C, Van Bommel J, Ince C (1999) PO2 measurements in the rat intestinal microcirculation. Am J Physiol - Gastrointest Liver Physiol.
15. Zheng L, Golub AS, Pittman RN (1996) Determination of PO2 and its heterogeneity in single capillaries. Am J Physiol - Hear Circ Physiol.
16. Zuurbier CJ, Van Iterson M, Ince C (1999) Functional heterogeneity of oxygen supply-consumption ratio in the heart. Cardiovasc. Res.
17. Johannes T, Mik EG, Ince C (2006) Dual-wavelength phosphorimetry for determination of cortical and subcortical microvascular oxygenation in rat kidney. J Appl Physiol.
18. Johannes T, Ince C, Klingel K, et al (2009) Iloprost preserves renal oxygenation and restores kidney function in endotoxemia-related acute renal failure in the rat. Crit Care Med.
19. Johannes T, Mik EG, Klingel K, et al (2009) Low-dose dexamethasone-supplemented fluid resuscitation reverses endotoxin-induced acute renal failure and prevents cortical microvascular hypoxia. Shock.
20. Johannes T, Mik EG, Ince C (2009) Nonresuscitated endotoxemia induces microcirculatory hypoxic areas in the renal cortex in the rat. Shock.

21. Johannes T, Mik EG, Klingel K, et al (2009) Effects of 1400w and/or nitroglycerin on renal oxygenation and kidney function during endotoxaemia in anaesthetized rats. Clin Exp Pharmacol Physiol.
22. Esipova T V., Karagodov A, Miller J, et al (2011) Two new "protected" oxyphors for biological oximetry: Properties and application in tumor imaging. Anal Chem.
23. Fercher A, Borisov SM, Zhdanov A V., et al (2011) Intracellular O2 sensing probe based on cell-penetrating phosphorescent nanoparticles. In: ACS Nano
24. Gillanders RN, Arzhakova O V., Hempel A, et al (2010) Phosphorescent oxygen sensors based on nanostructured polyolefin substrates. Anal Chem.
25. Poulson R (1976) The enzymic conversion of protoporphyrinogen IX to protoporphyrin IX in mammalian mitochondria. J Biol Chem.
26. Fukuda H, Casas A, Batlle A (2005) Aminolevulinic acid: From its unique biological function to its star role in photodynamic therapy. Int. J. Biochem. Cell Biol.
27. Dalton J, McAuliffe CA, Slater DH (1972) Reaction between molecular oxygen and photo-excited protoporphyrin IX [10]. Nature
28. Chantrell SJ, McAuliffe CA, Munn RW, et al (1977) Excited states of protoporphyrin IX dimethyl ester: Reaction on the triplet with carotenoids. J Chem Soc Faraday Trans 1 Phys Chem Condens Phases.
29. Mik EG (2013) Special article: measuring mitochondrial oxygen tension: from basic principles to application in humans. Anesth Analg 117:834–46.
30. Mik EG, Ince C, Eerbeek O, et al (2009) Mitochondrial oxygen tension within the heart. J Mol Cell Cardiol 46:943–51.
31. Mik EG, Johannes T, Zuurbier CJ, et al (2008) In vivo mitochondrial oxygen tension measured by a delayed fluorescence lifetime technique. Biophys J
32. Harms FA, Bodmer SI a, Raat NJH, et al (2012) Validation of the protoporphyrin IX-triplet state lifetime technique for mitochondrial oxygen measurements in the skin. Opt Lett 37:2625–7
33. Harms F, Stolker RJ, Mik E (2016) Cutaneous Respirometry as Novel Technique to Monitor Mitochondrial Function: A Feasibility Study in Healthy Volunteers. PLoS One 11:e0159544.
34. Ubbink R, Bettink MAW, Janse R, et al (2017) A monitor for Cellular Oxygen METabolism (COMET): monitoring tissue oxygenation at the mitochondrial level. J Clin Monit Comput 31:1143–1150.
35. Bodmer SIA, Balestra GM, Harms FA, et al (2012) Microvascular and mitochondrial PO(2) simultaneously measured by oxygen-dependent delayed luminescence. J Biophotonics 5:140–51.
36. Harms FA, de Boon WMI, Balestra GM, et al (2011) Oxygen-dependent delayed fluorescence measured in skin after topical application of 5-aminolevulinic acid. J Biophotonics 4:731–9.
37. Golub AS, Popel AS, Zheng L, Pittman RN (1997) Analysis of phosphorescence in heterogeneous systems using distributions of quencher concentration. Biophys J 73:452–65.
38. Dunphy I, Vinogradov S a, Wilson DF (2002) Oxyphor R2 and G2: phosphors for measuring oxygen by oxygen-dependent quenching of phosphorescence. Anal Biochem 310:191–8
39. Balestra GM, Aalders MCG, Specht PAC, et al (2015) Oxygenation measurement by multi-wavelength oxygen-dependent phosphorescence and delayed fluorescence: Catchment depth and application in intact heart. J Biophotonics.
40. Ince C, Mik EG (2016) Microcirculatory and mitochondrial hypoxia in sepsis, shock, and resuscitation. J Appl Physiol 120:226–35.
41. Harms FA, Voorbeijtel WJ, Bodmer SIA, et al (2013) Cutaneous respirometry by dynamic measurement of mitochondrial oxygen tension for monitoring mitochondrial function in vivo. Mitochondrion 13:507–14.

42. Harms FA, Bodmer SIA, Raat NJH, Mik EG (2015) Non-invasive monitoring of mitochondrial oxygenation and respiration in critical illness using a novel technique. Crit Care 19:343.

43. Harms FA, Bodmer SIA, Raat NJH, Mik EG (2015) Cutaneous mitochondrial respirometry: non-invasive monitoring of mitochondrial function. J Clin Monit Comput 29:509–519.

44. Römers LHL, Bakker C, Dollée N, et al (2016) Cutaneous Mitochondrial PO2, but Not Tissue Oxygen Saturation, Is an Early Indicator of the Physiologic Limit of Hemodilution in the Pig. Anesthesiology 125:124-32.

45. O'Brien EO, Schmidt U (2016) Cellular Hypoxia in a Brand New Light. Anesthesiology 125:20–21

Chapter 2

Aims and outline of this thesis

An adequate supply of oxygen to organs and tissues is essential to sustain mammalian life. Oxygen is used for aerobic metabolism, maintained by inhaling air (21% oxygen) in the lungs. Oxygen is bound by hemoglobin within the red blood cells and transported towards the tissue via blood circulation.

Hemoglobin-bound oxygen flows from the macro- towards the microcirculation and diffuses into the tissue cells, bringing oxygen to the mitochondria.

In the mitochondria, oxygen is used in oxidative phosphorylation to efficiently produce adenosine triphosphate (ATP) that acts as the energy source for many cellular processes.

Accurate measurements of oxygen at various levels, e.g., in blood, organ, tissue, and (intra) cellular compartments, are essential in research and clinical treatment of hypoxia. Hypoxia is an inadequate supply of oxygen to the tissue that results in ischemia. Over the last decades, many techniques have been developed for oxygen measurements in vivo [1, 2]. These techniques gained insight into the mechanisms of oxygen delivery, diagnosis, and treatment.

In the late 1980s, the phosphorescence quenching for the measurement of oxygen in biological samples was introduced [2, 3]. Although phosphorescence quenching of injectable phosphorescent dyes allowed measurement of oxygen at the microvascular and interstitial levels [4], the ultimate goal of measuring intracellular oxygen at the level of the mitochondria remained elusive. Furthermore, because it is dependent on the injection of metalloporphyrin derivatives, the technique in its original form has not been used in clinical applications.

In 2006 quenching of delayed fluorescence of protoporphyrin IX was introduced to measure oxygen tension (pO_2) in mitochondria mitoPO_2 [5]. This technique uses the optical properties of 5-aminolevulinic acid (ALA)–induced mitochondrial PpIX.

Oxygen-dependent quenching of delayed fluorescence of PpIX can be used in cultured cells, tissues, isolated organs, and in vivo. Until 2014, only a laboratory setup and a refrigerator-sized research device were available to study further the use of mitoPO_2 [6].

The step towards the clinical and human application of the delayed fluorescence lifetime technique to measure mitoPO_2 was possible with the introduction of COMET (Photonics Healthcare, Utrecht, The Netherlands), a cellular oxygen metabolism monitor. The COMET was CE approved in 2016 as medical device. It was transportable in a safe manner and measurements at the patient bedside and the operating theater as measurement location became available.

This thesis aims to study the clinical applications of mitochondrial oxygen tension measurement with the triplet state lifetime technique. Several fields were identified where oxygen plays

an important role, such as Anesthesiology, Dermatology, Hematology, Gastroenterology and Hepatology, and Cardio-Thoracic Surgery. The first pilot measurements and the COMET monitor description are presented in **chapter 3**. The first perioperative mitochondrial oxygen tension measurements are shown in combination with tissue oxygen saturation measurements. A case of decreased tissue flow is described and indicated that mitoPO$_2$ is sensitive for changes in flow leading to a decrease in mitoPO$_2$. In contrast, this was not detected by the usual tissue saturation technique.

Previous studies that used the protoporphyrin IX lifetime technique for cutaneous mitoPO$_2$ measurements in humans reported relatively high average mitoPO$_2$ values 44 mmHg (5.9kPa) [7] and 66 mmHg (8.8 kPa) [8]. In contrast, most textbooks mention normal values of mitochondrial tension as low as 7.5 mmHg (1kPa) [9].

Calibration of PpIX-TSLT, implemented in COMET, has been performed in cultured cells [10], liver, heart [11, 12], and cutaneous rat tissue [13]. In **chapter 4**, we aim to verify the calibration constants used in COMET on the human skin. Cyanide is applied to the skin to compare mitoPO$_2$ with local arterial oxygen partial pressure measured with a blood gas analyzer. The cyanide on the skin results in a temporary stop of mitochondrial respiration. After cessation of mitochondrial oxygen consumption, diffusion equilibrates the mitoPO$_2$ with arterial oxygen tension. As a result, these two measurement methods can be compared, even though they measure at different locations.

Next to mitoPO$_2$ measurements, the technique can be used to assess the parameter mitoVO$_2$ (a measure for oxygen consumption). Typically, mitoVO$_2$ shows much faster deoxygenation kinetics than hemoglobin-saturation-based techniques. The second aim of the study in **chapter 4** is to compare the dynamics of mitoPO$_2$ to several other techniques assessing tissue oxygenation in a stop-flow condition. Depletion of oxygen will be achieved by vascular occlusion.

To further explore the clinical application of COMET, a study is done within photodynamic therapy (PDT) at the dermatology department. PDT is successfully used in superficial cutaneous cancer treatment. The therapy involves three major interdependent factors, light, photosensitizer, and oxygen.

Because oxygen availability is one of the critical factors to produce reactive oxygen species (ROS) to induce cellular apoptosis is has been suggested to measure tissue oxygenation [14, 15]. The primary objective is to show that mitoPO$_2$ availability measurement is feasible during clinical ALA-PDT. Before and after the two fraction PDT treatment, with a 2-hour dark period in

between, mitoPO$_2$ and dynamic measurements were done. Extensive pain is one of the most severe and most often reported side effects during PDT treatment. Therefore, the secondary aim was to determine the pain sensation during a mitoPO$_2$ measurement sequence. The first application of COMET in ALA-PDT is discussed in **chapter 5**.

Another field where mitochondrial oxygen measurement can play an important role is in red blood cell transfusions (RBCT). An RBCT aims to restore an adequate oxygen supply. No objective and reliable measurements are available to determine an individual need for an RBCT [16]. MitoPO$_2$ not only depends on hemoglobin levels but also on local blood flow (e.g. capillary recruitment). The flow depends on cardiac output, which is dependent on preload. Due to the Frank-Starling effect, a fluid bolus can increase cardiac output. A patient group that receives an RBCT regularly are chronic anemia patients. Therefore we compared an RBCT with a fluid challenge in chronic anemia patients. We hypothesized that mitoPO$_2$ would increase upon an RBCT but not upon a fluid challenge. The objective of the study was to measure the response of mitoPO$_2$ during an RBCT. The results of this study are described in **chapter 6**.

It remains to be proven that the skin is a good predictor for inadequate macro circulatory oxygen supply. The intestinal mucosa is generally known to be susceptible to hypoxia and borderline ischemia. Therefore, we looked into the application of the PpIX-TSLT at the mucosa.

In collaboration with the Department of Gastroenterology and Hepatology, two studies are done to study the application of local oxygen tension measurement in the intestinal mucosa. The goal is to develop a reliable ischemia detection method in chronic mesenteric ischemia (CMI) patients. The gold standard in CMI diagnostics is mucosal oxygen saturation measurements with visible light spectroscopy (VLS). The first study compares the clinical applied technique VLS with a validated palladium porphyrin intravascular oxygen tension technique in an animal model. The comparison is made in **chapter 7**.

After that, a clinical pilot study is set up to perform mitoPO$_2$ measurements during an endoscopic procedure. PpIX expression is needed to measure mitoPO$_2$ on the skin, generally accomplished by an ALA-plaster. The plaster is not intended to be used on the intestinal mucosa. Therefore orally, ALA medication will be used, normally used in neurosurgery for tumor resection optimization. A dose-finding will be started, followed by the first intestinal mucosa mitoPO$_2$ measurements in healthy volunteers. This endoscopic application of mucosal mitoPO$_2$ is described in **chapter 8**.

Lastly, a study has been done at the Cardio-Thoracic Surgery department. With the use of extracorporeal circulation (ECC), cardiac and pulmonary functions are bypassed and taken over. ECC uses an artificial oxygenator to provide sufficient oxygen saturation and clears the carbon dioxide produced. Current monitoring techniques are not always sufficient to determine adequate oxygenation. Inadequate oxygenation could lead to acute kidney injury, which is unfortunately still a common complication after cardiothoracic surgery.

MitoPO_2 could be of significance to determine adequate oxygen tension at the mitochondrial level. Six hours pre-operatively, patients receive 5-aminolevulinic acid plates on the upper arm to facilitate the mitoPO_2 measurement. MitoPO_2 and StO_2 will be compared in this perioperative study. In this pilot, we study the influence of hemodynamic variation, pulsatility, ECC duration on mitoPO_2 and StO_2. Patients are observed until discharge for the development of acute kidney injury. This study can be found in **chapter 9**.

The results of this thesis are summarized in **chapter 10**, followed by a general conclusion, and ends with the future perspectives **chapter 11** of mitoPO_2 measurement. Finally, this thesis is concluded with a Dutch summary in **chapter 12.**

References

1. Springett R, Swartz HM (2007) Measurements of Oxygen *In Vivo* : Overview and Perspectives on Methods to Measure Oxygen Within Cells and Tissues. Antioxid Redox Signal 9:1295–1302. https://doi.org/10.1089/ars.2007.1620.
2. Swartz HM, Dunn JF (2003) Measurements of oxygen in tissues: overview and perspectives on methods. Adv Exp Med Biol 530:1–12.
3. Vanderkooi JM, Maniara G, Green TJ, Wilson DF (1987) An optical method for measurement of dioxygen concentration based upon quenching of phosphorescence. J Biol Chem 262:5476–82.
4. Wilson DF, Finikova OS, Lebedev AY, et al (2011) Measuring oxygen in living tissue: Intravascular, interstitial, and "tissue" oxygen measurements. In: Advances in Experimental Medicine and Biology
5. Mik EG, Stap J, Sinaasappel M, et al (2006) Mitochondrial PO_2 measured by delayed fluorescence of endogenous protoporphyrin IX. Nat Methods 3:939–45. https://doi.org/10.1038/nmeth940.
6. Harms FA, Bodmer SIA, Raat NJH, Mik EG (2015) Cutaneous mitochondrial respirometry: non-invasive monitoring of mitochondrial function. J Clin Monit Comput 29:509–519. https://doi.org/10.1007/s10877-014-9628-9.
7. Harms FA, Stolker RJ, Mik EG (2016) Cutaneous Respirometry as Novel Technique to Monitor Mitochondrial Function: A Feasibility Study in Healthy Volunteers. PLoS One 11:e0159544. https://doi.org/10.1371/journal.pone.0159544.
8. Baumbach P, Neu C, Derlien S, et al (2018) A pilot study of exercise-induced changes in mitochondrial oxygen metabolism measured by a cellular oxygen metabolism monitor (PICOMET). Biochim Biophys Acta - Mol Basis Dis. https://doi.org/10.1016/j.bbadis.2018.12.003.
9. Chambers D, Huang C, Matthews G (2019) Basic physiology for anaesthetists. Cambridge University Press.
10. Mik EG, Stap J, Sinaasappel M, et al (2006) Mitochondrial PO_2 measured by delayed fluorescence of endogenous protoporphyrin IX. Nat Methods 3:939–45. https://doi.org/10.1038/nmeth940.
11. Mik EG, Johannes T, Zuurbier CJ, et al (2008) In vivo mitochondrial oxygen tension measured by a delayed fluorescence lifetime technique. Biophys J 95:3977–90. https://doi.org/10.1529/biophysj.107.126094.
12. Mik EG, Ince C, Eerbeek O, et al (2009) Mitochondrial oxygen tension within the heart. J Mol Cell Cardiol 46:943–51. https://doi.org/10.1016/j.yjmcc.2009.02.002.
13. Harms FA, Bodmer SI a, Raat NJH, et al (2012) Validation of the protoporphyrin IX-triplet state lifetime technique for mitochondrial oxygen measurements in the skin. Opt Lett 37:2625–7.
14. Busch TM (2006) Local physiological changes during photodynamic therapy. Lasers Surg Med 38:494–9. https://doi.org/10.1002/lsm.20355.
15. Piffaretti F, Novello AM, Kumar RS, et al (2012) Real-time, in vivo measurement of tissular PO_2 through the delayed fluorescence of endogenous protoporphyrin IX during photodynamic therapy. J Biomed Opt 17:115007. https://doi.org/10.1117/1.jbo.17.11.115007.
16. Goodnough LT, Levy JH, Murphy MF (2013) Concepts of blood transfusion in adults. Lancet 381:1845–1854. https://doi.org/10.1016/S0140-6736(13)60650-9.

Chapter 3

A monitor for Cellular Oxygen METabolism (COMET): monitoring tissue oxygenation at the mitochondrial level

Rinse Ubbink[1], Mark A. Wefers Bettink[1], Rineke Janse[1], Floor A. Harms[1], Tanja Johannes[1], F. Michael Münker[2], Egbert G. Mik[1,3]

[1]Department of Anesthesiology, Laboratory for Experimental Anesthesiology, Erasmus MC – University Medical Center Rotterdam, Rotterdam, The Netherlands
[2]Photonics Healthcare B.V., Utrecht, The Netherlands
[3]Department of Intensive Care, Erasmus MC – University Medical Center Rotterdam, Rotterdam, The Netherlands

Published in:
Journal of clinical monitoring and computing, 2017;31(6):1143-1150

Abstract

After introduction of the protoporphyrin IX-triplet state lifetime technique as a new method to measure mitochondrial oxygen tension *in vivo*, the development of a clinical monitor was started. This monitor is the “COMET”, an acronym for Cellular Oxygen METabolism.

The COMET is a non-invasive electrically powered optical device that allows measurements on the skin. The COMET is easy to transport, due to its lightweight and compact size. After 5-aminolevulinic acid application on the human skin, a biocompatible sensor enables detection of PpIX in the mitochondria. PpIX acts as a mitochondrially located oxygen-sensitive dye. Three measurement types are available in the touchscreen-integrated user interface, ‘Single’, ‘Interval’ and ‘Dynamic measurement’.

COMET is currently used in several clinical studies in our institution. In this first description of the COMET device we show an incidental finding during neurosurgery. To treat persisting intraoperative hypertension a patient was administered clonidine, but due to rapid administration an initial phase of peripheral vasoconstriction occurred. Microvascular flow and velocity parameters measured with laser-doppler (O2C, LEA Medizintechnik) decreased by 44% and 16% respectively, but not the venous-capillary oxygen saturation. However, mitochondrial oxygen tension in the skin detected by COMET decreased from a steady state of 48 mmHg to 16 mmHg along with the decrease in flow and velocity.

We conclude that COMET is ready for clinical application and we see the future for this bedside monitor on the intensive care, operating theater, and testing of mitochondrial effect of pharmaceuticals.

Introduction

Because of the importance of adequate tissue oxygen supply, many techniques have been developed for measuring oxygen *in vivo* over the last decades [1, 2]. The ultimate goal of measuring oxygen at the level of the mitochondria has recently become reality. We introduced the protoporphyrin IX-triplet state lifetime technique (PpIX-TSLT) for measuring mitochondrial oxygen tension (mitoPO$_2$) in 2006 [3]. In the mean time, the technique has been proven to be useful in isolated cells, isolated organs and *in vivo* in animal studies [4–7].

PpIX-TSLT is based on the principle of oxygen-dependent quenching of the excited triplet state of protoporphyrin IX (PpIX). Application of the porphyrin precursor 5-aminolevulinic acid (ALA) induces PpIX in the mitochondria where it acts as a mitochondrial located oxygen-sensitive dye. After photo-excitation with a pulse of green light PpIX emits delayed fluorescence of which the lifetime is inversely related to the amount of oxygen. The technique is non-invasive and can be safely used in humans [8].

The ability to measure optically intracellular oxygen is providing the possibility to assess oxygenation at the end of the oxygen cascade [3, 9]. Measurements in the intracellular compartment are complementary to for example hemoglobin-based oxygen measurements. Pulse-oximetry typically measures at the arteriolar side of the microcirculation [10] while near-infrared and visible light spectroscopy are biased toward the venous compartment [11, 12]. Interstitial oxygen measurements with e.g. oxygen electrodes measure close to the cellular compartment, but are cumbersome and tissue destructive [1]. Measuring at the end of the oxygen cascade is important since (pathologic) shunting in the microcirculation or the development of tissue edema can cause cellular hypoxia, which is otherwise not detectable [13].

Besides measuring mitoPO$_2$ PpIX-TSLT also provides the possibility to get insight in local tissue oxygen consumption at the mitochondrial level [14]. Mitochondrial oxygen consumption (mitoVO$_2$) can be estimated by measuring the oxygen disappearance rate (ODR) in the measuring volume [15]. Recently we have demonstrated that this enables bedside non-invasive monitoring of an important aspect of mitochondrial function in animal models of critical illness [16, 17].

A clinical device featuring PpIX-TSLT has now been developed and recently entered use in clinical trials in our institution. This monitor is called “COMET”, an acronym for Cellular Oxygen METabolism. The COMET measuring system enables physicians to measure oxygen tension and oxygen consumption at the subcellular level in the mitochondria. This paper is the

first description of this CE-marked device (Photonics Healthcare, Utrecht, The Netherlands). It provides the technical background, the construction of the device, and its use together with two examples of measurements in human skin.

Methods

Background of PpIX-TSLT

Protoporphyrin IX (PpIX) is the final precursor of heme in the heme biosynthetic pathway and is synthesized inside the mitochondria [13]. The conversion of PpIX to heme in the mitochondria is a rate-limiting step. Therefore, administration of the porphyrin precursor 5-aminolevulinic acid (ALA) enhances the mitochondrial PpIX concentration [18]. Administration of ALA does not only enhance PpIX to detectable levels, but it also ensures mitochondrial origin of the delayed fluorescence signal [3, 6, 7].

Delayed fluorescence can be observed after pulsed excitation of PpIX as delayed luminescence with the same spectrum as prompt fluorescence (red light). In contrast to prompt fluorescence delayed fluorescence has a lifetime of tens to hundreds of microseconds [3]. Delayed fluorescence is the result of photon emission due to spontaneous relaxation of the excited triplet state via bi-directional intersystem crossing. Oxygen is a very effective quencher of the excited triplet state. In the process of quenching, energy is transferred to oxygen and PpIX relaxes to the ground state without emission of a photon. This causes the lifetime of the triplet state, and thus the lifetime of the emitted delayed fluorescence, to be oxygen-dependent.

The delayed fluorescence lifetime is inversely proportional to the amount of oxygen according to the Stern-Volmer equation [8, 19] . With the assumption of a homogenous distribution of oxygen this relationship can be used to calculate the mitochondrial oxygen tension:

$$mitoPO_2 = \frac{\frac{1}{\tau} - \frac{1}{\tau_0}}{k_q} \quad (1)$$

Where τ is the measured delayed fluorescence lifetime, τ_0 is the delayed fluorescence lifetime in the absence of oxygen (i.e. the lifetime of spontaneous relaxation), and k_q is the quenching constant.

Signal analysis

Oxygen however is heterogeneously distributed in tissues *in vivo*. Previous studies have shown that this also applies for mitoPO$_2$ [6, 7, 13]. Delayed fluorescence from a heterogeneous system does not decay mono-exponentially, but the signal contains a lifetime distribution. Fitting equation 1 to a distribution of lifetimes generally leads to an underestimation of the mean

PO_2 in the measuring volume [20]. A much better estimation of the mean PO_2 can be found by alternatively fitting a distribution of quencher concentration to the delayed fluorescence signal. The fitting function for a simple rectangular distribution with a mean mitoPO_2 Q_m and a mitoPO_2 range from Q_m-δ till Q_m+ δ is [21]:

$$Y_R(t) = \exp\left(-\left(\frac{1}{\tau_0} + k_q \langle mitoPO_2 \rangle\right) t\right) \frac{\sinh(k_q \delta t)}{k_q \delta t} \quad (2)$$

where $Y_R(t)$ is the normalized delayed fluorescence data, <mitoPO_2> is the mean mitoPO_2 within the sample volume and t is the factor time.

Fitting of equation 2 is fast and very robust when applied to weak delayed fluorescence signals and noisy real world signals. In a previous analysis we have shown that fitting equation 2 allows for reliable retrieval of mitoPO_2 values from data with signal-to-noise ratios (SNR) as low as 10 [5]. For time-domain delayed luminescence measurements SNR is defined as the maximum amplitude of the delayed fluorescence divided by the maximum amplitude of the noise. Generally a SNR above 20 is well achievable and the noise-induced error in the measurement remains below 2%.

For analysis of the delayed fluorescence signals COMET uses equation 2 to calculate mean mitoPO_2 in the measuring volume under the probe. The absolute value for mitoPO_2 is directly displayed on the screen without further processing. COMET also evaluates the signal quality, which is calculated from the SNR value; an increase of 1 in SNR is approximately 1% in signal quality up till a SNR of 50. Beyond a SNR 50 the increase in signal quality percentage will flatten out. As long as SNR is within an acceptable range, a SNR greater than 5, COMET will show a percentage and a calculated mitoPO_2. If COMET cannot detect a signal, or SNR is too low, less than or equal to 5, the used version of the firmware makes COMET to display “no signal found” and to provide the unrealistic value of “999”.

Monitor description

The COMET is a medical device and class IIa classified according to the Medical Device Directive 93/42/EEC. The legal manufacturer is Photonics Healthcare B.V., Utrecht, The Netherlands. It weighs 10 kg and sizes 22 x 33 x 29 cm without cradle and port cover on the side. The COMET measurement system exists of two components shown in figure 1. The first component is the monitor which includes the multi-touch screen integrated user interface, light source, detection system and processing units. The second component is the COMET Skin Sensor developed for use on the human skin.

Figure 1. COMET monitor and skin sensor.

Hardware

The COMET is an electrically powered system (rated power consumption of 250 W). The light source and the detection system are the two core components. A 515 nm pulsed laser, pulse duration 60ns, with a 10Hz repetition rate illuminates the intra cellular accumulated PpIX. The fluorescent signal is projected on a gated red-sensitive photomultiplier tube. Users can interact via a multi-touch 12" TFT-LCD screen. Apart from the main switch to turn on the device, the COMET has no physical buttons. If a USB storage device is inserted in the USB-port on the rear panel the data is exported in a comma separated file format for further processing in programs like MS Excel. The COMET can be used on a flat surface or be mounted on a trolley or arm through a VESA 75/100 compatible adapter plate.

Software

Lifetimes of the raw data are calculated on an embedded control board. The embedded calculation software is written in C code to simplify the development process as per IEC 62304

as required for certification. The user interface (UI) is running on a separate Linux based operating system to enhance device usability experience.

There are three different types of measurement to distinguish, shown in table 1.

Table 1 The COMET different measurement types.

Single measurement	One measurement per activation of the touchscreen non physical button.
Interval measurement	The COMET will measure in a set interval: At the start of the interval a measurement is done, and the interval time can be chosen (60 min, 20 min, 5 min, 1 min).
Dynamic measurement	The COMET can conduct a series of up to 120 measurements, one measurement per second.

Location of the measurement

The COMET measures oxygen tension in mitochondria by measuring the triplet-state lifetime of PpIX. Under normal (non-sensitized) conditions PpIX is present in very low concentrations in the human skin and not detectable with the COMET. This can be overcome by the exogenous administration of ALA that leads to higher concentrations of PpIX in the mitochondria.

ALA synthase is the first and the rate-limiting enzyme of the porphyrin synthetic pathway. Under normal conditions the level of heme synthesis and the intracellular concentration of PpIX are mainly regulated by heme control of the ALA synthase activity. As a small molecule, ALA penetrates the stratum corneum [22]. Exogenously provided ALA bypasses the negative feedback controls in the heme biosynthetic pathway and leads to overproduction of PpIX [23].

The COMET can measure in healthy skin as well as in skin lesions. After ALA application the measurement area needs to be covered, to avoid consumption of PpIX by light. A priming time for ALA, typically 4 hours or more, is needed to synthesize a suitable concentration of PpIX to enable measurements of mitoPO_2 and oxygen disappearance rate.

After topical administration on healthy skin, PpIX is synthesized in the epidermis but not (significantly) in the dermis [24]. While ALA penetrates into the dermis the heme-synthesis pathway in most dermis cells is inactive. The conversion of ALA to PpIX requires energy and an intact heme cycle, thus PpIX is not synthesized in the metabolically inactive cells of the stratum corneum. In healthy skin this limits the intradermal measurement location and signal origin of the COMET to the epidermis with a thickness of about 0,1mm [25].

The recommended measurement location is the skin of the sternum seen in figure 2. This provides a central measurement location less influenced by temperature changes, movement and peripheral vasoconstriction [26].

Figure 2. COMET skin sensor position on the sternum

Skin sensor

The biocompatible housing (70x20x20mm) of the Skin Sensor, shown in figure 3, holds two optical fibers; the excitation and the detection fiber. A flexible metal tube protects the vulnerable optical fibers against external mechanical forces. The optical design of the sensor can collect light at approximately a right angle to the sensor cable. The light emitted by the sensor is divergent and safe for eyesight at any distance.

Ambient light entering the detection path might overload or even damage the photomultiplier tube. For protection, a photodiode in the Skin Sensor determines the ambient light before each measurement. Sensor temperature, used as an approximation of skin temperature, is measured with an electrical resistive sensor.

Figure 3. Detailed view of skin sensor

Oxygen-consumption measurement

The COMET provides the opportunity for measurements in dynamic situations by taking a series of 120 samples of the mitoPO$_2$ acquired at 1Hz. This can be used to determine the oxygen disappearance rate (ODR) and reperfusion. Typically, mitochondrial oxygen availability is measured for 10-20 seconds in an undisturbed and stable situation. Subsequently light pressure is applied with a hand onto the sensor, to give occlusion of the microcirculation and stop local blood flow in the measurement volume, for about 45 seconds. After these 45 seconds the pressure is released and restoration of microcirculatory blood flow and mitochondrial re-oxygenation will appear.

Previously, we have described the fundamental principles behind the technology and have provided a working implementation of the technique for mitoVO$_2$ measurements in vivo [14]. In summary, the ODR is generally dependent on two factors; oxygen consumption (VO$_2$(t)) and Diffusive Oxygen Influx into the measurement volume (DOI(t)). The method to calculate ODR from the mitoPO$_2$ kinetics is:

$$ODR = dPO_2/dt = -VO_2(t) + DOI(t)$$

The VO$_2$(t) is oxygen-dependent and, according to Michaelis-Menten kinetics, can be described as:

$$VO_2 = (V_{max} \cdot PO_2(t))/(P_{50} + PO_2(t))$$

Where V$_{max}$ is the not supply-dependent maximal tissue oxygen consumption and P$_{50}$ is the PO$_2$ at which cellular oxygen consumption is reduced to ½ V$_{max}$. PO$_2$(t) denotes the PO$_2$ in the measurement volume at time point t.

In human measurements

Using COMET a dynamic measurement was performed on a healthy volunteer. Preceding the measurements an ALA plaster 4 cm^2 (2mg 5-amino-4oxopentacid / cm^2) was applied for approximately 10 hours (overnight) onto the skin of the sternum. A baseline of 20 seconds was measured before the microcirculation was occluded. The microcirculation occlusion was accomplished by application of external pressure by hand on the Skin Sensor.

Secondly, we report an incidental finding we made during an ongoing feasibility study of the COMET. The study is performed in accordance with the declaration of Helsinki and patients are consented with a protocol approved by local ethics committee METC (CCMO number NL51937.078.15). This study is set up to determine the applicability, stability, and reproducibility

of the COMET measurement over a longer period of time during neurosurgery. The shown incidental finding is an observation that occurred during non-protocolled administration of the central alpha-receptor agonist clonidine.

MitoPO$_2$ was measured intraoperatively, simultaneously to tissue oxygenation saturation and perfusion parameters (O2C, oxygen to see version 2424, Lea Medizintechnik GmbH, Germany). The O2C measures three parameters: The local capillary venous saturation (SO$_2$), the local velocity of blood given in velocity units (VU) and the local micro vascular blood flow given in flow units (FU). Both the COMET Skin Sensor and the O2C probe (LFX-43) were positioned on the sternum next to each other.

Results

Oxygen-consumption measurement

A typical example of an oxygen-consumption measurement on the healthy volunteer, is shown in figure 4. Mean mitoPO$_2$ ($t_{0\text{-}19}$) gave a baseline mitoPO$_2$ of 22.7 ± 2.1 mmHg (mean ± SD). After 20 seconds direct pressure with the probe was given to occlude microvascular blood flow in the skin. The available oxygen was consumed and resulted in an oxygen disappearance rate of 6.3 mmHg.s^{-1}. When the pressure was released and direct oxygen recovery up to 60-70 mmHg in mitoPO$_2$ was seen. At 120 seconds the mitoPO$_2$ returned to baseline values.

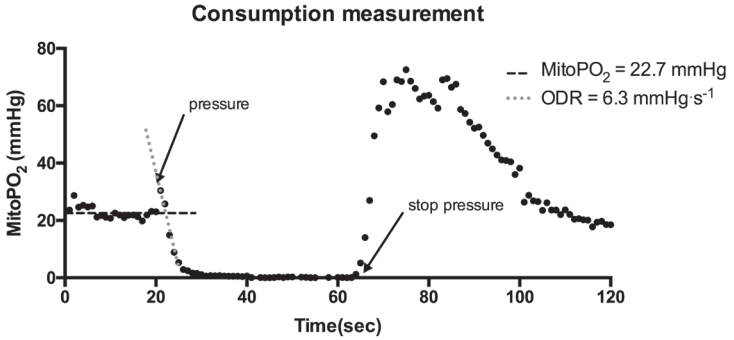

Figure 4. A typical dynamic measurement of mitochondrial partial oxygen pressure (mitoPO$_2$) by COMET measurement system. A sample of 120 seconds is shown. In the first 20 seconds the baseline was determined, afterwards light pressure was applied on the sensor to stop microcirculation and the oxygen disappearance rate (ODR) was measured. At 60 seconds pressure was released.

Incidental finding during ongoing clinical study

In one of the measured patients during an ongoing feasibility study in neurosurgery patients, clonidine was given intravenously due to persistent hypertension. Clonidine is a central

inhibitor of noradrenergic neurotransmitter transmission but also a peripheral α1-agonist. Given in a short period of time clonidine leads to initial peripheral vasoconstriction, followed by a slow onset of vasodilatation. In this particular case 150 microgram of clonidine was given as a bolus application. A direct onset effect of vasoconstriction on flow and velocity but not on capillary venous oxygen saturation (SO_2) was seen as measured by O2C figure 5. Flow decreased by 44% and velocity by 16%. Although SO_2 did not change, a transient drop in mitoPO$_2$ was measured with the COMET. MitoPO$_2$ dropped from a steady state of 48 mmHg to 16 mmHg. After the fast clonidine administration the restoration of blood flow and velocity, mitoPO$_2$ returned to baseline in approximately 15 minutes.

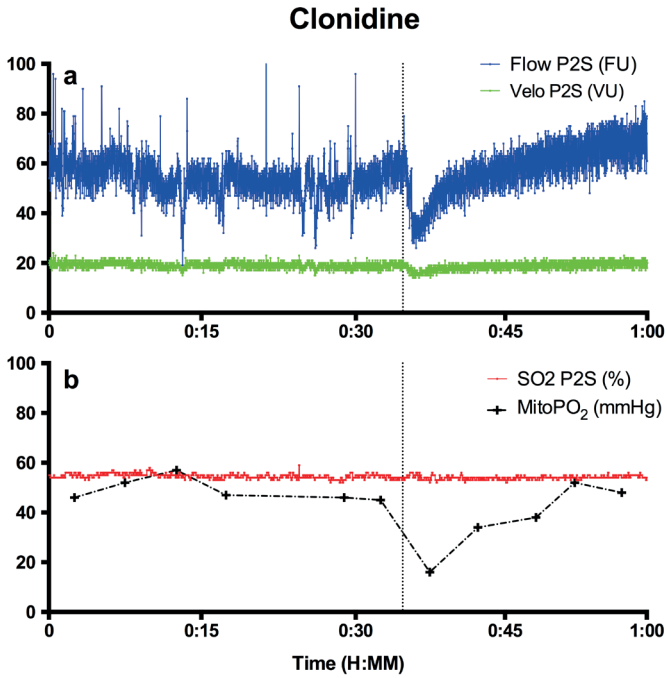

Figure 5 A. Flow in arbitrary flow units (FU) and arbitrary velocity in velocity units (VU) of microcirculation as measured with probe 2 (P2S) O2C. **B** Capillary venous saturation (SO_2) as measured by O2C and mitochondrial partial oxygen pressure (mitoPO$_2$) as measured by the COMET.

Discussion

The COMET measurement system is the successor of the first clinical prototype previously described in this journal [17]. This new clinical monitor is safe to be used, easy to transport and applicable for *in vivo* measurement of mitochondrial oxygen tension and consumption in the human skin. The sternal skin is an easy accessible and non-invasive measurement location. The clinical significance of measuring in the skin arises from the fact that, like the gut, the skin can be

regarded as a canary of the body [27]. The idea is that cutaneous mitochondrial PO_2 changes foretell changes in other vital organs and systemic parameters. Indeed, in an animal model mitoPO_2 appeared an earlier indicator of approaching the limit of physiological compensation during hemodilution than e.g. venous saturation and lactate [27, 28]. The “canary” function of human skin in relation to organ function still needs further investigation but important is that also changes in cutaneous mitochondrial oxygen consumption correlate with ODR changes in other organs and tissues [17]. The ODR from the dynamic measurement 6.3 $mmHg.s^{-1}$ in this example corresponds with previous data from healthy volunteers 5.8 ± 2.3 $mmHg.s^{-1}$ [29] .

In this paper we describe the case of clonidine given to a patient within a short period of time. This incidental finding occurred during an ongoing neurosurgery feasibility study. This patient group was chosen because in general we aim at hemodynamic stability during surgery over a longer time period. Therefore the incidental finding of an abrupt drop in cutaneous mitoPO_2 after a bolus clonidine came clearly forward. In line with clinical observations the effects of clonidine administration resulted in initial vasoconstriction and subsequent vasodilatation after a couple of minutes. Using online monitoring we observed a direct decline in microvascular blood flow and velocity, followed by an increase in flow and velocity as measured by the O2C. With the change of flow and velocity a decrease in the oxygen supply to the tissue is expected. In consequence a decrease in mitoPO_2 of 30mmHg is observed as measured by the COMET.

However, interestingly, the capillary-venous oxygen saturation measured by the O2C did not show any decrease in the minutes following clonidine administration. Two main phenomena could explain the unchanged capillary-venous oxygen saturation. First, the SO_2 is measured with the absorbance of visible light; the velocity and flow are measured with the hemoglobin laser doppler frequency shift. The different wavelengths of light, giving a different tissue penetration and therefore measurement compartment [30, 31], used in these techniques may explain why a difference in flow but not of SO_2 after clonidine administration could be observed. A second explanation could be a total stop flow of some capillaries. The part of the capillary tree without flow does not contribute to venous-capillary saturation. Thus, the oxygen extraction in the measurement volume stays the same. For the COMET measurements heterogeneity of the oxygen content in the measurement volume could be demonstrated [8]. Therefore a heterogeneous bimodal distribution could explain the decrease in flow and a constant oxygen capillary venous saturation. The reader should keep in mind that for practical reasons the O2C and COMET measurements were performed in close proximity of each other, but not in exactly the same area of the skin. However, we do think that for a valid comparison of the measurements the fact that SO_2 and mitoPO_2 were measured at the same depth in skin is of more importance. Based on our findings it is clear that measuring oxygen availability directly at cellular level provides complementary data and new insight.

While COMET is the first clinical device for measuring mitochondrial oxygen and oxygen consumption, the used technology has some limitations. Currently the typical application time of the ALA on the skin is 4 hours. This makes the measurement technique not yet applicable in acute situations. Furthermore, the combination of topical ALA administration and the green excitation light cause a very shallow measurement depth. While this does enable the oxygen consumption measurements, the oxygen measurements become more sensitive to tissue heterogeneity and background light.

Till now the feasibility of measuring mitoPO$_2$ and mitoVO$_2$ with PpIX-TSLT was tested in healthy volunteers [29] and is currently further evaluated with COMET in the perioperative setting. However, the original main development idea of COMET was the *in vivo* determination of aspects of mitochondrial (dys)function in critical illness. Indeed, in the laboratory setting the effectiveness of this technique in determining mitochondrial function under septic circumstances could be demonstrated [16].

Furthermore, mitochondrial oxygen measurements could potentially provide a new physiological transfusion trigger for decision-making in transfusion medicine. In a very recent animal study we have shown that mitoPO$_2$ can be used as an early detector of reaching the individual limit of hemodilution before changes in systemic oxygen consumption and lactate levels occur [27]. If this concept can be translated into the anemic human situation, it is indeed potentially an individual physiological parameter to guide blood transfusions. The technique used in COMET is not limited to measurements in skin, since ALA can be administered systemically [32, 33]. Therefore, endoscopic or intraoperative measurement of mitoPO$_2$ is technically feasible but such attempts should always take into account extensive safety considerations related to potential photodynamic toxicity.

Conclusion

This report provides a description of the novel COMET measurement system. The enhanced protoporphyrin IX concentration in the skin is used as endogenous oxygen-sensitive probe. The method gives the possibility to measure cellular oxygen availability and the oxygen disappearance rate at the bedside on a mitochondrial level. In the future the COMET could play a role in clinical practice to assess tissue viability, to manage oxygen transport, and to recognize and possibly to treat mitochondrial inhibition in critically ill patients. Furthermore it potentially can be used as an individual blood transfusion trigger and may enable testing mitochondrial effects of pharmaceutical substances research.

References

1. Springett R, Swartz HM (2007) Measurements of oxygen in vivo: overview and perspectives on methods to measure oxygen within cells and tissues. Antioxid Redox Signal 9:1295–301. doi: 10.1089/ars.2007.1620
2. Swartz HM, Dunn JF (2003) Measurements of oxygen in tissues: overview and perspectives on methods. Adv Exp Med Biol 530:1–12.
3. Mik EG, Stap J, Sinaasappel M, et al (2006) Mitochondrial PO_2 measured by delayed fluorescence of endogenous protoporphyrin IX. Nat Methods 3:939–45. doi: 10.1038/nmeth940
4. Balestra GM, Mik EG, Eerbeek O, et al (2015) Increased in vivo mitochondrial oxygenation with right ventricular failure induced by pulmonary arterial hypertension: mitochondrial inhibition as driver of cardiac failure? Respir Res 16:6. doi: 10.1186/s12931-015-0178-6
5. Bodmer SIA, Balestra GM, Harms FA, et al (2012) Microvascular and mitochondrial PO(2) simultaneously measured by oxygen-dependent delayed luminescence. J Biophotonics 5:140–51. doi: 10.1002/jbio.201100082
6. Mik EG, Ince C, Eerbeek O, et al (2009) Mitochondrial oxygen tension within the heart. J Mol Cell Cardiol 46:943–51. doi: 10.1016/j.yjmcc.2009.02.002
7. Mik EG, Johannes T, Zuurbier CJ, et al (2008) In vivo mitochondrial oxygen tension measured by a delayed fluorescence lifetime technique. Biophys J 95:3977–90. doi: 10.1529/biophysj.107.126094
8. Mik EG (2013) Special article: measuring mitochondrial oxygen tension: from basic principles to application in humans. Anesth Analg 117:834–46. doi: 10.1213/ANE.0b013e31828f29da
9. Treacher DF, Leach RM (1998) Oxygen transport-1. Basic principles. BMJ 317:1302–6. doi: 10.1136/bmj.317.7168.1302
10. Alexander CM, Teller LE, Gross JB (1989) Principles of pulse oximetry: theoretical and practical considerations. Anesth Analg 68:368–76.
11. Franceschini MA, Boas DA, Zourabian A, et al (2002) Near-infrared spiroximetry: noninvasive measurements of venous saturation in piglets and human subjects. J Appl Physiol 92:372–84.
12. Benaron DA, Parachikov IH, Friedland S, et al (2004) Continuous, noninvasive, and localized microvascular tissue oximetry using visible light spectroscopy. Anesthesiology 100:1469–75. doi: 10.1097/00000542-200406000-00019
13. Ince C, Mik EG (2016) Microcirculatory and mitochondrial hypoxia in sepsis, shock, and resuscitation. J Appl Physiol 120:226–35. doi: 10.1152/japplphysiol.00298.2015
14. Harms FA, Voorbeijtel WJ, Bodmer SIA, et al (2013) Cutaneous respirometry by dynamic measurement of mitochondrial oxygen tension for monitoring mitochondrial function in vivo. Mitochondrion 13:507–14. doi: 10.1016/j.mito.2012.10.005
15. Harms FA, Mik EG (2015) In vivo assessment of mitochondrial oxygen consumption. Methods Mol Biol 1264:219–29. doi: 10.1007/978-1-4939-2257-4_20
16. Harms FA, Bodmer SIA, Raat NJH, Mik EG (2015) Non-invasive monitoring of mitochondrial oxygenation and respiration in critical illness using a novel technique. Crit Care 19:343. doi: 10.1186/s13054-015-1056-9
17. Harms FA, Bodmer SIA, Raat NJH, Mik EG (2015) Cutaneous mitochondrial respirometry: non-invasive monitoring of mitochondrial function. J Clin Monit Comput 29:509–519. doi: 10.1007/s10877-014-9628-9
18. Fukuda H, Casas A, Batlle A (2005) Aminolevulinic acid: from its unique biological function to its star role in photodynamic therapy. Int J Biochem Cell Biol 37:272–6. doi: 10.1016/j.biocel.2004.04.018

19. Mik EG, Donkersloot C, Raat NJH, Ince C (2002) Excitation pulse deconvolution in luminescence lifetime analysis for oxygen measurements in vivo. Photochem Photobiol 76:12–21. doi: 10.1562/0031-8655(2002)076<0012

20. Johannes T (2005) Dual-wavelength phosphorimetry for determination of cortical and subcortical microvascular oxygenation in rat kidney. J Appl Physiol 100:1301–1310. doi: 10.1152/japplphysiol.01315.2005

21. Golub AS, Popel AS, Zheng L, Pittman RN (1997) Analysis of phosphorescence in heterogeneous systems using distributions of quencher concentration. Biophys J 73:452–65. doi: 10.1016/S0006-3495(97)78084-6

22. Kennedy JC, Pottier RH (1992) Endogenous protoporphyrin IX, a clinically useful photosensitizer for photodynamic therapy. J Photochem Photobiol B 14:275–92.

23. Malik Z, Kostenich G, Roitman L, et al (1995) Topical application of 5-aminolevulinic acid, DMSO and EDTA: protoporphyrin IX accumulation in skin and tumours of mice. J Photochem Photobiol B 28:213–8.

24. Goff BA, Bachor R, Kollias N, Hasan T (1992) Effects of photodynamic therapy with topical application of 5-aminolevulinic acid on normal skin of hairless guinea pigs. J Photochem Photobiol B 15:239–51.

25. Sandby-Møller J, Poulsen T, Wulf HC (2003) Epidermal thickness at different body sites: relationship to age, gender, pigmentation, blood content, skin type and smoking habits. Acta Derm Venereol 83:410–3. doi: 10.1080/00015550310015419

26. Campbell I (2008) Body temperature and its regulation. Anaesth Intensive Care Med 9:259–263. doi: 10.1016/j.mpaic.2008.04.009

27. Römers LHL, Bakker C, Dollée N, et al (2016) Cutaneous Mitochondrial PO_2, but Not Tissue Oxygen Saturation, Is an Early Indicator of the Physiologic Limit of Hemodilution in the Pig. Anesthesiology 125:124–32. doi: 10.1097/ALN.0000000000001156

28. O'Brien EO, Schmidt U (2016) Cellular Hypoxia in a Brand New Light. Anesthesiology 125:20–21. doi: 10.1097/ALN.0000000000001157

29. Harms F, Stolker RJ, Mik E (2016) Cutaneous respirometry as novel technique to monitor mitochondrial function: A feasibility study in healthy volunteers. PLoS One 11:163399. doi: 10.1371/journal.pone.0159544

30. Meglinsky IV, Matcher SJ (2001) Modelling the sampling volume for skin blood oxygenation measurements. Med Biol Eng Comput 39:44–50. doi: 10.1007/BF02345265

31. Vongsavan N, Matthews B (1993) Some aspects of the use of laser Doppler flow meters for recording tissue blood flow. Exp Physiol 78:1–14.

32. Guyotat J, Pallud J, Armoiry X, et al (2016) 5-Aminolevulinic Acid-Protoporphyrin IX Fluorescence-Guided Surgery of High-Grade Gliomas: A Systematic Review. Adv Tech Stand Neurosurg 61–90. doi: 10.1007/978-3-319-21359-0_3

33. Namikawa T, Yatabe T, Inoue K, et al (2015) Clinical applications of 5-aminolevulinic acid-mediated fluorescence for gastric cancer. World J Gastroenterol 21:8769–75. doi: 10.3748/wjg.v21.i29.8769

Chapter 4

Mitochondrial oxygen monitoring with COMET: verification of calibration in man and comparison with vascular occlusion tests in healthy volunteers

R. Ubbink[1], M.A. Wefers Bettink[1], W. van Weteringen[2], E.G. Mik[1]

[1]Department of Anesthesiology, Erasmus MC,
University Medical Center Rotterdam, The Netherlands
[2]Department of Pediatric Surgery, Erasmus MC – Sophia Children's Hospital,
University Medical Center Rotterdam, The Netherlands

Published in:
Journal of clinical monitoring and computing,2020: 1-10

Abstract

Mitochondria are the primary consumers of oxygen and therefore an important location for oxygen availability and consumption measurement. A technique has been developed for mitochondrial oxygen tension ($mitoPO_2$) measurement, incorporated in the COMET. In contrast to most textbooks, relatively high average $mitoPO_2$ values have been reported. The first aim of this study was to verify the validity of the COMET calibration for $mitoPO_2$ measurements in human skin. The second aim was to compare the dynamics of $mitoPO_2$ to several other techniques assessing tissue oxygenation.

Firstly, we performed a two-point calibration. Mitochondrial oxygen depletion was achieved with vascular occlusion. A high $mitoPO_2$ was reached by local application of cyanide. $MitoPO_2$ was compared to the arterial oxygen partial pressure (PaO_2). Secondly, for deoxygenation kinetics we compared COMET variables with the LEA O2C, SenTec OxiVenT™ and Medtronic INVOS™ parameters during a vascular occlusion test.

Twenty healthy volunteers were recruited and resulted in 18 datasets (2 times 9 subjects). The lowest measured $mitoPO_2$ value per subject had a median [IQR] of 3.0 [1.0 – 4.0] mmHg, n=9 . After cyanide application the $mitoPO_2$ was 94.1 mmHg [87.2 – 110.9] and did not differ significantly (n=9, p=0.5) from the PaO_2 of 101.0 [98.0 – 106.0] mmHg. In contrast to O2C, OxiVenT™ and INVOS parameters, $mitoPO_2$ declined within seconds with pressure on the probe. The kinetics from this decline are used to mitochondrial oxygen consumption ($mitoVO_2$).

This study validates the calibration of the COMET device in humans. For $mitoVO_2$ measurements not only blood flow cessation but application of local pressure is of great importance to clear the measurement site of oxygen-carrying erythrocytes.

Introduction

Mitochondria are small intracellular organelles that generate energy for the cells in the form of adenosine triphosphate (ATP). Oxygen is of critical importance for efficient ATP generation through the process of oxidative phosphorylation, also called mitochondrial respiration. This function makes mitochondria the primary consumers of oxygen in the body and therefore the most desired location for measuring oxygen availability and consumption.

An optical noninvasive technique has been developed for measuring mitochondrial oxygen tension (mitoPO$_2$). MitoPO$_2$ is determined with the protoporphyrin IX-Triplet State Lifetime Technique (PpIX-TSLT) by measuring the oxygen-dependent delayed fluorescence lifetime of 5-aminolevulinic acid (ALA)-induced PpIX [1–3]. This measurement technique is incorporated in a medical device called the Cellular Oxygen METabolism monitor (COMET) [4].

Previous studies that used the protoporphyrin IX lifetime technique for cutaneous mitoPO$_2$ measurements in humans reported some remarkable results. Most importantly, relatively high average mitoPO$_2$ values of around 44 mmHg (5.9 kPa) [5] and 66 mmHg (8.8 kPa) [6] have been reported. In contrast, most textbooks mention normal values of mitochondrial oxygen tension as low as 7.5 mmHg (1 kPa) or less [7]. The calibration constants used in the COMET have been determined in animal studies [8]. A direct calibration in man has been lacking to preclude the high PO$_2$ values being a result of improper calibration. The first aim of this study was therefore to verify the calibration of COMET in human skin.

No other clinical device is able to measure oxygenation at the mitochondrial level at the bedside. A direct comparison with other measurement techniques is thus unreliable because every tissue compartment, from intravascular to intracellular, has a different oxygen tension, leading to oxygen gradients. Due to the lack of a gold standard we aimed at using the same approach as used for in vivo calibration in animals, i.e. to use a combination of blocking oxygen supply by microvascular occlusion and blocking mitochondrial respiration by cyanide cream [8]. This provides a two-point calibration with a minimal mitoPO$_2$ value during microvascular occlusion and a known mitoPO$_2$ value after blockage of mitochondrial oxygen consumption.

Next to mitoPO$_2$ measurements, the COMET system can be used to assess the parameters mitoVO$_2$ (a measure for oxygen consumption) and mitoDO$_2$ (as a measure for oxygen delivery) [3, 6]. Several methods have been developed over the years for measuring tissue oxygen consumption non-invasively. Most of these methods use hemoglobin-based measurement techniques, measuring a vascular or microvascular hemoglobin oxygen saturation in combination with a vascular occlusion test [9]. Typically, the mitoVO$_2$ measurements with

COMET show much faster deoxygenation kinetics than those other approaches [10]. Therefore, the second aim of this study is to compare COMET variables to spectroscopic and transcutaneous techniques during vascular occlusion testing.

In short, in this study we compare mitoPO$_2$ with an arterial blood gas to verify the validity of the COMET calibration for mitoPO$_2$ measurements in human skin and compared the dynamics of mitoPO$_2$ to several other techniques for assessing tissue oxygenation in a series of healthy volunteers.

Methods

The study was approved by the local medical ethical committee and registered on www.toetstingonline.nl [NL61767.078.17]. The study complies with the Helsinki declaration on research ethics. Healthy volunteers were recruited at Erasmus Medical Center Rotterdam, the Netherlands. Informed consent was obtained prior to participant inclusion. Inclusion criteria were: subjects between 18 and 50 years of age and ASA-1-2. Exclusion criteria were: mental disability, presence of mitochondrial disease, diabetes, anemia, hemoglobinopathy, mild to severe COPD, porphyria and/or use of anti-coagulant medication.

Measuring mitochondrial oxygen tension

The COMET (Photonics Healthcare BV, Utrecht, The Netherlands) was used for mitoPO$_2$ and mitoVO$_2$ measurements. COMET uses the protoporphyrin IX triplet state lifetime technique (PpIX-TSLT) to measure oxygen availability. It provides quantitative measures, does not affect the measured tissue, and does not need recalibration before use [1]. For the extensive description of COMET internal components and the implemented algorithm, we refer to previous work [4]. We have described the fundamental principles behind the technology and have provided a working implementation of the technique as well as a method for calculating mitoVO$_2$ from the mitoPO$_2$ kinetics [11].

Before mitoPO$_2$ measurements can be performed 5-Aminolevulinic acid (ALA) has to be applied to the skin to induce sufficient mitochondrial PpIX for detection of delayed fluorescence [1, 12]. To this end we cutaneously applied a 4 cm^2 plaster, containing 8mg ALA (Photonamic, Hamburg, Germany). Six to eight hours previous to the measurements the ALA-plaster was applied to the lower arm. The COMET Skin Sensor was fixated onto the skin using a double-sided adhesive transparent plaster without optical interference (LEA Medizintechnik GmbH, Giessen, Germany).

Verification of COMET calibration

Since no gold standard exists to which COMET can be compared, verification of COMET calibration had to rely on creating predictable mitochondrial oxygen levels. We chose a two-point verification aiming at approximating zero oxygen conditions and arterial oxygen tension. In earlier experiments in cells and animals the oxygen tension was decreased by flushing or breathing nitrogen to wash out all available oxygen.

In healthy human volunteers tissue-deoxygenation with nitrogen to a near-zero level is not a safe and viable option. A method that is applicable in humans is temporal arterial occlusion of a limb in combination with local pressure on the measuring probe. Arterial and microvascular occlusion inhibits blood flow and thus the oxygen supply to the measurement site. Ongoing cellular oxygen consumption will decrease local mitochondrial oxygen tension to very low values, approximating the desired zero oxygen conditions.

In addition to measurements near zero oxygen conditions we applied a method to compare mitoPO$_2$ to arterial oxygen tension in a blood gas sample, in order to create a second calibration point at a higher PO$_2$ level. A known high mitochondrial oxygen tension can be achieved by abolishing the oxygen gradient between arterial blood and the tissue cells. After cessation of mitochondrial oxygen consumption diffusion equilibrates the mitochondrial and arterial oxygen tension. Mitochondrial respiration can be temporarily inhibited by locally applying cyanide [13–15], which has previously been demonstrated in cells and animals [8]. In the transient absence of mitochondrial oxygen metabolism, the measured mitoPO$_2$ can be compared to the oxygen partial pressure measured in an arterial blood gas (ABG) sample [13–15].

To diminish the influence of external factors like temperature and atmospheric oxygen a gas-sealed incubator was used to control internal air temperature and oxygen concentration, as shown in Figure 1a. During the measurements the subject's arm was inserted into the incubator, which was set to an internal temperature of 37 degrees Celsius. The oxygen concentration within the incubator was measured with a Fibox 4 trace (PreSense Precision Sensing GmbH, Regensburg, Germany). Prior to the mitoPO$_2$ measurements the arterial blood pressure was taken.

The first mitoPO$_2$ measurement was done in the incubator at a low surrounding PO$_2$ achieved by filling the incubator with nitrogen gas (PO$_2$ <5 mmHg), and with the blood pressure cuff pressurized to 50 mmHg above systolic pressure. After verification of the cessation of blood flow with an O2C laser-doppler monitor with an LFX-43 probe (oxygen to see version 2424, Lea Medizintechnik GmbH, Germany), local pressure was applied with the measurement

probe of the COMET to empty and occlude the microvessels in the measured tissue in order to perform a dynamic measurement showing the decreasing mitoPO$_2$ (120 measurements at 1 Hz). With the combination of flow cessation with the pressure cuff, local pressure on the sensor, and mitochondrial oxygen consumption the minimal mitoPO$_2$ was determined in the arm during occlusion. The lowest measured mitoPO$_2$ during this measuring sequence was taken as lowest measurable mitoPO$_2$ per subject.

An arterial blood sample was taken from the radial artery to determine arterial oxygen tension (PaO$_2$) with a blood gas analyzer (ABL 800 Flex, Radiometer, Brønshøj, Denmark). Nitrogen gas was mixed with room air to set the oxygen concentration in the incubator to a level equal to the arterial PaO$_2$ (range ±5 mmHg).

In this study, topical application of cyanide was used to equalize mitoPO$_2$ to PaO$_2$ by blocking oxygen consumption at the skin measurement location. Cyanide ions (CN) bind with high affinity to the mitochondrial cytochrome c oxidase, blocking its activity. As a result, electron transport in the enzyme chain of oxidative phosphorylation and subsequently mitochondrial ATP production and mitochondrial oxygen metabolism are inhibited [16]. The applied cyanide cream was locally produced and contained a concentration of 1% potassium cyanide (Sigma-Aldrich, St. Louis, Missouri) mixed with hydrophilic cremor Lanette (Lanette cream I FNA, Bipharma, Weesp, The Netherlands). After 1 minute the cream was removed and the lower arm was placed in the air mixture equal to the sampled PaO$_2$, after which the mitoPO$_2$ was measured.

To test blockage of mitochondrial respiration after topical application of cyanide the absence of oxygen consumption was checked. After 20 measurements in a sequence of 120 measurements at 1 Hz pressure was applied to the COMET skin sensor. Without cyanide a decrease in mitoPO$_2$ within seconds was seen, as illustrated in figure 5a. While the mitochondrial respiration was blocked the mitoPO$_2$ remained constant as illustrated in figure. 5c. Fifteen minutes after cyanide application the mitoVO$_2$ was measured in the skin to assess recovery of mitochondrial respiration (figure 5d).

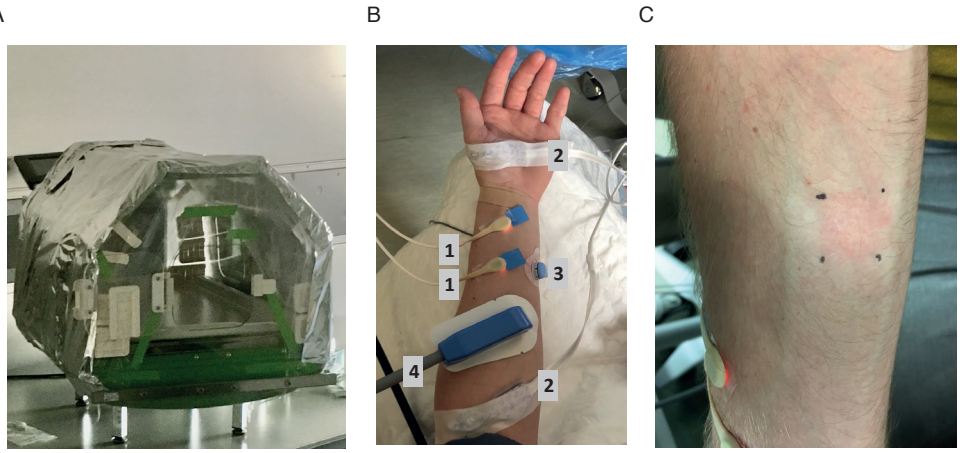

Figure 1. A) The incubator, sealed to prevent nitrogen gas leakage and provide a controlled air temperature of 370C. **B)** Probe position of 1. O2C LFX-43 probe, 2. INVOS, 3. SenTec OxiVenT, and 4. COMET Skin Sensor on the lower arm. **C)** The ALA application side after cyanide application. A temporary hyperemia phase was seen as a red square on the arm.

Comparison during vascular occlusion testing

To compare the behavior of mitoVO_2 of COMET to other oxygen metabolism-related measurements, a variety of clinical bedside monitoring devices with a temporal resolution of seconds were used. The following devices were included;

1. Oxygen To See with the LFX-43 probe (O2C version 2424, Lea Medizintechnik GmbH, Germany), which combines direct (infra)red light spectroscopy with laser doppler. It measures local capillary venous saturation (SO_2), and local microvascular blood flow is provided in flow units (FU).
2. Near-infrared spectroscopy (INVOS), which measures the tissue saturation and 3) a SenTec Digital Monitoring System with an OxiVenT™ Sensor (SenTec AG, Therwil, Switzerland) which transcutaneously measures blood gases and provides tcPCO_2 values. The location of the different probes on the arm can be seen in Figure 1b.

We measured during and after an arterial occlusion test of the arm. Arterial occlusion was achieved by insufflation of a cuff to at least 50 mmHg above the systolic blood pressure. The absence of skin blood flow was confirmed with laser-doppler blood flow measurement with the O2C. During 2 minutes the COMET monitor measured mitoPO_2 with a frequency of 1 Hz. The O2C, INVOS, and SenTec OxiVenT all collected data during arterial occlusion to

determine the oxygen level and consumption, as well as carbon dioxide (CO_2) accumulation in the measurement volume. In this setup no pressure was applied to the COMET skin sensor in order to be able to compare the deoxygenation rates of the different measurements.

The mitoVO_2 measurement was done with the following procedure; after a stationary measurement of 10 seconds direct pressure on the COMET Skin Sensor probe was applied. This halted the microcirculation, and with it oxygen delivery to the measured tissue volume. The mitoVO_2 was measured directly after local occlusion of the oxygen supply by a linear fit of mitoPO_2. This simple procedure created reproducible stop-flow conditions and induced measurable oxygen consumption rates, consequential to a cessation of microvascular oxygen supply and ongoing cellular oxygen consumption. MitoPO_2 was measured before, during and after application of pressure at an interval of 1 Hz.

Statistical analysis and software

Software version v.016.5b.184 of COMET was used, during the cyanide measurements, the adjusted timing software was used. Statistical analysis and visualization were done with R version 3.4.2 [17] and GraphPad Prism 6. MitoPO_2 and Arterial Blood Gas were compared using a two sided Wilcoxon-Mann-Whitney U-test. Significance was determined by p-values <0.05. Values are given as median and interquartile ranges or stated otherwise.

The average of the last 3 MitoPO_2 values measured before pressure was applied were used as a baseline. Linear slope comparison (as measure for the deoxygenation rate, or oxygen disappearance rate) between COMET, INVOS, SenTec OxiVenT was performed with GraphPad Prism linear regression model from the descending part of the data. MitoVO_2 linear fit was done with LabVIEW (Version 13, National Instruments, Austin, TX, USA) with the first 4 samples after pressure had been applied by the sensor to compare mitoVO_2 with previous published results [10]. To visually compare the oxygenation decline rate between the devices the data is transformed into z-score (datapoint – mean)/ standard deviation.

Results

A total of 20 healthy volunteers were recruited and provided informed consent. Of the 20 volunteers 10 underwent the entire study protocol. One subject dropped out due to beta-thalassemia that was missed during the inclusion procedure. The first 10 inclusions (session 1) resulted therefore in 9 complete datasets. Analysis of this first dataset showed that cyanide application led to unmeasurable delayed fluorescence in all but 1 subject. This unforeseen result was analyzed in cooperation with the manufacturer of the COMET device. It appeared

to be caused by the relatively long photomultiplier gate duration in comparison to the very short delayed fluorescence lifetimes after cyanide application, illustrated in Figure 2.

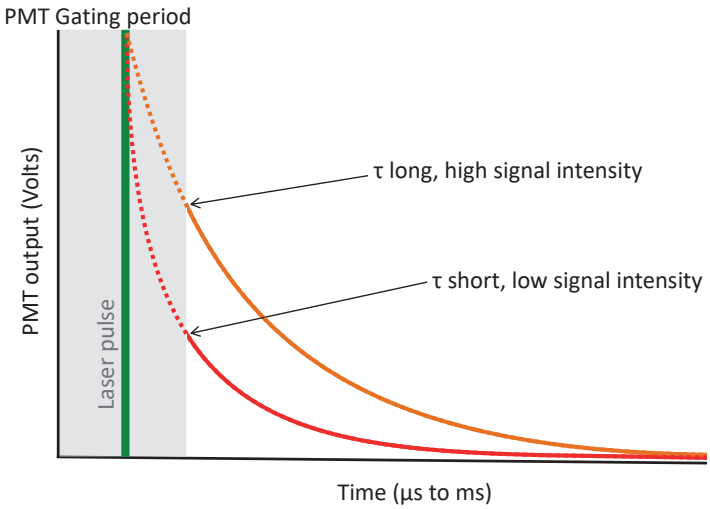

Figure 2. This illustration shows the decrease in signal intensity measured by the photomultiplier (PMT) with short lifetimes (several µs). If the lifetime is short the oxygen tension is high. The laser pulse (green) is followed by a PMT gating period (gray) to protect the PMT from prompt fluorescence. At the PMT most of the short lifetime signal intensity (red) will be lost. In low oxygen tension and thus a long lifetime (orange) the signal intensity will hardly be influenced by the PMT gating period.

A temporary change in the firmware of the COMET, kindly supported by the manufacturer, was suggested and used to overcome this problem. Therefore, a second series of measurements (session 2) with the cyanide cream was performed in 10 subjects. One subject had insufficient signal quality after the baseline measurement. This resulted in 9 datasets of new volunteers in the second session. A flow diagram of the inclusions is shown in Figure 3.

Demographic characteristics of the 18 analyzed healthy volunteers can be found in Table 1.

Table 1: Volunteer characteristics

	Session 1 (n=9) Median [IQR]	**Session 2 (n=9) Median [IQR]**
Plaster application time (min)	365 [360-450]	434 [425-455]
Blood pressure systole (mmHg)	123 [120-125]	129 [124-130]
Blood pressure diastole (mmHg)	84 [78-85]	85 [80-90]
Body length (cm)	184 [173-190]	178 [173-181]
Weight (kg)	84 [65-90]	77 [71-80]
Age (years)	28 [26-30]	28 [23-32]
Gender (female)	22%	33%

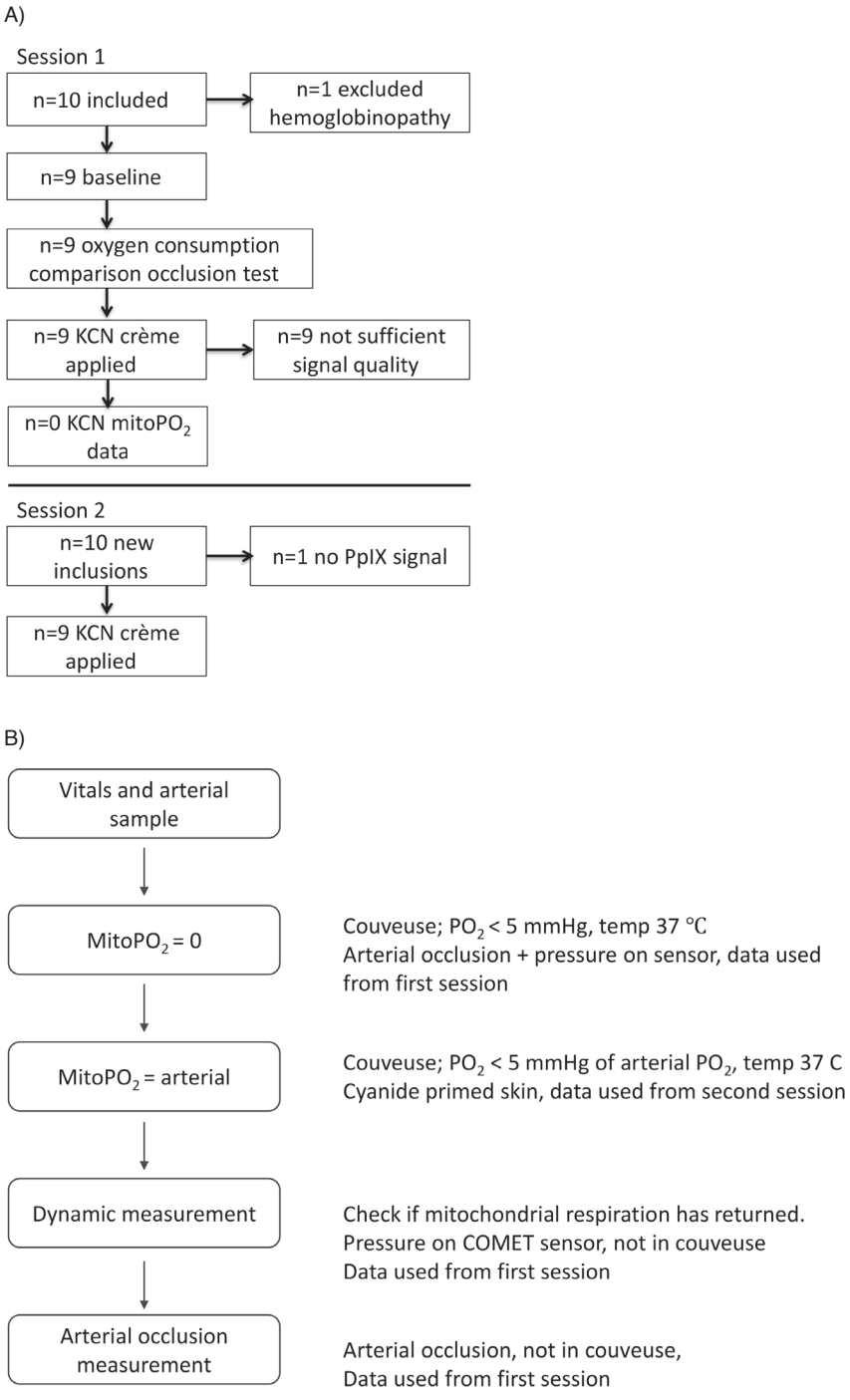

Figure 3. A)Diagram of study subject flow, B) Diagram of methods timeline

Zero and arterial blood gas oxygen tension validation

While the arm was in the incubator with an oxygen tension < 5 mmHg, the blood supply to the arm was occluded and pressure was applied to the skin sensor to approximate zero oxygen conditions. In all cases mitoPO$_2$ dropped and reached an equilibrium. The lowest measured mitoPO$_2$, median [IQR] minimum value was 3.0 [1.0 – 4.0] mmHg. In one case the steady state did not go below 5 mmHg and reached an equilibrium at 15 mmHg, seen in Figure 4a.

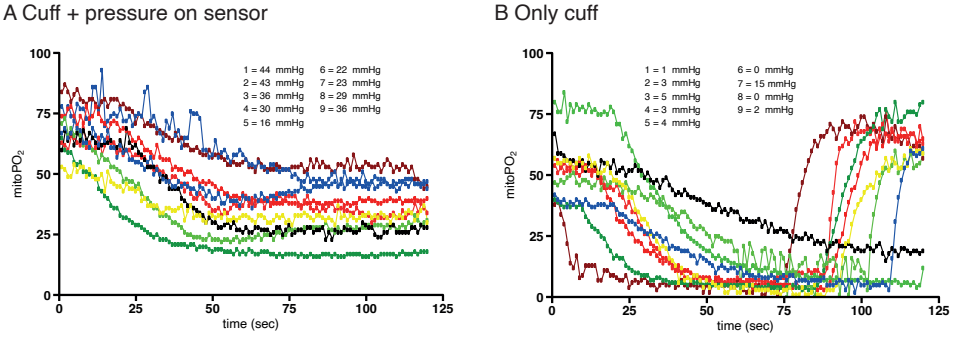

Figure 4. A) mitoPO$_2$ measurements in the incubator with pressure applied to the COMET skin sensor and an inflated upper arm cuff, pressurized to 50 mmHg above systolic blood pressure to stop the arterial flow in the arm. The listed values are the individual minimum mitoPO$_2$ levels just before the pressure is released.
B) mitoPO$_2$ measurements of the arm in which only the cuff around the upper arm was pressurized to 50 mmHg above systolic blood pressure to stop the arterial blood flow in the arm. The listed mitoPO$_2$ values are the equilibrium value at the end of the measurement.

The additional effect of local pressure on the tissue with the COMET skin sensor on the deoxygenation kinetics compared to use of only a blood pressure cuff can clearly be seen in Figure 4. In the experiments shown in Figure 4b only an upper arm cuff was pressurized to stop the arterial blood flow. As a result, the mitoPO$_2$ stabilized at median of 30.0 [24.5 – 36.0] mmHg, greatly contrasting with the low mitoPO$_2$ 3.0 [1.3 – 4.8] mmHg when pressure is also applied on the skin sensor itself. If pressure is applied to the skin sensor the decrease in oxygen tension is faster, 2.1 [1.0 – 2.9] mmHg/s compared to 1.3 [1.2 – 1.4] mmHg/s without pressure.

Application of cyanide cream on the skin in the first session led to low signal quality and, except for one case, mitoPO$_2$ readings well below the corresponding PaO$_2$ values (Figure 5a). This COMET behavior was analyzed in cooperation with the manufacturer and appeared to be caused by the detector gating. Due to the specific timing of this gating, the very short delayed fluorescence lifetimes resulting from the high intracellular PO$_2$ were omitted from the signal analysis, leading to an erroneously low steady mitoPO$_2$ around 66 mmHg.

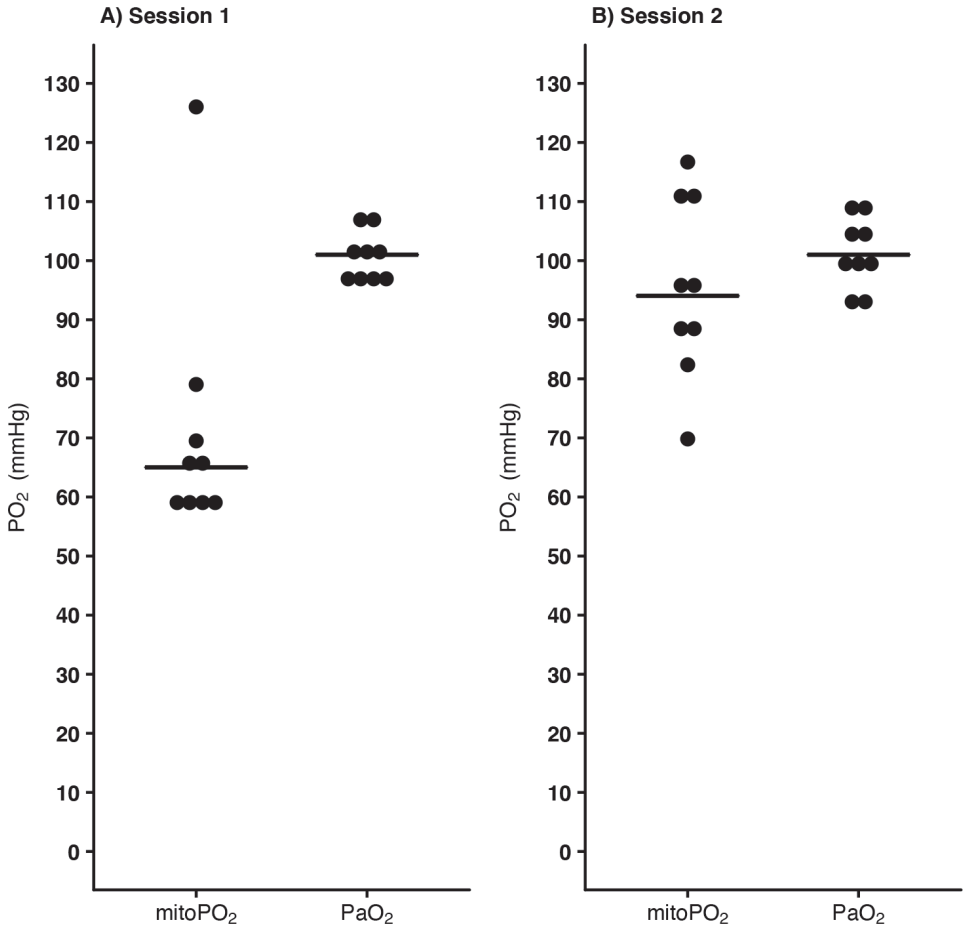

Figure 5. Comparison between COMET mitoPO_2 after cyanide cream had been applied to block mitochondrial respiration and arterial blood gas PaO_2 taken from a radialis. A) Data from session 1, even though the delayed fluorescence was insufficient a mitoPO_2 was displayed around 65 mmHg. One subject with a strong signal the short lifetime was measurable, seen as black dot 126 mmHg. B) Data from session 2 with adjusted software. No significant difference was seen in session 2 between mitoPO_2 and PaO_2.

To enable accurate detection of high mitoPO_2 values the timing of the gating was adjusted by a temporary adaptation in the firmware. During session 2 data was collected with this adjusted software. Now, the median [IQR] mitoPO_2 was 94.1 mmHg [87.2 – 110.9] and did not differ significantly (p=0.5) from the sampled PaO_2 of 101.0 mmHg [98.0 – 106.0]. When pressure was applied to the skin sensor the mitoPO_2 did not decrease, indicating the absence of mitochondrial respiration, as shown in Figure 6C. Within all subjects the mitochondrial respiration returned after approximately 15 minutes. No major adverse events caused by the

cyanide application were witnessed. Apart from a temporarily red skin, no pain, skin irritation or other effects of the cyanide cream were reported.

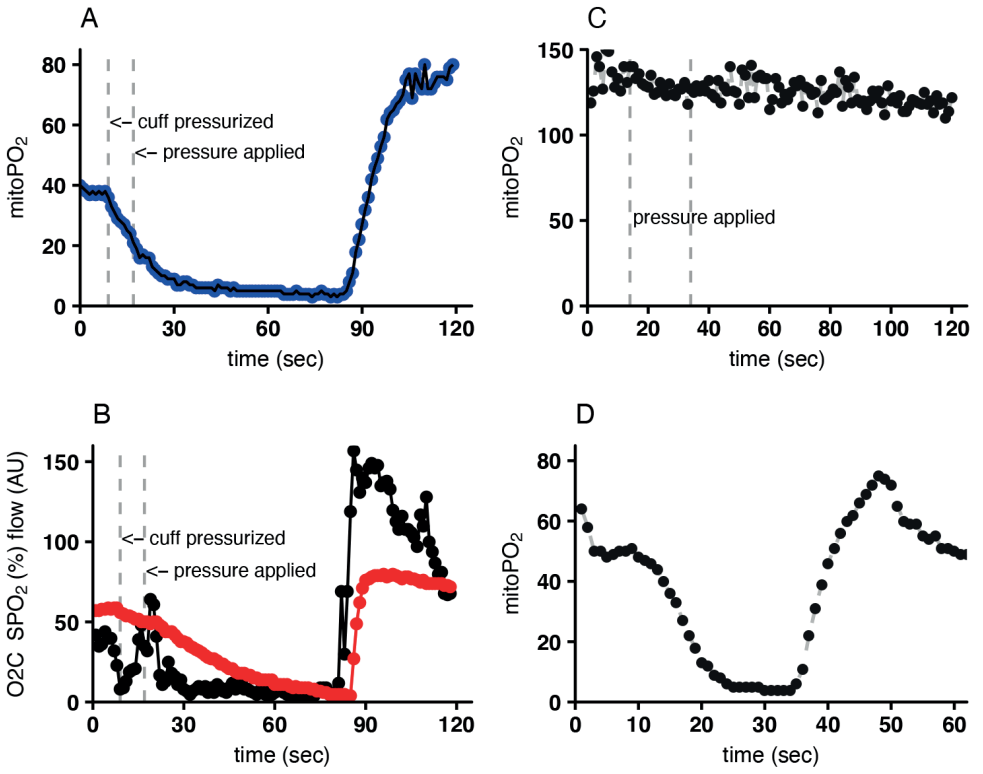

Figure 6. A) MitoPO_2 baseline measurement, at t=9 (sec) blood pressure cuff inflated to 50 mmHg above systolic blood pressure, t=17 (sec) manual pressure on the COMET skin sensor, at t=84 (sec) release of pressure from skin sensor and cuff. B) O2C microvascular blood flow (black) and tissue oxygenation SpO_2 (red) with the pressure cuff applied and pressure on the skin sensor. C) Cyanide was applied to the skin to block mitochondrial respiration. While pressure was applied no sudden drop was seen, indicating cyanide-induced blockage of mitochondrial respiration. D) Ten minutes after cyanide application a mitochondrial respirational check was done.

Comparison of monitors

Arterial occlusion of the arm led to an immediate decline and subsequent stop of microcirculatory blood flow measured by the O2C. MitoPO_2 and tissue oxygen saturation followed. A linear regression of the measured decline during the arterial occlusion with the cuff provided different slopes for all measurements as shown in Table 2. An example of measurements is shown in Figure 7A, with the mean of the z score of all subjects shown in Figure 7B.

Table 2: Linear fit of arterial occlusion of the arm with a pressurized cuff

	Baseline value Median [IQR]	Decline Mean ± SD	z-score* Decline Mean
$MitoPO_2$ (mmHg)	68 [61-76.5]	-0,75 ± 0,06	-0,089
Flow O2C (FU)	35 [20-57]	-2,30 ± 0,37	-0,15
sat O2C (%)	49 [43-65]	-0,51 ± 0,05	-0,062
NIRS (%)	76 [72-82]	-0,21 ± 0,04	-0,058
$TcPCO_2$ OxiVenT (mmHg)	51 [47-56]	$-0,37*10^{-3}$ ± 0,03	-0,010
Heating OxiVenT (mWatt)	130 [123-142]	$-0,95*10^{-1}$ ± 0,06	-0,050

*z-score = (data point-average)/standard deviation

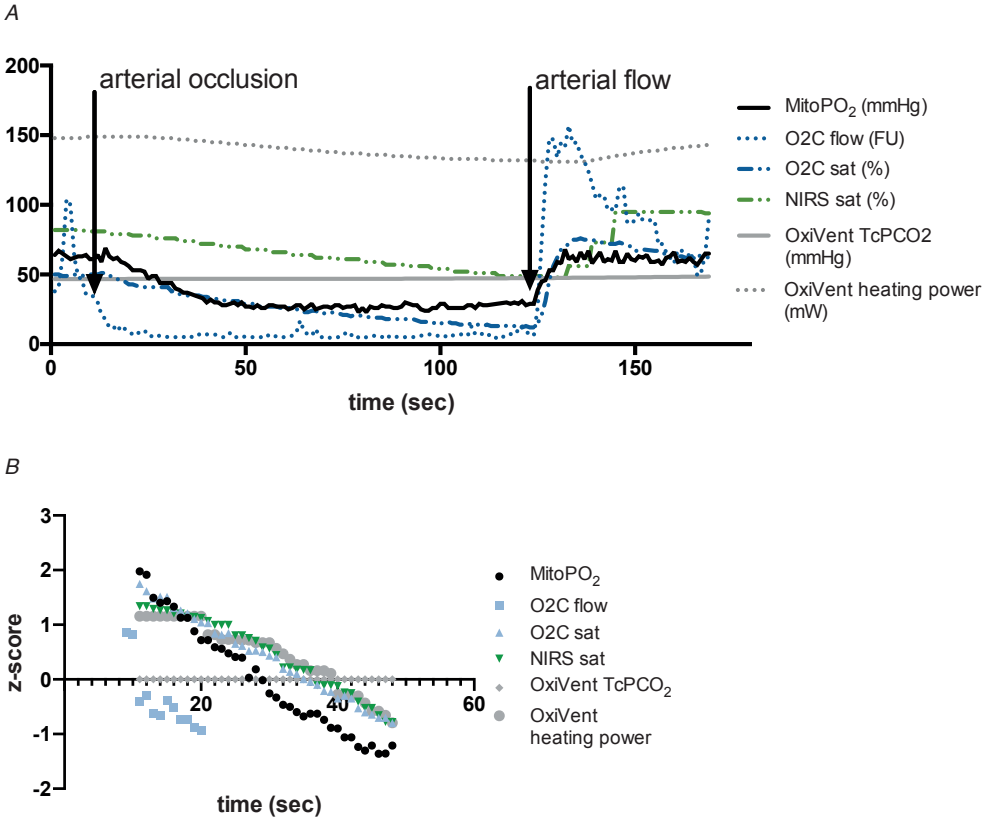

Figure 7. A)Typical example of arterial occlusion of the forearm. At t=10 seconds the blood pressure cuff was inflated to 50 mmHg above the blood pressure measured earlier. At t=120 seconds the blood pressure cuff was released and arterial flow returned. B) Average data of 9 subjects. Data shown in z-score transformation, z=(data point – mean)/standard deviation to compare the overall decline part of the data.

Interestingly the $tcPCO_2$ measurement was stable during this short arterial stop, although the heating power required to maintain a stable sensor temperature of 43 °C changed slightly. After a relatively long delay an increase in $tcPCO_2$ was seen.

Discussion

This study demonstrates that the calibration of COMET device, originally determined in animal experiments, is adequate for cutaneous $mitoPO_2$ measurements in man. Furthermore, dynamic oxygenation measurements aimed at gaining insight in tissue oxygen consumption depend on the specific measuring technique and method to cease oxygen supply to the measurement spot.

The COMET measurement system measures relatively high $mitoPO_2$ values compared to the general idea that $mitoPO_2$ should be very low in order to drive oxygen diffusion [6, 18, 19]. This study shows that such high $mitoPO_2$ values are not the result of an inadequate calibration. On the contrary, in this study the COMET showed the tendency to underestimate $mitoPO_2$ in the case intracellular PO_2 was artificially increased to arterial oxygen levels.

The $mitoPO_2$ measured with the COMET monitor is higher than expected. $MitoPO_2$ appears to be, depending on the measurement site and respiratory rate of the tissue, much closer to microvascular oxygen tension [20, 21], and thus closer to tissue and/or interstitial oxygen levels [22, 23], than anticipated [7]. There are several reasons why mean $mitoPO_2$ in a tissue sample cannot be an order of magnitude lower than microvascular and interstitial oxygen tension; First, oxygen does not disappear stepwise but gradual, so several mitochondria will see aPO_2 close to intravascular values. Second, oxygen diffuses also from large vessels so contribute to cellular oxygen delivery [24], so several mitochondria have a higher PO_2 than capillary oxygen tension. Third, the $mitoPO_2$ will not be substantially lower than interstitial PO_2 because the oxygen gradient over the cell membrane is small [1]. Typically reported baseline $mitoPO_2$ values are 40-70 mmHg. Other oxygen measurements in the skin are matching these values [23]. Importantly, it has been demonstrated in both a preclinical [25] and clinical setting [4] that $mitoPO_2$ provides different information than hemoglobin saturation-based techniques like near-infrared spectroscopy.

Application of cyanide on the skin led to a temporary block of mitochondrial respiration and abolishment of the oxygen gradient. In the first series of 9 investigated subjects, the timing between the laser pulse and the end of the off-gating of the photomultiplier (PMT) in the COMET proofed too long to adequately detect the short delayed fluorescence lifetimes caused by the artificially high intracellular PO_2. The gating itself is necessary to prevent

damage to the sensitive detector due to laser light and prompt fluorescence [4], and its timing is a trade-off between several factors, foremost the ability to accurately measure high mitoPO$_2$ (supraphysiological) and protecting the detector. After adjustment of this timing in the firmware, PMT gating interference was sufficiently reduced to allow collection of the delayed fluorescence signal after topical application of cyanide. Due to this adaptation, we were able to demonstrate that mitoPO$_2$, as measured with COMET, corresponds well to PaO$_2$ in the absence of mitochondrial oxygen consumption. Under more physiological circumstances the timing of the PMT gating is much less critical as delayed fluorescence lifetimes are longer and easier to detect. COMET measured very low mitoPO$_2$ after oxygen deprivation and overall the calibration of the device seems adequate for its purpose.

This study also presents the comparison of different oxygen consumption measurements in the arm. The COMET was compared to O2C, INVOS and SenTec OxiVenT™ during an arterial occlusion test in nine subjects. During arterial occlusion all oxygenation parameters show a decline in a comparable rate. Also, the measured decline in NIRS saturation of 0.21%/sec (12.6%/min) in this study is comparable to previously found values of 10.8, 13.2, 22.8%/min during occlusion of an extremity [26]. However, during a dynamic measurement for measuring mitochondrial oxygen consumption (mitoVO$_2$), with pressure on the measurement probe, a faster decline is seen. This decline is seen in all but one subject in figure 4 A with an equilibrium at 15 mmHg. Since the curve of this individual shows similarities to the measurements without local pressure on the probe, we think that probably the effect of local pressure on the sensor was inadequate. We hypothesize that in this case an equilibrium emerges between the still saturated hemoglobin and mitochondrial respiration, similar to the situation in laboratory animals [27]. Also, when a mitoVO$_2$ procedure is done on the sternum we do not see such equilibrium at a high mitoPO$_2$ value. Therefore, we think that the pressure on the skin sensor did not adequately push away the erythrocytes in the measurement volume.

MitoVO$_2$ measurements should preferably be done on skin above a bone structure to allow the buffer of erythrocytes to be pushed away. The arm is therefore not the preferred site because the skin is not located above a flat bone. This likely resulted in a relatively slow median mitoVO$_2$ of 2.1 mmHg/s in comparison to measurements done on the sternum with a median mitoVO$_2$ 5.8 mmHg/s measured on healthy volunteers in our lab [10]. When the skin sensor is on top of a bone structure, with a little pressure the microcirculation is blocked and the erythrocytes are pushed out of the measurement volume. In this study the applied pressure was not measured but this could add to the standardization of a mitoVO$_2$ maneuver and improve the repeatability. However, arterial occlusion tests can only be done on an extremity and therefore the mitoVO$_2$ values are different from other healthy volunteer studies [6, 10]. Whilst the forearm is not a

preferred measurement site a large difference in mitoVO_2 could be demonstrated if pressure is exerted onto the COMET Skin Sensor, 2.1 mmHg/s compared to 1.3 mmHg/s during arterial occlusion. The oxygen buffer available in microcirculation likely accounts for the difference of 0.8 mmHg/s.

Both the mode of measurement (hemoglobin-based versus non-hemoglobin-based) and differences in tissue penetration depth per technique might account to the observed differences in oxygen disappearance rates. The COMET has a penetration depth of less than a mm, in contrast to infra-red optical techniques (>900nm wavelength) with a penetration depth of several cm. Since O2C and INVOS measure deeper in the tissue, and thus in a different tissue compartment, the decline in oxygen saturation represents a larger measurement volume. After the occlusion an equilibrium emerges between the available oxygen, mainly dependent on the concentration and amount of arterial and venous hemoglobin available in the vessels, and mitochondrial respiration. It is not possible to push away or largely reduce the number of erythrocytes in the infra-red measurement volume. A large measurement volume that contains erythrocytes without the ability to reduce the oxygen buffer results in a slower decrease in saturation. When performing a dynamic measurement with the COMET local pressure with the Skin Sensor leads to largely eliminating the available erythrocytes from the microcirculation and therefor the dynamic measurement may be less dependent on the availability of the oxygen buffer.

Conclusion

This study shows that mitochondrial oxygen partial pressures measured with Pp-IX lifetime technique are comparable to the arterial PaO_2 during blockade of mitochondrial respiration with topical application of cyanide. Therefore, this study demonstrates that the calibration of COMET device, originally determined in animal experiments, is valid in human cutaneous mitoPO_2 measurements.

For mitochondrial oxygen consumption measurements not only blood flow occlusion, but applying pressure on the COMET Skin Sensor is of great importance to clear the measurement site of available oxygen-carrying erythrocytes. Without a technique to eliminate this oxygen buffer the consumption measurement underestimates the actual mitochondrial oxygen consumption.

References

1. Mik EG, Stap J, Sinaasappel M, et al (2006) Mitochondrial PO_2 measured by delayed fluorescence of endogenous protoporphyrin IX. Nat Methods 3:939–45. https://doi.org/10.1038/nmeth940
2. Mik EG (2013) Special article: measuring mitochondrial oxygen tension: from basic principles to application in humans. Anesth Analg 117:834–46. https://doi.org/10.1213/ANE.0b013e31828f29da
3. Harms FA, Bodmer SIA, Raat NJH, Mik EG (2015) Cutaneous mitochondrial respirometry: non-invasive monitoring of mitochondrial function. J Clin Monit Comput 29:509–519. https://doi.org/10.1007/s10877-014-9628-9
4. Ubbink R, Bettink MAW, Janse R, et al (2017) A monitor for Cellular Oxygen METabolism (COMET): monitoring tissue oxygenation at the mitochondrial level. J Clin Monit Comput 31:1143–1150. https://doi.org/10.1007/s10877-016-9966-x
5. Harms F, Stolker RJ, Mik E (2016) Cutaneous Respirometry as Novel Technique to Monitor Mitochondrial Function: A Feasibility Study in Healthy Volunteers. PLoS One 11:e0159544. https://doi.org/10.1371/journal.pone.0159544
6. Baumbach P, Neu C, Derlien S, et al (2018) A pilot study of exercise-induced changes in mitochondrial oxygen metabolism measured by a cellular oxygen metabolism monitor (PICOMET). Biochim Biophys acta Mol basis Dis. https://doi.org/10.1016/j.bbadis.2018.12.003
7. Chambers D, Huang C, Matthews G (2019) Oxygen Cascade. In: Basic Physiology for Anaesthetists. Cambridge University Press, pp 80–81.
8. Harms FA, Bodmer SI a, Raat NJH, et al (2012) Validation of the protoporphyrin IX-triplet state lifetime technique for mitochondrial oxygen measurements in the skin. Opt Lett 37:2625–7.
9. Steenhaut K, Lapage K, Bové T, et al (2017) Evaluation of different near-infrared spectroscopy technologies for assessment of tissue oxygen saturation during a vascular occlusion test. J Clin Monit Comput 31:1151–1158. https://doi.org/10.1007/s10877-016-9962-1
10. Harms FA, Stolker RJ, Mik EG (2016) Cutaneous Respirometry as Novel Technique to Monitor Mitochondrial Function: A Feasibility Study in Healthy Volunteers. PLoS One 11:e0159544. https://doi.org/10.1371/journal.pone.0159544
11. Harms FA, Voorbeijtel WJ, Bodmer SIA, et al (2013) Cutaneous respirometry by dynamic measurement of mitochondrial oxygen tension for monitoring mitochondrial function in vivo. Mitochondrion 13:507–14. https://doi.org/10.1016/j.mito.2012.10.005
12. Mik EG, Johannes T, Zuurbier CJ, et al (2008) In vivo mitochondrial oxygen tension measured by a delayed fluorescence lifetime technique. Biophys J 95:3977–90. https://doi.org/10.1529/biophysj.107.126094.
13. Ballantyne B, Boardman SP, Bright J, et al (1972) Proceedings: Tissue cyanide concentrations and cytochrome oxidase in experimental cyanide poisoning. Br J Pharmacol 44:382P.
14. Camerino PW, King TE (1966) Studies on cytochrome oxidase II. A reaction of cyanide with cytochrome oxidase in soluble and particulate forms. J Biol Chem 241:970–979.
15. Piantadosi CA, Sylvia AL, Jöbsis FF (1983) Cyanide-induced cytochrome a, a3 oxidation-reduction responses in rat brain in vivo. J Clin Invest 72:1224–1233.
16. Clausen T, Zauner A, Levasseur JE, et al (2001) Induced mitochondrial failure in the feline brain: Implications for understanding acute post-traumatic metabolic events. Brain Res 908:35–48. https://doi.org/10.1016/S0006-8993(01)02566-5
17. R Core Team (2017) R: A Language and Environment for Statistical Computing.

18. Wittenberg BA, Wittenberg JB (1989) Transport of oxygen in muscle. Annu Rev Physiol 51:857–78. https://doi.org/10.1146/annurev.ph.51.030189.004233

19. Hsia CCW, Schmitz A, Lambertz M, et al (2013) Evolution of air breathing: Oxygen homeostasis and the transitions from water to land and sky. Compr Physiol 3:849–915. https://doi.org/10.1002/cphy.c120003

20. Bodmer SIA a, Balestra GM, Harms FA, et al (2012) Microvascular and mitochondrial PO(2) simultaneously measured by oxygen-dependent delayed luminescence. J Biophotonics 5:140–51. https://doi.org/10.1002/jbio.201100082

21. Balestra GM, Aalders MCG, Specht PAC, et al (2015) Oxygenation measurement by multi-wavelength oxygen-dependent phosphorescence and delayed fluorescence: catchment depth and application in intact heart. J Biophotonics 8:615–28. https://doi.org/10.1002/jbio.201400054

22. De Santis V, Singer M (2015) Tissue oxygen tension monitoring of organ perfusion: Rationale, methodologies, and literature review. Br J Anaesth 115:357–365. https://doi.org/10.1093/bja/aev162

23. Keeley TP, Mann GE (2019) Defining physiological normoxia for improved translation of cell physiology to animal models and humans. Physiol. Rev.

24. Ellsworth ML, Pittman RN (1990) Arterioles supply oxygen to capillaries by diffusion as well as by convection. Am J Physiol 258:H1240-3. https://doi.org/10.1152/ajpheart.1990.258.4.H1240

25. Römers LHL, Bakker C, Dollée N, et al (2016) Cutaneous Mitochondrial PO_2, but Not Tissue Oxygen Saturation, Is an Early Indicator of the Physiologic Limit of Hemodilution in the Pig. Anesthesiology 125:124-32. https://doi.org/10.1097/ALN.0000000000001156

26. Hyttel-Sorensen S, Hessel TW, Greisen G (2014) Peripheral tissue oximetry: Comparing three commercial near-infrared spectroscopy oximeters on the forearm. J Clin Monit Comput. https://doi.org/10.1007/s10877-013-9507-9

27. Harms FA, Bodmer SIA, Raat NJH, Mik EG (2015) Non-invasive monitoring of mitochondrial oxygenation and respiration in critical illness using a novel technique. Crit Care 19:343. https://doi.org/10.1186/s13054-015-1056-9

Chapter 5

Quantitative intracellular oxygen availability before and after 5-aminolevulinic acid skin photodynamic therapy

R. Ubbink [1], E.P. Prens [2], E.G. Mik [1]

[1] Erasmus Medical Center, Anesthesiology, Erasmus MC University Medical Center, Rotterdam, the Netherlands
[2] Erasmus Medical Center, Dermatology, Erasmus MC University Medical Center, Rotterdam, the Netherlands

Published in:
Photodiagnosis and Photodynamic Therapy 36 (2021) 102599

Abstract

Background, during photodynamic therapy (PDT) oxygen is transformed into reactive oxygen species (ROS) to induce cellular apoptosis in (pre)malignant cells. Real time oxygen availability measurement is clinically available with the Cellular Oxygen Metabolism (COMET) monitor.

Methods, Primary objective is to show that mitochondrial oxygen availability (mitoPO$_2$) measurement is possible during clinical ALA-PDT. The secondary aim was to determine the pain sensation, because it is the most commonly reported side effect of PDT. Before and after the two fraction PDT treatment, with a 2-hour dark period, mitoPO$_2$ was measured and reported pain was documented with a visual analog scale (VAS) 0-100.

Results, nine patients were included. Before the first PDT session the median signal quality was [IQR] 55.0% [34.2-68.0], which decreased after session one to 0% [0.0-10.0]. MitoPO$_2$ was 40.0 [17.7-53.8] mmHg and increased afterwards to 61.8 [38.2-64.8] mmHg. This likely the result of the delay time between the illumination stop and the mitoPO$_2$ measurements in a vasodilated, visibly red lesion.

Before session two signal quality was 10.4 [0-20.15 %, 40% lower than at the start. In 5 patients the signal quality after session 2 was too low because of photobleaching and insufficient regeneration of PpIX, median 0 [0-10]%. Subjects reported low median VAS scores, all below 3, directly after the mitoPO$_2$ measurements.

Conclusion, with COMET we were able to reliably measure mitochondrial oxygen concentrations during photodynamic therapy. Signal quality drastically decreases after a PDT session because of PpIX deterioration during the illumination phase.

Introduction

Photodynamic therapy (PDT) is successfully used for treatment of superficial cutaneous cancers. The therapy requires three interdependent factors, light, photosensitizer, and oxygen. The photosensitizer absorbs light and reacts with oxygen, resulting in the creation of reactive oxygen species (ROS). The PDT results in cellular and vascular damage and an immunological response that leads to apoptosis and necrosis of (pre)malignant tissue [1]. The availability of oxygen is a crucial factor for the amount of apoptosis induced during PDT [2].

PDT has a high complete clinical response rate of 90% in human superficial basal cell carcinoma [3]. Unfortunately the recurrence rate is around 21.1% and no clinical clearance is seen in 14.7% [4].The cytotoxicity variation after PDT *in vivo* is multifactorial and depends on the photosensitizing molecule penetration, its localization, light dose and time, type of irradiation and time, and type of tumor and its level of oxygenation [5–7]. In order to improve the clinical response a two fraction treatment scheme, with a dark period in between two illumination sessions, can be used [8]. Such two-fraction treatment scheme is common in the Netherlands. However, although it has been proven to improve the clinical response the exact mechanism is not fully understood.

Because oxygen availability is one of the key factors for the induction of ROS and cellular apoptosis, it has been suggested to measure oxygen to be capable of adjusting the light dosimetry in real time for an optimal usage of the photosensitizer [9–11].

One of the most used photosensitizers in PDT is 5-aminolevulinic acid (ALA)-induced Protoporphyrin IX (PpIX). PpIX occurs naturally in cells and is endogenously produced in the mitochondrial heme-cycle. Under normal circumstances the accumulation of PpIX is avoided by a negative feedback mechanism of heme [12]. External administration of ALA bypasses this negative feedback inhibition, which in combination with the rate-limiting incorporation of iron into PpIX for the formation of heme, results in PpIX accumulation in the mitochondria [13].

Real time oxygen availability measurement became possible with the introduction of the Triplet State Lifetime Technique (TSLT) [14]. As in ALA-PDT this technique also uses ALA-induced PpIX as an intra cellular endogenous oxygen probe. The PpIX exhibits prompt fluorescence, but also an oxygen-dependent delayed fluorescence in the same spectrum with a lifetime of several hundred microseconds [15]. Spontaneous regression via a bi-directional intersystem crossing from the excited triplet state, is accompanied by delayed fluorescence. Oxygen is a very effective quencher of the excited PpIX in the triplet state, it takes over the energy and PpIX will relax to its ground state without emission of a photon. The delayed fluorescent lifetime

of the PpIX is therefore inversely proportional to the amount of intracellular oxygen [15]. The detailed description of the measurement technique has been published elsewhere [15–17]. Currently a device, called COMET, is available that has incorporated the TSLT and enables measurements of mitochondrial oxygen (mitoPO$_2$) availability and oxygen disappearance rate (ODR) in the skin [17].

The primary aim of this pilot study is to demonstrate that the measurement of oxygen availability is possible with COMET in the current daily clinical ALA-PDT practice. The second aim was to determine the pain sensation caused by the oxygen measurement technique and of the PDT treatment [18].

Materials and Methods

This single center study was ethical approved by ethical research board Rotterdam and registered at www.toetsingonline.nl [NL51187.078.14]. All adult patients (age > 18 years) who were scheduled for ALA-PDT in 2015 and 2016 in the Erasmus Medical Center Rotterdam were included. Patients came in around 9:00 am for 20% ALA gel application (Fagron, Oud Beijerland, The Netherlands) on the skin lesion. The area was subsequently covered with an occlusive dressing (Tegaderm, 3M, Leiden, The Netherlands) for light protection. This coverage ensures a proper accumulation of PpIX, blocks the location for excessive sunlight, and prevents photo degradation PpIX.

Two illumination sessions were scheduled with the Omnilux light source (Waldmann Phototherapeutics, London, United Kingdom), emitting a wavelength of 633 nm with a bandwidth of 20 nm in a continuous mode. Light fractions were delivered at a fluence rate of 80mW cm^{-2}. Four hours after ALA application the first illumination session (20 J cm^{-2}) started. Subsequently the second illumination session (80 J cm^{-2}) was started after a two-hour dark interval.

Before and after each PDT illumination session the oxygen availability (as mitochondrial oxygen tension, mitoPO$_2$) and oxygen disappearance rate (ODR) were measured with COMET (Photonics Healthcare BV, Utrecht, the Netherlands). One measurement is a sequence of 120 measurements (1Hz). After approximately 15 seconds, pressure was applied on the probe to temporarily occlude the local microcirculation. In this period the mitochondria locally use the oxygen in the cells and therefore the oxygen disappearance rate can be determined, after 30 to 40 seconds pressure was released and the influx of oxygen into the cell can be seen. A detailed description of COMET, the measurement technique, and the signal quality calculation have been described elsewhere [17].

PDT is known to be painful in a selective group of patients. The sensation of the oxygen measurement with COMET specific was determined with a visible analogue scale (VAS score). The VAS goes from 0, no sensation, to 100, the worst pain ever felt. Before and after illumination a close-up digital photograph was taken. Patients needed to report their pain sensation with a pencil stroke between 0-100. Afterwards the length from 0 to the indication was measured with a digital caliper.

Oxygen availability was calculated as the average of six measurements prior to the point where pressure was applied on the skin sensor to occlude the microcirculation. Oxygen disappearance rate was determined with a least square linear fit of the first part of the oxygen disappearance curve [19]. Because the availability of oxygen is unlimited for the consuming cells, the calculated coefficient dPO_2/dt approximates the cellular oxygen respiration. A detailed description of the analysis technique can be found in an article on cutaneous respirometry by Harms et al. 2016 [20].

Data were analyzed using R version 3.4.2 [21]. Boxplot shows the median in the middle with hinges first and third quartiles (25 and 75% percentiles). Whiskers are min max value within 1.5*IQR. Group comparison for $mitoPO_2$ levels was done with Wilcoxon-Mann-Whitney test. Significance was determined by *p*-values < 0.05. All values reported are expressed as median with the first and third inter quartile range. Due to the exploratory nature of this study, no corrections for multiple comparisons were applied.

Results

Nine patients were measured. Seventy eight percent (78%) of patients were treated with ALA-PDT for basal cell carcinoma (BCC) and 22% for actinic keratosis (AK). The overview of demographic data can be found in Table 1. In one occasion COMET failed to measure in the morning because of high humidity in the summer period, after acclimatization in the air-conditioned area it started working, therefore only before and after the second illumination phase the $mitoPO_2$ was measured. In another case the pain in session one was non-bearable and the PDT session was stopped and no measurements could be done afterwards. The data and patient flow scheme can be found in Figure 1. An example of an oxygen availability measurement with an oxygen disappearance rate measurement is shown in Figure 2.

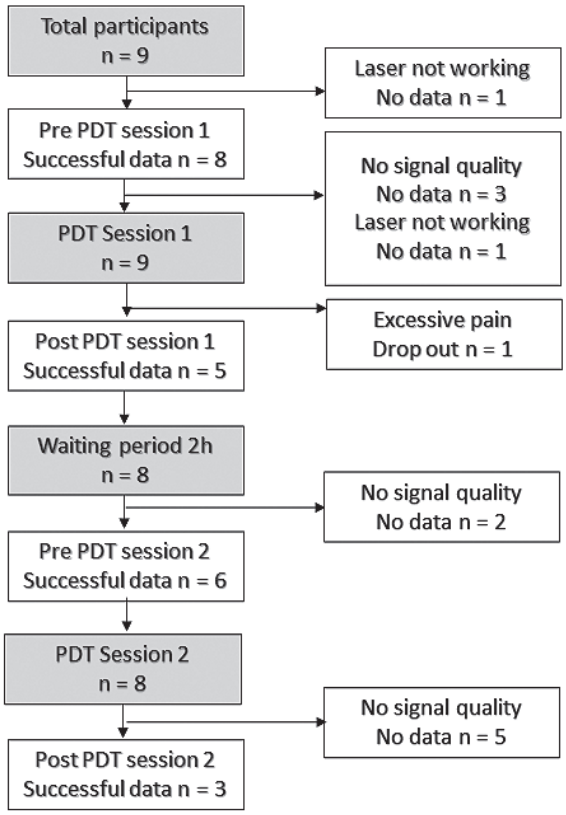

Figure 1. Patient and data flow scheme

Table 1: Patient characteristics

Diagnosis	Age	M/F	Skin type	Lesion size mm2	Result PDT	Days after PDT
BCC	51	F	White	4	Good	20
BCC	64	M	White	16	Good	16
BCC	65	M	Light brown	4	Good	51
BCC	82	F	Light brown	4	Good	84
AK	68	M	White	Complete limb	Good	57
AK	76	M	Light brown	5	Inconclusive	176
BCC	33	F	White	5	Inconclusive	45
BCC	60	F	White	6	Good	129
BCC	64	F	White	45	Partial response	87

AK: Actinic keratosis, BCC: Basal cell carcinoma, F: Female, M: Male, PDT: Photo Dynamic Therapy,

Illumination session 1

Before the first PDT session the signal quality was adequate (defined as > 20% [17]) in all patients, median [IQR] 55.0% [34.2-68.0] and decreased after the PDT session to 0% [0.0-10.0]. Oxygen availability before the start of PDT was 40.0 [17.7-53.8] mmHg *n*=8 in the lesion. After the first PDT session 3 patients did have insufficient signal quality and no mitoPO$_2$ could be gathered. The oxygen availability increased after session one to 61.8 [38.2-64.8] mmHg *n*=5. Oxygen disappearance rate (ODR) before was 5.6 [3.0-8.4] mmHg/sec and increased to 6.4 [1.8-6.6] mmHg/sec. In one patient the oxygen consumption measurement could not be performed after the PDT session because of insufficient signal quality in subsequent measurements to calculate the ODR.

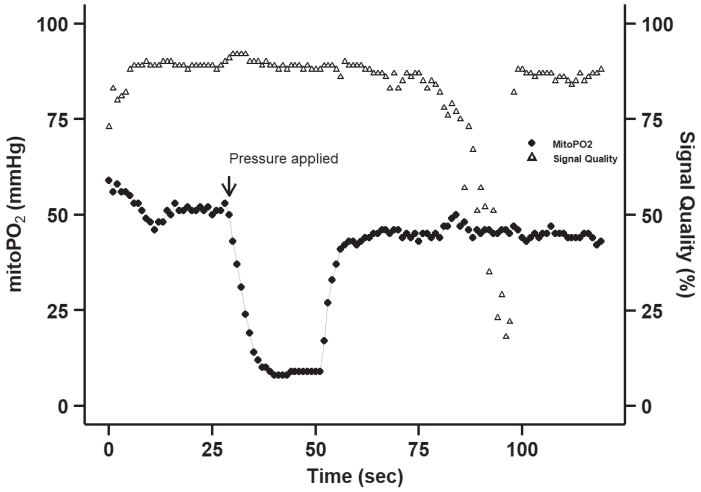

Figure 2. An example of mitoPO$_2$ measurement (black) and signal quality (blue), before photodynamic therapy session 1. MitoPO$_2$ is 51.2 mmHg calculated as average from the 6 measurement points before pressure is applied to the sensor resulting in a drop in the mitoPO$_2$.

Illumination session 2

After a 2-hour interval in the dark, to re-accumulate PpIX, one patient regained a signal, the mitoPO$_2$ increased further to 86.3 [41.8-164.1] mmHg *n*=6 before the second PDT illumination. It decreased to 60.0 [30.0-82.7] mmHg, *n*=3. The signal quality started with a median 10.4 [0-20.15]% what is 40% lower compared to the start illumination 1. In 5 patients the signal quality after session 2 was too low to measure mitoPO$_2$ and resulted in a median 0 [0-10]%. The ODR after the 2h dark period was 6.6 [5.4-8.1] mmHg/s, and decrease to 1.4 [0.7-5.7] mmHg/s. An overview is given in Figure 3.

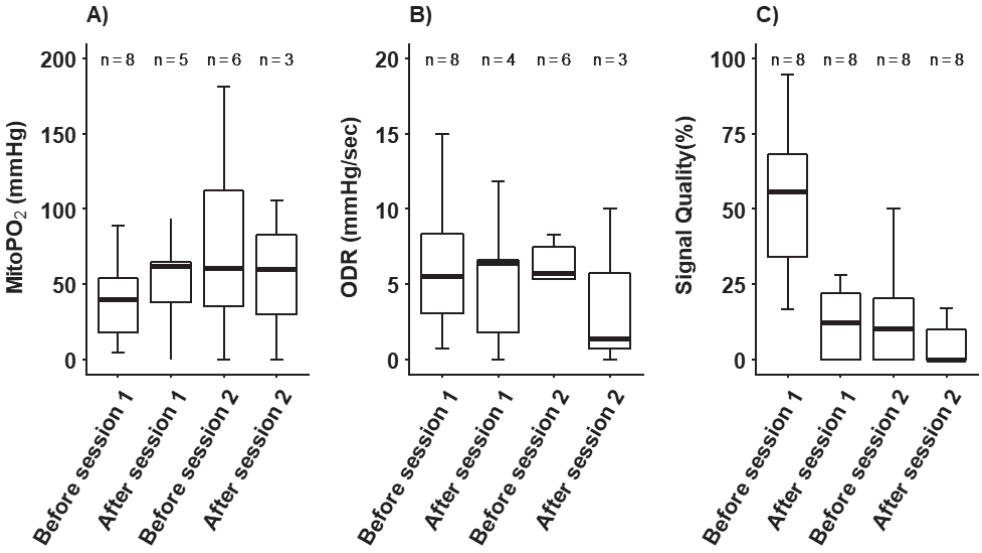

Figure 3. A) Oxygen availability in the lesion (*MitoPO$_2$).* B) Oxygen disappearance rate. C) Signal quality

Measurement sensation

Subjects were asked to report the sensation after the measurement with COMET specific. Time points before the illumination session tend to be close to zero VAS median with IQR 1.5 [0.6-3.5], VAS-scores afterwards have the tendency to be higher 2.3 [0.9-9.7]. Before session 2 it was lower compared to session 1 VAS 1.6 [0.6-1.6] and after the PDT session VAS 1.9 [1.2-2.6]. It was hard for the subjects to distinguish between the pain felt after the PDT session and during the COMET measurement itself, an overview can be found in Figure 4. Photographs of the lesions before the first and after the second PDT session are seen in Figure 5.

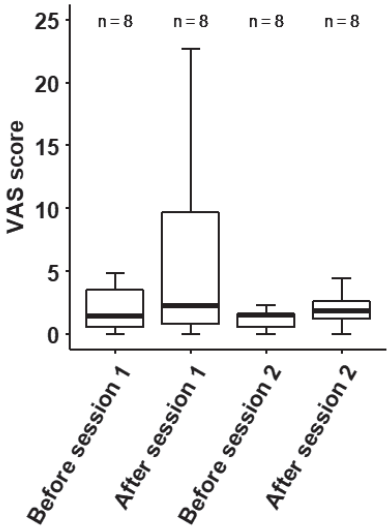

Figure 4. From 9 included patients 8 reported pain sensation with the Visual Analogue Scale from 0 (no pain) to 100 (worse pain ever felt).

Typical finding

One of the measurements had a typical finding showing that the oxygen availability was 0 mmHg after the usage of an anesthetic lidocaine with adrenaline. In session 1 so much pain was experienced that the patient asked for an anesthetic. Before and after the PDT session with an adequate signal quality, 0 mmHg mitoPO_2 was measured, seen in Figure 6.

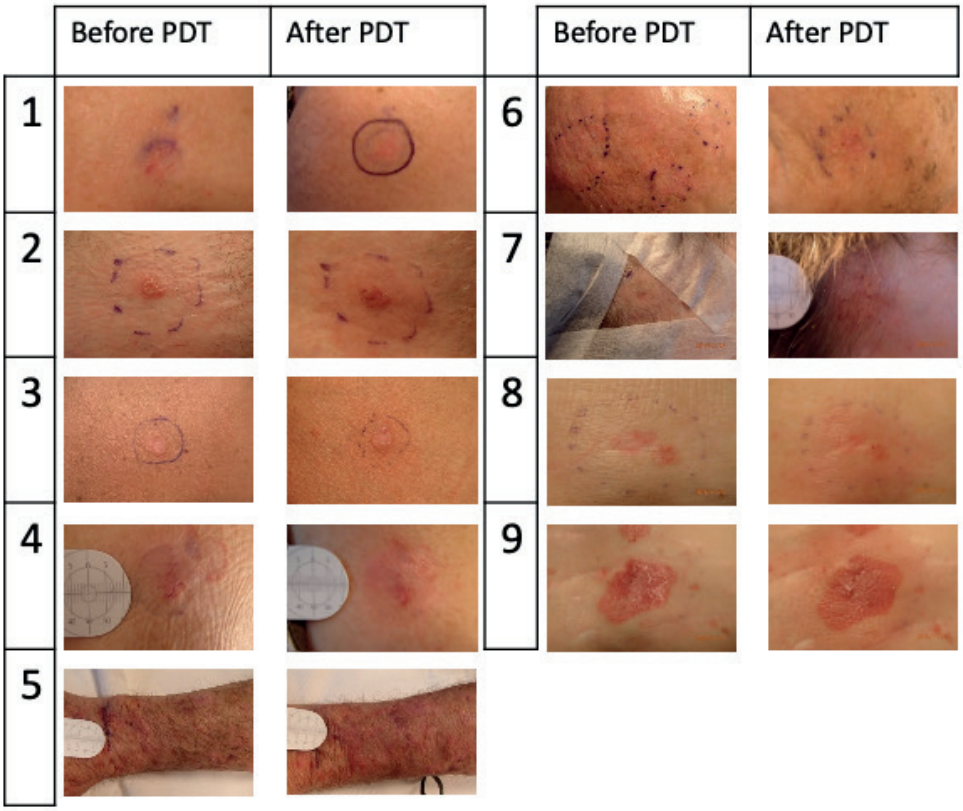

Figure 5. Photograph before photo dynamic therapy (PDT) and after illumination.

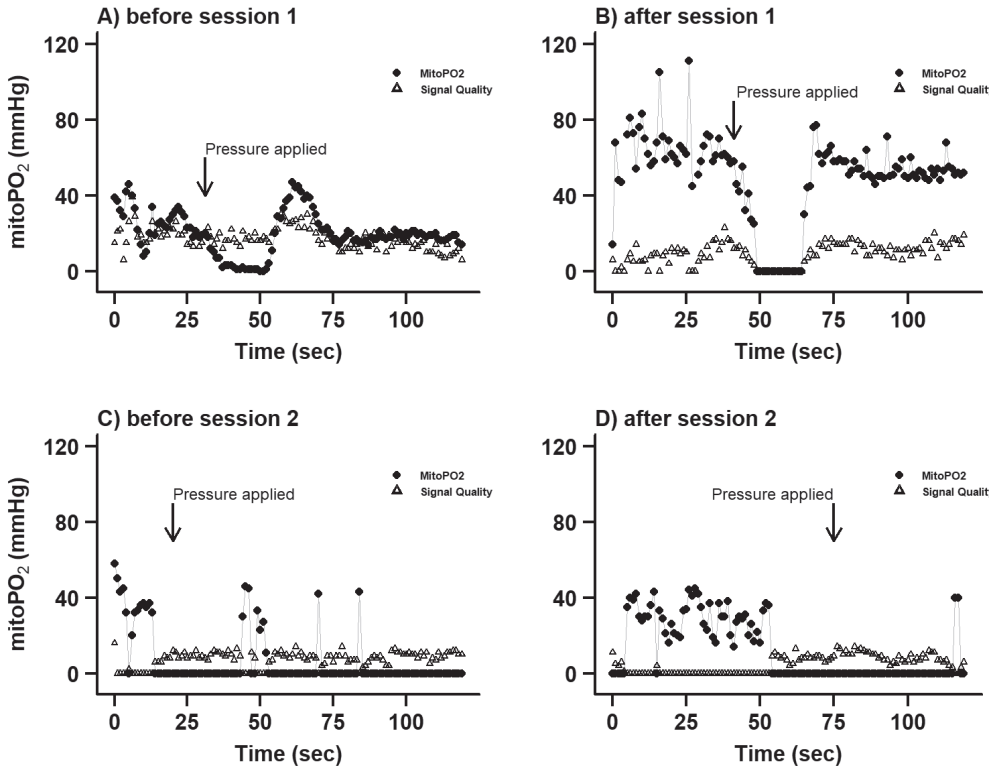

Figure 6. A) Before session 1 an oxygen disappearance curve is seen. After 30 seconds pressure was applied on the probe and released after 25 seconds. This occludes the microcirculation and results in a drop of mitoPO$_2$. After skin sensor release an influx of oxygen is seen with an overshoot, stabilizing after 10 seconds. B) After session 1 an increase in overall mitoPO$_2$ is seen. After the 2-hour dark period session 2 started, because of extreme pain session 1 an anesthetic (lidocaine + adrenaline) was used. C) Before session 2, 0 mmHg mitoPO$_2$ was measured. D) After session 2 searching for the correct lesion location with adequate signal quality 0 mmHg was measured.

Discussion and Conclusion

This study was designed to explore the usability of COMET during ALA-PDT. For the mitochondrial oxygen availability measurement, a sufficient conversion of ALA in PpIX is necessary to get an adequate delayed fluorescence signal. The signal quality before ALA-PDT was sufficient to determine the mitoPO$_2$ and ODR adequately.

Before session one, eight patients were measured with COMET. The use of COMET in a non-air-conditioned room during summer with high humidity led to occasional laser miss fire of the excitation light source in the COMET device.

Before the illumination session the signal quality was sufficient for every patient to measure reliable mitoPO$_2$. After session one an increase of mitoPO$_2$ was seen. In the majority of cases

the signal quality decreased drastically after the PDT illumination and resulted in non-reliable measurements. It was expected that the signal quality would decrease after PDT sessions because of PpIX photobleaching and photodegradation of PpIX [22].

One of the main mechanisms of PDT is the utility of oxygen conversion into reactive oxygen species that leads to apoptosis and necrosis. Therefore, we expected that the oxygen would be depleted after an illumination phase. Surprisingly, the median oxygen availability increased after the first PDT session. This is likely the result of the delay between the illumination stop and the mitoPO_2 measurements. The inflow of oxygen into the microcirculation is in order of seconds and could occur right after the stop and is reflected in the increased mitoPO_2 after session 1. To substantiate this theory, the skin was macroscopically erythematous after the session, which is a consequence of vasodilatation and increased blood flow.

Extensive pain is one of most severe and most often reported side effects during PDT treatment. All patients experience some discomfort or even unbearable pain during the PDT. VAS scores found for PpIX PDT were $\geq$ 70 in 58% of the cases [23] and in 85% of the cases reported by Piffaretti et al. [24], in comparison the COMET did not induce any significant pain sensation with a median VAS of 1.5 and 1.6 seen in Figure 4. Bias is introduced in the VAS-score after a PDT session because it was hard to distinguish between the pain felt from the ALA-PDT and the oxygen measurement. Therefore the VAS scores after the treatment were higher compared to pre-PDT sessions, but still negligible compared to the pain felt during PDT.

One patient that started with a low mitoPO_2 stood out, due to extreme pain during the photodynamic session. No measurements were done after the first session and the second session was not started. These low mitoPO_2 (<10 mmHg) values were not seen in any other measured subject, maybe the initial low oxygen and the fast usage of all the oxygen have led to nerve signaling with a pain sensation. A second interesting case was the use of lidocaine with adrenaline shown in Figure 6. After using the anesthetic with an adequate signal quality 0 mmHg oxygen availability was measured. It is likely that due to vasoconstriction of the adrenaline a small amount of oxygen enters the lesion and is consumed right away. Therefor results in 0 mmHg, since PDT efficacy is oxygen dependent, this may negatively influence the PDT treatment effectiveness.

The application of the 20% ALA-gel 4 hours before the PDT treatment was done proportional to the lesion size. Most lesions measured a few millimeters in diameter. Therefore, the measurement location was also a few mm^2 in size. The skin sensor head of COMET is not designed for such small lesions. A high signal quality indicated the head was positioned

properly. It was hard to find location with good signal quality with on these small lesions, and when found, to measure and hold the Skin Sensor steady in position.

A smaller skin sensor, steady secured, over the lesion would increase the reproducibility of the measurements. It is known that the mitoPO_2 is heterogenic distributed in the skin surface so not the exact same volume of cells is measured before and after the PDT treatment [16, 25].

Clearly in the data is seen that the signal quality is dramatically decreased after a PDT session. This is expected because the red-light illumination during PDT will use all the available PpIX and will also bleach and destroy the PpIX ring integrity.

Over the years several mechanisms have been developed to improve PDT and implement a form of individual dosimetry. Singlet oxygen measurement, oxygen phosphorescence with palladium porphyrin, and photobleaching are a few examples of this [2, 24, 26].

One of the potential clinical improvements for PDT with COMET is dosimetry with oxygen availability feedback mechanism. The PDT treatment depends mainly on the creation reactive oxygen. The COMET could provide feedback to ensure enough oxygen inflow in the lesion. This may improve the individual PDT dosimetry and therefore outcomes [10, 27–29].

Recently a pilot has been published by Scholtz et al. (2020) that uses a delayed fluorescence imaging system during ALA-PDT to detect mitochondrial oxygen tension in tumors in mice. It showed that oxygen is tumors is heterogenous, and that the redistribution of oxygen in the lesion after a light dosage of 5J/cm^2 can take up to 10-60 min. Furthermore the study showed that the oxygen depletion rate was dependent on the PpIX concentration, which in itself was heterogenous distributed in the lesions [11].

Photobleaching-based PDT dosimetry is a technique to provide dosimetry feedback. It can be used when sufficient or a high concentration of O_2 is available. Especially with low oxygen concentrations, this approach becomes unreliable and is therefore not practical in clinical PDT dosimetry [30].

Another technique to evaluate PDT dosimetry is photon count from $^1O_2$ singled oxygen luminescence (SOL). It is stated that the amount SOL is related to the cell toxicity [2]. Unfortunately, this technique is costly, complex and measures a very weak signal, therefore it is unlikely to be clinically available in the short term. This technique showed that if the illumination is increased and the oxygen availability depleted no extra apoptosis will be induced. Rather a time in the dark to reintroduce oxygen in the lesion, is beneficial for lesion apoptosis [2].

An existing well-known technique to measure intravascular oxygen tension, is the phosphorescence technique with palladium porphyrin, introduced in PDT over 2 decades ago [26]. The phosphorescence lifetime is detectable besides the fluorescence of the PpIX and can be used simultaneously with the PDT illumination. A drawback of this technique is the extra infusion of potential toxic metalophorphyrin in the bloodstream. Second compared to mitoPO$_2$ the vascular compartment is measured, instead of the intra cellular compartment where its used.

In conclusion, the COMET measurement system can be used in ALA photodynamic therapy to measure *in vivo* mitochondrial oxygen concentration. Signal quality was adequate in all patients before the PDT session started. Afterwards the signal quality was drastically decreased. It was safely applicable; in small lesions it was hard to perform steady measurements, because of a large skin sensor in comparison. Since only a small number of patients was included for this pilot, no conclusions could be drawn about the relationship between mitoPO$_2$ and clinical outcome.

It is recommended to further look into the oxygen availability and the treatment effect of PDT. A study should be designed to compare the illuminated area with a non-illuminated area. Small intermittent stops could be introduced in the PDT illumination to evaluate the oxygen concentration. This may act as a feedback loop to further recuperates oxygen into the lesion in the dark intermittent phase. This may individualize treatment per lesion or individual. After this exploration this may open a new monitoring tool for PDT to deliver personal and lesion-specific light dosimetry guided by oxygen delivery in the lesion.

References

1. Schmidt R (2006) Photosensitized generation of singlet oxygen. Photochem Photobiol 82:1161–1177. https://doi.org/10.1562/2006-03-03-IR-833
2. Jarvi MT, Patterson MS, Wilson BC (2012) Insights into photodynamic therapy dosimetry: simultaneous singlet oxygen luminescence and photosensitizer photobleaching measurements. Biophys J 102:661–71. https://doi.org/10.1016/j.bpj.2011.12.043
3. van der Snoek EM, Robinson DJ, van Hellemond JJ, Neumann HAM (2008) A review of photodynamic therapy in cutaneous leishmaniasis. J Eur Acad Dermatol Venereol 22:918–22. https://doi.org/10.1111/j.1468-3083.2008.02805.x
4. Drucker AM, Adam GP, Rofeberg V, et al (2018) Treatments of Primary Basal Cell Carcinoma of the Skin: A Systematic Review and Network Meta-analysis. Ann Intern Med 169:456–466. https://doi.org/10.7326/M18-0678
5. Dolmans DEJGJ, Fukumura D, Jain RK (2003) Photodynamic therapy for cancer. Nat Rev Cancer 3:380–387. https://doi.org/10.1038/nrc1071
6. Oleinick NL, Morris RL, Belichenko I (2002) The role of apoptosis in response to photodynamic therapy: what, where, why, and how. Photochem Photobiol Sci 1:1–21. https://doi.org/10.1039/b108586g
7. Plaetzer K, Krammer B, Berlanda J, et al (2009) Photophysics and photochemistry of photodynamic therapy: fundamental aspects. Lasers Med Sci 24:259–68. https://doi.org/10.1007/s10103-008-0539-1
8. De Haas ERM, Kruijt B, Sterenborg HJCM, et al (2006) Fractionated illumination significantly improves the response of superficial basal cell carcinoma to aminolevulinic acid photodynamic therapy. J Invest Dermatol 126:2679–2686. https://doi.org/10.1038/sj.jid.5700460
9. Busch TM (2006) Local physiological changes during photodynamic therapy. Lasers Surg Med 38:494–9. https://doi.org/10.1002/lsm.20355
10. Piffaretti F, Novello AM, Kumar RS, et al (2012) Real-time, in vivo measurement of tissular pO_2 through the delayed fluorescence of endogenous protoporphyrin IX during photodynamic therapy. J Biomed Opt 17:115007. https://doi.org/10.1117/1.jbo.17.11.115007
11. Scholz M, Petusseau AF, Gunn JR, et al (2020) Imaging of hypoxia, oxygen consumption and recovery in vivo during ALA-photodynamic therapy using delayed fluorescence of Protoporphyrin IX. Photodiagnosis Photodyn Ther 30:101790. https://doi.org/10.1016/j.pdpdt.2020.101790
12. Gardner LC, Smith SJ, Cox TM (1991) Biosynthesis of delta-aminolevulinic acid and the regulation of heme formation by immature erythroid cells in man. J Biol Chem 266:22010–8
13. Gardner LC, Cox TM (1988) Biosynthesis of heme in immature erythroid cells. The regulatory step for heme formation in the human erythron. J Biol Chem 263:6676–82
14. Mik EG, Stap J, Sinaasappel M, et al (2006) Mitochondrial PO_2 measured by delayed fluorescence of endogenous protoporphyrin IX. Nat Methods 3:939–45. https://doi.org/10.1038/nmeth940
15. Mik EG, Stap J, Sinaasappel M, et al (2006) Mitochondrial PO_2 measured by delayed fluorescence of endogenous protoporphyrin IX. Nat Methods 3:939–45. https://doi.org/10.1038/nmeth940
16. Mik EG (2013) Special article: measuring mitochondrial oxygen tension: from basic principles to application in humans. Anesth Analg 117:834–46. https://doi.org/10.1213/ANE.0b013e31828f29da
17. Ubbink R, Bettink MAW, Janse R, et al (2017) A monitor for Cellular Oxygen METabolism (COMET): monitoring tissue oxygenation at the mitochondrial level. J Clin Monit Comput 31:1143–1150. https://doi.org/10.1007/s10877-016-9966-x

18. Ibbotson SH (2011) Adverse effects of topical photodynamic therapy. Photodermatol Photoimmunol Photomed 27:116–130. https://doi.org/10.1111/j.1600-0781.2010.00560.x

19. Harms FA, Bodmer SIA, Raat NJH, Mik EG (2015) Cutaneous mitochondrial respirometry: non-invasive monitoring of mitochondrial function. J Clin Monit Comput 29:509–519. https://doi.org/10.1007/s10877-014-9628-9

20. Harms F, Stolker RJ, Mik E (2016) Cutaneous Respirometry as Novel Technique to Monitor Mitochondrial Function: A Feasibility Study in Healthy Volunteers. PLoS One 11:e0159544. https://doi.org/10.1371/journal.pone.0159544

21. R Core Team (2017) R: A Language and Environment for Statistical Computing.

22. Valentine RM, Ibbotson SH, Brown CTA, et al (2011) A quantitative comparison of 5-Aminolaevulinic acid- and methyl aminolevulinate-induced fluorescence, photobleaching and pain during photodynamic therapy. Photochem Photobiol. https://doi.org/10.1111/j.1751-1097.2010.00829.x

23. Middelburg TA, Nijsten T, Neumann MHA, et al (2013) Red light ALA-PDT for large areas of actinic keratosis is limited by severe pain and patient dissatisfaction. Photodermatol Photoimmunol Photomed 29:276–8. https://doi.org/10.1111/phpp.12055

24. Piffaretti F, Zellweger M, Kasraee B, et al (2013) Correlation between protoporphyrin IX fluorescence intensity, photobleaching, pain and clinical outcome of actinic keratosis treated by photodynamic therapy. Dermatology 227:214–225. https://doi.org/10.1159/000353775

25. Mik EG, Johannes T, Zuurbier CJ, et al (2008) In vivo mitochondrial oxygen tension measured by a delayed fluorescence lifetime technique. Biophys J 95:3977–90. https://doi.org/10.1529/biophysj.107.126094

26. McIlroy BW, Curnow A, Buonaccorsi G, et al (1998) Spatial measurement of oxygen levels during photodynamic therapy using time-resolved optical spectroscopy. J Photochem Photobiol B Biol 43:47–55. https://doi.org/10.1016/S1011-1344(98)00081-5

27. Thompson MS, Johansson A, Johansson T, et al (2005) Clinical system for interstitial photodynamic therapy with combined on-line dosimetry measurements. Appl Opt 44:4023–31. https://doi.org/10.1364/ao.44.004023

28. Zhu TC, Finlay JC (2008) The role of photodynamic therapy (PDT) physics. Med Phys 35:3127–36. https://doi.org/10.1118/1.2937440

29. van Veen RLP, Robinson DJ, Siersema PD, Sterenborg HJCM (2006) The importance of in situ dosimetry during photodynamic therapy of Barrett's esophagus. Gastrointest Endosc 64:786–8. https://doi.org/10.1016/j.gie.2006.06.056

30. Dysart JS, Singh G, Patterson MS (2005) Calculation of singlet oxygen dose from photosensitizer fluorescence and photobleaching during mTHPC photodynamic therapy of MLL cells. Photochem Photobiol 81:196–205. https://doi.org/10.1562/2004-07-23-RA-244

Chapter 6

Effects of red cell transfusion on mitochondrial oxygen tension in chronic anemia patients: a pilot study

Rinse Ubbink[1], Lucia W.J. M. Streng[1], Nicolaas J.H. Raat[1], Floor A. Harms [1], Peter. A.W te Boekhorst[2], Robert J Stolker[1], Egbert.G. Mik[1]

[1] Department of Anesthesiology, Erasmus MC - University Medical Center Rotterdam, Rotterdam, The Netherlands
[2] Department of Hematology, Erasmus MC - University Medical Center Rotterdam, Rotterdam, The Netherlands

Submitted for publication
Haemotologica

Abstract

In light of the associated risks, the question has been raised if the decision to give a blood transfusion should solely be based on hemoglobin level. As mitochondria are the final destination of oxygen transport, mitochondrial parameters are suggested to be of added value. The aim of this pilot study was to investigate the effect of a red blood cell transfusion on mitochondrial oxygenation as measured by the COMET device in chronic anemia patients. To correct for the effect of volume load on mitochondrial oxygenation, a red blood cell transfusion and a saline infusion were given in random order. 21 patients were included, of which 12 participated twice. If patients participated twice, the order of infusion was reversed. In both the measurements wherein a blood transfusion was given first and wherein 500 ml of 0.9% saline was given first, median mitochondrial oxygen tension decreased after red blood cell transfusion. This can either be explained by compensation of the patients, because of the chronic nature of their disease or the timing of the measurements. Potentially, the effect of the red blood cell transfusion cannot be seen during or directly after the transfusion, but hours later. The results of this study have strengthened the need for further research into the effect of blood transfusion tissue oxygenation and the potential role for mitochondrial parameters herein.

Introduction

Since 98% of oxygen in the blood is bound by hemoglobin, red blood cells constitute the cornerstone of oxygen transport from the alveoli in the lungs to the tissue of the entire body [1]. In the cells, mitochondria use the oxygen for oxidative phosphorylation to create adenosine triphosphate (ATP). This oxygen-dependent process is highly efficient in generating ATP. In comparison, anaerobic glycolysis results in 88 % less ATP per glucose molecule [2]. Therefore, a reduced level of red blood cells, or anemia, compromises metabolic capacity and the processes depending upon it.

Anemia can be restored by administering a red blood cell transfusion (RBCT). However, a RBCT has various risks. These may involve blood-transmitted bacterial or viral pathogens, immunological reactions such as an acute hemolytic reaction or acute lung injury related to transfusions (TRALI), hemodynamic or electrolyte disorders, or simply administration of the wrong product through human error [3]. It follows that a RBCT should only be given to patients for whom the benefits outweigh the risks [4].

Currently, the decision to transfuse erythrocytes in most clinical cases is mainly based on a level of hemoglobin specified as a transfusion trigger. To prevent unnecessary RBCT, studies have compared the effects of transfusion trigger levels, with particular attention to differences between liberal (9.0 g/dL to 10.0 g/dL) or restrictive (7.0 g/dL) transfusion triggers [5–8]. Nevertheless, finding a 'one size fits all' hemoglobin level below which blood transfusion is beneficial remains difficult [9,10]. Consequently, the question has been raised whether the decision for RBCT should be based on hemoglobin level alone [11].

In the efforts to find a patient-based transfusion trigger, the focus has been shifted towards oxygen delivery and consumption. To investigate this possibility of more personalized transfusion medicine, studies have suggested the measurement of tissue oxygenation (StO_2) using near-infrared spectroscopy (NIRS) [12–14]. Although multiple studies have reported a positive correlation between hemoglobin and StO_2, the results are inconclusive and hampered by lack of a gold standard StO_2 value for standardization [11,15,16].

Considering that mitochondria are the final destination for oxygen, mitochondrial oxygenation tension ($mitoPO_2$) measurement can theoretically give essential information about the adequacy of oxygen delivery capacity and the occurrence of cellular hypoxia. $MitoPO_2$ can be measured non-invasively by the COMET device (Photonics Healthcare BV, Utrecht, the Netherlands) which employs the protoporphyrin IX triplet state lifetime technique [17]. The PpIX-TSLT is based on the delayed fluorescent properties of protoporphyrin IX. To stimulate the synthesis of endogenous mitochondrial PpIX through the conversion of 5-aminolevulinic

acid (ALA) an ALA plaster (Alacare, Photonamic GmbH und Co.KG. Pinneberg, Germany) has to be applied to the skin for several hours. After subsequent excitation with light, the accumulated protoporphyrin IX emits a delayed red fluorescence. The delayed fluorescence lifetime is oxygen-dependent. Short lifetimes resemble high partial oxygen pressure and long lifetimes resemble low oxygen pressure [18].

The potential of monitoring mitoPO_2 as an early detection method for adequate oxygen delivery capacity has been highlighted in the pre-clinical study by Römers et al. in 2016. Both StO_2 using NIRS and mitoPO_2 were measured in pigs during a hemodilution protocol. Whereas mitoPO_2 showed a decrease preceding the decline of hemodynamic parameters and rise of lactate, NIRS values remained stable even though ischemia occurred [19].

The aim of this pilot study is to explore the effect of RBCT on oxygenation at a mitochondrial level. To this end, the effect of RBCT on mitoPO_2 is investigated in chronic anemia patients before, during, and after transfusion. To account for the effects of volume load, the patients will first receive a blood transfusion followed by saline infusion or vice versa. The hypothesis is that mitoPO_2 will increase after RBCT and not after saline infusion in anemic patients, provided the patient is not hypovolemic.

Methods

This single-center pilot study was performed at Erasmus Medical Center (EMC) in Rotterdam, The Netherlands. The protocol was approved by the Institutional Research Board of the EMC and registered in the CCMO register (NL55664.078.15). Written informed consent was obtained from all patients.

Eligible patients were above 18 years of age and either presented with clinical symptoms related to a low Hb level or had a Hb level below 4.0 – 5.5 mmol/L, depending on their age (<4.0 mmol/L for patients below 25 years of age, <5.5 mmol/L for patients aged above 70 years of age). Exclusion criteria consisted of intellectual disability, porphyria, hemoglobinopathy or heart- or kidney failure with fluid restriction.

PpIX-TSLT technique

In-depth detail of the method to calculate mitochondrial oxygen tension from PpIX delayed fluorescence can be found in Mik et al [18,20]. Additional information on the implementation of the technique into a clinical monitor and a detailed description of the COMET device have been described by Ubbink et al [17].

Procedures

An ALA plaster was applied to the sternum at least four hours before the measurements. In order to account for a potential effect of fluid responsiveness, the RBCT was given before or after infusion of 500 ml of 0.9% saline. The order of the RBCT and fluid challenge was decided using sealed envelopes opened on the measurement day. A patient could participate twice; in that case, the sequence was reversed for the second measurement. The volume of transfused RBC units was decided by the hematologist and varied between 270 to 870 ml. Neither the erythrocytes nor the saline were warmed prior to infusion, as per local protocol.

Data analysis

The primary study parameter was mitoPO$_2$ (kPa) as measured by the COMET device. The secondary study parameters included hemodynamic parameters and RBC age. As this was a pilot study, no a priori sample size was calculated. The IRB agreed on 16 inclusions per group.

Data was tested for normality with Shapiro-Wilk at every time point. Change in mean mitoPO$_2$ from baseline after RBCT and saline infusion was analyzed using an ANOVA repeated measures test. The pairwise t-test was used for comparison of the primary and secondary parameters. To correct for multiple testing a Bonferroni correction was applied for the α-level. A linear regression model was used to assess the relation between delta mitoPO$_2$ and the age of the given erythrocytes. Data analysis was performed using R statistics [21].

Results

21 patients were enrolled. 12 of these patients were measured on two occasions, whereby one time they first received RBCT or a fluid challenge with saline and the second time vice versa. The other nine either received RBCT or a fluid challenge. From the 33 observations, two measurements were not included in the analysis as a result of insufficient signal quality of the mitoPO$_2$ measurement. This resulted in 31 observations from 20 patients. 50% of the patients were diagnosed with myelodysplastic syndrome or acute myeloid leukemia. Patient characteristics can be seen in Table 1. All patients remained hemodynamically stable throughout the measurements, as can be seen in Table 2.

Table 1. Patient demographics and diagnosis. Values in mean ± sd.

Demographics:	**n=20**
Gender male (%)	*n=14* (70%)
Inpatient (%)	*n*=7 (35%)
Age (years)	63 ± 10
Length (cm)	176 ± 10
Weight (kg)	80 ± 22
Diagnosis (%)	
Myelodysplastic syndrome	*n*=5 (25%)
Acute myeloid leukemia	*n*=5 (25%)
Acute lymphocytic leukemia	*n*=4 (20%)
Primary myelofibrosis	*n*=3 (15%)
Mantle cell lymphoma	*n*=1 (5%)
Sideroblastic anemia	*n*=1 (5%)
Aplastic anemia	*n*=1 (5%)

Table 2: Values during baseline, end of red blood cell transfusion and fluid challenge

	Red blood cell transfusion first				**Fluid challenge first**			
	Baseline	**RBCT**	**FC**	***p***	**Baseline**	**FC**	**RBCT**	***p***
Hb (mmol/L)a	5.0 ± 0.4	-	-		5.0 ± 0.4	-	-	NS
RBCT age (days)b	-	19.1 ± 6.5	-		-	-	19.7 ± 5.4	NS
Body temp (0C)c,d	36.9 [36.7-37.1]	37.0 [36.7-37.5]	36.8 [36.6-37.2]	NS	37.0 [36.7-37.2]	36.8 [36.5-37.2]	36.7 [36.7-37.2]	NS
$SaPO_2$ (%)e	96.8 ± 1.8	97.6 ± 1.6	97.9 ± 1.7	NS	96.6 ± 2.5	96.7 ± 2.5	97.1 ± 2.5	NS
Systolic NIBP (kPa)e	16.2 ± 2.0	17.1 ± 3.3	17.1 ± 2.4	NS	16.2 ± 1.3	16.8 ± 1.7	17.1 ± 1.3	NS
Diastolic NIBP (kPa)e	8.6 ± 1.1	9.6 ± 1.1	9.6 ± 1.4	NS	8.7 ± 1.0	8.9 ± 1.1	9.5 ± 0.9	NS
HR (beats/min)d	69.5 [66.5-88.3]	64.0 [61.8-87.5]	63.0 [62.0-83.5]	NS	71.0 [60.0-77.5]	70.0 [61.0-77.5]	73.0 [57.5-75.5]	NS

FC: Fluid Challenge, Hb: Hemoglobin, HR: Heart rate, NS: Not Significant, NIBP: Non-invasive blood pressure, RBCT: Red blood cell transfusion, $SaPO_2$: Arterial saturation
a Sample t-test, not paired
b RBCT→FC *n*=13, FC-->RBCT *n*=12, sample-t-test not paired
c body temperature, location tympanic
d Kruskal-wallis test, paired true
e. Repeated ANOVA

$MitoPO_2$ after RBCT and fluid challenge

Figure 1. shows an example of the response in $mitoPO_2$ after RBCT followed by a fluid challenge. $MitoPO_2$ was measured with an interval of 1 minute. In resemblance to the overall response of the measurements, $mitoPO_2$ dropped during the RBCT and did not change during the fluid challenge.

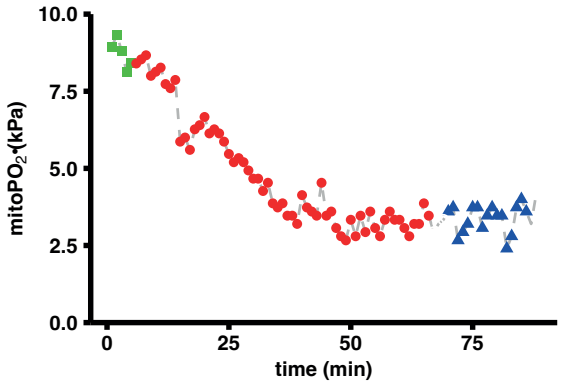

Figure 1. **An example of mitochondrial oxygen tension (mitoPO$_2$) measurements as measured by the COMET monitor (interval in minutes).** The red dots represent the values during red blood cell transfusion and the blue triangles the values during a subsequent fluid challenge (FC). The first five green squares are baseline measurements.

Overall, in the group who received a RBCT first mean mitoPO$_2$ measurements decreased significantly from baseline upon a RBCT (8.07 ± 1.82 kPa to 5.12 ± 1.78 kPa (n=16; p<0.05; mean ± SD)). After the subsequent FC an insignificant rise in mean mitoPO$_2$ to 5.36 ± 1.58 kPa was observed. In the group who started with the fluid challenge followed by the RBCT the mean baseline mitoPO$_2$ was 8.45 ± 3.92 kPa, which slightly decreased to 7.09 ± 2.80 kPa after the fluid challenge. Mean mitoPO$_2$ significantly reduced to 5.08 ± 2.04 kPa after RBCT. The above mentioned results are displayed in figure 2.

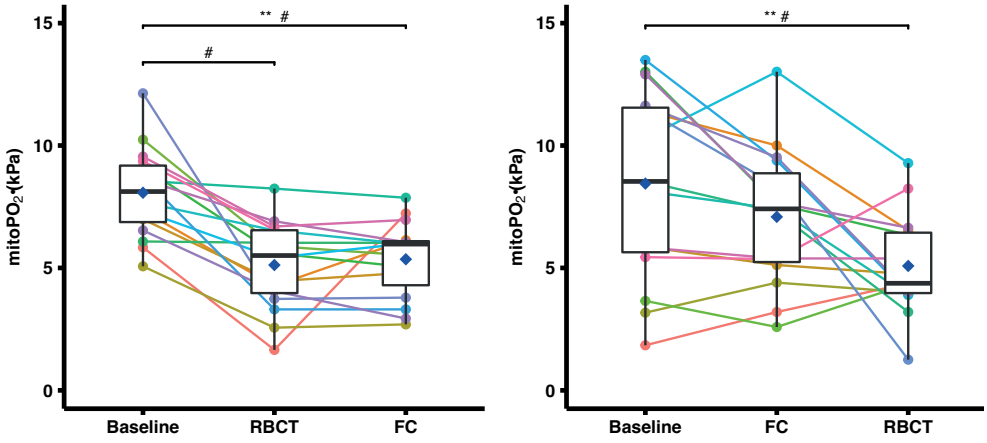

Figure 2. The mitochondrial oxygen tension (mitoPO$_2$) in kPa for each group. Boxplot shows the median in the middle with hinges first and third quartiles (25 and 75% percentiles). Whiskers are min-max values within 1.5*IQR. Lines represent one data sequence per patient. # Pairwise t-test with Bonferroni correction, ** ANOVA repeated measures test, blue diamond is mean value.

Hb level in relation to mitoPO$_2$

No correlation could be found between neither baseline Hb level and baseline mitoPO$_2$ (R^2=0.002, intercept=7,01 kPa, slope=0.25 kPa, p=0.82) nor baseline Hb level and delta mitoPO$_2$ (R^2=0.0002, intercept=-2,88 kPa, slope=0.08 kPa, p=0.94). Delta mitoPO$_2$ was calculated as the change in mitoPO$_2$ value between either baseline and after RBCT or the last part of both the fluid challenge and RBCT, depending on the order in which the fluids were administered. Figure 3 displays the corresponding graphs.

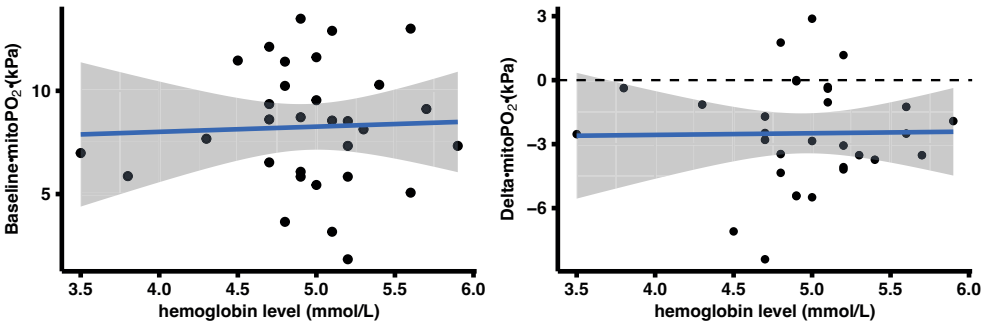

Figure 3. Correlation between baseline hemoglobin level and baseline hemoglobin level. A) Linear regression model (blue line) of the relationship between delta mitoPO$_2$ (dots) and baseline hemoglobin level. **B)** Delta mitoPO$_2$ was calculated as the change in mitoPO$_2$ value between either baseline and after RBCT or the last part of both the FC and RBCT, depending on the order in which the fluids were administered. The gray area is the standard error around the linear model.

Delta mitoPO$_2$ in relation to RBC-unit age

Delta mitoPO$_2$ in relation to RBC-unit age could be analyzed in 25 of the 31 RBCT casus. In the measurements of the group who received a RBCT first, delta mitoPO$_2$ constituted baseline to RBCT and in the measurements group who received a fluid challenge first the difference in mitoPO$_2$ after a fluid challenge and after RBCT.

No correlation could be found between delta mitoPO$_2$ and age for all given erythrocytes R^2=0.02, intercept=-1.87 ∆ kPa decrease, slope=-0.05 ∆ kPa/day, p=0.54, as can be seen in figure 4.

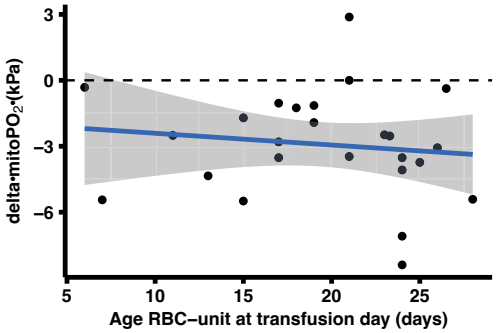

Figure 4. Correlation red blood cell unit age and change in mitochondrial oxygen tension. Linear regression model (blue line) of the relationship between delta mitoPO$_2$ (dots) and age of the administered erythrocytes. Delta mitoPO$_2$ was calculated as the change in mitoPO$_2$ value between either baseline and after RBCT or the last part of both the FC and RBCT, depending on the order in which the fluids were administered. Gray area is the standard error around the linear model.

DISCUSSION

In this pilot clinical study (31 observations) we were able to continuously monitor mitoPO$_2$ during RBCT in chronic anemic patients. Since the goal of a RBCT is to increase tissue oxygenation, the hypothesis was that mitoPO$_2$ would increase after the RBCT, unless mitoPO$_2$ proved to be low as a result of hypovolemia. However, the most prominent effect of RBCT on median mitoPO$_2$ was a decrease. This effect was not seen after infusion of 500 ml of saline.

Potential mechanisms of decreased mitoPO$_2$

The decrease in mitoPO$_2$ after RBCT can be explained by several mechanisms. The first of these is that cell-free plasma hemoglobin may scavenge the important vasodilator nitric oxide (NO) and could decrease microvascular flow due to vasoconstriction in the skin [22–24]. Moreover, the transfused RBCs could be less deformable [25,26] and aggregate in the microcirculation and reduce blood flow [25,27]. Microcirculatory flow could be additionally affected by an alteration in plasma hematocrit ratio (Fahraeus-Lindqvist effect) [28,29].

Finally, 2,3- disphosphoglycerate (2,3-DPG) is a metabolic intermediate that allosterically affects hemoglobin oxygen affinity. After ten days of storage, almost all red blood cell 2,3-DPG is depleted [30], and the oxyhemoglobin dissociation curve has shifted to the left and less oxygen is released to the tissue. As can be seen in figure 5, our analysis revealed no correlation between delta mitoPO$_2$ and the age of all given erythrocytes. This can be explained by the fact that only 2 of the given erythrocyte units were younger than 10 days, implying that in the majority of these units the 2,3-DPG was already depleted.

Yuruk et al. measured thenar and sublingual tissue oxygen saturation with NIRS in chronic anemic patients before and after RBCT and showed a small increase from 81 to 85% [31]. Although the average tissue oxygen saturation increased, the individual patient response was mixed, as was also seen in our results. The fact that the mitoPO$_2$ and NIRS appear to behave differently does not necessarily mean a discrepancy between the studies. NIRS measures mixed vessel Hb saturation levels; therefore, it reflects mainly venous Hb saturation levels. A decreased mitoPO$_2$ in combination with an increased venous oxygen content suggests suboptimal functioning of the microcirculation, and can in particular be explained by shunting.

In 2017 a systematic review by Nielsen et al. reviewed all articles between 1947 and 2017 which measured the effect of RBCT on tissue oxygenation or microcirculatory parameters in patients admitted to the intensive care unit (ICU) [32]. The used techniques included lactic acid measurement, gastric tonometry, NIRS and Sidestream Dark Field Imaging (SDF). The authors concluded that generally, RBCT did not improve the tissue oxygenation or microcirculatory parameters in ICU patients with moderate anemia 4.34 - 6.21 mmol/L (7-10 g/dL) [32]. However, several of the studies also showed that patients with disturbances in tissue oxygenation or microcirculatory parameters did show improvement upon RBCT. For these patients, the pre-transfusion baseline parameters for oxygenation and microcirculatory flow were correlated to the post-transfusion values, suggesting a difference in benefit from RBCT [32].

In our results, we also observed singular cases in which mitoPO$_2$ increased after RBCT in contrast to the overall trend in the rest of the patients. However, we could not link this difference in response to RBCT to baseline hemoglobin level as delta mitoPO$_2$ and baseline hemoglobin level were not correlated. The concept of a critical Hb concentration offers an explanation for this phenomenon. If the critical Hb concentration is reached, compensatory physiological responses to anemia are unable to maintain tissue oxygenation [33]. Further decline in Hb concentration will therefore lead to a decrease in the delivery of oxygen and oxygen consumption [34]. Aside from being patient and disease dependent, the critical Hb can also vary over time as the compensatory responses to anemia may be affected by different comorbidities. This could explain why a part of our cohort demonstrated improved mitochondrial oxygenation after RBCT at the standardized hemoglobin level, whilst the rest did not [33] Moreover, both the observed difference in effect and the concept of critical hemoglobin concentration support the idea that parameters of oxygen delivery, tissue oxygenation and oxygen consumption can provide vital information for RBCT strategies.

Limitations

This study has several limitations. First, this is a pilot study with a sample size of 20 patients and 31 observations. Apart from the overall decrease in mitoPO$_2$, an increase in mitoPO$_2$ of more than 10% upon a RBCT was observed in four patients. As a result of the small sample size and the lack of post-RBCT parameters, however, we cannot clarify whether the difference between increase and decrease in mitoPO$_2$ is associated with an improvement in health complaints, microcirculatory parameters, hemodynamic parameters or laboratory values.

Furthermore, the study population consisted of chronic anemia patients as these patients regularly receive a RBCT at a planned appointment, which enables placement of the ALA plaster four hours before the measurement. However, patients with chronic anemia have had time to physiologically adapt to compensate for the low Hb level and maintain necessary oxygen delivery [35]. This makes it difficult to translate our results to patients with acute anemia.

Lastly, we only measured mitoPO$_2$ before, during and shortly after RBCT. The decrease in mitoPO$_2$ could be a transient effect after which patients mitigate the negative effects of the RBCT. This period could potentially be hours or days. In support of this theory, several patients reported regaining energy after a few days after the RBCT. Future studies should therefore measure over the course of several days.

Conclusion

In this pilot study the effect of RBCT on mitochondrial oxygenation in chronic anemia patients was demonstrated. In contrast with the expectation that the mitoPO$_2$ would increase after a RBCT, mean mitoPO$_2$ decreased after RBCT. The clinical significance of the decrease in mitoPO$_2$ in terms of outcome remains to be elucidated. Our results should be validated in a larger, powered trial. Future research should preferably combine mitochondrial oxygenation and microvascular blood flow measurements, include additional outcome measures. In addition, it should measure over the course of days to investigate if the effect is transient. To conclude, in combination with microvascular parameters, mitochondrial oxygenation measurements provide novel insight into the effect of RBCT on cellular oxygenation. The results of this study encourage the exploration of mitoPO$_2$ as a potential transfusion trigger or means to personalized transfusion medicine.

Reference

1. Rhodes CE, Denault D, Varacallo M. Physiology, Oxygen Transport. Treasure Island (FL).
2. Winslow RM. Oxygen: the poison is in the dose. Transfusion 2013;53(2):424–437.
3. Bolcato M, Russo M, Trentino K, Isbister J, Rodriguez D, Aprile A. Patient blood management: The best approach to transfusion medicine risk management. Transfusion and apheresis science : official journal of the World Apheresis Association : official journal of the European Society for Haemapheresis 2020;59(4):102779.
4. Goodnough LT, Levy JH, Murphy MF. Concepts of blood transfusion in adults. The Lancet 2013;381(9880):1845–1854.
5. Carson JL, Stanworth SJ, Roubinian N, et al. Transfusion thresholds and other strategies for guiding allogeneic red blood cell transfusion. The Cochrane database of systematic reviews 2016;10(10):CD002042.
6. Akyildiz B, Ulgen Tekerek N, Pamukcu O, et al. Comprehensive Analysis of Liberal and Restrictive Transfusion Strategies in Pediatric Intensive Care Unit. Journal of tropical pediatrics 2018;64(2):118–125.
7. Jairath V, Kahan BC, Gray A, et al. Restrictive versus liberal blood transfusion for acute upper gastrointestinal bleeding (TRIGGER): a pragmatic, open-label, cluster randomised feasibility trial. Lancet (London, England) 2015;386(9989):137–144.
8. Møller A, Nielsen HB, Wetterslev J, et al. Low vs high hemoglobin trigger for transfusion in vascular surgery: a randomized clinical feasibility trial. Blood 2019;133(25):2639–2650.
9. Cortés Buelvas A, Buelvas AC. Anemia and transfusion of red blood cells. Cortés BA/ Colombia Médica 2013;44(4):236-242.
10. Refaai MA, Blumberg N. The transfusion dilemma--weighing the known and newly proposed risks of blood transfusions against the uncertain benefits. Best practice & research Clinical anaesthesiology 2013;27(1):17–35.
11. Carson JL, Stanworth SJ, Dennis JA, et al. Transfusion thresholds for guiding red blood cell transfusion. The Cochrane database of systematic reviews 2021;12(12):CD002042.
12. Torella F, Haynes SL, McCollum CN. Cerebral and peripheral near-infrared spectroscopy: an alternative transfusion trigger? Vox sanguinis 2002;83(3):254–257.
13. Leal-Noval SR, Arellano-Orden V, Muñoz-Gómez M, et al. Red Blood Cell Transfusion Guided by Near Infrared Spectroscopy in Neurocritically Ill Patients with Moderate or Severe Anemia: A Randomized, Controlled Trial. Journal of neurotrauma 2017;34(17):2553–2559.
14. Vretzakis G, Georgopoulou S, Stamoulis K, et al. Monitoring of brain oxygen saturation (INVOS) in a protocol to direct blood transfusions during cardiac surgery: a prospective randomized clinical trial. Journal of cardiothoracic surgery 2013;8145.
15. Crispin P, Forwood K. Near Infrared Spectroscopy in Anemia Detection and Management: A Systematic Review. Transfusion medicine reviews 2021;35(1):22–28.
16. Kleiser S, Nasseri N, Andresen B, Greisen G, Wolf M. Comparison of tissue oximeters on a liquid phantom with adjustable optical properties. Biomedical optics express 2016;7(8):2973–2992.
17. Ubbink R, Bettink MAW, Janse R, et al. A monitor for Cellular Oxygen METabolism (COMET): monitoring tissue oxygenation at the mitochondrial level. Journal of clinical monitoring and computing 2017;31(6):1143–1150.
18. Mik EG. Special article: measuring mitochondrial oxygen tension: from basic principles to application in humans. Anesthesia and analgesia 2013;117(4):834–46.

19. Römers LHL, Bakker C, Dollée N, et al. Cutaneous Mitochondrial PO_2, but Not Tissue Oxygen Saturation, Is an Early Indicator of the Physiologic Limit of Hemodilution in the Pig. Anesthesiology 2016;125(1):124–32.
20. Mik EG, Balestra GM, Harms FA. Monitoring mitochondrial PO_2: the next step. Current opinion in critical care 2020;26(3):289–295.
21. R Core Team. R: A Language and Environment for Statistical Computing.
22. Aubron C, Nichol A, Cooper DJ, Bellomo R. Age of red blood cells and transfusion in critically ill patients. Annals of Intensive Care 2013;3(1):2.
23. Lee JS, Gladwin MT. Bad Blood: The risks of red cell storage. Nature Medicine 2010;16(4):381–382.
24. Risbano MG, Kanias T, Triulzi D, et al. Effects of Aged Stored Autologous Red Blood Cells on Human Endothelial Function. American journal of respiratory and critical care medicine 2015;192(10):1223–33.
25. Beutler E, Kuhl W, West C. The osmotic fragility of erythrocytes after prolonged liquid storage and after reinfusion. Blood 1982;59(6):1141–1147.
26. Van Bommel J, de Korte D, Lind A, et al. The effect of the transfusion of stored RBCs on intestinal microvascular oxygenation in the rat. Transfusion 2001;41(12):1515–23.
27. Suzuki Y, Tateishi N, Soutani M, Maeda N. Flow behavior of erythrocytes in microvessels and glass capillaries: effects of erythrocyte deformation and erythrocyte aggregation. International journal of microcirculation, clinical and experimental 1996;16(4):187–94.
28. Fahraeus R. The suspension stability of the blood. Physiological Reviews 1929;9(3):399–431.
29. Fahraeus R, Lindvist T. The viscosity of the blood in narrow capillary tubes. American Journal of Physiology Legacy Content 1931;96(3):562–568.
30. Högman CF, Löf H, Meryman HT. Storage of red blood cells with improved maintenance of 2,3-bisphosphoglycerate. Transfusion 2006;46(9):1543–52.
31. Yuruk K, Bartels SA, Milstein DMJ, Bezemer R, Biemond BJ, Ince C. Red blood cell transfusions and tissue oxygenation in anemic hematology outpatients. Transfusion 2012;52(3):641–646.
32. Nielsen ND, Martin-Loeches I, Wentowski C. The Effects of red Blood Cell Transfusion on Tissue Oxygenation and the Microcirculation in the Intensive Care Unit: A Systematic Review. Transfusion medicine reviews 2017;31(4):205–222.
33. McLellan SA, McClelland DBL, Walsh TS. Anaemia and red blood cell transfusion in the critically ill patient. Blood reviews 2003;17(4):195–208.
34. Shah A, Oczkowski S, Aubron C, Vlaar AP, Dionne JC. Transfusion in critical care: Past, present and future. Transfusion medicine (Oxford, England) 2020;30(6):418–432.
35. Hébert PC, Van der Linden P, Biro G, Hu LQ. Physiologic aspects of anemia. Critical care clinics 2004;20(2):187-212.

Chapter 7

Evaluation of Endoscopic Visible Light Spectroscopy: Comparison with Microvascular Oxygen Tension Measurements in a Porcine Model

Rinse Ubbink, Msc*[1], Louisa J.D. van Dijk, MD*[2,3] Desirée van Noord, MD, PhD[2,4], Tanja Johannes MD, PhD[1], Patricia A. C. Specht, BSc[1], Marco J. Bruno MD, PhD[2], Egbert G. Mik MD, PhD[1,5]

[1]Department of Anesthesiology, Laboratory for Experimental Anesthesiology, Erasmus MC University Medical Center, Rotterdam, the Netherlands
[2] Department of Gastroenterology and Hepatology, Erasmus MC University Medical Center, Rotterdam, the Netherlands
[3]Department of Radiology, Erasmus MC University Medical Center, Rotterdam, the Netherlands
[4]Department of Gastroenterology and Hepatology, Franciscus Gasthuis & Vlietland, Rotterdam, the Netherlands
[5]Department of Intensive Care, Erasmus MC University Medical Center, Rotterdam, the Netherlands

* Both authors contributed equally to this manuscript.
Published in:
Journal of Translational medicine 2019;17:65

Abstract

Background: Visible light spectroscopy (VLS) is a technique used to measure the mucosal oxygen saturation during upper gastrointestinal endoscopy to evaluate mucosal ischemia, however in vivo validation is lacking. We aimed to compare VLS measurements with a validated quantitative microvascular oxygen tension (μPO_2) measurement technique.

Methods: Simultaneous VLS measurements and μPO_2 measurements were performed on the small intestine of five pigs. First, simultaneous measurements were performed at different FiO_2 values (18%-100%). Thereafter, the influence of bile was assessed by comparing VLS measurements in the presence of bile and without bile. Finally, simultaneous VLS and μPO_2 measurements were performed from the moment a lethal dose potassium chloride intravenously was injected.

Results: In contrast to μPO_2 values that increased with increasing FiO_2, VLS values decreased. Both measurements correlated poorly with R^2= 0.39, intercept 18.5, slope 0.41 and a bias of -16%. Furthermore, the presence of bile influenced VLS values significantly (median (IQR)) before bile application 57.5% (54.8-59.0%) versus median with bile mixture of the stomach 73.5% (66.8-85.8), p=$<2.2*10^{-16}$; median with bile mixture of small bowel 47.6% (41.8-50.8) versus median after bile removal 57.0% (54.7-58.6%), p=$<2.2*10^{-16}$). Finally, the VLS mucosal oxygen saturation values did not decrease towards a value of 0 in the first 25 minutes of asystole in contrast to the μPO_2 values.

Conclusions: These results suggest that VLS measures the mixed venous oxygen saturation rather than mucosal capillary hemoglobin oxygen saturation. Further research is needed to establish if the mixed venous compartment is optimal to assess gastrointestinal ischemia.

Key words: visible light spectroscopy, chronic mesenteric ischemia, diagnostics, microvascular oxygen tension measurements

Background

Visible light spectroscopy (VLS) is a technique used to measure the mucosal capillary hemoglobin oxygen saturation based on reflectance spectrophotometry [1]. The mucosal oxygen saturation can be calculated by the marked difference in the absorption spectra of oxygenated and deoxygenated hemoglobin. Endoscopic VLS measurements are performed during upper GI endoscopy [2-4]. As determined previously by van Noord et al., measurements are defined positive for ischemia if the measured saturation is lower than 63% in the antrum of the stomach, lower than 62% in the duodenal bulb and 58% in the descending duodenum [4].

VLS is used in clinical practice in the work-up of the diagnosis of chronic mesenteric ischemia (CMI). CMI is defined as ischemic symptoms caused by insufficient blood supply to the gastrointestinal (GI) tract [5]. The main cause of CMI is stenosis of one or more mesenteric arteries due to atherosclerosis [6]. Other occlusive causes are external compression of the celiac artery and/or celiac ganglion by the median arcuate ligament and diaphragmatic crura (median arcuate ligament syndrome (MALS)) and mesenteric artery stenosis due to vasculitis. However, CMI can exist in the absence of mesenteric artery stenosis. Non-occlusive mesenteric ischemia (NOMI) is caused by hypo-oxygenation due to underlying conditions such as cardiac and pulmonic insufficiency, spasms of small arteries, shunts, occlusion of smaller arteries e.g. by micro-emboli, and autonomic dysfunction [7].

The diagnosis of CMI is a clinical challenge because of the diverse presentation of CMI. Symptoms overlap largely with many other disorders and the high prevalence of asymptomatic mesenteric artery stenosis in the general population of (3-29% [8, 9]) due to the existence of an extensive collateral circulation. However, mesenteric artery stenosis can become symptomatic if this collateral circulation is not sufficient and/or the extent of the stenosis becomes significant. Accurate identification of patients with CMI is important to select those patients who will benefit of therapy, but to withhold invasive therapy from those who will not. Treatment consists of endovascular revascularization with expandable metal stents or surgical revascularization of obstructed vessels, both methods that are invasive, costly and not without side-effects. A functional test to determine mucosal ischemia of the GI tract is therefore essential.

In the absence of one specific test for the diagnosis of CMI [10], the diagnosis is established by consensus in a multidisciplinary meeting attended by gastroenterologists, vascular surgeons and interventional radiologists. Symptoms alone do not accurately predict the diagnosis of CMI [7, 11, 12]. Therefore, consensus diagnosis is based on the combination of symptoms, imaging of the mesenteric vasculature and functional assessment of mucosal ischemia with

gastric-jejunal tonometry [13, 14] or VLS [1, 4]. The diagnosis is confirmed if successful therapy results in symptom relief. This method for the diagnosis of CMI has an acceptable diagnostic yield [15] and this method is excepted in absence of a gold standard test [10].

Endoscopic mucosal oxygen saturation measurements with VLS are already used in clinical practice to evaluate CMI, however no extensive validation studies have been performed for this intended use. In the current study, VLS mucosal oxygen saturation is compared with a validated microvascular oxygen tension (μPO_2) measurement technique [16, 17].

The microvascular oxygen tension technique used in this study is a Palladium (Pd) porphyrin phosphorescence lifetime technique that measures oxygen tension, introduced by Van der Kooi at the end of the 1980s [18]. Palladium porphine (Pd-porphyrin) bound to albumin, has become a standard phosphorescent dye for μPO_2 measurements *in vivo* [16, 17]. This quantitative measurement is also located in the microcirculation making it a convenient comparison to mucosal oxygen saturations measured with VLS.

The objective of this study was to validate the VLS technique. This validation consisted of 3 experiments in a porcine model: 1) comparison of VLS mucosal oxygen saturation and μPO_2 measurements at different levels of FiO_2, 2) VLS mucosal oxygen saturation measurements in the presence of bile and 3) comparison of VLS mucosal oxygen saturation and μPO_2 measurements during asystole.

Methods

Ethical statement

This study was approved by the local Animal Research Committee of the Erasmus MC University Medical Center in accordance with the National Guidelines for Animal Care and Handling (protocol number DEC 129-13-06 EMC3185). To enhance transparency this article is written according to the ARRIVE guidelines for animal research [19].

Experimental animals

In total, 5 female crossbred Landrace x Yorkshire pigs, with mean body weights of 28.1±0.6 kg (mean±standard error of mean), age 2-3 months were used for the experiments. Sample size calculation determined that 5 animals were sufficient to detect a difference of at least 5% in mucosal saturation measured with VLS before and after bile per location with an alpha of 0.05 and a power of 90% [20].

Experimental procedures

After an overnight fast with free access to water, the animals were sedated with an intramuscular injection of tilatamine/zolazepam (6/6 mg/kg; Virbac Laboratories, Carros, France), xylazine (2 mg/kg; AST Farma B.V., The Netherlands) and atropine sulfate (0.5 mg/animal; Centrafarm Services BV, Etten-Leur, The Netherlands). After a 15 min induction period, anesthesia was induced with tilatamine/zolazepam (50-100 mg/animal) through a cannula (20G Venflon (Becton, Dickinson and Company, USA) in an auricular vein. Tracheal intubation was performed with a size 7.0 Portex® endotracheal tube (Smiths Medical International Ltd., United Kingdom). For maintenance of anesthesia, the animals received continuous infusion of ketamine (5 mg kg^{-1} h^{-1}; Alfasan Nederland B.V., The Netherlands), midazolam (1.5 mg kg^{-1} h^{-1}; Atavis Group PCT, Iceland), sufentanil (4 μg kg^{-1} h^{-1}; Janssen-Cilag B.V., The Netherlands), and rocuroniumbromide (4 mg kg^{-1} h^{-1}; Fresenius Kabi Austria GmbH, Austria). All animals received 500 ml of colloid solution (Voluven®; Fresenius Kabi AG, Germany) at start and a continuous infusion of crystalloid (Sterofundin® ISO 10 ml kg^{-1} h^{-1}; B. Braun, Germany). Each pig received a bolus of magnesium sulfate (500 mg; Pharmachemie BV, Haarlem, The Netherlands), as arrhythmia prophylaxis, added to the first bag of crystalloid solution. To prevent infections during the experiment, Cefazolin (1000 mg/animal; Kefzol ® EuroCept BV, Ankeveen, The Netherlands), an antibiotic used for the treatment of a widespread of bacteria was given intravenous.

Pressure-controlled mechanical ventilation (Servo 300; Siemens-Elema, Solna, Sweden) was performed with a FiO_2 between 24% and a positive end-expiratory pressure of 5 cmH_2O while no intervention was done. Normothermia, measured nasal, was maintained between 38° and 39°C, with two heating pads underneath and an electric heating blanket above the animal. Furthermore, hearth rate, MAP, SpO_2 and temperature were monitored continuously throughout the entire experiment. Arterial blood samples were collected to determine the arterial oxygen pressure and arterial oxygen saturation (ABL 800Flex (Radiometer, Denmark).

A 4Fr thermodilution catheter (Pulsion Medical Systems AG München, Germany) was placed in the left femoral artery for arterial blood sampling. An 9Fr introducer sheath (Arrow International Inc., USA) was placed in the right jugular vein for infusion of palladium porphyrin. Both catheters were placed using the Seldinger technique. A lower midline abdominal incision was made to insert a cystostomy tube into the urinary bladder with purse-string sutures for urine collection.

The animals were placed in supine position and an incision was made to open the abdomen. A small intestinal loop was dissected and a small incision was made at the non-vascularized side to expose the intestinal mucosa (Figure 1).

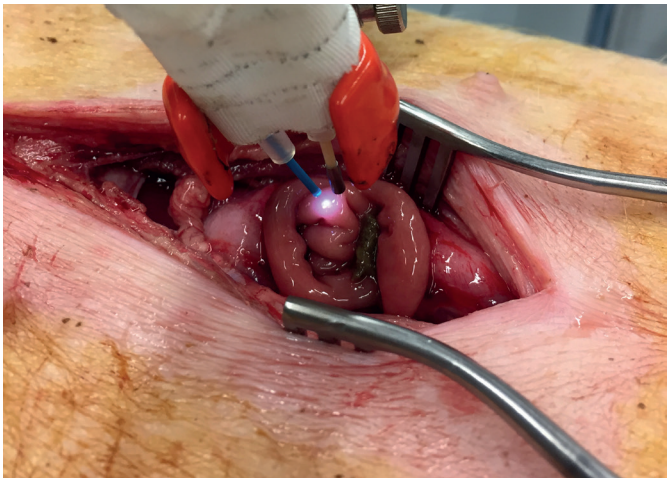

Figure 1. Set-up of the experiment of the VLS-probe (blue) and the μPO_2 probe fixated together positioned 1 to 5 mm above the mucosa of the small intestinal loop.

Mucosal oxygen saturation measurements were performed with a fiberoptic probe (Endoscopic T-Stat Sensor; Spectros, Portola Valley, California, USA) connected to the VLS oximeter (T-Stat 303 Microvascular Oximeter, Spectros, Portola Valley, California).

Microvascular oxygen tension measurements were done with oxygen dependent phosphorescent dye palladium porphine (Pd-porphyrin). Palladium porphyrin is a large molecule with optical properties that can absorb energy and react with oxygen. In the absence of oxygen it will release the absorbed energy from an excitation source via phosphorescent light with a specific decay time, i.e. lifetime. The lifetime is related to the amount of oxygen surrounding the Pd-porphyrin described by the Stern-Volmer relation [18]. It has been tested for pH, temperature and diffusivity dependency [17]. Calibration experiments are done and determine the O_2 accuracy of 5% independent of phosphorescence intensity itself [17].

For the laboratory experimental setup of the μPO_2 measurements the excitation source was an Opolette 355-I tunable laser (Opotek, Carlsbad, CA, USA) set to a wavelength of 524nm. An optical fiber developed by TNO and produced by Light Guide Optics was used that would fit through the working channel of a gastroduodenal endoscope. It has one central located excitation fiber with several surrounding detection fibers.

The phosphorescence was collected with a gated micro channel plate photomultiplier tube (MCP-PMT R5916U series, Hamamatsu Photonics, Hamamatsu, Japan). Phosphorescence lifetime analysis was done with a self-written software program in Labview (version 13.0, National Instruments, Austin, TX, USA). For the detailed setup description we refer elsewhere [21].

The probe palladium porphyrin was Pd(II) meso-Tetra (4-carboxyphenyl)porphine (80 mg/animal) (Frontier Scientific, Logan, USA) dissolved in 1ml DMSO and TRIS Trisma® Base (Sigma, St. Louis, MO) was combined with a 4% bovine serum albumin solution solved in phosphate buffered saline. This method has been validated *in vitro* and *in vivo* [17]. Pd-porphyrin bound to albumin, forms a high-molecular-weight complex, confining it mainly to the vascular compartment when infused intravenously.

Both optical fibers were fixated together to perform stable simultaneous mucosal oxygen saturation and μPO_2 measurements of the same mucosal spot of the small intestine (Figure 1).

Mucosal oxygen saturation versus μPO_2 measurements at different FiO_2 values

Simultaneous VLS mucosal oxygen saturation and μPO_2 measurements were performed at different FiO_2 values ranging from 18%-100%. The mucosal oxygen saturation and μPO_2 measurements were simultaneously performed for two minutes at a specific FiO_2 value. When a new FiO_2 value was set, the start of a set of new measurements was awaited for the first two minutes. To compare the two measurement techniques the μPO_2 was converted into a corresponding saturation. For the μPO_2 conversion, for every measured value in mmHg the corresponding % was calculated called micro-vascular oxygen saturation converted (μSO_2. converted). The conversion can be found in Figure 2.

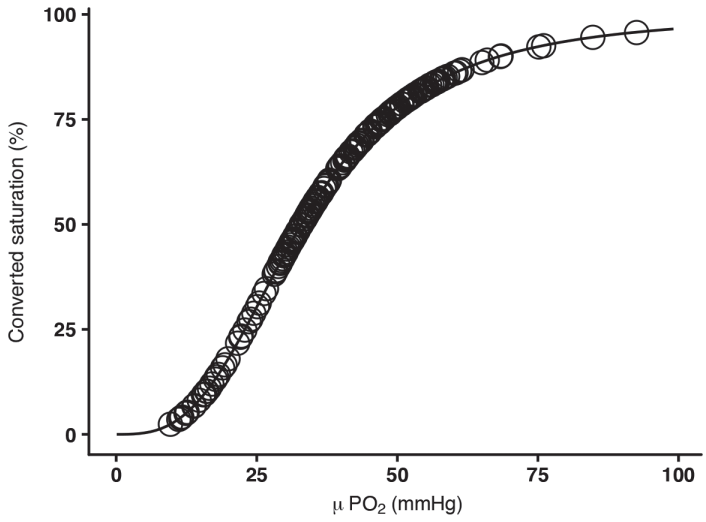

Figure 2. Conversion of μPO_2 into saturation according to the found relationship by Serianni et al [23].

Influence of bile on mucosal oxygen saturation

Furthermore, the influence of bile on mucosal oxygen saturation values measured with VLS was assessed. Mucosal oxygen saturation measurements were performed of the small intestine mucosa in presence of bile. Two different types of bile were used: fluid obtained during upper GI endoscopy from the stomach of the animal and fluid obtained from the small intestine of the animal. The sticky viscosity of the bile ensured the fixation of the bile on the measurement area and continuous visual confirmation ensured that the bile measurements were performed on surface covered with bile. The amount of bile applied to the mucosa, the thickness of the bile applied and the exact content of the bile applied were not controlled. The mucosal oxygen saturations in presence of bile were compared with the mucosal oxygen saturations before the bile was applied to the mucosa (baseline) and the mucosal oxygen saturations every time after the bile was removed with saline fluid as control. For every step approximately 30 measurements were done.

Mucosal oxygen saturation versus μPO_2 during asystole

Finally, simultaneous mucosal oxygen saturation and μPO_2 measurements were performed from the moment a lethal dose potassium chloride was intravenously injected. A measurement period of 25 minutes after injection was considered long enough to ensure a steady state since Benaron. et al. showed detection of local ischemia with VLS within 120 seconds [22].

Experimental outcomes

Mucosal oxygen saturation values were defined in percentage tissue hemoglobin saturation. The μPO_2 measurements were defined in mmHg.

Analytical and Statistical methods

Statistical analysis was performed with R Statistics software (v3.2.4). Normal distribution was assessed visually and with the Shapiro-Wilk normality test. Normal distributed data is presented as mean±standard deviation (SD) and abnormally distributed data is presented as median with interquartile range (IQR). A linear regression model was used for the FiO_2, mucosal oxygen saturations, and μPO_2. A scatter plot was used to show the mucosal oxygen saturation versus the μPO_2 measurements at different FiO_2 values. To compare the two measurement techniques, the μPO_2 was converted from mmHg to % porcine hemoglobin saturation. To determine the saturation a porcine-specific hemoglobin saturation formula published by R. Serianni et al. was used(23): $(\%/100) = (0.13534 \cdot P_{O2})^{3.02} / [(0.13534 \_ P_{O2})^{3.02} + 91.2]$. The

formula was derived from 213 data point at pH 7.4 and 37 degrees with an excellent fit.

To compare the saturation, the difference in measurement frequency had to be overcome. The mucosal oxygen saturation has a fixed measurement interval whereas the μPO_2 is measured on demand. To equally compare the two measurements the mucosal oxygen saturation was averaged over same period as one μPO_2 was done. Thereafter these results were visualized with linear regression and with a Bland-Altman comparison plot [24].

The Wilcoxon signed-rank test was used to compare the measurement before, with and after application of bile. A two-tailed p value of <0.05 was considered significant. After the potassium chloride injection mucosal oxygen saturation measurements were compared with μPO_2. Because VLS measures every second, a symmetrical moving average of 20 samples was taken to smooth the data, for example the eleventh sample is an average of sample 1-21.

Results

Baseline data

All 5 animals were in good clinical condition before the start of the experiment.

Mucosal oxygen saturation versus μPO_2 measurements at different FiO_2 values

The mucosal oxygen saturation levels versus the μPO_2 levels different values of FiO_2 in 5 animals were measured. The mucosal oxygen saturation decreased with increasing FiO_2 in contrast to the μPO_2 values that increased with increasing FiO_2. The spread of the mucosal oxygen saturation levels and the FiO_2 levels was large, shown in Figure 3.

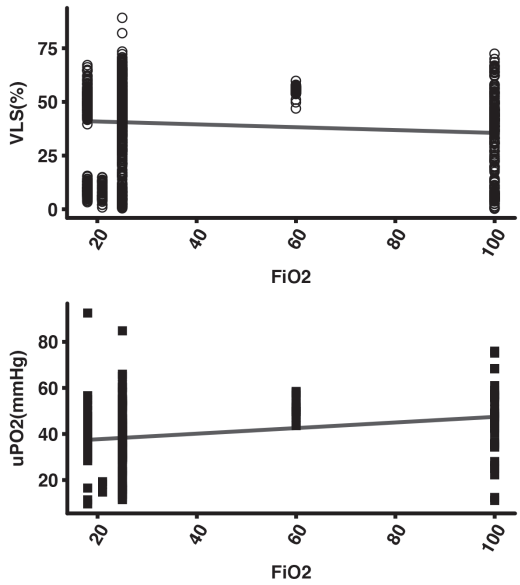

Figure 3. Scatter plot n=5 of mucosal oxygen saturation versus μPO_2 measurements at different FiO_2 values. VLS (R^2 =-0.01, Intersect=42.19, Slope=-0.07), μPO_2 (R^2=0.06, intersect=35.56, slope=0.14).

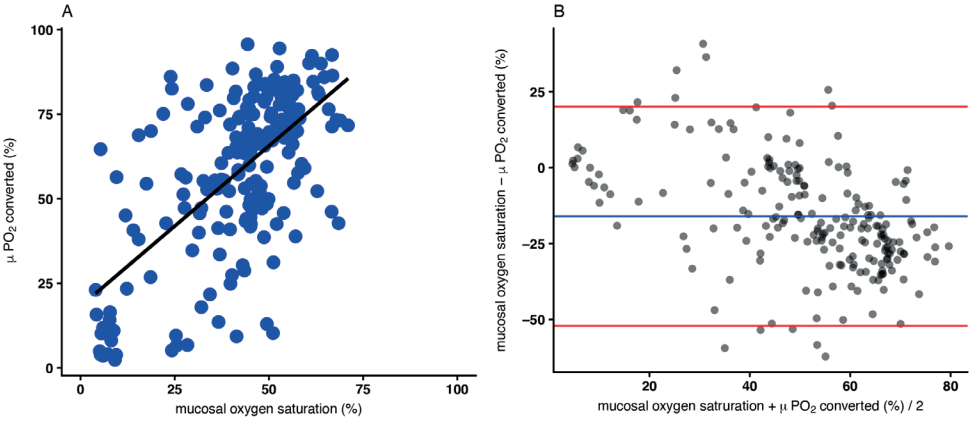

Figure 4. A) Correlation between mucosal oxygen saturation and the converted μPO_2 saturation. R^2= 0.39, intercept 18.5 slope 0.41. B) Blant-Altman plot of the mucosal oxygen saturation and the converted μPO_2 saturation.
VLS – μPO_2_saturation: -16.00974, 2.5% limit: -52.83358 , 97.5% limit: 20.81410, SD(diff): 18.41192

Figure 4A shows the correlation between mucosal oxygen saturation and the converted μPO_2 saturation. There is a poor linear correlation with an r^2=0.39, an interception of 18.5% and a

slope of 0.41. In the Bland-Altman plot (Figure 4b) also a poor correlation is seen with a mean difference of -16%. If the saturation increases the mucosal oxygen saturation undervalues the saturation even more.

Influence of bile on mucosal oxygen saturation

Figure 5 shows the mucosal oxygen saturation measurements without the presence of bile, with the presence of a bile mixture from the stomach and with the presence of a bile mixture from the small bowel and measurements without any of the bile mixtures measured in a total of 2 animals. The mucosal oxygen saturation measurements before application of the bile mixtures and after the bile mixtures were removed were not significantly different (mucosal oxygen saturation before application of bile mixture median (IQR) 57.5% (54.8-59.0%) versus mucosal oxygen saturation after removal bile mixture 57.0% (54.7-58.6%), p= 0.2743). However, a significant increase of the mucosal oxygen saturation was seen when the bile mixture from the stomach was applied compared to the mucosal oxygen saturation before application of the bile mixtures (median mucosal oxygen saturation with mixture of the stomach (IQR) 73.5% (66.8-85.8) p= $<2.2*10^{-16}$). When the bile mixture from the small bowel was applied, the mucosal oxygen saturation was significantly lower with a median (IQR) 47.6% (41.8-50.8), p=$<2.2*10^{-16}$ compared to mucosal oxygen saturation measurements with bile mixture form the stomach and the mucosal oxygen saturation increased significantly after the bile mixtures had been removed (p=$<2.2*10^{-16}$).

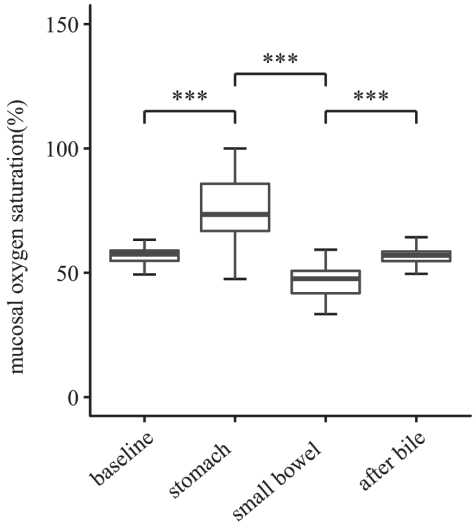

Figure 5. Mucosal oxygen saturation measurements without the presence of bile, with the presence of a bile mixture from the stomach, with a bile mixture from the small bowel and measurements without any of the bile mixtures. The baseline mucosal oxygen saturations did not significantly differ from the mucosal oxygen saturations after the bile had been removed shown as “after bile”. *** = p $<2.2*10^{-16}$

Mucosal oxygen saturation versus μPO_2 during asystole

The mucosal oxygen saturation measurements and μPO_2 measurements during the minimally first 25 minutes of asystole in 5 animals are shown in Figure 6. In all 5 animals the μPO_2 measurements decreased towards a value of 0. The mucosal oxygen saturation measured with VLS decreased and increased variably during the measurement period and the mucosal oxygen saturation never reached a stable state around 0%.

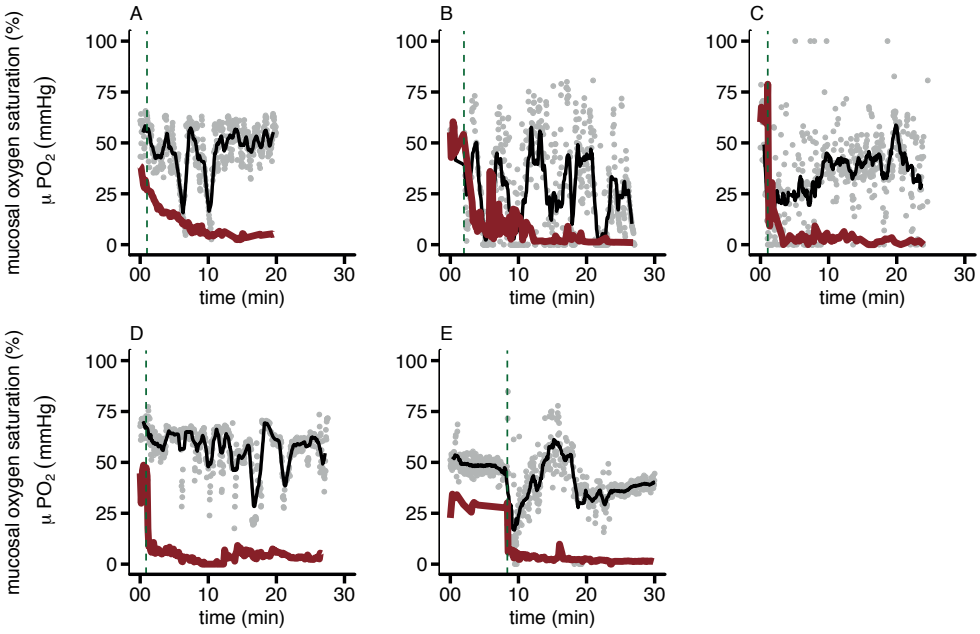

Figure 6. Average mucosal oxygen saturation measurements measured by VLS (black) over 21 data points (gray) and μPO_2 measurements (red) during the minimally first 20 minutes of asystole in 5 pigs. Green vertical dashed line represents the time a lethal potassium dose was injected.

Adverse events

No adverse events occurred during the 5 porcine experiments.

Discussion

In this study we validated mucosal oxygen saturation measurements by comparing VLS with calibrated μPO_2 measurements. This study showed that the mucosal oxygen saturation values decreased with increasing FiO_2 in contrast to the μPO_2 values that increased with increasing FiO_2 with a large spread of the measured mucosal oxygen saturation levels and FiO_2 levels and a poor linear correlation. Furthermore, a significant influence of bile on the mucosal oxygen saturation values was shown. Finally, this study showed that the mucosal oxygen saturation values, in contrast to the μPO_2 values, did not decrease towards a value of 0 in the first 25 minutes of asystole.

The found inverse relationship of the mucosal oxygen saturation measurements by VLS with FiO_2 is remarkable. Mucosal oxygen saturations measured with VLS are expected to increase with increasing FiO_2 if VLS measures the capillary oxygen saturation level. However, VLS measures not only arterial saturation but also a large venous compartment. If a large mixed venous saturation determines the overall saturation value the influence of FiO_2 is expected to be minimal. Potentially due to hyperoxic vasoconstriction the actual venous saturation can decrease more compared to normoxic situations. The high FiO_2 values will be measured by the μPO_2. Furthermore, the measured values, both VLS as μPO_2 values, have a great spread. Possibly, the oxygen tension was very variable in the gastrointestinal vessels as intestinal ischemia is also patchy and heterogenic distributed [5]. During the experiment the hemodynamic state of the animals worsened by all experimental handlings, also contributing to a great spread of measured values.

Significant influence of bile on the mucosal oxygen saturation values measured with VLS was confirmed. Therefore it is advised and mentioned in the prescription to remove any bile remnants before the start of the VLS measurements. The bile has its own absorption spectrum of light. It also absorbs light in the same wavelengths as oxyhemoglobin and deoxyhemoglobin [25], and influences the result to determine the mucosal oxygen saturation. The amount of bile applied to the mucosa, the thickness of the bile applied and the exact content of the bile applied were not controlled in this experiment. However, these factors contribute to the light absorption by the bile and thus influence its effects on the VLS signal. Therefore, we advise to remove any fluid on the measuring area of the GI mucosa before the VLS measurements.

The idea that VLS measures mixed venous oxygen saturation is further confirmed by the fact that VLS measured still a reasonable oxygen saturation 25 minutes after asystole. The saturation in the capillaries is decreased towards zero over time due to diffusion of oxygen towards the still oxygen consuming cells. However, in the venous compartment the oxygen

will desaturate slowly by the large buffer capacity. Therefore, the oxygen saturation will not decrease towards zero immediately after asystole. Dips in oxygen saturation are seen in the mixed venous compartment measured by VLS as shown in Figure 6 due to spasm in the supplying arteries. After such a peristaltic contraction the blood flow stabilizes and no decrease in saturation is seen.

VLS is a powerful technique to measure oxygen saturation at a microvascular level. In the microvasculature oxyhemoglobin/deoxyhemoglobin is proportional mainly located in the venous compartment of the microvasculature. Therefore the saturation measured by the VLS is mainly represented by the venous compartment. For detection of an oxygen transport problem that results in ischemia, the microvascular arterial saturation is of importance, a part that is underexposed by VLS. This is endorsed by the fact that after a lethal potassium chloride the saturation does not drop in comparison to μPO_2, which is an exaggerated model of instant ischemia.

This study has some limitations. First, the experiments performed in this study were designed to enable generalizability in humans. However, to enable stable oxygen saturation measurements with VLS and μPO_2 of the mucosa of the small intestine of a pig, the abdomen had to be opened to open the small intestinal loop. The mucosa of this small intestinal loop was exposed to room air and room temperature. This will result in oxygen diffusion into the tissue and rapid decrease in temperature for the exposed tissue. Furthermore, the abdominal anatomy of a pig is different from the human abdominal anatomy. The GI tract of a pig is monogastric like the human GI tract, however the colon lies in a spiral. The mesenteric vascularization in humans consists of individual variable, mesenteric vessel formations with arcades, lateral branches and anastomoses in the bowel wall [26]. The mesenteric vascularization in pigs consists of bundles of vessel branched of the main stem arising from the mesentery and passing directly into the bowel wall without any branching of arcades [26].

Conclusion

This study showed that VLS measures the mixed venous hemoglobin oxygen saturation and not the mucosal capillary hemoglobin oxygen saturation. The presence of bile significantly influences the oxygen saturation levels measured with VLS. VLS is currently used in clinical practice in the clinical work-up of CMI. Further research is needed to establish if the mixed venous compartment is optimal for mucosal hemoglobin saturation measurements to assess GI ischemia.

References

1. Benaron DA, Parachikov IH, Cheong WF, Friedland S, Rubinsky BE, Otten DM, et al. Design of a visible-light spectroscopy clinical tissue oximeter. J Biomed Opt. 2005;10(4):44005.
2. Friedland S, Soetikno R, Benaron D. Reflectance spectrophotometry for the assessment of mucosal perfusion in the gastrointestinal tract. Gastrointest Endosc Clin N Am. 2004;14(3):539-53, ix-x.
3. Friedland S, Benaron D, Coogan S, Sze DY, Soetikno R. Diagnosis of chronic mesenteric ischemia by visible light spectroscopy during endoscopy. Gastrointestinal endoscopy. 2007;65(2):294-300.
4. Van Noord D, Sana A, Benaron DA, Pattynama PM, Verhagen HJ, Hansen BE, et al. Endoscopic visible light spectroscopy: a new, minimally invasive technique to diagnose chronic GI ischemia. Gastrointestinal endoscopy. 2011;73(2):291-8.
5. Writing C, Bjorck M, Koelemay M, Acosta S, Bastos Goncalves F, Kolbel T, et al. Editor's Choice - Management of the Diseases of Mesenteric Arteries and Veins: Clinical Practice Guidelines of the European Society of Vascular Surgery (ESVS). Eur J Vasc Endovasc Surg. 2017;53(4):460-510.
6. Clair DG, Beach JM. Mesenteric Ischemia. N Engl J Med. 2016;374(10):959-68.
7. Mensink PB, Moons LM, Kuipers EJ. Chronic gastrointestinal ischaemia: shifting paradigms. Gut. 2011;60(5):722-37.
8. Roobottom CA, Dubbins PA. Significant disease of the celiac and superior mesenteric arteries in asymptomatic patients: predictive value of Doppler sonography. AJR Am J Roentgenol. 1993;161(5):985-8.
9. Jarvinen O, Laurikka J, Sisto T, Salenius JP, Tarkka MR. Atherosclerosis of the visceral arteries. Vasa. 1995;24(1):9-14.
10. Rutjes AW, Reitsma JB, Coomarasamy A, Khan KS, Bossuyt PM. Evaluation of diagnostic tests when there is no gold standard. A review of methods. Health Technol Assess. 2007;11(50):iii, ix-51.
11. Sana A, Vergouwe Y, van Noord D, Moons LM, Pattynama PM, Verhagen HJ, et al. Radiological imaging and gastrointestinal tonometry add value in diagnosis of chronic gastrointestinal ischemia. Clinical gastroenterology and hepatology : the official clinical practice journal of the American Gastroenterological Association. 2011;9(3):234-41.
12. ter Steege RW, Sloterdijk HS, Geelkerken RH, Huisman AB, van der Palen J, Kolkman JJ. Splanchnic artery stenosis and abdominal complaints: clinical history is of limited value in detection of gastrointestinal ischemia. World J Surg. 2012;36(4):793-9.
13. Mensink PB, Geelkerken RH, Huisman AB, Kuipers EJ, Kolkman JJ. Twenty-four hour tonometry in patients suspected of chronic gastrointestinal ischemia. Digestive diseases and sciences. 2008;53(1):133-9.
14. Otte JA, Geelkerken RH, Oostveen E, Mensink PB, Huisman AB, Kolkman JJ. Clinical impact of gastric exercise tonometry on diagnosis and management of chronic gastrointestinal ischemia. Clinical gastroenterology and hepatology : the official clinical practice journal of the American Gastroenterological Association. 2005;3(7):660-6.
15. Sana A, Moons LM, Hansen BE, Dewint P, van Noord D, Mensink PB, et al. Use of visible light spectroscopy to diagnose chronic gastrointestinal ischemia and predict response to treatment. Clinical gastroenterology and hepatology : the official clinical practice journal of the American Gastroenterological Association. 2015;13(1):122-30 e1.
16. Lo LW, Koch CJ, Wilson DF. Calibration of oxygen-dependent quenching of the phosphorescence of Pd-meso-tetra (4-carboxyphenyl) porphine: a phosphor with general application for measuring oxygen concentration in biological systems. Anal Biochem. 1996;236(1):153-60.

17. Sinaasappel M, Ince C. Calibration of Pd-porphyrin phosphorescence for oxygen concentration measurements in vivo. Journal of applied physiology (Bethesda, Md : 1985). 1996;81(5):2297-303.
18. Vanderkooi JM, Maniara G, Green TJ, Wilson DF. An optical method for measurement of dioxygen concentration based upon quenching of phosphorescence. J Biol Chem. 1987;262(12):5476-82.
19. Kilkenny C, Browne WJ, Cuthill IC, Emerson M, Altman DG. Improving bioscience research reporting: the ARRIVE guidelines for reporting animal research. PLoS Biol. 2010;8(6):e1000412.
20. Chow SCW, H.; Shao, J. Sample Size Calculations in Clinical Research. 1st ed: Taylor & Francis Group; 2003.
21. Harms FA, de Boon WM, Balestra GM, Bodmer SI, Johannes T, Stolker RJ, et al. Oxygen-dependent delayed fluorescence measured in skin after topical application of 5-aminolevulinic acid. Journal of biophotonics. 2011;4(10):731-9.
22. Benaron DA, Parachikov IH, Friedland S, Soetikno R, Brock-Utne J, van der Starre PJ, et al. Continuous, noninvasive, and localized microvascular tissue oximetry using visible light spectroscopy. Anesthesiology. 2004;100(6):1469-75.
23. Serianni R, Barash J, Bentley T, Sharma P, Fontana JL, Via D, et al. Porcine-specific hemoglobin saturation measurements. Journal of applied physiology (Bethesda, Md : 1985). 2003;94(2):561-6.
24. Bland JM, Altman DG. Statistical methods for assessing agreement between two methods of clinical measurement. Lancet. 1986;1(8476):307-10.
25. Nachabe R, Evers DJ, Hendriks BH, Lucassen GW, van der Voort M, Wesseling J, et al. Effect of bile absorption coefficients on the estimation of liver tissue optical properties and related implications in discriminating healthy and tumorous samples. Biomed Opt Express. 2011;2(3):600-14.
26. von Trotha KT, Butz N, Grommes J, Binnebosel M, Charalambakis N, Muhlenbruch G, et al. Vascular anatomy of the small intestine-a comparative anatomic study on humans and pigs. Int J Colorectal Dis. 2015;30(5):683-90.

Chapter 8

Oxygen-dependent delayed fluorescence of protoporphyrin IX measured in the Stomach and Duodenum during Upper Gastrointestinal Endoscopy

Rinse Ubbink*[3], Louisa J.D. van Dijk*[1,2], Luke G. Terlouw[1,2], Desirée van Noord[1,4], Egbert G. Mik[3], Marco J. Bruno[1]

[1] Department of Gastroenterology and Hepatology, Erasmus MC University Medical Center, Rotterdam, the Netherlands
[2] Department of Radiology, Erasmus MC University Medical Center, Rotterdam, the Netherlands
[3] Department of Anesthesiology, Laboratory for Experimental Anesthesiology, Erasmus MC University Medical Center, Rotterdam, the Netherlands
[4] Department of Gastroenterology and Hepatology, Franciscus Gasthuis & Vlietland, Rotterdam, the Netherlands

* Both authors contributed equally to this manuscript.

Published in:
Journal of Biophotonics, 2019;12(10):1-11

Abstract

Protoporphyrin IX-triplet state lifetime technique (PpIX-TSLT) is a method used to measure oxygen (PO_2) in human cells. The aim of this study was to assess the technical feasibility and safety of measuring oxygen-dependent delayed fluorescence of ALA-induced PpIX during upper gastrointestinal (GI) endoscopy.

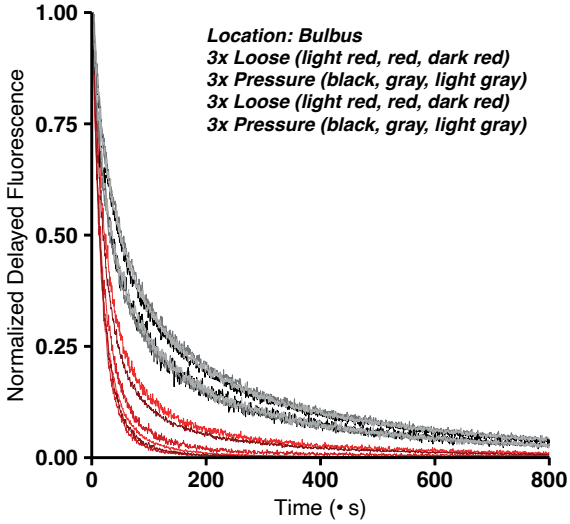

Endoscopic delayed fluorescence measurements were performed 4 hours after oral administration of 5-aminolevulinic acid (ALA) in healthy volunteers. The ALA dose administered was 0,1,5 or 20mg/kg. Measurements were performed at three mucosal spots in the gastric antrum, duodenal bulb and descending duodenum with the catheter above the mucosa and while applying pressure to induce local ischemia and monitor mitochondrial respiration. During two endoscopies, measurements were performed both before and after intravenous administration of butylscopolamine.

Delayed fluorescence measurements were successfully performed during all 10 upper GI endoscopies. ALA dose of 5 mg/kg showed adequate signal-to-noise ratio (SNR) values >20 without side effects. All pressure measurements showed significant prolongation of delayed fluorescence lifetime compared to measurements performed without pressure ($p<0.001$). Measurements before and after administration of butylscopolamine did not differ significantly in the duodenal bulb and descending duodenum.

Measurements of oxygen-dependent delayed fluorescence of ALA-induced PpIX in the GI tract during upper GI endoscopy are technically feasible and safe.

Graphical abstract and text

Oxygen tension (PO_2) can be measured in human cells by delayed fluorescence lifetime quenching of 5-aminolevulinic acid-induced protoporphyrin IX. This study aimed to assess the technical feasibility and safety of this technique during upper gastrointestinal endoscopy in the gastrointestinal (GI) tract. The endoscopic delayed fluorescence lifetime measurements in the GI tract were technically feasible and safe. Local mucosal ischemia was introduced temporarily by applying pressure with the probe on the mucosa. The lifetime prolongation demonstrated the oxygen-dependence of the signal.

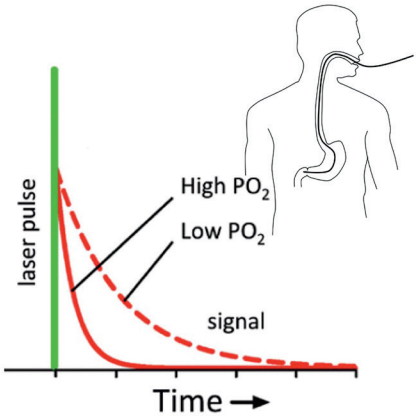

Introduction

Protoporphyrin IX (PpIX) is an endogenous compound synthesized in active mitochondria which can be induced by administration of its precursor 5-aminolevulinic acid (ALA). PpIX exhibits oxygen-dependent delayed fluorescence after photoexcitation [1]. The fluorescence lifetime depends directly on oxygen concentration, since oxygen acts as a quencher of excited PpIX molecules. In other words, upon collision of oxygen with an excited PpIX molecule energy transfer to oxygen will relax PpIX to the ground state without emission of a photon. More oxygen leads to more collisions and quenching, thereby shortening the delayed fluorescence lifetime. This phenomenon is described quantitatively by the Stern-Volmer relationship(2), relating the lifetime to the amount of oxygen (e.g. oxygen concentration or oxygen tension). A detailed description of the principles of the PpIX-triplet state lifetime technique (PpIX-TSLT) can be found in the article written by Harms et al. [3]. Introduction of the COMET monitor (Photonics Healthcare BV, Utrecht, The Netherlands) made PpIX-TSLT clinically available for measurements on the skin [4]. The main goal of this study was to investigate the technical feasibility of delayed fluorescence measurements in the gastrointestinal (GI) tract during endoscopy.

Oxygen tension (PO_2) measurements in cells of the gastrointestinal (GI) tract during endoscopy could be of great value, e.g. for the diagnostic work-up of patients suspected to be suffering from chronic mesenteric ischemia (CMI). CMI is the result of insufficient blood supply to the GI tract caused by obstruction of mesenteric arteries and/or veins [5]. CMI is in >90% caused by atherosclerosis of minimally one mesenteric artery. Typical symptoms of CMI are postprandial abdominal pain and weight loss, however more atypical symptoms as nausea, constant abdominal discomfort, vomiting, diarrhea or constipation are also reported [5]. Symptoms alone are of limited value for the diagnosis of CMI [6]. Mesenteric artery stenosis can be detected by CT-angiography, however the presence of mesenteric artery stenosis will not necessarily result in symptomatic disease (CMI) due to an abundant collateral mesenteric network. The prevalence of mesenteric artery stenosis in the asymptomatic general population is high (3-29%), increasing with age [7, 8]. CMI occurs when extensive mesenteric artery stenosis and/or an insufficient collateral network is present. Therefore, a functional test detecting GI ischemia is highly desired. Currently, visible light spectroscopy (VLS) and tonometry are used as functional tests for the diagnostic work-up of patients suspected to be suffering from CMI.

VLS measures the mucosal capillary hemoglobin oxygen saturation during upper GI endoscopy [9, 10] and is less invasive than tonometry measuring luminal pCO_2 with a nasogastric and nasojejunal catheter connected to a capnography [10, 11]. However, the sensitivity of VLS for CMI is 90% and the specificity is 60%(12), indicating the need to improve the accuracy of the

diagnostic workup. Since in the original reports of PpIX-TSLT the lifetimes were shown to be related to mitochondrial oxygen levels [1, 13] this technique shows promise for diagnosing CMI. The COMET monitoring device was designed for cutaneous measurements and has been adapted for endoscopic delayed fluorescence lifetime measurements. Therefore the primary aim of this study was to assess the technical feasibility of delayed fluorescence measurements of the GI tract during upper GI endoscopy. Secondary aims were:

1. to determine the dose of 5-aminolevulinic acid (ALA) needed for endoscopic measurements;
2. to determine the specific measurements locations;
3. to demonstrate oxygen-dependent signal and,
4. to determine the influence of butylscopolamine on the measurements.

Methods

Study design and setting

This work describes a single center study in healthy volunteers. The institutional review board of the Erasmus MC University Medical Center approved this study (NL59177.078.16, NL63050.078.17). The study complies with the Helsinki declaration on research ethics.

Participants

Healthy volunteers were recruited by distributing information leaflets. Before inclusion the medical history and existence of GI complaints were evaluated. Blood samples were taken to detect impaired renal function, and liver test abnormalities, defined as eGFR <90 ml/min/m3 or liver test abnormalities >1.5 times upper limit of normal. Healthy volunteers were eligible if they were able to give written informed consent, had an unremarkable medical history, and had no GI complaints. Volunteers were excluded in case of pregnancy, acute or chronic porphyria, and a known ALA or porphyrin hypersensitivity.

Study procedures and setup

The healthy volunteers were fasted for at least 6 hours and ALA (Gliolan, Medac GmbH, Wedel, Germany) was administered orally 4 hours before the upper GI endoscopy. The volunteers were discharged after the endoscopy. They were instructed to report any side effects. Furthermore, they were instructed to avoid exposure to sunlight as much as possible, and take precautions (e.g. sunglasses, long sleeves) during the first 24 hours after administration of ALA, since phototoxicity after sunlight exposure is a known side effect of ALA. Adverse events were collected during 7 days.

A probe that could be passed safely through the accessory channel of the endoscope was used for endoscopic detection of fluorescence light (designed by TNO, produced and CE-marked by LightGuideOptics, Mechenheim, Germany). The diameter of the accessory channel of the endoscope is 3.2 to 4.2 mm and therefore the tip of the probe is slightly smaller than 3.2 mm. The probe is a fiber optic assembly with one excitation fiber in the middle directly surrounded by seven detection fibers. The used detection fibers all have a diameter of 365 μm, and the excitation fiber is 470 μm in diameter. The fibers have a numerical aperture (NA) of 0.22±0.2. The tips of the fibers are fixed together in a ferrule. The position of the fiber tips within the ferrule and distance compared to each other is fixed and does not change when pressure is applied on the mucosa with the probe tip or while passing the probe tip through the accessory channel of the endoscope. The excitation fiber of the probe was connected to the light source in the COMET, a pulsed 515nm laser. The detection fiber was connected to the photomultiplier detection system of the COMET. To protect the highly sensitive detection system from indirect laser light a long pass filter (575nm with OD 4, Edmund Optics, Barrington, NJ, USA) was introduced in the optical path of the detection branch. During endoscopy peripheral saturation was continuously monitored and oxygen was administered intranasally to maintain a saturation level ≥95%. See figure 1 for the setup.

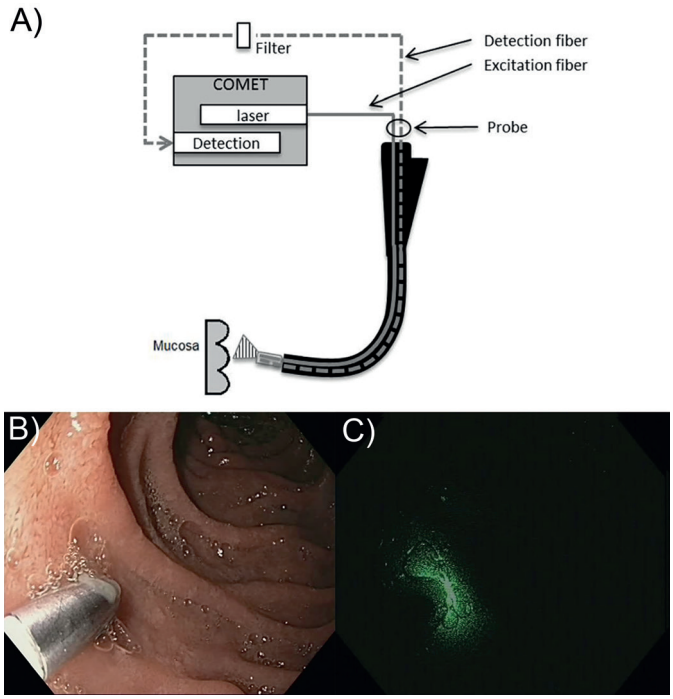

Figure 1. The setup for upper GI endoscopic delayed fluorescence measurements: **A)** Schematic setup, **B)** Probe in the descending duodenum during upper GI endoscopy, and **C)** Probe in the descending duodenum during endoscopic measurement (endoscopic light is switched off).

Delayed fluorescence lifetime measurements were performed similar to VLS measurements at three anatomical locations in the descending duodenum, duodenal bulb, and antrum of the stomach [12]. The fiber was positioned approximately 1-5 mm above the mucosa of the target area. A perpendicular angle of the fiber tip and the target area is optimal for the signal quality, however this is not an important parameter for the outcome of the lifetime measurements. To minimize interference by background noise the light of the endoscope was switched off during the measurements. Raw delayed fluorescent traces were stored with an external computer connected via the serial (rs-232) port. A python script written to store the raw data in a comma-separated file was used to read the serial buffer. The raw data was analyzed with software written in LabVIEW (version 13.0, National Instruments, Austin, TX, USA). Lifetimes were calculated using a rectangular distribution fit, taking into account the heterogeneity in lifetimes underlying the measured delayed fluorescence signal [13] unless stated otherwise. The mitochondrial oxygen tension (mitoPO_2) reading by COMET was not used since COMET is developed and tested for measurement on skin and links the measured lifetimes to the calibration constants for skin cells. Because this is the first report on delayed fluorescence measurements via an endoscope, we judged to exercise some restraint in reporting absolute values of PO_2. Therefore all delayed fluorescence measurements are represented as reciprocal lifetimes $1/\tau$ (with τ in microseconds) in order to obtain a positive association between oxygen and lifetime. According to the Stern-Volmer relationship the reciprocal lifetime is linearly related to the actual oxygen tension. Based on our current understanding of the technology, PO_2 measurements with a reciprocal lifetime $>0.1\ \mu s^{-1}$ should be considered as non-physiological in humans with a normal arterial oxygen tension [1].

Determination necessary ALA dose

The appropriate dose of ALA was determined by performing delayed fluorescence lifetime measurements with different doses of ALA. Since PpIX is endogenously present and accumulates in metabolic active cells, such as mucosal cells, measurements were performed during one upper GI endoscopy without administration of ALA. In neurosurgery 20mg/kg ALA is used to induce enough PpIX to visually determine the tumor fluorescence under blue light [14]. This was expected to be an abundant dose for detection of delayed fluorescence in the duodenal region because of the high cellular turnover and metabolic rate compared to neurological tissue. Therefore, five upper GI endoscopies were performed using a dose of 20mg/kg, two upper GI endoscopies were performed after administration of 1mg/kg ALA and two using a dose of 5mg/kg. Optimal dosage was based on signal quality and adverse events. Quality is expressed as signal-to-noise ratio (SNR). A SNR >20 is considered adequate [4].

Determining measurement locations and demonstrating oxygen-dependent signal

Measurements were obtained at each anatomical location with the probe hovering 1-5 mm above the mucosal surface. In order to confirm that the measured delayed fluorescence lifetimes depend on the oxygen concentration, measurements were performed while inducing local mucosal ischemia. Temporary ischemia was achieved by applying pressure to the mucosa with the probe. The oxygen supply to the tissue under the probe is compromised by compression of the capillaries. Because the oxygen is used within the cells, and the supply compromised, a prolongation of lifetime was expected due to the decrease in PO_2 during application of pressure. After minimally two seconds of pressure, three consecutive measurements were taken while pressure was applied. This process was repeated at two more sites within each anatomical location. In the situation without pressure the tip of the probe was positioned under view in close proximity of the tissue or just on the tissue without visible deformation of the mucosa. While providing pressure the probe is pushed on the tissue and caused tissue deformation similar to the procedure performed when obtaining tissue biopsies for diagnostic purposes. The exact amount of pressure applied was not controlled or measured. Measurements started in the descending duodenum and subsequently measurements with and without applying pressure were performed in the duodenal bulb and gastric antrum.

An oxygen consumption curve was made in two volunteers who received 5mg/kg ALA by taking repeated measurements with an interval of one second. Measurements were performed without applying pressure for minimally five seconds; the next 20 seconds measurements were performed while applying pressure to visualize mitochondrial respiration [15]. SNR and reciprocal lifetime were used to determine appropriate locations for measurements.

It is known that local oxygen tension will be heterogeneously distributed within the tissue [16]. Further analysis was done on the raw fluorescent traces to determine the effect of local applied pressure on the reciprocal lifetime and its distribution, caused by e.g. oxygen heterogeneity. By assuming the PpIX to be homogenous distributed among the GI tract the underlying lifetime distribution can be obtained with a method described by Golub et al. [17]. The trace can be described by a sum of rectangular distributions and the fractional contribution per reciprocal lifetime can be recovered. This method was successfully used by our group to recover oxygen distribution histograms [16, 18, 19] and is used on specific traces in this study to determine the distribution of (reciprocal) lifetimes in the signal as a measure of heterogeneity in the tissue. The fractional distribution within a trace describes the heterogeneity on a microvascular and

cellular scale. To investigate the heterogeneity on a larger tissue scale all data recorded above the tissue is combined in a histogram and the individual contributions are visualized by color.

Determining influence of butylscopolamine

Intravenous administration of butylscopolamine is commonly used during upper GI endoscopy to reduce intestinal contractions. Since butylscopolamine is known to induce tachycardia causing increased cardiac output, GI tract tissue oxygen levels could be influenced. This possible influence was evaluated in two volunteers receiving 5mg/kg ALA. All measurements mentioned before were performed in the descending duodenum, duodenal bulb and gastric antrum. After intravenous administration of 20 mg butylscopolamine the measurements were repeated in exactly the same manner.

Statistical analyses

The SNR and reciprocal lifetime were not normally distributed and therefore described as medians and interquartile ranges (IQR). Differences in reciprocal lifetimes with and without pressure and before and after administration of butylscopolamine were determined using the Wilcoxon-Mann-Whitney Test. A two-tailed p value of <0.05 was considered significant. Statistical analysis was performed using R (version 3.4.2) [2].

Results

Participants

Ten upper GI endoscopies were performed in six healthy volunteers. Nine out of ten upper GI endoscopies were performed in females, with a median age of 30.0 years (IQR 28.5-34.0 years). All endoscopies were performed in non-smokers and all healthy volunteers gave informed consent. No oxygen or sedatives were administered during endoscopy. Delayed fluorescence lifetime measurements were successfully performed during all ten endoscopies.

Table 1. Signal-to-noise ratio (SNR) for measurements with probe position 1-5mm above tissue, data presented as median [IQR], total of 10 upper GI endoscopies.

Dose	0 mg/kg	1 mg/kg	5 mg/kg	20 mg/kg
SNR Antrum	2 [1-3]	4 [3-6]	6 [4-13]	19 [8-37]
SNR Duodenal bulb	3 [2-7]	233 [165-533]	702 [179-900]	617 [269-921]
SNR Descending duodenum	6 [5-6]	29 [18-56]	215 [156-684]	110 [77-248]
Adverse Events	0/1	0/2	0/2	3/5 phototoxicity

Determining necessary ALA dose

The SNR for each specific location and dose of ALA are presented in table 1 and figure 2. The endogenous amount of PpIX showed to be insufficient to measure delayed fluorescence, since SNR was below 20 at all locations. The dose of 1mg/kg ALA also showed to be insufficient with SNR values of the first quartile reaching maximal 18 in the descending duodenum and a median SNR of 29 just above the lower limit of 20.

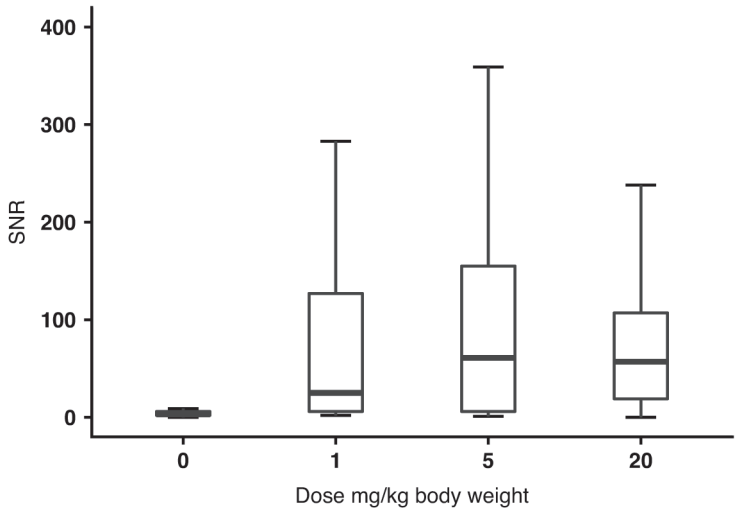

Figure 2. Signal-to-noise ratio (SNR) sorted by oral dose ALA combined for all measurement locations (gastric antrum, duodenal bulb, descending duodenum). Measurements are performed without pressure applied. Outliers are not presented since SNRs in 5 and 20mg/kg go up to 6000.

SNR in duodenal bulb and descending duodenum were adequate in the 5 and 20mg/kg group, however phototoxic side effects occurred in three out of five volunteers in the 20mg/kg group (table 1). The phototoxicity was observed on the skin of the face exposed to sunlight after the experiment in all three volunteers with phototoxicity and looked similar to a sunburned like reaction. Side effects resolved within 24 hours in all volunteers. Phototoxicity was not observed in the GI tract and volunteers did not experience abdominal complaints.

It was concluded that 5mg/kg was the best dose with sufficient SNR values and without reported side effects. This dose leaves a margin for suboptimal circumstances, for example less conversion of PpIX in patients and losses in the detection system due to the use of adaptors needed to couple the measuring probe to the COMET system.

Determining measurement locations

The SNR at the gastric antrum location was low compared to the SNR of the duodenal bulb and descending duodenum. Only in the 20 mg/kg group the upper quartile of the values reached a SNR >20 in the gastric antrum, therefore the signal quality in the gastric antrum showed insufficient for reliable measurements. The lifetime calculation became more inaccurate if the SNR dropped below 20, resulting in a scatter of lifetimes with a tendency to non-physiological lifetimes, see figure 3. Since the SNR values in the gastric antrum were too low and caused non-physiological lifetimes, measurements in gastric antrum were not included in the analysis of the influence of butylscopolamine.

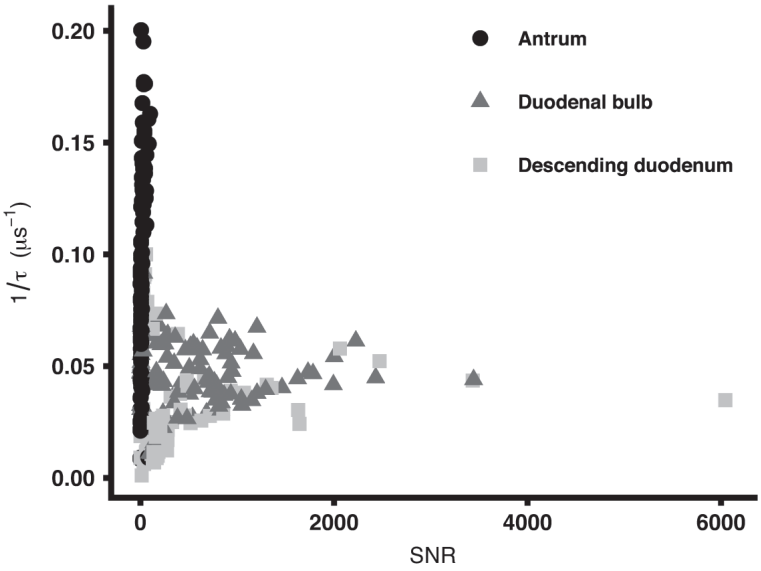

Figure 3. Reciprocal lifetimes 1/τ (with lifetime tau in microseconds) versus signal-to-noise ratio (SNR) of all measurements without pressure applied specified for each measurement location.

Demonstrating oxygen-dependent signal

Raw delayed fluorescence lifetime traces were recorded. When the probe was “loose” hovering above the GI tissue short lifetimes were measured. While pressure was applied the lifetime increased, shown in the Bulbus in figure 4.

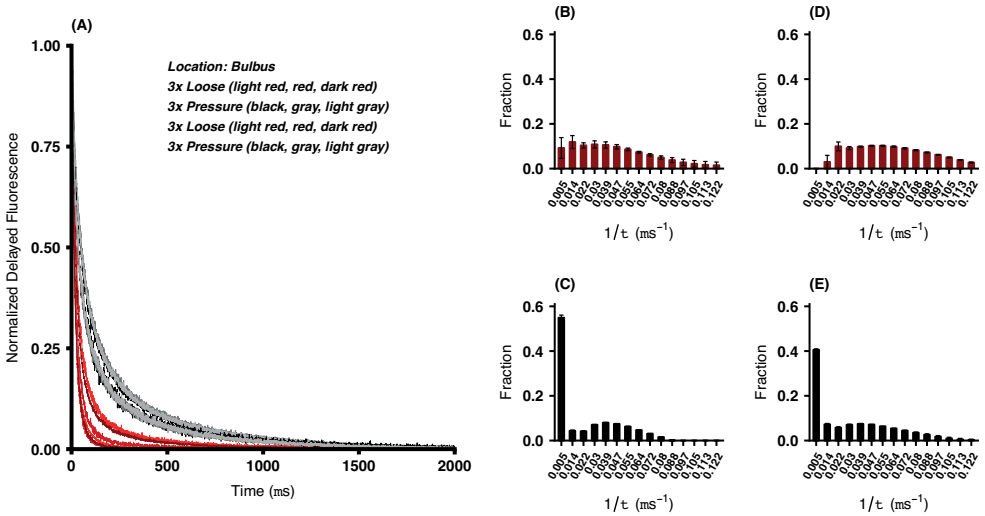

Figure 4. A) The normalized delayed fluorescence traces recorded in the Bulbus with 5mg/kg ALA. The traces represent 3 loose followed by 3 measurements while pressure was given with the probe on the tissue to induce local ischemia. This sequence was repeated for a second time. For the distribution analysis (histograms) a base of 15 reciprocal lifetimes equally distributed over a corresponding physiological PO_2 range (0-150 mmHg) assuming a quenching constant of 830 $mmHgs^{-1}$ and lifetime of spontaneous relaxation of 800 microseconds was taken(1). Histograms show reciprocal lifetime distributions of traces of the first panel. B and D) Average of 3 loose measurements. C and E) Average of 3 measurements while pressure was applied on the tissue with the optical probe. Histogram data presented as mean±SEM.

For the lifetime distribution analysis a base of 15 reciprocal lifetimes equally distributed over a corresponding physiological PO_2 range (0-150 mmHg) assuming a quenching constant of 830 $mmHgs^{-1}$ and lifetime of spontaneous relaxation of 800 microseconds was taken [1]. The distribution analysis was done on the 2 times 3 loose and 2 times 3 pressure traces. The averaged distributions of both the loose and pressure measurements are shown in figure 4. While pressure was applied a fraction of 0.55 of the signal fell in the bin with central reciprocal lifetime 0.005 μs^{-1}. Such lifetimes around 200 μs and even longer, as in this bin, indicate that a large part in the measurement volume is ischemic. The decrease in oxygen resulted in a distribution that has shifted to the left (lower PO_2) compared to the loose situation [3]. To analyze the heterogeneity between different spots of mucosal tissue, all “loose” data was combined into a histogram. To visualize the contribution of individual volunteers the data is color categorized per subject, shown in figure 5.

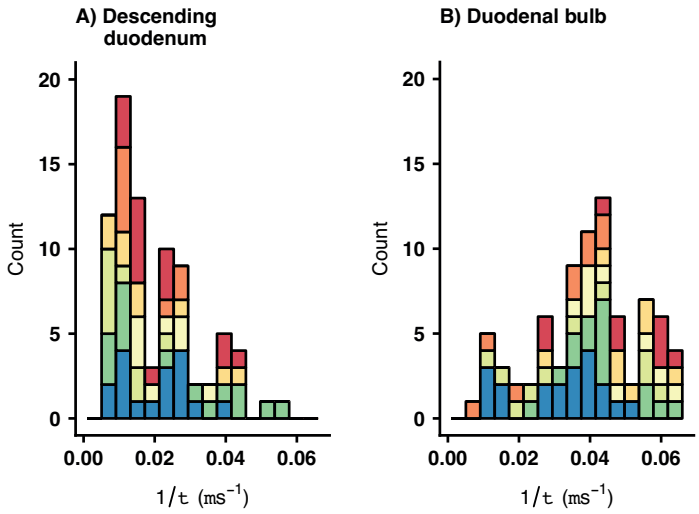

Figure 5. Histogram, 16 bins distributed over physiological reciprocal lifetimes, of the two measurement locations, included data is 5 and 20mg/kg ALA administration. The presented data is from two measurement location, a) Descending duodenum, b) Duodenal bulb, with the measurement probe hovering 5mm above the tissue. The colors indicate the individual measurement subject.

All measurements performed while applying pressure on the mucosa were significantly lower compared to measurements performed without pressure at all measurements locations (table 2). Figure 6 displays a decrease of reciprocal lifetime when pressure is applied with values decreasing further when pressure is maintained for a longer period of time. The oxygen disappearance curve (figure 7) supports this finding and shows a decrease of reciprocal lifetime over time, demonstrating disappearance of oxygen due to ongoing oxygen consumption, while temporary ischemia is induced.

Table 2. Reciprocal lifetime (in units, $1/\tau$ μs^{-1}) of GI tissue PO_2 measurements with and without pressure applied for each measurement location. ALA dose is 5mg/kg and 20mg/kg, total of seven upper GI endoscopies.

Location	$1/\tau$ loose median [IQR]	$1/\tau$ pressure median [IQR]	p-value
Antrum	0.092 [0.061-0.132]	0.052 [0.032-0.069]	<0.001
Duodenal bulb	0.041 [0.032-0.049]	0.013 [0.010-.0.022]	<0.001
Descending duodenum	0.016 [0.011-0.026]	0.009 [0.008-0.011]	<0.001

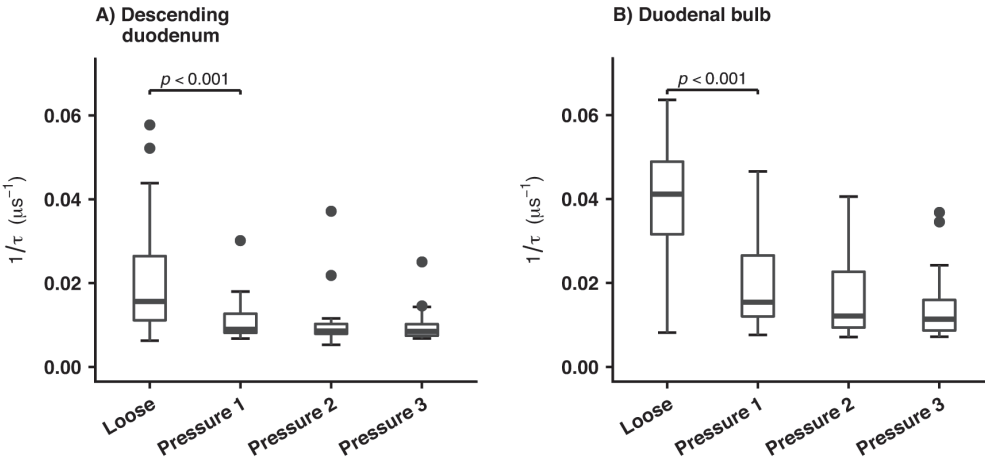

Figure 6. A) Measurements in the descending duodenum. X-axis shows measurements just above tissue (loose) and three consecutive measurements during pressure application (pressure 1, pressure 2, pressure 3). B) Measurements in the duodenal bulb. X-axis shows measurements just above tissue (loose) and three consecutive measurements during pressure application (pressure 1, pressure 2, pressure 3).

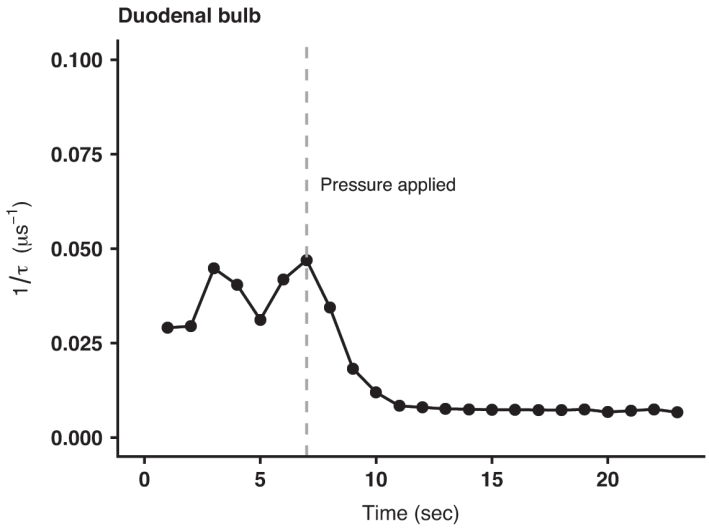

Figure 7. Oxygen consumption curve performed in the duodenal bulb.

Determining influence of butylscopolamine

Delayed fluorescence before and after administration of butylscopolamine did not differ significantly in the duodenal bulb (figure 8). In the descending duodenum, reciprocal lifetimes before administration of butylscopolamine were significantly lower than after

administration of butylscopolamine (figure 8). Measurements before and after administration of butylscopolamine did no longer differ significantly (p=0.281) when the lowest duodenal values before administration of butylscopolamine are excluded. These measurements were performed while unintended pressure was applied to the mucosa due to intestinal contractions

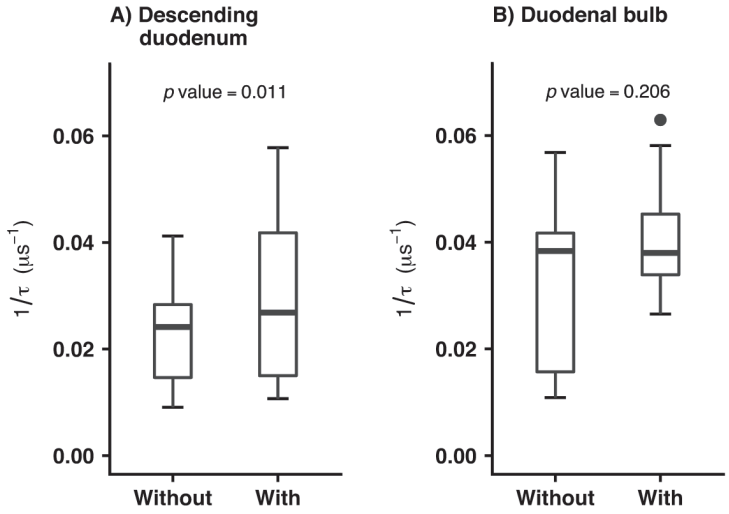

Figure 8. A) measurements with 5mg/kg ALA in duodenal bulb without butylscopolamine versus measurements with butylscopolamine and B) measurements with 5mg/kg ALA in descending duodenum without butylscopolamine versus measurements with butylscopolamine.

Discussion

This study showed that delayed fluorescence measurements of ALA-induced PpIX in the GI tract during upper GI endoscopy are technically feasible and that the measured signal is oxygen-dependent. We determined an optimal dose of 5mg/kg ALA and duodenal bulb and descending duodenum as suitable measurement locations. Administration of butylscopolamine during upper GI endoscopy did not influence the measured GI delayed fluorescence signal (reciprocal lifetimes).

ALA-induced enhancement of mitochondrial PpIX provided the first method to measure mitochondrial PO_2 in living cells [1]. In a time window of some hours after administration of ALA the PpIX is confined in the mitochondria as shown in animal studies in rat liver [18] and rat heart [19]. Since PpIX diffuses slowly out of the mitochondria, it will not solely remain in the mitochondria, making the localization of the signal less specific over time. The COMET system provides the clinical parameter "mitoPO_2" (mitochondrial oxygen tension), in order to distinguish the measurement from e.g. hemoglobin-based "tissue oxygen" measurements,

since such parameters provide other information from different tissue compartments(4). However, the reader should keep in mind that the origin of the PpIX delayed fluorescence signal is not only mitochondrial and depends on tissue type, and the amount of time after ALA administration.

Administration of ALA is needed for reliable endoscopic delayed fluorescence lifetime measurements since the amount of endogenously present PpIX is not sufficient for measurements using the current setup. The optimal dose of ALA is a compromise between sufficient signal quality and no or few side effects. The signal quality was high for a dose of 20mg/kg ALA, however phototoxicity was reported in 60%. Measured reciprocal lifetime values were disproportionally high at a dose of 1mg/kg ALA compared to the values measured with 5 or 20mg/kg ALA. This finding suggests the occurrence of disproportional high reciprocal lifetime values at low SNRs due to insufficient ALA dose. An explanation may be the occurrence of PpIX photobleaching, caused by the white xenon light source of the endoscope plus the potential photobleaching effect of the green laser light. The total amount of light exposure depends on the endoscopic observation time. But despite the endoscopic light source the measurements could be performed with sufficient signal quality. With technical and medical considerations in mind we advise an ALA dose of 5mg/kg for endoscopic oxygen-dependent delayed fluorescence measurements, since we showed reliable delayed fluorescence measurements without any side effects after administration of this dose.

The COMET device determines mitoPO_2 by the delayed fluorescence lifetime of PpIX after excitation with a laser pulse. The measurement has been calibrated for skin and in that case reciprocal lifetime is linear proportional to oxygen tension in mmHg [1]. The calibration constants in the human gastro-duodenal tract are unknown, as a consequence all data is represented in reciprocal lifetimes $1/\tau$ (μs^{-1}). The measured lifetimes in the gastric antrum were short, with a median value of 10.8 μs, that would have corresponded with non-physiological high PO_2 values if the current available calibration constants were used [1]. The reason why the gastric antrum has short delayed fluorescent lifetimes has not been studied. We consider the histological composition and function of the mucosa could interfere with the excitation light of the delayed fluorescent signal itself. It could be that the ability of these cells to accumulate PpIX is lower, e.g. due to a relatively slow cellular turnover, resulting in low SNRs and unreliable short lifetimes.

We determined the influence of administration of butylscopolamine on the endoscopic delayed fluorescence signal since butylscopolamine is commonly administered intravenously in clinical practice if intestinal contractions hamper the endoscopy. Delayed fluorescence

lifetimes before and after administration of butylscopolamine did not differ significantly in the duodenal bulb, however in the descending duodenum the reciprocal lifetimes before administration of butylscopolamine were significantly lower than after administration. These lower values were due to unintended application of pressure during measurements, caused by peristaltic movements of the bowels. During the endoscopic GI delayed fluorescence measurements the green light emitted by the laser is visible when the endoscopic light is switched off. When peristaltic movements of the bowels were present we frequently observed fading or even disappearance of the green light when the GI mucosa pressed against the fiber. At the same time, lower reciprocal lifetime values were noted. Since the endoscopic light has to be switched off during GI delayed fluorescence measurements, correcting the position of the probe in order to avoid contact with the mucosa is difficult in contractile bowels. After excluding the low values caused by unintended application of pressure, no significant differences in reciprocal lifetime before and after butylscopolamine remained. Therefore we conclude that butylscopolamine does not influence the endoscopic GI tissue reciprocal lifetime values, however when intestinal contractions are present measurements can be affected by unintended application of pressure. We advise to administer butylscopolamine during duodenal delayed fluorescence measurements when intestinal contractions are present, to increase the reliability of the measurements. Furthermore, future design of the probe with development of pressure sensors on the probe tip to avoid measurements during unintended application of pressure with the probe tip on the GI mucosa could be a solution for this problem.

This study has some limitations. First, the measured GI tract delayed fluorescence measurements in this study are presented as reciprocal lifetime since the calibration constants for the mucosa of the GI tract are unknown yet. Second, during the GI tissue measurements the light of the endoscope has to be switched off to minimize background noise. Furthermore, the probe tip currently consists of sharp edges, which can possibly damage the GI mucosa. Finally, the amount of endogenous PpIX is far from sufficient to measure GI delayed fluorescence using COMET. Necessity to administrate ALA causes a delay between oral intake and the first measurement opportunity, aside from potential phototoxic effects. Fortunately we did not register any adverse events with 5mg/kg ALA. The use of a commercial device limited our choice to an excitation wavelength of 515 nm, since this is the excitation wavelength of the COMET device, which is designed for cutaneous delayed fluorescence measurements after topical application of ALA [4]. This wavelength is a tradeoff between melatonin and hemoglobin absorption, topical applied ALA penetration depth, and measurement volume depth. The penetration depth of green light in the gut is very limited [21], and in our application the use of 515 nm excitation light likely limits the measurement depth to the mucosa. However,

since ALA is systemically administered in this application, other excitation wavelengths could provide more efficient photo excitation and improve SNR, or alter the penetration depth and increase measurement volume.

For the interpretation of the signal in terms of quantitative oxygen measurements additional research into the localization of PpIX and the photo-physical properties of the delayed fluorescence would be very helpful. For example, Vinklárek et al. described a Singlet Oxygen Feedback-Induced mechanism (SOFDF) that influences the delayed fluorescence of PpIX under certain non-physiologic circumstances [22]. It is currently unknown to what extent other mechanisms than T-type delayed fluorescence, like this SOFDF mechanism, contribute to the *in vivo* delayed fluorescence signal. Although we are determined to improve our measurement and eventually hope to be able to convert the measured lifetimes to PO_2 levels this in itself is not necessary for successful clinical application. The only relevant question here is whether the measured lifetimes in healthy subjects differ from patients with e.g. CMI. Sensitivity and specificity of the technique could equally well be studied and calculated on reciprocal lifetimes instead of oxygen tensions.

In conclusion, measurement of oxygen-dependent delayed fluorescence of ALA-induced PpIX during upper GI endoscopy is feasible and safe. Further research is needed for the clinical applicability of this technique in the diagnostic work-up of CMI, starting with endoscopic GI delayed fluorescence measurements in patients suspected of CMI to determine its discriminative ability and to determine cut-off values for the inverse lifetime measurements for mucosal ischemia. Further research has to determine whether a more accurate diagnosis of CMI can be established when the presence of mucosal ischemia detected by endoscopic delayed fluorescence measurements is combined with the symptoms and imaging of the mesenteric arteries, and ultimately whether its use results in less patients treated for suspected CMI (with the associated risks and costs of revascularization therapy) who will not experience relief of symptoms since they are false positively diagnosed by current standards.

References

1. Mik EG, Stap J, Sinaasappel M, Beek JF, Aten JA, van Leeuwen TG, et al. Mitochondrial PO_2 measured by delayed fluorescence of endogenous protoporphyrin IX. Nature methods. 2006;3(11):939-45.
2. Vanderkooi JM, Maniara G, Green TJ, Wilson DF. An optical method for measurement of dioxygen concentration based upon quenching of phosphorescence. J Biol Chem. 1987;262(12):5476-82.
3. Harms FA, de Boon WM, Balestra GM, Bodmer SI, Johannes T, Stolker RJ, et al. Oxygen-dependent delayed fluorescence measured in skin after topical application of 5-aminolevulinic acid. Journal of biophotonics. 2011;4(10):731-9.
4. Ubbink R, Bettink MA, Janse R, Harms FA, Johannes T, Munker FM, et al. A monitor for Cellular Oxygen METabolism (COMET): monitoring tissue oxygenation at the mitochondrial level. Journal of clinical monitoring and computing. 2016.
5. Bjorck M, Koelemay M, Acosta S, Bastos Goncalves F, Kolbel T, Kolkman JJ, et al. Editor's Choice - Management of the Diseases of Mesenteric Arteries and Veins: Clinical Practice Guidelines of the European Society of Vascular Surgery (ESVS). Eur J Vasc Endovasc Surg. 2017;53(4):460-510.
6. ter Steege RW, Sloterdijk HS, Geelkerken RH, Huisman AB, van der Palen J, Kolkman JJ. Splanchnic artery stenosis and abdominal complaints: clinical history is of limited value in detection of gastrointestinal ischemia. World J Surg. 2012;36(4):793-9.
7. Roobottom CA, Dubbins PA. Significant disease of the celiac and superior mesenteric arteries in asymptomatic patients: predictive value of Doppler sonography. AJR Am J Roentgenol. 1993;161(5):985-8.
8. Jarvinen O, Laurikka J, Sisto T, Salenius JP, Tarkka MR. Atherosclerosis of the visceral arteries. Vasa. 1995;24(1):9-14.
9. Benaron DA, Parachikov IH, Cheong WF, Friedland S, Rubinsky BE, Otten DM, et al. Design of a visible-light spectroscopy clinical tissue oximeter. J Biomed Opt. 2005;10(4):44005.
10. Otte JA, Geelkerken RH, Oostveen E, Mensink PB, Huisman AB, Kolkman JJ. Clinical impact of gastric exercise tonometry on diagnosis and management of chronic gastrointestinal ischemia. Clinical gastroenterology and hepatology : the official clinical practice journal of the American Gastroenterological Association. 2005;3(7):660-6.
11. Mensink PB, Geelkerken RH, Huisman AB, Kuipers EJ, Kolkman JJ. Twenty-four hour tonometry in patients suspected of chronic gastrointestinal ischemia. Digestive diseases and sciences. 2008;53(1):133-9.
12. Van Noord D, Sana A, Benaron DA, Pattynama PM, Verhagen HJ, Hansen BE, et al. Endoscopic visible light spectroscopy: a new, minimally invasive technique to diagnose chronic GI ischemia. Gastrointestinal endoscopy. 2011;73(2):291-8.
13. Mik EG. Special article: measuring mitochondrial oxygen tension: from basic principles to application in humans. Anesth Analg. 2013;117(4):834-46.
14. Stummer W, Novotny A, Stepp H, Goetz C, Bise K, Reulen HJ. Fluorescence-guided resection of glioblastoma multiforme by using 5-aminolevulinic acid-induced porphyrins: a prospective study in 52 consecutive patients. J Neurosurg. 2000;93(6):1003-13.
15. Harms FA, Voorbeijtel WJ, Bodmer SI, Raat NJ, Mik EG. Cutaneous respirometry by dynamic measurement of mitochondrial oxygen tension for monitoring mitochondrial function in vivo. Mitochondrion. 2013;13(5):507-14.
16. Johannes T, Mik EG, Ince C. Dual-wavelength phosphorimetry for determination of cortical and subcortical microvascular oxygenation in rat kidney. Journal of applied physiology (Bethesda, Md : 1985). 2006;100(4):1301-10.

17. Golub AS, Popel AS, Zheng L, Pittman RN. Analysis of phosphorescence in heterogeneous systems using distributions of quencher concentration. Biophysical journal. 1997;73(1):452-65.
18. Mik EG, Johannes T, Zuurbier CJ, Heinen A, Houben-Weerts JH, Balestra GM, et al. In vivo mitochondrial oxygen tension measured by a delayed fluorescence lifetime technique. Biophysical journal. 2008;95(8):3977-90.
19. Mik EG, Ince C, Eerbeek O, Heinen A, Stap J, Hooibrink B, et al. Mitochondrial oxygen tension within the heart. Journal of molecular and cellular cardiology. 2009;46(6):943-51.
20. Team RC. R: A Language and Environment for Statistical Computing 2017 [Available from: http://www.R-project.org/.
21. Sinaasappel M, van Iterson M, Ince C. Microvascular oxygen pressure in the pig intestine during haemorrhagic shock and resuscitation. J Physiol. 1999;514 (Pt 1):245-53.
22. Vinklarek IS, Scholz M, Dedic R, Hala J. Singlet oxygen feedback delayed fluorescence of protoporphyrin IX in organic solutions. Photochemical & photobiological sciences : Official journal of the European Photochemistry Association and the European Society for Photobiology. 2017;16(4):507-18.

Chapter 9

Mitochondrial oxygenation during cardiopulmonary bypass: a pilot study

F. Harms[1], R. Ubbink[1], C.J. de Wijs[1], M.P. Ligtenberg[1,2], M. ter Horst[1], E.G. Mik[1]

[1]Laboratory of Experimental Anesthesiology, Erasmus MC, Department of Anesthesiology, University Medical Centre Rotterdam, Rotterdam, The Netherlands

[2] Educational program Technical Medicine; Leiden University Medical Center, Delft University of Technology & Erasmus University Medical Center Rotterdam.

Published in:
Front. Med. - Intensive Care Medicine and Anesthesiology, Submitted on:
29 Sep 2021 (2022)

Abstract

Objective: Ensuring adequate oxygenation is essential for the preservation of organ function during cardiac-surgery and cardiopulmonary bypass (CPB). Both hypoxia and hyperoxia result in undesired outcomes and a narrow window for optimal oxygenation exists. Current perioperative monitoring techniques are not always sufficient to monitor adequate oxygenation. The non-invasive COMET® could be a tool to monitor the oxygenation, measuring the cutaneous mitochondrial oxygen tension (mitoPO$_2$). This pilot study examines the feasibility of the cutaneous mitoPO$_2$ measurements during cardiothoracic procedures. The cutaneous mitoPO$_2$ will be compared to the tissue oxygenation (StO$_2$) as measured by Near Infrared Spectroscopy.

Design and method: This single center observational study examined 41 cardiac-surgery patients requiring CPB. Pre-operatively, patients received a 5-aminolevulinc acid plaster on the upper arm to enable the mitoPO$_2$ measurements. After induction of anesthesia, both the cutaneous mitoPO$_2$ and StO$_2$ were measured throughout the procedure. Patients were observed until discharge for the development of acute kidney insufficiency (AKI).

Results: The cutaneous mitoPO$_2$ was successfully measured in all patients and was 63.5 [40.0 – 74.8] mmHg at the surgery start and decreased significantly (p<0.01) to 36.4 [18.4 – 56.0] mmHg by the end of the CPB run. The StO$_2$ at surgery start was 80.5 [76.8-84.3] %, and did not change significantly. Cross-clamping of the aorta and the switch to non-pulsatile flow resulted in a median cutaneous mitoPO$_2$ decrease of 7 mmHg (p<0.01). The cessation of the aortic cross-clamping period resulted in an increase of 4 mmHg (p<0.01). Four patients developed AKI these all had a lower pre-operative eGFR of 52 ml/min versus 81 ml/min in the non-AKI group. The AKI group spent 32% of the operation time with a cutaneous mitoPO$_2$ value under 20 mmHg as compared to 8% in the non-AKI group.

Conclusion: This pilot study illustrated the feasibility of measuring the cutaneous mitoPO$_2$ with the COMET® during cardiothoracic procedures. Moreover, in contrast to StO$_2$, the mitoPO$_2$ decreased significantly with increased CPB run time. The cutaneous mitoPO$_2$ also significantly decreased during the aortic cross-clamping period and increased upon release of the clamp, the StO$_2$ did not. This emphasized the sensitivity of the cutaneous mitoPO$_2$ to detect circulatory and microvascular changes.

Introduction

The use of cardiopulmonary bypass (CPB) during cardiac surgery has a profound effect on the human body, since circulation, respiration, homeostasis, and thermoregulation are all affected by the CPB. Maintaining an adequate tissue oxygen supply, is essential to preserve cellular oxygenation and subsequently the preservation of organ function during CPB. The supply of oxygen is dependent on the red blood cell (RBC) count as well as the macrovascular and microvascular perfusion. Inadequate macro/micro-vascular perfusion and/or shortage of RBCs (anemia) can lead to an inadequate supply of oxygen resulting in tissue hypoxia. It is widely understood that hypoxia is an independent risk factor for postoperative complications, such as acute kidney injury (AKI), postoperative cognitive dysfunction (POCD), and post-operative delirium [1, 2]. Cardiac surgery-associated kidney injury (CSA-AKI) is unfortunately common as the kidneys are especially susceptible for periods of low mean arterial blood pressure and hypoxia due to their high metabolic activity [3]. Currently, no individual estimate can determine the minimum mean arterial blood pressure or critical oxygen tension before tissue injury or ischemia occurs. It is known that there is an oxygen reserve which must be depleted before the onset of ischemia. Thus only a longer period of low oxygen levels contribute to potential ischemia resulting in acute kidney injury.

On the other hand, striving for a hyperoxic state during CPB has not proven clinically beneficial [4]. This is due to the fact that hyperoxia can lead to the generation of oxygen radicals which play a role in the development of ischemic reperfusion injury [4]. Moreover, hyperoxia can lead to alveolar collapse resulting in atelectasis, which is one of the main contributing factors for post-operative hypoxia [4]. This highlights the fact that both hypoxia and hyperoxia can result in undesired outcomes and thus a narrow window for optimal oxygenation exists during CPB.

The current perioperative monitoring techniques seem to be sufficient for the maintenance of adequate tissue oxygenation in most patients. However, in high-risk patients the optimal oxygenation window during CPB is narrow and not completely understood [5]. This accentuates the need for novel monitoring techniques which can measure tissue oxygenation. The recently introduced COMET® monitor (Photonics Healthcare, Utrecht) could be of significance for these patients.

The Cellular Oxygen METabolism (COMET®) monitor enables non-invasive, in-vivo measurements of cutaneous mitochondrial oxygenation ($MitoPO_2$). In order to measure the cutaneous $MitoPO_2$ the COMET® device utilizes the Protoporphyrin IX - Triplet State lifetime Technique (PpIX –TSLT) [6-8]. This technique relies on the accumulation of an oxygen-sensitive delayed fluorescent porphyrin, namely Protoporphyrin IX (PpIX), which is

endogenously generated in the mitochondria through the administration of 5-aminolevulinc acid [6-8]. The subsequent PpIX singlet excited state intersystem cross into triplet states these long-lived triplet states are quenched efficiently by molecular oxygen which is the only known quencher in vivo [6-8]. The pioneering work conducted by E.G. Mik validated that the delayed fluorescence quenching by molecular oxygen was able to consistently quantify the MitoPO_2 in isolated cells, isolated organs and in vivo [6]. Moreover, the fact that mitochondria are the end users of oxygen, the mitoPO_2 reflects the local balance between oxygen supply and oxygen consumption within the cell [6, 7, 9]. This technique has also been proven feasible in measuring the cutaneous mitoPO_2 in healthy volunteers [10-12].

Near-infrared spectroscopy (NIRS) is a technique utilized to monitor tissue oxygenation, especially for the prevention of cerebral hypoxia [13]. However, Chan et al conducted a systematic review of 11 randomly controlled trials and found that current reference values for NIRS are varied and that the information on any association between NIRS measurements and outcomes such as POCD is limited [14]. In recent laboratory and clinical studies the cutaneous mitoPO_2 has shown to be more sensitive in measuring subtle changes in local oxygen supply and demand, than the NIRS technique. This sensitivity was demonstrated for the first time in a porcine model. In this experiment hemodilution in pigs resulted in an earlier decrease of the cutaneous mitoPO_2 than the NIRS tissue oxygenation saturation measurements (StO_2) [15]. Secondly, a recently completed pilot study in chronic anemia patients [16] has shown variable individual responses of the cutaneous mitoPO_2 measurements during red blood cell transfusion. This further supports the potential of cutaneous mitoPO_2 measurements to provide an insight into tissue oxygenation. Therefore, it is assumed that the cutaneous mitoPO_2 measurements can be an earlier indicator for tissue hypoxia than StO_2.

This pilot study's primary aim was to examine the feasibility of this measurement technique during cardiothoracic surgical procedures requiring a CPB. The impact of hemodynamic changes during CPB and its run time on the cutaneous mitoPO_2 were also analyzed. Examining the impact of CPB run time on the cutaneous mitoPO_2 is essential since it is widely understood that long CPB run times lead to worse clinical outcomes [17]. This decrease in clinical outcome is primarily attributed to increased myocardial stunning and increased inflammatory mediators during long CPB run time. The resulting inflammatory reaction contributes to an increased vascular permeability leading to an efflux of intravascular fluid into the interstitial space, causing microvascular dysfunction and an increased distance from the blood circulation to the target cell mitochondria [18, 19]. Therefore, the expectation was that long CPB run times are associated with reduced mitochondrial oxygenation, tissue hypoxia and poor outcomes.

Moreover, the importance or superiority of pulsatile flow during CPB has remained controversial and unresolved [17]. There are two major CPB methods namely, continuous flow or a pulsatile flow utilizing a rotary pulsatile flow pump. However, in this academic hospital only a continuous flow pump is used Therefore, in order to examine the effects of non-pulsatile flow on a mitochondrial level, the cutaneous mitoPO$_2$ will be examined during the CPB aortic cross-clamp period (a period in which patients have no pulsatile flow) and will be contrasted to the CPB period in which the patients have their own cardiac output.

In conclusion, as well as providing an impression of the cutaneous mitoPO$_2$ and its behavior during CPB. The cutaneous mitoPO$_2$ was also compared to simultaneously conducted StO$_2$ measurements. The correlation between perioperative cutaneous mitoPO$_2$ measurements and clinical outcomes in cardiac surgery have also been investigated.

Materials and Methods

Study population

This single center observational pilot study was approved by the local medical ethics committee, and was conducted in the Erasmus Medical Center (Erasmus MC), Rotterdam, the Netherlands. The subjects which could participate were patients planned for cardiothoracic surgery requiring CPB with the use of extracorporeal circulation. This included varying cardiothoracic operations namely, a coronary artery bypass graft (CABG), myectomy, cardiac valve replacement or repair and aortic root replacements.

The inclusion criteria were, over 18 years of age, acceptable proficiency of the Dutch language, cardiac surgery requiring CPB. The exclusion criteria were, not having an indication for invasive intra-arterial blood pressure monitoring, presence of mitochondrial disease, pregnancy or lactation, emergency surgery, intracardiac shunts, or skin lesions on upper arm or shoulder that could impede with cutaneous mitoPO$_2$ measurements. Patients eligible and willing to participate signed informed consent form prior to their surgery.

Patient demographic characteristics, including age, sex, height and weight were extracted from their electronic patient files. Intraoperative parameters and lab results, were automatically recorded with the electronic recording system, e.g. heart rate, arterial blood pressure, and CPB settings.

Sample size

This pilot study is the first observational cutaneous mitoPO$_2$ COMET® study in cardiothoracic surgery patients. Due to the amount of variables such as, hemodynamic changed brought on

by CPB and vaso-active agents, it is unknown what their effects will be on the mitochondrial function. Therefore, it is difficult to predict the variation in cutaneous mitoPO$_2$.

The sample size is thus based on the available data from a study in which the feasibility of cutaneous mitoPO$_2$ measurements were examined in healthy volunteers [10]. The healthy volunteers had a mean cutaneous mitoPO$_2$ of 44mmHg ± 17mmHg. In oxygen-supplemented patients cutaneous mitoPO$_2$ is expected to be slightly higher and is assumed to be around 55 mmHg.

Therefore, if an accuracy of 10% is assumed with the expected mean 55 mmHg there is a 5.5 mmHg margin of error. A Confidence interval of 95% corresponding with t=1.96 and s=17mmHg as standard deviation gives a sample size n of 36.7 subjects. However, due to the assumptions an estimation of 37 subjects was made. The fact that this patient population is more heterogeneous than the healthy volunteers which results in its own variability it was determined that a minimum of 41 successfully included subjects was a realistic sample size.

Lastly, the correct and timely application of the 5-aminolevulinic acid (ALA) plaster is crucial to obtain an adequate signal quality for reliable cutaneous mitoPO$_2$ measurements. To prevent a loss of power subjects with an initial signal quality (signal quality is calculated and displayed by the COMET® monitor) below 20% will be replaced, as this indicates a problem in the preparation phase. The cause of failure in cases with low signal quality will be examined to ensure proper action for future prevention.

Cardiopulmonary bypass

The CPB circuit consisted of the Quadrox HMOD 71000 with integrated Quart HBF140 arterial filter, a venous hard-shell cardiotomy reservoir and the revolution pump for the heart-lung machine, Stöckert S5 (Sorin Group). All surfaces were coated with Safeline® coating (Maquet Cardiopulmonary) or PHYSIO® coating (Sorin Group). The priming solution consisted of Gelofusine® (B.Braun, Melsungen AG, Germany) and Mannitol 200 g/l (Baxter Healthcare, Utrecht, The Netherlands). The initial heparin (Leo Pharmaceuticals, Weesp, The Netherlands) dosage was 300 IU/kg bodyweight, with an additional 7500 IU in the CPB circuit prime solution. Anti-coagulation through active clotting time was monitored using the Hemochron® Jr. (J.T.C. Europe, Rodano, Italy). Values >440 seconds were considered safe for CPB. The oxygenation was regulated by using in-line blood gas monitoring CDI-500® (Terumo Corporation, Tokyo, Japan) in α-stat method, combined with a Mass flow meter (Brooks Instruments, Hartfield, PA, USA). Intraoperative hemodynamic management targeted an arterial non-pulsatile flow of 2.4 L/min/m^2 and mean arterial pressure >60 mmHg. The targeted value for PaO$_2$ during the CPB time was 150mmHg. Cardioplegia was induced by the administration of St. Thomas Hospital solution.

Cutaneous mitoPO$_2$ measurement

Cutaneous mitoPO$_2$ measurement is an optical technique based on the PpIX-TSLT [6]. PpIX-TSLT is based on the principle of oxygen-dependent quenching of the excited triplet state of PpIX. Application of the porphyrin precursor ALA induces PpIX in the mitochondria. After photoexcitation with a pulse of green light PpIX emits delayed fluorescence of which the lifetime is inversely related to the amount of oxygen [6]. The PpIX-TSLT is incorporated in a clinical monitoring device COMET® [7].

The day before surgery an Alacare plaster (photonamic, Wedel, Germany), containing ALA, was applied on the upper arm or shoulder. Before the induction of anesthesia the COMET® probe was fixated on the pre-medicated skin. The area around the probe was covered with gausses to minimize interference of ambient light. Cutaneous mitoPO$_2$ in mmHg was measured perioperatively with a 5 minute interval. At the end of the operation the COMET® probe was removed and skin was covered with a plaster to protect it against light exposure.

Included patients with an initial signal quality below 20% as indicated by COMET® device were excluded and replaced as to ensure reliable measurements during the complete surgery period. Cutaneous mitoPO$_2$ measurements with an absolute value of 0 mmHg or a signal quality lower than 20%, as reported by the COMET®, were excluded.

StO$_2$ vs. Cutaneous mitoPO$_2$

The StO$_2$ was measured using the INVOS® device (Medtronic, Minneapolis, MN), which uses near-infrared spectroscopy to determine the regional oxygen saturation [20]. The INVOS® probe was fixated on the skin near the COMET® probe. StO$_2$ was recorded with the default INVOS® sampling interval of approximately 30 seconds and was defined as a percentage (%) hemoglobin saturation. At the end of the surgery both the probes of the COMET® and INVOS® were removed simultaneously, the last measurements of both devices were used as a reference to synchronize the two systems in time.

Start vs. end of CPB period

There is an expectation that the cutaneous mitoPO$_2$ will be negatively impacted by CPB run time due to previously discussed negative effects. Therefore, the cutaneous mitoPO$_2$ values were compared at the start and end of the CPB run time. Establishing a baseline with the first 20 minutes of CPB time compared to the last 20 minutes of the CPB period. The StO$_2$ measurements were taken during the same time frame as the cutaneous mitoPO$_2$ measurements.

Cutaneous mitoPO$_2$ vs. StO$_2$ change over time

The cardiothoracic surgical procedures in which CPB is utilized often take around 1 to 3 hours. This resulted in the need to clustered the data in order to compare it during operation time. Ten-minute windows were used to resample both cutaneous mitoPO$_2$ and StO$_2$ data. For each ten-minute time window, a median and inter quartile range (IQR) was calculated. For example if the surgery took 60 minutes, six time windows were created, and 3 hours will correspond with 18 time windows.

CPB with aortic cross-clamp vs. CPB without aortic cross-clamp

During cardiothoracic procedures in the Erasmus MC the heart delivers the pulsatile flow and pressure, a pulsatile state. When full flow extracorporeal circulation is given, and the aortic cross-clamp is set, a constant flow with a centrifugal pump results in a constant blood pressure and flow, a non-pulsatile state. A pulsatile and non-pulsatile period are both present in one CPB procedure, therefore the influence on oxygen delivery at the mitochondrial level was also investigated.

CPB without aortic cross-clamp was defined by the presence of cardiac output (arterial blood pressure swings) after the start of extracorporeal circulation till the aortic cross-clamp. Even though the CPB pump delivers a constant pressure, cardiac output creates a pulsatile pressure pattern on top of that. When the aorta is cross-clamped and cardioplegia is given by the administration of St. Thomas Hospital solution, the blood flow becomes non pulsatile defined as CPB with aortic cross-clamp.

Pulsatile flow before and after aortic cross-clamp

Two calculation methods were used to investigate the effect of pulsatile flow on cutaneous mitoPO$_2$. In the first method, cutaneous mitoPO$_2$ was measured right before and 5 minutes after aortic cross-clamp. In the second method, cutaneous mitoPO$_2$ was measured before and 5 minutes after the release of the aortic cross-clamp. This creates two datasets within a patient firstly, when the aortic cross-clamp is set (pulsatile → non-pulsatile) and secondly, when it is released (non-pulsatile → pulsatile).

Pulsatile flow for valve surgery versus coronary bypass graft surgery

The effect of pulsatile flow on the cutaneous mitoPO$_2$ was compared between patients undergoing valve surgery and CABG. This is due to the fact that after the initiation of CPB patients undergoing valve surgery receive the aortic cross-clamp almost immediately whilst

for patients undergoing a CABG procedure the aortic cross-clamp is placed approximately 30 minutes later. The reason is that once CPB has commenced during the CABG procedures the surgeon can properly inspect the coronary arteries and decide where to place the anastomoses. Throughout this time period the flow is still pulsatile due to the patient's own cardiac output, and only after aortic cross-clamping, the flow becomes non-pulsatile.

After 15 minutes of extracorporeal circulation during the CPB the cutaneous mitoPO$_2$ data was collected for 20-minutes. During this time window (15 – 35 min) the cutaneous mitoPO$_2$ was averaged to get a CABG CPB without aortic cross-clamp data point and a valve surgery aortic cross-clamp data point. This is illustrated in figure 1 which clarifies the valve surgery with aortic cross-clamp and CABG without aortic cross-clamp groups.

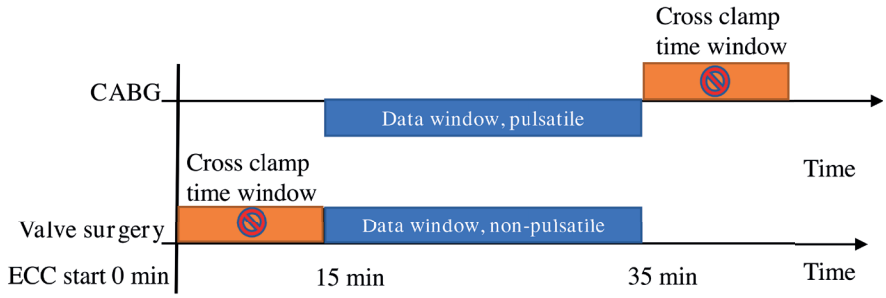

Figure 1. Illustrates aortic cross-clamp data window preparation. The data window time period is the same for the CABG cohort and the valve surgery cohort namely, 15 minutes after the start of extracorporeal circulation. In the CABG group the flow is pulsatile in the data window and in the valve surgery group it is non-pulsatile, since the aortic cross-clamp has been set.

Time below a cutaneous mitoPO$_2$ threshold in correlation with acute kidney injury

CSA-AKI is a unfortunately common and is generally associated with longer CPB run times [3]. This is due to a wide range of factors including hypoxia as previously discussed in the introduction. The cutaneous mitoPO$_2$ could therefore, provide a new insight in the prediction of CSA-AKI. In order to investigate this, three different ranges of cutaneous mitoPO$_2$ were chosen namely, cutaneous mitoPO$_2$ below 20 mmHg, between 20 and 40 mmHg, and above 40 mmHg. It was hypothesized that the longer the cutaneous mitoPO$_2$ is in a low range during CPB the greater the risk of developing AKI.

The COMET® measurement interval varied occasionally as the interval was changed from every 5 minutes to every minute or an extra 'single measurement' was taken. To determine the number of minutes below a threshold the data was interpolated to create a data point for every

minute. This was done with an approximation function in R version 3.5.2 [21]. The 'approxfun', in R, returns a list of points which linearly interpolate given data points. Having a data point for every minute the subsequent number of minutes that cutaneous mitoPO$_2$ was within one of the ranged could be determined.

The patients were grouped retrospective in AKI and non-AKI according to the AKI criteria [22].

- Increase in serum creatinine by ≥ 26.5 umol/L within 48 hours; or
- Increase in serum creatinine to ≥ 1.5 times baseline, which is known or presumed to have occurred within the prior 7 days; or
- Urine volume <0.5 ml/kg/h for 6 hours.

A group comparison was done between the AKI and non-AKI groups comparing the absolute number of minutes, and as percentage of the total CPB run time the cutaneous mitoPO$_2$ was below a threshold.

Statistics

Normality was tested with Shapiro-Wilk test. Normally distributed data are presented as means ± SD and non-normally distributed data as medians with 25-75th percentiles. Start and end period cutaneous mitoPO$_2$, StO$_2$, pulsatility before and after the aortic cross clamp were compared with a paired Mann–Whitney U-test. Pulsatility for valve surgery and CABG group comparison is done using an unpaired student t-test.

For categorical data namely, patient characteristics a two-sided Fisher's exact test done. For continuous values a Mann-Whitney U test was used. Significance was determined by p-values <0.05.

Results

COMET® data was successfully retrieved from all 41 patients whom underwent cardiothoracic surgery requiring CPB. In total, 0 patients were excluded or replaced, this is illustrated by a flow chart in figure 2. The INVOS® device which was used for StO$_2$ measurements was not available for 10 patients, thus they do not have any StO$_2$ data. This is due to the introduction of a new NIRS monitor which was not used for this study to ensure data compatibility. Table 1 describes the baseline patient characteristics.

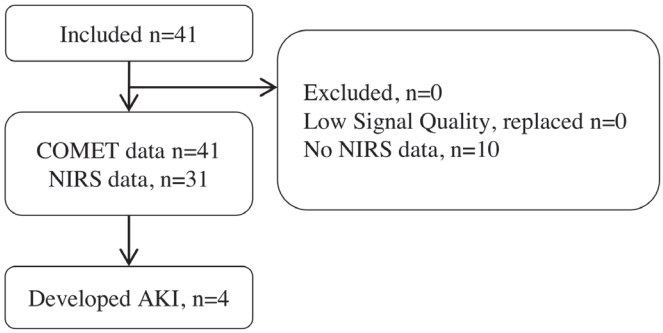

Figure 2. Patient study flowchart

Table 1: Patient characteristics

	All (n=41)	Non-AKI(n=37)	AKI (n=4)	*p*
Female (n)	15 (37%)	14	1	1*
CABG (n)	13 (32%)	12	1	1*
Valve surgery (n)	27 (66%)	24	3	1*
Re operation (n)	3 (7%)	3	0	1*
Age (years)	65 [57-73]	65 [57-73]	64 [58-70]	1∞
Weight (kg)	81 ± 13	81 [71-89]	88 [89- 91]	0.15∞
Length (cm)	176 ± 95	174 [170-180]	187 [181-188]	0.17∞
Duration surgery (min)	250 [202-297]	250 [201-296]	290 [228-392]	0.33∞
Duration CPB (min)	152 [111-200]	148 [106-187]	193 [163-240]	0.13∞
Hb preop (mmol/L)	8.35 ± 1.1	8.4 [7.6-9.2]	8.85 [8.30-9.10]	0.65∞
Hb begin cpb (mmol/L)	6.0 ± 0.8	5.9 [5.5-6.4]	6.6 [6.0-7.0]	0.34∞
Hb end cpb (mmol/L)	5.8 ± 0.8	5.8 [5.2-6.3]	5.6 [5.1-6.0]	0.67∞
Delta Creatinine (*μ*mol/L) Post-Pre	-5 [-10-12]	-5 [-11-4]	39.5 [31.5-48.5]	0.001∞
eGFR Pre-Op	73 ± 20	81 [61-88]	52 [47-59.8]	0.06∞
eGFR Post-Op	75 [50-98]	85 [56-99]	37. 5 [32.5-42]	0.004∞

* Fischer Exact test two sided, ∞ Mann-Whitney U test Represented as Mean ± SD or Median [IQR]

CPB start and end cutaneous mitoPO$_2$, StO$_2$ comparison

The median and IQR of CPB time was 152 [111-200] min. At the start CPB the median cutaneous mitoPO$_2$ was 63.5 [40.0-74.8] mmHg and decreased significantly $p<0.01$, $n=41$ to 36.4 [18.4-56.0] mmHg by the end of the CPB time. The average cutaneous mitoPO$_2$ was 44.1 [30.6-53.3] mmHg.

The StO$_2$ at the start of CPB was 80.5 [76.8-84.3] %, and did not change significantly by the end of the CPB time, 80.0 [75.8-84.8] %, *p*=NS, *n*=31. This is portrayed in figure 3.

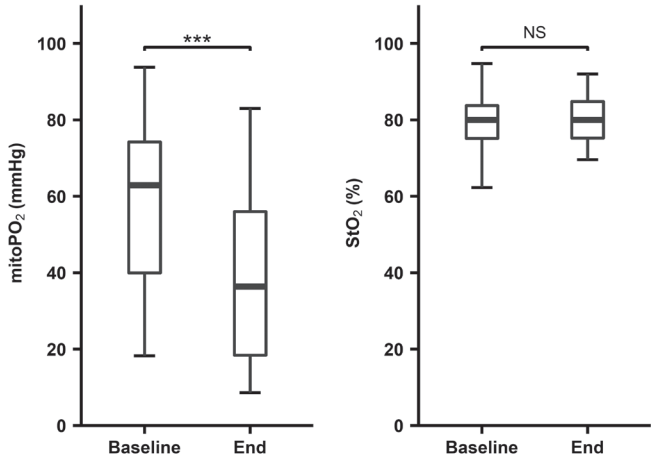

Figure 3. First and last 4 values during CPB, COMET® cutaneous mitoPO$_2$ n=41, ***p<0,01, INVOS® StO$_2$, n=31, p=not significant (NS). Boxplot with median, IQR box and whisker 1.5 times IQR

Cutaneous MitoPO$_2$ and StO$_2$ change over time

For the StO$_2$ and cutaneous mitoPO$_2$ 10 minute data windows from 31 patients were used. Cutaneous MitoPO$_2$ started at a mean of 62 ± 23 mmHg and slowly dropped to 44 ± 27 mmHg after 1 hour and becomes steady after approximately 90 minutes CPB time, see figure 4A. Overall the deviation of cutaneous mitoPO$_2$ was large however, as mentioned in section 4.1 they all had a decrease in the cutaneous mitoPO$_2$ during the CPB runs.

Longer durations of CPB run time resulted in lower cutaneous mitoPO$_2$ levels. However, the StO$_2$ showed no clear changes during CPB, as illustrated in figure 4B.

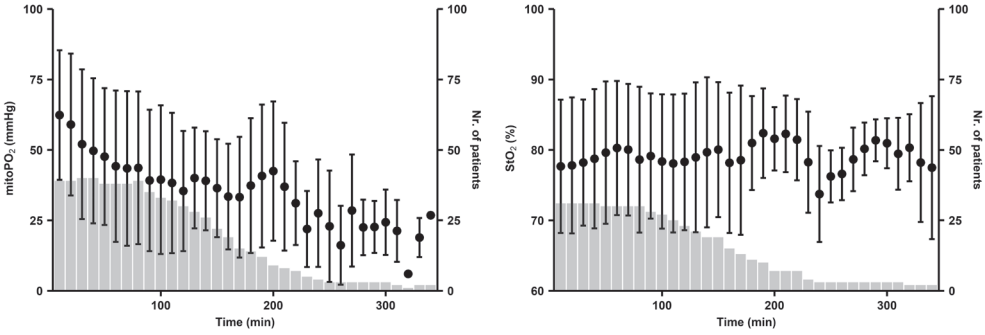

Figure 4. A) Distribution of cutaneous mitoPO$_2$ during CPB and B) Distribution of StO$_2$ during CPB, with start of CPB at t=0. Dots represent the mean value of patients averaged cutaneous mitoPO$_2$ per 10-minute windows. Whiskers demonstrate the standard deviation. Bars represent the number of patients.

Effect of aortic cross-clamp

Two methods were used to determine the effect of aortic cross-clamp on the cutaneous mitoPO$_{2.}$ The first method looked at cutaneous mitoPO$_2$ pre and post aortic cross-clamp.

Effect of aortic cross-clamp:

When the aortic cross-clamp was set the median cutaneous mitoPO$_2$ decreased by 7 mmHg, n = 41, p<0.01, and when it was released it increased 4 mm Hg, n = 41, p<0.01, as seen in figure 5.

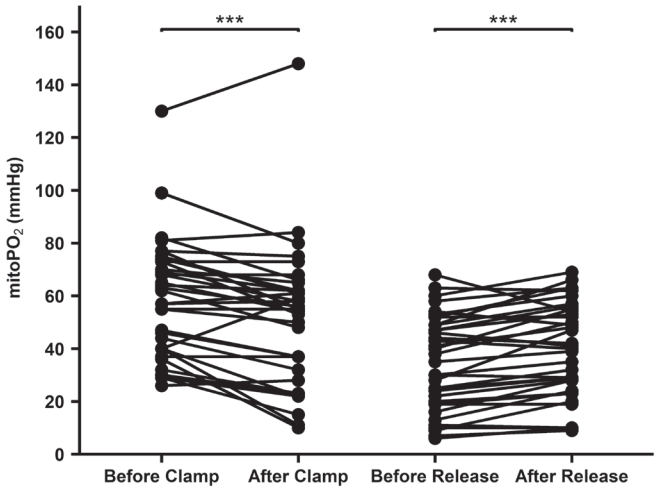

Figure 5. Cutaneous MitoPO$_2$ values before and after aortic clamping and cutaneous mitoPO$_2$ values before and after the release of aortic clamp. WU test paired p<0,01***.

Effect of aortic cross clamp at the start of CPB:

Within the second method the non-pulsatile flow occurring during the 20 minute window after commencing extracorporeal circulation during valve surgery n=19,was compared to the compared to the CABG group n=8, in which the aortic cross-clamp has not been placed. The cutaneous mitoPO$_2$ was 17.7 mmHg lower in the valve surgery group when compared to the CABG group n=8, 48.4 ± 28.8 vs. 66.0 ± 21.7 mm Hg, p=0.03. This is shown in figure 6.

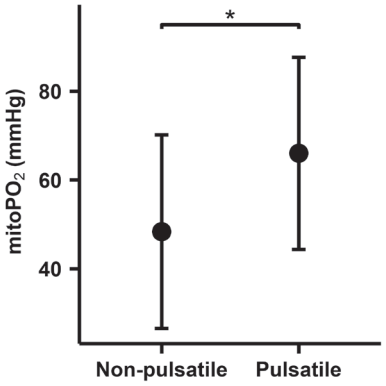

Figure 6: Comparison between valve-surgery aortic cross-clamp period and CABG non aortic cross-clamp period. An average of the 20-minute data window after the extracorporeal circulation has been running for 15 minutes per patient. Mean SD plot of cutaneous mitoPO$_2$.

Time below cutaneous mitoPO$_2$ threshold in correlation with kidney injury

4 of the 41 included patients, 9.8 %, developed post-operative CSA-AKI according to the AKICS criteria [22]. Figure 7 shows the calculation method that determines the number of minutes the cutaneous mitoPO$_2$ was below the set threshold.

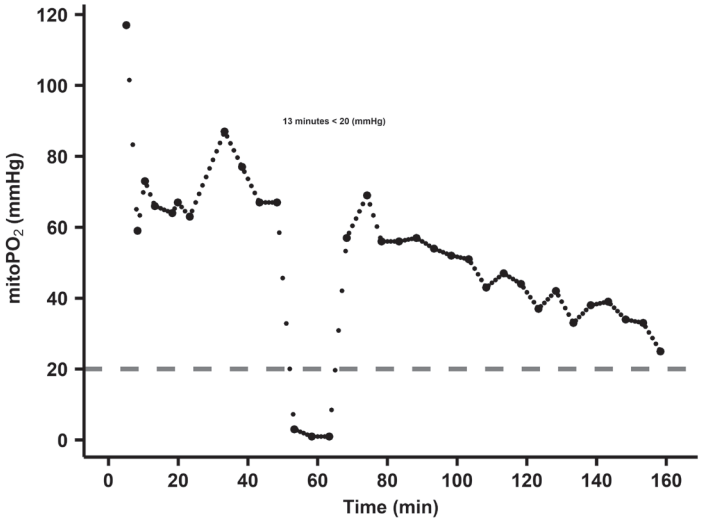

Figure 7: Example of minutes below threshold calculation. Red dots are cutaneous mitoPO$_2$ values, black dots are linear interpolated values to create a data pointfor every minute. The blue line is the threshold set on 20 mmHg. In this case the cutaneous mitoPO$_2$ was below the threshold for 13 minutes.

Within the AKI and non-AKI group the number of minutes below 20 mmHg, between 20 and 40 mmHg, and above 40 mmHg were examined. This resulted in a 50-minute median difference in duration in the lowest cutaneous mitoPO$_2$ group between AKI (58 minutes, n = 4) and non-AKI (8 minutes ,n = 37). The other threshold levels did not show larger differences as seen in figure 8A.

When examining the percentage of the procedure time spent below 20 mmHg threshold the AKI group spent 32% of CPB run time below this threshold, whereas the non-AKI group spent 8% of CPB time below this threshold, as seen in figure 8B.

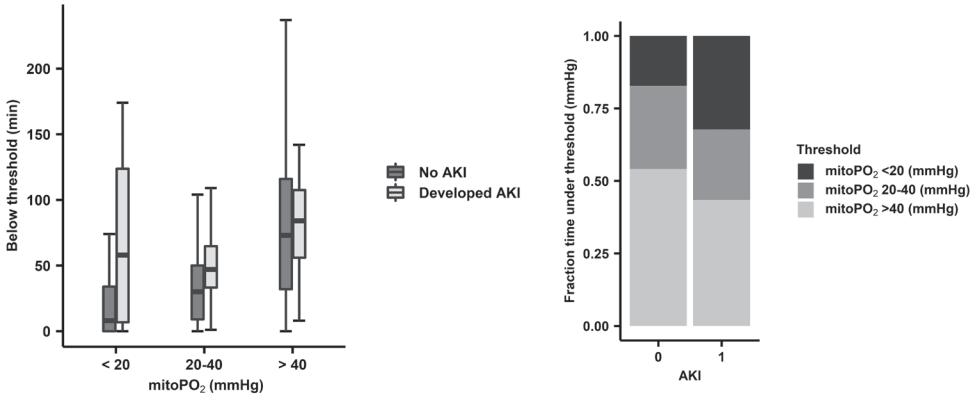

Figure 8: A) Absolute time within cutaneous mitoPO$_2$ ranges for AKI (n=4) patients and non-AKI (n=37) patients. The cutaneous mitoPO$_2$ ranges were below 20mmHg, between 20 and 40 mmHg, and above 40mmHg. Boxplot with median, IQR box and whisker 1.5 times IQR, outliers are not shown, **B*)*** Time spent within a range as a proportion of CPB/extracorporeal circulation duration. Proportion is achieved by dividing the number of minutes below threshold by CPB duration.

Discussion

This pilot study demonstrates that it is feasible to examine the cutaneous mitoPO$_2$ in patients undergoing cardiothoracic surgery requiring a CPB. The cutaneous mitoPO$_2$ was successfully measured intraoperatively using the COMET® device based on the PpIX-TLST to monitor oxygen delivery on a mitochondrial level [7]. Moreover, it was also evident that it was logistically feasible to measure the cutaneous mitoPO$_2$ during cardiothoracic procedures as all 41 patients were measured successfully without any major incidents.

The COMET® enables the non-invasive measurement of in-vivo cutaneous mitoPO$_2$ values. In this study the mean cutaneous mitoPO$_2$ level at the start of surgery was 62 ± 23 mmHg. Which is in-line with the typically reported cutaneous mitoPO$_2$ levels under baseline circumstances of 40-70 mmHg [9, 23]. This is substantially higher than the classically derived and theorized

mitoPO$_2$ values which are based on a gradual decline in PO$_2$ from the vascular, interstitial and cytosolic compartments [24-26]. Historically most studies reported low compartmental/ tissue PO$_2$ levels with values ranging from 10-17 mmHg based on measurements with oxygen electrodes [27, 28]. This has resulted in the classically derived and estimated mitoPO$_2$ value of several mmHg [24-26]. However, after the introduction of less invasive measurement techniques it was found that tissue oxygen levels were substantially higher than those measured by oxygen electrodes [29]. This has been exemplified by Bodmer et al. through the use of phosphorescence-based microvascular PO$_2$ measurements of the liver in which they measured tissue oxygen values of 60mmHg [30] as opposed to classical studies using oxygen electrode measurements in which the measured tissue oxygen was between 10-20 mmHg [31]. These recent insights into microvascular PO$_2$ suggest that the classical estimations of the mitoPO$_2$ are potentially underestimated, and are likely to be in the order of several tens of mmHg [32-34]. This is in line with the average cutaneous mitoPO$_2$ as measured by the COMET®.

It is important to note that the cutaneous mitoPO$_2$ as measured with the COMET® is an average mitochondrial oxygen tension in the measurement area under the COMET® sensor, and not the oxygen tension of a single mitochondrion. The oxygen tension in individual mitochondria is heterogenic because of the presence of an oxygen gradient necessary to drive the oxygen flux. The mitochondria in the measurement site have differing mitoPO$_2$ values influenced by the location of each mitochondrion and its oxygen consumption rate. Mitochondria in close proximity to large vessels can have a higher oxygen tension than capillaries and mitochondria located further away from capillaries and large vessels have a lower mitoPO$_2$ [35]. Our current understanding of mitoPO$_2$ advocates that it should be interpreted as an oxygen balance, depending on both oxygen supply and consumption [36].

The information emphasized in the two previous paragraphs is important for the interpretation and understanding of the cutaneous mitoPO$_2$. As of yet there is no clear threshold at which it is safe to say that the cutaneous mitoPO$_2$ as measured by the COMET® is too low and at which point an intervention must be made to increase it. In general, our knowledge about in vivo mitochondrial oxygen tension and oxygen-dependent functional and metabolic adaptation is limited. In-vitro studies have previously shown that tissue cells start adapting to available oxygen at higher mitochondrial oxygen levels than isolated mitochondria. Isolated mitochondria only experience oxygen-limited ATP production at very low mitochondrial oxygen levels of ($<$ 2 mmHg). This is due to the high oxygen affinity of the mitochondrial respiratory chain [37]. However, a study examining physiological hearts found that tissue cells started adapting to available oxygenation levels at values as high as 20-40 mmHg [38]. This oxygen-

dependence is driven through oxygen sensing mechanisms such as hypoxia-inducible factor [38-40]. Such mechanisms result in oxygen-limited ATP production at much higher oxygen levels than previously assumed. However, as the mitoPO$_2$ is an averaged value of all the mitochondria measured under the sensor a low mitoPO$_2$ value could indicate that some of these mitochondria are hypoxic and in a state of shock whilst others are not. In order to improve the understanding and interpretation of the cutaneous mitoPO$_2$ multiple clinical trials are currently being conducted.

NIRS was included in this study as it is a clinically available means to non-invasively asses tissue saturation, a measure for tissue oxygenation but actually measured in the vasculature. Unlike NIRS, in which the tissue saturation values are not calibrated, the values of the cutaneous mitoPO$_2$ are calibrated [9]. In contrast to the changes exhibited by the cutaneous mitoPO$_2$ during the CPB run times the StO$_2$ measured with NIRS did not show any significant changes. In our patient cohort only during extreme intraoperative events such as deep hypothermia with circulatory arrest the StO$_2$ also decreased. This apparent earlier or more sensitive response of cutaneous mitoPO$_2$ to microcirculatory alterations compared to NIRS has been previously demonstrated in a hemodilution study in pigs. During hemodilution cutaneous mitoPO$_2$ dropped well before the StO$_2$ did [15].

In this study we found that the cutaneous mitoPO$_2$ progressively decreases with the length of the CPB run time. This is further highlighted when comparing the baseline cutaneous mitoPO$_2$ at the start of the CPB and the cutaneous mitoPO$_2$ at the end of the CPB run, which was significantly reduced. However, after a CPB run time of 180 minutes there were few patients left, this potentially resulted in a bias as the differences in cutaneous mitoPO$_2$ were especially pronounced after 180 minutes. As previously mentioned in the introduction long CPB run times are associated with poor clinical outcomes [17]. This can be due to a myriad of factors, one of which is that patients with prolonged CPB run times are often in a worse preoperative clinical condition requiring more complex surgeries than those with shorter run times augmenting the effect of the CPB run times. However, it is widely understood that a CPB with extracorporeal circulation results in multiple physiological changes namely, a decreased blood pressure, hemodilution, hypothermia, hyperoxia and cardiac arrest each of these negatively influencing the microcirculation [41]. Moreover, the heart lung machine also influences the pharmacokinetics of drugs during CPB run times [42]. The heart lung machine itself also negatively impacts the microcirculation as contact of the non-endothelialized synthetic surface with the patient's blood leads to an activation of the innate immune system this immune reaction associated with CPB carries many similarities to the systemic immune response syndrome [19, 43, 44].

Currently, there is still no consensus whether pulsatile or non-pulsatile flow is preferred during CPB. Mainly because no clinical difference in outcome can be found, and the lack of clinical monitoring techniques to monitor differences. This study tried to evaluate if mitoPO$_2$ could be able to detect changes related to pulsatile flow. This was attempted by comparing two distinct surgery groups namely, the CABG group and the valve surgery group. As previously discussed in the methods section these two groups have different states of flow after commencing CPB. Due to the differing aortic cross-clamp times, as after cross-clamping the continuous blood flow is a result of the CPB pump. The cutaneous mitoPO$_2$ decreased significantly when the aorta was cross-clamped and increased significantly upon release and re-establishment of partial cardiac output. Other studies demonstrated similar results with Koning et al. showing that the initiation of non-pulsatile flow reduced microcirculatory perfusion and oxygenation [45]. Furthermore, when comparing on-pump versus off-pump surgeries studies have shown that off-pump CABG surgeries resulted in a less significant decrease of microcirculatory perfusion and oxygenation when compared to on-pump CABG surgeries [41, 46]. This can partially be explained by the fact that rhythmic flow variations allow for increased oxygen offloading in the microcirculation [41, 47]. These afore mentioned studies further reinforce the fact that non-pulsatile flow results in a poor microcirculatory environment, concurring with the cutaneous mitoPO$_2$ measurements found in this study.

The changes in cutaneous mitoPO$_2$ during aortic cross-clamping and before aortic cross-clamping were not only witnessed on an individual level as previously mentioned but were also witnessed when comparing patients undergoing CABG and patients undergoing valve surgery. This is because these surgeries have different aortic cross-clamping times after commencing extracorporeal circulation and thus different moments in time when the aorta is cross-clamped. The cutaneous mitoPO$_2$ was significantly higher during the period in which cardiac output with extracorporeal circulation co-existed in the 15-35 minute time frame after commencing CPB in the CABG cohort when compared to the immediate aortic cross-clamping and CPB flow during valve surgery. This further exemplifies that the patient's own cardiac output most likely improves the oxygen availability in the skin during cardiothoracic surgery requiring a CPB.

The development of AKI is a major postoperative complication after cardiothoracic surgery with an occurrence of approximately 18% [1]. The causes of AKI are multifactorial in origin with no clear single parameter or factor augmentation being able to prevent AKI. Hypotension and anemia which both result in decreased oxygen delivery capacity will synergistically contribute to the development of AKI [48]. However, the cutaneous mitoPO$_2$ measured the overall end result of oxygen delivery in which all the factors that potentially contribute to the

development in AKI play an important role. Therefore, it is hypothesized that the cutaneous mitoPO$_2$ might just be sensitive enough to detect potential perfusion issues. This is mainly due to the fact that poor perfusion in the skin and gastrointestinal tract usually prelude poor perfusion in other organs [49]. The cutaneous mitoPO$_2$ can be measured as the accumulated time below a certain low oxygen level threshold potentially highlighting poor perfusion. In this study a method has been developed to determine the number of minutes below a set threshold cutaneous mitoPO$_2$.

When comparing the duration of time that the cutaneous mitoPO$_2$ was below a certain threshold in the AKI and the non-AKI group, an association was found between the duration of time they each spent below certain thresholds. This is most evident when the cutaneous mitoPO$_2$ was below 20 mmHg where the AKI group spent more time below this threshold in absolute minutes and as a percentage of the operation's duration. However, there was a bias in this data as the more prolonged procedures also had generally lower cutaneous mitoPO$_2$ values and the negative effects associated with prolonged CPB run times, such as an increased inflammatory response, also become more pronounced [17]. It is also important to note that the eGFR in the AKI group was lower than in the non-AKI group, as a lower eGFR is a risk factor for the development of AKI. Nonetheless, as this study was not powered for a AKI and non-AKI comparison it is not possible to draw any substantial conclusions but this is of great interest in further research utilizing the COMET®.

In conclusion, this pilot study was successful in demonstrating the feasibility of this measurement technique during cardiothoracic surgical procedures. The cutaneous mitoPO$_2$ seems more sensitive to hemodynamic alterations during these surgeries than the StO$_2$. The COMET® device could potentially become a vital supplementary monitoring technique during cardiothoracic surgeries however, further specific research must be conducted to prove this.

References

1. Thiele RH, Isbell JM, Rosner MH. AKI associated with cardiac surgery. Clin J Am Soc Nephrol. 2015;10(3):500-14.
2. Holmgaard F, Vedel AG, Rasmussen LS, Paulson OB, Nilsson JC, Ravn HB. The association between postoperative cognitive dysfunction and cerebral oximetry during cardiac surgery: a secondary analysis of a randomised trial. Br J Anaesth. 2019;123(2):196-205.
3. Cartin-Ceba R, Kashiouris M, Plataki M, Kor DJ, Gajic O, Casey ET. Risk factors for development of acute kidney injury in critically ill patients: a systematic review and meta-analysis of observational studies. Crit Care Res Pract. 2012;2012:691013.
4. Young RW. Hyperoxia: a review of the risks and benefits in adult cardiac surgery. J Extra Corpor Technol. 2012;44(4):241-9.
5. Spoelstra-de Man AM, Smit B, Oudemans-van Straaten HM, Smulders YM. Cardiovascular effects of hyperoxia during and after cardiac surgery. Anaesthesia. 2015;70(11):1307-19.
6. Mik EG, Stap J, Sinaasappel M, Beek JF, Aten JA, van Leeuwen TG, et al. Mitochondrial PO2 measured by delayed fluorescence of endogenous protoporphyrin IX. Nat Methods. 2006;3(11):939-45.
7. Ubbink R, Bettink MAW, Janse R, Harms FA, Johannes T, Munker FM, et al. A monitor for Cellular Oxygen METabolism (COMET): monitoring tissue oxygenation at the mitochondrial level. J Clin Monit Comput. 2017;31(6):1143-50.
8. Ubbink R, Wefers Bettink MA, van Weteringen W, Mik EG. Mitochondrial oxygen monitoring with COMET: verification of calibration in man and comparison with vascular occlusion tests in healthy volunteers. J Clin Monit Comput. 2020.
9. Mik EG, Balestra GM, Harms FA. Monitoring mitochondrial PO2: the next step. Curr Opin Crit Care. 2020;26(3):289-95.
10. Harms FA, Stolker RJ, Mik EG. Correction: Cutaneous Respirometry as Novel Technique to Monitor Mitochondrial Function: A Feasibility Study in Healthy Volunteers. PLoS One. 2016;11(9):e0163399.
11. Harms FA, Brandt-Kerkhof ARM, Mik EG. Monitoring of mitochondrial oxygenation during perioperative blood loss. BMJ Case Rep. 2021;14(1).
12. Harms FA, Mik EG. In Vivo Assessment of Mitochondrial Oxygen Consumption. Methods Mol Biol. 2021;2277:175-85.
13. Murkin JM, Arango M. Near-infrared spectroscopy as an index of brain and tissue oxygenation. Br J Anaesth. 2009;103 Suppl 1:i3-13.
14. Chan MJ, Chung T, Glassford NJ, Bellomo R. Near-Infrared Spectroscopy in Adult Cardiac Surgery Patients: A Systematic Review and Meta-Analysis. J Cardiothorac Vasc Anesth. 2017;31(4):1155-65.
15. Romers LH, Bakker C, Dollee N, Hoeks SE, Lima A, Raat NJ, et al. Cutaneous Mitochondrial PO2, but Not Tissue Oxygen Saturation, Is an Early Indicator of the Physiologic Limit of Hemodilution in the Pig. Anesthesiology. 2016;125(1):124-32.
16. Ubbink R, te Boekhorst PAW, Mik EG. Novel technique to monitor effect of transfusion on mitochondrial oxygenation 2015.
17. Madhavan S, Chan SP, Tan WC, Eng J, Li B, Luo HD, et al. Cardiopulmonary bypass time: every minute counts. J Cardiovasc Surg (Torino). 2018;59(2):274-81.
18. Barry AE, Chaney MA, London MJ. Anesthetic management during cardiopulmonary bypass: a systematic review. Anesth Analg. 2015;120(4):749-69.

19. Dekker NAM, Veerhoek D, Koning NJ, van Leeuwen ALI, Elbers PWG, van den Brom CE, et al. Postoperative microcirculatory perfusion and endothelial glycocalyx shedding following cardiac surgery with cardiopulmonary bypass. Anaesthesia. 2019;74(5):609-18.
20. Lee JH, Park YH, Kim HS, Kim JT. Comparison of two devices using near-infrared spectroscopy for the measurement of tissue oxygenation during a vascular occlusion test in healthy volunteers (INVOS(R) vs. InSpectra). J Clin Monit Comput. 2015;29(2):271-8.
21. Team RDC. R: A Language and Environment for Statistical Computing. 2019.
22. Summary of Recommendation Statements. Kidney International Supplements. 2012;2(1):8-12.
23. Keeley TP, Mann GE. Defining Physiological Normoxia for Improved Translation of Cell Physiology to Animal Models and Humans. Physiol Rev. 2019;99(1):161-234.
24. Wittenberg BA, Wittenberg JB. Transport of oxygen in muscle. Annu Rev Physiol. 1989;51:857-78.
25. Gnaiger E, Lassnig B, Kuznetsov A, Rieger G, Margreiter R. Mitochondrial oxygen affinity, respiratory flux control and excess capacity of cytochrome c oxidase. J Exp Biol. 1998;201(Pt 8):1129-39.
26. Gayeski TE, Honig CR. Intracellular PO2 in individual cardiac myocytes in dogs, cats, rabbits, ferrets, and rats. Am J Physiol. 1991;260(2 Pt 2):H522-31.
27. Rumsey WL, Pawlowski M, Lejavardi N, Wilson DF. Oxygen pressure distribution in the heart in vivo and evaluation of the ischemic “border zone”. Am J Physiol. 1994;266(4 Pt 2):H1676-80.
28. Trochu JN, Bouhour JB, Kaley G, Hintze TH. Role of endothelium-derived nitric oxide in the regulation of cardiac oxygen metabolism: implications in health and disease. Circ Res. 2000;87(12):1108-17.
29. Wilson DF. Quantifying the role of oxygen pressure in tissue function. Am J Physiol Heart Circ Physiol. 2008;294(1):H11-3.
30. Bodmer SI, Balestra GM, Harms FA, Johannes T, Raat NJ, Stolker RJ, et al. Microvascular and mitochondrial PO(2) simultaneously measured by oxygen-dependent delayed luminescence. J Biophotonics. 2012;5(2):140-51.
31. Jamieson D, van den Brenk HA. Electrode size and tissue pO2 measurement in rats exposed to air or high pressure oxygen. J Appl Physiol. 1965;20(3):514-8.
32. Kekonen EM, Jauhonen VP, Hassinen IE. Oxygen and substrate dependence of hepatic cellular respiration: sinusoidal oxygen gradient and effects of ethanol in isolated perfused liver and hepatocytes. J Cell Physiol. 1987;133(1):119-26.
33. Giraudeau C, Djemai B, Ghaly MA, Boumezbeur F, Meriaux S, Robert P, et al. High sensitivity 19F MRI of a perfluorooctyl bromide emulsion: application to a dynamic biodistribution study and oxygen tension mapping in the mouse liver and spleen. NMR Biomed. 2012;25(4):654-60.
34. Liu S, Shah SJ, Wilmes LJ, Feiner J, Kodibagkar VD, Wendland MF, et al. Quantitative tissue oxygen measurement in multiple organs using 19F MRI in a rat model. Magn Reson Med. 2011;66(6):1722-30.
35. Golub AS, Popel AS, Zheng L, Pittman RN. Analysis of phosphorescence in heterogeneous systems using distributions of quencher concentration. Biophys J. 1997;73(1):452-65.
36. Mik EG. Special article: measuring mitochondrial oxygen tension: from basic principles to application in humans. Anesth Analg. 2013;117(4):834-46.
37. Wilson DF, Harrison DK, Vinogradov SA. Oxygen, pH, and mitochondrial oxidative phosphorylation. J Appl Physiol (1985). 2012;113(12):1838-45.
38. Tuckerman JR, Zhao Y, Hewitson KS, Tian YM, Pugh CW, Ratcliffe PJ, et al. Determination and comparison of specific activity of the HIF-prolyl hydroxylases. FEBS Lett. 2004;576(1-2):145-50.
39. Yu AY, Frid MG, Shimoda LA, Wiener CM, Stenmark K, Semenza GL. Temporal, spatial, and oxygen-regulated expression of hypoxia-inducible factor-1 in the lung. Am J Physiol. 1998;275(4):L818-26.

40. Majmundar AJ, Wong WJ, Simon MC. Hypoxia-inducible factors and the response to hypoxic stress. Mol Cell. 2010;40(2):294-309.
41. Koning NJ, Atasever B, Vonk AB, Boer C. Changes in microcirculatory perfusion and oxygenation during cardiac surgery with or without cardiopulmonary bypass. J Cardiothorac Vasc Anesth. 2014;28(5):1331-40.
42. Holley FO, Ponganis KV, Stanski DR. Effect of cardiopulmonary bypass on the pharmacokinetics of drugs. Clin Pharmacokinet. 1982;7(3):234-51.
43. Rosenthal LM, Tong G, Wowro S, Walker C, Pfitzer C, Bottcher W, et al. A Prospective Clinical Trial Measuring the Effects of Cardiopulmonary Bypass Under Mild Hypothermia on the Inflammatory Response and Regulation of Cold-Shock Protein RNA-Binding Motif 3. Ther Hypothermia Temp Manag. 2020;10(1):60-70.
44. Robich M, Ryzhov S, Kacer D, Palmeri M, Peterson SM, Quinn RD, et al. Prolonged Cardiopulmonary Bypass is Associated With Endothelial Glycocalyx Degradation. J Surg Res. 2020;251:287-95.
45. Koning NJ, Vonk AB, van Barneveld LJ, Beishuizen A, Atasever B, van den Brom CE, et al. Pulsatile flow during cardiopulmonary bypass preserves postoperative microcirculatory perfusion irrespective of systemic hemodynamics. J Appl Physiol (1985). 2012;112(10):1727-34.
46. De Backer D, Dubois MJ, Schmartz D, Koch M, Ducart A, Barvais L, et al. Microcirculatory alterations in cardiac surgery: effects of cardiopulmonary bypass and anesthesia. Ann Thorac Surg. 2009;88(5):1396-403.
47. Kislukhin VV. Stochasticity of flow through microcirculation as a regulator of oxygen delivery. Theor Biol Med Model. 2010;7:29.
48. Haase M, Bellomo R, Story D, Letis A, Klemz K, Matalanis G, et al. Effect of mean arterial pressure, haemoglobin and blood transfusion during cardiopulmonary bypass on post-operative acute kidney injury. Nephrol Dial Transplant. 2012;27(1):153-60.
49. Dantzker DR. The gastrointestinal tract. The canary of the body? JAMA. 1993;270(10):1247-8.

Chapter 10

Summary and Conclusion

Mitochondria are the powerhouses of a cell and are essential to maintain energy availability with the usage of oxygen. Although several measurement techniques are available to evaluate oxygen consumption and mitochondrial metabolism, no clinical measurement technique was available on the bedside to monitor mitochondrial oxygen tension. Harms et al. introduced the first clinical device to measure mitochondrial oxygen tension with the triplet state lifetime technique. This clinical research device brought the laboratory setup to the clinic. The next step was the development of a relatively small, transportable, and certified device for medical use. Such a device was developed and put on market in 2016.

The newly available monitoring device COMET (Photonics Healthcare, Utrecht, The Netherlands) was first introduced in the operating theatre. The introduction of COMET has been reported in **chapter 3**. After the application of 5-aminolevulinic acid plaster on the human skin, an adequate signal of PpIX could be detected in the majority of patients. An incidental finding was done during neurosurgery. One patient got administered clonidine to treat persisting intraoperative hypertension, but an initial phase of peripheral vasoconstriction occurred due to too rapid administration. Microvascular flow and velocity measured with laser-doppler (O2C, LEA Medizinetechnik, Heuchelheim, Germany) decreased by 44 and 16%, respectively. The venous-capillary oxygen saturation did not decrease during the vasoconstriction. Mitochondrial oxygen tension also decreased from 48 to 16 mmHg and provided complimentary data as a newly available parameter compared to hemoglobin saturation-based measurements.

The Pp-IX lifetime technique used in COMET has been calibrated in cell cultures, isolated organs (heart and liver), and in vivo animals. The first reported values of mitoPO_2 in healthy volunteers were around 44 mmHg (5.9kPa) and 66 mmHg (8.8 kPa). These reported mitoPO_2 values deviate from the tension reported to a textbook of 7.5mmHg (1kPa) at the mitochondrial level. Therefore, there was a need to validate the mitoPO_2 values in the human skin. This was done in **chapter 4**, which describes the comparison of mitoPO_2 with arterial blood gas samples. With topical application of cyanide on the skin that blocks mitochondrial respiration, mitoPO_2 could be compared with arterial blood gas PaO_2 levels. After cyanide application, the mitoPO_2 measurements done with COMET was median 94.1 mmHg [87.2-110.9] and did not differ significantly (n=9, p=0.5) from the PaO_2 of 101.0 [98.0-106.0]. These results demonstrated that animal experiments initially determined calibration parameters are valid for human cutaneous measured mitoPO_2.

In the second part of this study, we compared the mitoPO_2 deoxygenation kinetics with O2C, OxiVenT™, and INVOS parameters during a vascular occlusion test. During arterial occlusion, all oxygenation parameters show a decline in a comparable rate. However, during a dynamic measurement for measuring mitochondrial oxygen consumption (mitoVO_2), a faster decline

is seen with pressure on the measurement probe. As a result, this part showed that applying pressure on the COMET Skin Sensor is of great importance to clear the measurement site of available oxygen-carrying erythrocytes. Without a technique to eliminate this oxygen buffer, the consumption measurement underestimates the actual mitochondrial oxygen consumption.

At the dermatology department, photodynamic therapy (PDT) is used to treat superficial skin lesions. The same precursor (5-aminolevulinic acid) is used for photodynamic treatment compared to mitoPO$_2$ measurements. Oxygen availability is one of the critical components in PDT to create reactive oxygen species that sequentially will induce cellular apoptosis. We report in **chapter 5** a study that measured mitoPO$_2$ before and after a PDT session. Overall, the signal quality was adequate in all patients before the PDT session started. Afterwards, the signal quality was drastically decreased, primarily due to photobleaching. In general, most skin lesions were a few millimeters in size, included in this study. The COMET Skin Sensor is 70x20 mm in size. Therefore, it was hard first to find the small lesion's exact location and perform steady measurements.

In **chapter 6,** we describe the use of COMET during a red blood cell transfusion. We hypothesized that the mitoPO$_2$ would increase if RBCTs were given. The hypothesis was tested with the inclusion of chronic anemia patients because they regularly get an RBCT prescribed. The mitoPO$_2$ could increase because of two main mechanisms. Firstly, the increase in RBC oxygen transport capacity, secondly a volume increase that results in an increased cardiac output. To evaluate the volume effect also a fluid challenge was given before or after an RBCT.

In contrast to our hypothesis, the mitoPO$_2$ did not increase during an RBCT, nor did it upon a fluid challenge; it even tended to decrease during an RBCT for chronic anemic patients.

Only in a few cases when the mitoPO$_2$ baseline was low, the mitoPO$_2$ increased after an RBCT. An increase during RBCT while the mitoPO$_2$ is relatively low was also seen is a case study intraoperatively and an animal hemodilution study. It suggests that the mitoPO$_2$ will not increase directly on every RBCT, but there is an individual threshold under which RBCT directly benefits the mitoPO$_2$.

Tissue ischemia is the result of an inadequate oxygen supply towards the tissues. Ischemia can result from inadequate RBC oxygen transport capacity, treated by RBCT, or caused by inadequate flow. Arterial stenosis can cause a flow limitation that also leads to ischemia. Stenosis in mesenteric arteria can lead to chronic mesenteric ischemia (CMI). Currently, the standard diagnostic tool in CMI diagnosis is visible light spectroscopy (VLS).

Chapter 7 describes a study done in a porcine model that compared VLS with a calibrated palladium porphyrin-based oxygen tension measurement. We showed that VLS measured

a reasonable saturation after asystole of 25 minutes. Furthermore, there was an inverse relationship between the fraction of inspired oxygen and VLS saturation. Therefore, VLS showed a low correlation with local ischemia. It showed that VLS measures mixed venous hemoglobin oxygen saturation rather than the mucosal capillary oxygen saturation. It remains the question of whether mixed venous hemoglobin oxygen saturation is the correct measure for mucosal ischemia.

In CMI, there is a need for a reliable, easy-to-use functional test. Since mitoPO$_2$ measures the oxygen tension where the oxygen is used, it is reasonable to study the feasibility of mitoPO$_2$ in CMI. With the installed large skin sensor on COMET, this was not possible. In **chapter 8,** we describe the development of the configuration that could be used through the working channel of an endoscope. The pilot study showed that measurement of oxygen-dependent delayed fluorescence of ALA-induced PpIX during upper GI endoscopy is feasible and safe. Further research is needed for the clinical applicability of this technique in the diagnostic workup of CMI.

Lastly, mitoPO$_2$ was measured perioperatively in patients on cardiopulmonary bypass (CPB). The use of CPB during cardiac surgery has a profound effect on the human body. Since circulation, respiration, homeostasis, and thermoregulation are all affected by CPB. It is essential to supply an adequate oxygen supply to preserve organ function. Unfortunately, acute kidney injury (AKI) is still a common complication after cardiac surgery, mainly because of susceptibility to hypoxia due to their high metabolic activity. Near-infrared spectroscopy (NIRS) is a widely used technique to monitor cerebral tissue saturation (StO$_2$) during CPB. In **chapter 9**, the pilot study compared StO$_2$ with mitoPO$_2$ during CPB. Furthermore, the influence of hemodynamic variation on mitoPO$_2$ has been studied, and if the development of AKI correlates with mitoPO$_2$ levels.

In total, 41 patients were included in this study. The median MitoPO$_2$ at the start of surgery was 63.5 mmHg and significantly decreased to 36.4 mmHg ($p<0.01$) by the end of surgery. The median StO$_2$ was 80.5% and did not change significantly to 80.0 by the end of surgery. Also, during the change from pulsatile to non-pulsatile flow resulting from aortic clamping, the mitoPO$_2$ significantly decreased. The mitoPO$_2$ did prove sensitive to hemodynamic alterations during the surgeries and could prove to be a vital supplementary monitoring technique during these operations.

Conclusion

Mitochondrial oxygen tension is entering a new phase in which it can be explored in a wide variety of fields. This thesis describes the applicability of mitoPO$_2$ within Anesthesiology, Dermatology, Hematology, Gastro- hepatology, and Thoracic Surgery.

Oxygen is such a fundamental and essential element used in cellular metabolism and a research topic with many open research questions. Several applications have been studied within this thesis, but since this is only the introduction of a new measurement parameter. It led to many more questions than answers. We realize that the more we discover about the mitochondria and their use of oxygen, the more we do not know. Further research is needed in each field to investigate its potential.

Chapter 11

General discussion and Future perspectives

We reported the use of non-invasive mitochondrial oxygen tension measurements with the Pp-IX triplet state delayed fluorescence technique. With the introduction of COMET, we were able to measure at different locations and types of patients. The main goal was to investigate the clinical applicability of mitochondrial oxygen tension with the triplet state lifetime technique. We successfully measured in the operating theatre during neuro and thoracic surgery, at the dermatology department before and after a photodynamic therapy session, during a red blood cell transfusion at the hematology department, and through a working channel of an endoscope at the gastroenterology department. Each study can be seen as an introduction or a pilot study to evaluate the applicability and potential.

We brought the mitoPO$_2$ measurement technique to the operating theatre for the first time and performed successful measurements during neurosurgery. Furthermore, in **chapter 3**, we demonstrate that mitochondrial oxygen tension is sensitive for microcirculatory flow alternations. Compared with venous-capillary saturation measurement techniques, mitoPO$_2$ provided information from a different location. Hemoglobin saturation-based techniques gather information from blood, arterial/venous, or a combination of both. MitoPO$_2$ gives intracellular information about where the oxygen is actually used and can be seen as complementary information [1].

Pp-IX used for the mitoPO$_2$ measurement is present in cells with active mitochondria [2]. Although present, insufficient in concentration for mitoPO$_2$ measurement with the current measurement signal sensitivity and setup. The conversion of the precursor ALA applied on the skin takes around 4- hours minimum. Therefore, the mitoPO$_2$ measurement cannot be used in an emergency setup. Patients need to be pre-selected, and the targeted measurement area should be given a precursor of Pp-IX in advance.

Another point of care for the mitoPO$_2$ measurement, in general, is the sensitivity for external pressure. We demonstrated in **chapter 4** that pressure applied on the COMET Skin Sensor pushes away the erythrocytes from the measurement area and stops the superficial microvascular flow. This can be used to do mitoVO$_2$ measurements without the erythrocyte buffer. However, since the microcirculatory pressure is low, the flow can be alternated with a small amount of external pressure. Even traction on the skin might influence microcirculation. Therefore, the Skin Sensor itself should be applied with great care.

MitoPO$_2$ has been calibrated in cell cultures, isolated organs, and in vivo animals [3–5]. The first reported values were around 44 mmHg (5.9kPa) [6] and 66 mmHg (8.8 kPa) [7] in healthy volunteers. These reported values deviate from the tension reported to a textbook of 7.5 mmHg (1kPa) at the mitochondrial level [8]. In **chapter 4,** we validated the calibration

constants for mitoPO$_2$ on the human skin. In comparison with the 'gold standard' blood gas analyzer, the values did not differ significantly.

As shown in **chapter 5,** mitoPO$_2$ can be measured in 5-aminolevulinic acid photodynamic therapy (ALA-PDT) at the dermatology department. An adequate Pp-IX signal was detected after the 4 hour application period on the lesions. After the illumination session, de Pp-IX signal deteriorated, mainly because of photobleaching.

At the hematology department, red blood cell transfusions (RBCT) are given on a regular basis to chronic anemic patients. In **chapter 6,** we show that against our hypothesis, the mitoPO$_2$ decreases in the majority of transfusions. Only in a few cases when the mitoPO$_2$ baseline was low the mitoPO$_2$ increased after an RBCT. If we look at the limited amount of studies done at the microvascular level, we also see that not all RBCT improve microvascular parameters [9]. Only in non-adapted/ compensated patients for low hemoglobin levels, such as trauma or cardiothoracic patients, an increase of microcirculatory values is seen [10, 11]. This might correspond with our finding that not all RBCT will directly improve mitoPO$_2$. The question remains what the main mechanisms are that may influence this oxygen balance on a cellular level. It is a difficult study topic since many mechanisms influence this balance, such as, RBC deformability, viscosity, 2-3 DPG, nitric oxide, chronic compensation, and metabolic need.

MitoPO$_2$ is generally measured on the skin because of easy accessibility and the non-invasiveness. Measurement on the skin can be seen as a 'canary' function for inadequate oxygen supply [12, 13]. On the other hand, intestinal ischemia is commonly accepted as the first site to suffer from inadequate oxygen supply. Currently, visible light spectroscopy is used to diagnose chronic mesenteric ischemia. we demonstrated that VLS still measured a reasonable saturation after 25 minutes of asystole of a porcine model. It showed that VLS measures mixed venous hemoglobin oxygen saturation rather than the mucosal capillary oxygen saturation. It remains the question of whether mixed venous hemoglobin oxygen saturation is the correct measure for mucosal ischemia. Therefore, we demonstrated in **chapter 8** that mitoPO$_2$ measurements are feasible with an optical fiber through an endoscope after orally ALA intake.

We demonstrated in **chapter 9** that mitoPO$_2$ can be of importance during cardiopulmonary bypass during cardiac surgery. The mitoPO$_2$ did prove sensitive to hemodynamic alterations during the surgeries and could prove to be a vital supplementary monitoring technique during these operations.

In each field, oxygen plays an essential role in treatment, but surprisingly, in most cases, we do not understand the precise mechanism of oxygen delivery and consumption on a mitochondrial level. With the non-invasive mitoPO$_2$ measurement, we could gain more knowledge on the cellular and subcellar levels.

Intraoperatively we have seen that mitoPO$_2$ is sensitive to hemodynamic changes. MitoPO$_2$ reflects changes in oxygen delivery on a tissue level. Further research could be done to detect whether there is a mitoPO$_2$ threshold for hypoxia. We have reported that mitoPO$_2$ might not improve directly upon a red blood cell transfusion (RBCT) for every patient. We hypothesize that a certain mitoPO$_2$ threshold is present before the mitoPO$_2$ will increase upon an RBCT. In anemia patients, this might be lower because of improved individual coping of hypoxemia due to adaptation [9]. MitoPO$_2$ could play a role in the search for a guide in managing RBCT on an individual level. The overall question remains what a sufficient oxygen supply is in an individual. The lack of knowledge becomes evident with RBCT but also during cardio pulmonary bypass (CPB). In both cases, there is no individual estimate of what the patient minimally needs.

The question of adequate oxygen supply on a tissue level is evident in the following cases but not limited to this list:

- The decision to give a red blood cell transfusion;
- The decision to give a fluid challenge if vascular underfilling is the underlying cause;
- Individual need of oxygen supply during cardiopulmonary bypass;
- Individual need of oxygen supply extracorporeal life support;
- Free tissue flap evaluation in plastic surgery;
- Adequate oxygen supply during warm oxygen perfusion;
- Oxygen tension measurement in tumor tissue during photodynamic therapy;
- In septic patients, whether oxygen supply is the root cause for decreased cellular function or mitochondrial dysfunction results in reduced cellular functionality;
- Evaluation of oxygen supply towards the extremities after percutaneous transluminal angioplasty to improve blood flow;
- Evaluation of chronic mesenteric ischemia.

As a study example, I would suggest that we look into the individual need of oxygen supply during cardiopulmonary bypass to prevent the common complication of acute kidney injury. A minimum amount of oxygen delivery has been suggested of 270 ml/min/m^2 during CPB [14].

A longer period of time below this value has been associated with AKI [15]. Currently, the suggested flow, cardiac output, is determined by the 2,4*BSA of the patient. However, with fever, obesity, sepsis, or other pathophysiological changes, the VO_2 can vary and deviate from the calculated given DO_2 from BSA. Several parameters can measure the imbalance of DO_2/VO_2. With mitoPO_2 oxygen disappearance rate (mitoVO_2), we can determine the cellular respiration at a given time point. Since the input and output of oxygen can be measured during CPB, we can calculate the VO_2. We could try in this setting to validate the mitoVO_2 with the VO_2 during CPB. The mitoPO_2 is a balance between oxygen delivery towards the cells and consumption simultaneously. From this balance, we should be able to determine the minimum DO_2 value of 270 ml/min/m^2.

It would be interesting to look at the correlation between the mitoVO_2 during bypass and the calculated VO_2 from the blood. Anaerobic parameters such as lactate elevation and respiration quotient >1 could detect an oxygen deficit and CO_2 production corresponding with a DO_2/VO_2 imbalance and anaerobic metabolism.

Temperature is also known to influence mitochondrial metabolism. The measured mitoVO_2 changes during temperature change should also correspond to the change in VO_2 calculated from the DO_2 delivered and oxygen content that returns in the venous line of the CPB. Potentially preoperative mitoVO_2 might determine an individual CPB flow instead of general BSA or change CPB treatment during low hematocrit status or increased VO_2.

A major step forwards on the technical side would be that the delay of 4 hours ALA application time would be overcome. Either by increased PpIX signal sensitivity, and a decrease of external disturbing factors such as light and sensor stability. This will increase the potential to measure in an emergency situation, and guide decision making when time is critical.

The future perspective is that we further understand the mitochondrial need for such a fundamental parameter as oxygen tension and consumption on an individual level.

References

1. Mik EG, Stap J, Sinaasappel M, et al (2006) Mitochondrial PO_2 measured by delayed fluorescence of endogenous protoporphyrin IX. Nat Methods 3:939–45. https://doi.org/10.1038/nmeth940
2. Gardner LC, Smith SJ, Cox TM (1991) Biosynthesis of delta-aminolevulinic acid and the regulation of heme formation by immature erythroid cells in man. J Biol Chem 266:22010–8.
3. Mik EG, Ince C, Eerbeek O, et al (2009) Mitochondrial oxygen tension within the heart. J Mol Cell Cardiol 46:943–951. https://doi.org/10.1016/j.yjmcc.2009.02.002
4. Mik EG, Johannes T, Zuurbier CJ, et al (2008) In vivo mitochondrial oxygen tension measured by a delayed fluorescence lifetime technique. Biophys J 95:3977–90. https://doi.org/10.1529/biophysj.107.126094
5. Mik EG, Stap J, Sinaasappel M, et al (2006) Mitochondrial PO_2 measured by delayed fluorescence of endogenous protoporphyrin IX. Nat Methods 3:939–45. https://doi.org/10.1038/nmeth940
6. Harms FA, Stolker RJ, Mik EG (2016) Cutaneous Respirometry as Novel Technique to Monitor Mitochondrial Function: A Feasibility Study in Healthy Volunteers. PLoS One 11:e0159544. https://doi.org/10.1371/journal.pone.0159544
7. Baumbach P, Neu C, Derlien S, et al (2018) A pilot study of exercise-induced changes in mitochondrial oxygen metabolism measured by a cellular oxygen metabolism monitor (PICOMET). Biochim Biophys acta Mol basis Dis. https://doi.org/10.1016/j.bbadis.2018.12.003
8. Chambers D, Huang C, Matthews G (2019) Basic physiology for anaesthetists. Cambridge University Press.
9. Liu W, He H, Ince C, Long Y (2021) The effect of blood transfusion on sublingual microcirculation in critically ill patients: A scoping review. Microcirculation 28:1–10. https://doi.org/10.1111/micc.12666
10. Yuruk K, Bartels SA, Milstein DMJ, et al (2012) Red blood cell transfusions and tissue oxygenation in anemic hematology outpatients. Transfusion 52:641–646. https://doi.org/10.1111/j.1537-2995.2011.03312.x
11. Yuruk K, Almac E, Bezemer R, et al (2011) Blood transfusions recruit the microcirculation during cardiac surgery. Transfusion 51:961–967. https://doi.org/10.1111/j.1537-2995.2010.02971.x
12. Römers LHL, Bakker C, Dollée N, et al (2016) Cutaneous Mitochondrial PO_2, but Not Tissue Oxygen Saturation, Is an Early Indicator of the Physiologic Limit of Hemodilution in the Pig. Anesthesiology 125:124–32. https://doi.org/10.1097/ALN.0000000000001156
13. O'Brien EO, Schmidt U (2016) Cellular Hypoxia in a Brand New Light. Anesthesiology 125:20–21
14. Ranucci M, Romitti F, Isgrò G, et al (2005) Oxygen delivery during cardiopulmonary bypass and acute renal failure after coronary operations. Ann Thorac Surg 80:2213–2220. https://doi.org/10.1016/j.athoracsur.2005.05.069
15. de Somer F, Mulholland JW, Bryan MR, et al (2011) O2delivery and CO2production during cardiopulmonary bypass as determinants of acute kidney injury: Time for a goal-directed perfusion management? Crit Care 15:. https://doi.org/10.1186/cc10349

Chapter 12

Nederlandse samenvatting

Nederlandse samenvatting

Mitochondriën zijn kleine organellen in een cel die verantwoordelijk zijn voor de energieproductie. Ze gebruiken zuurstof om efficiënt energie voor de cel te maken. In 2015 is het eerste klinische apparaat ontwikkeld die de hoeveelheid zuurstof en het zuurstofverbruik op mitochondriaal niveau kan meten. Dit apparaat, de COMET, is een relatief kleine en transporteerbare monitor die in 2016 een CE-certificaat heeft verkregen. De COMET kwam in 2016 op de markt en wordt sinds die tijd in verschillende centra voor klinisch onderzoek ingezet.

De COMET (Photonics Healthcare, Utrecht, The Netherlands) werd als eerste gebruikt in de operatiekamer van het Erasmus MC. De monitor zelf en het eerste klinische gebruik hiervan wordt beschreven in **hoofdstuk 3** van dit proefschrift. De COMET meet zuurstof op basis van zuurstofafhankelijke optische eigenschappen van de lichaamseigen stof protoporfyrine IX (PpIX). Voor de meting wordt er een 5-amininolevulinezuur (ALA) pleister op de huid gepakt. De ALA uit de pleister wordt door de mitochondriën in PpIX omgezet en door locale PpIX ophoping is er genoeg PpIX om de mitochondriale zuurstofspanning (mitoPO$_2$) te kunnen meten. Om mitoPO^2 te meten, bestralen we de PpIX met groen licht, wat vervolgens zelf weer licht uitstraalt in de vorm van rode directe fluorescentie en vertraagde fluorescentie. Hoe lang deze PpIX moleculen vertraagd licht geven, uitgedrukt als de uitdooftijd van de vertraagde fluorescentie, is afhankelijk van de hoeveel zuurstof. De techniek is gevoelig voor verstoring van buitenaf, maar we hebben in deze studie laten zien dat met de COMET in de klinische setting van een operatiekamer mitoPO$_2$ kan worden gemeten.

Er is daarnaast gezien dat bij een patiënt die een bolus kreeg van medicatie die bloedvaten kan vernauwen er een sterke afname was in mitoPO$_2$. Opvallend was dat deze daling niet werd gezien met een weefsel saturatie meter (O2C, LEA Medizinetechnik, Heuchelheim, Duitsland). De weefsel saturatie is het percentage rode bloedcellen waar zuurstof aan gebonden is op het niveau van de microcirculatie. Dit resultaat suggereert dat mitoPO$_2$ gevoeliger is om een tekort aan zuurstof op weefselniveau te detecteren en een toevoeging is ten opzichte van de huidige meetmethoden.

De meettechniek die gebruikt wordt om mitoPO$_2$ te meten is gekalibreerd in cellijnen en proefdiermodellen, echter nog niet op de menselijke huid. In **hoofdstuk 4** valideren we de eerder verkregen kalibratie. Door de mitochondriën van de huid tijdelijk geen zuurstof te laten gebruiken, door lokale toediening van een stof die de mitochondriale ademhalingsketen blokkeert (Cyanide), is de mitoPO$_2$ tijdelijk gelijk aan de zuurstofspanning in het arteriële bloed die met een valideerde techniek kan worden gemeten. Het resultaat laat zien dat onder zulke omstandigheden de mitoPO$_2$ en de arteriële zuurstofspanning gelijk zijn en dat dus de bepaalde kalibratie constanten valide zijn voor het toepassen op de menselijke huid.

In het tweede deel van deze studie, ook beschreven in **hoofdstuk 4**, hebben we de kinetiek van de daling van mitoPO$_2$ door zuurstofverbruik vergeleken met de kinetiek van zuurstofdaling zoals die met andere monitoring technieken zoals O2C, OxiVent™ en INVOS wordt gemeten. We hebben zuurstof verbruik bekeken na het snel afsluiten van de bloedtoevoer naar de arm met een bloeddrukband. Het effect van deze regionale zuurstofblokkade is vergeleken met het effect van lokale zuurstofblokkade die kan worden verkregen door de COMET skin sensor in de huid te duwen (hierdoor worden lokaal de kleine bloedvaten afgesloten). Hiermee hebben we laten zien dat het drukken op de COMET Skin Sensor belangrijk is omdat dit de rode bloedcellen, die zuurstof bevatten, uit het meetgebied evacueert. Zonder deze druktechniek zorgen de rode bloedcellen voor een zuurstofvoorraad in het meetvolume en zal het mitochondriale zuurstof verbruik in werkelijkheid hoger zijn dan wat gemeten wordt.

In de dermatologie wordt fotodynamische therapie (PDT) gebruikt voor het behandelen van oppervlakkige huidaandoeningen. Hierbij wordt dezelfde medicatie gebruikt als bij de mitoPO$_2$ meting, namelijk ALA dat omgezet wordt naar PpIX. De zuurstofbeschikbaarheid in de aandoening van de huid is één van de cruciale factoren bij fotodynamische therapie om het goed te laten werken. Door het toegediende licht tijdens PDT wordt zuurstof omgezet in zuurstofradicalen die zorgen dat cellen in geprogrammeerde celdood gaan. In **hoofdstuk 5** geven we de resultaten van mitoPO$_2$ metingen in patiënten voor en na een PDT-sessie. De signaalkwaliteit was bij alle patiënten goed voordat de eerste PDT-sessie startte. Hierna nam de kwaliteit van het signaal drastisch af, hoofdzakelijk doordat door overbelichting van PpIX het molecule openbreekt, een proces dat “photo bleaching” wordt genoemd. Over het algemeen bleken de behandelde huidaandoeningen klein te zijn in afmeting. Door deze kleine afmetingen was de Skin Sensor van de COMET in verhouding groot, wat het vinden van de juiste meetplek als ook het doen van stabiele metingen lastig maakte.

In **hoofdstuk 6** beschrijven we het gebruik van de COMET tijdens het geven van een bloedtransfusie. Er is bij chronisch anemische patiënten (patiënten met chronisch tekort aan rode bloedcellen) gemeten omdat deze groep regelmatig een bloedtransfusie krijgt. De verwachting was dat na het geven een bloedtransfusie er hogere mitoPO$_2$ waarden zouden worden gemeten.

In tegenstelling tot onze verwachting nam de mitoPO$_2$ tijdens een bloedtransfusie niet toe. Er was eerder een neerwaartse trend tijdens de bloedtransfusie te zien. Enkel bij een paar patiënten is er een toename gezien. Bij deze patiënten was sprake van een lage mitoPO$_2$ voor het begin van de bloedtransfusie. Een herstel van een lage mitoPO$_2$ door bloedtransfusie is ook eerder tijdens een operatie gezien en tijdens een bloedverdunning studie bij dieren. Dit laat zien dat waarschijnlijk de mitoPO$_2$ niet altijd direct zal toenemen bij een bloedtransfusie, maar alleen indien er sprake is van een disbalans tussen zuurstofaanbod en zuurstofverbruik op weefselniveau. Deze balans

verschuift waarschijnlijk door fysiologische adaptatie op het moment dat iemand langere tijd weinig rode bloedcellen heeft. Momenteel denken we dat een lage mitoPO$_2$ een uiting kan zijn van het feit dat de individuele compensatiemechanismen hun grens hebben bereikt en dat meten van mitoPO$_2$ een rol kan spelen in het individualiseren van bloedtransfusiebeleid.

Ischemie (een tekort aan zuurstof) van de weefsels wordt veroorzaakt door te weinig toevoer van zuurstof naar de weefsels. Ischemie kan het resultaat zijn van een tekort aan rode bloedcellen en daarmee de transportcapaciteit, maar het kan ook liggen aan de afname van de doorstroming. Een afname in doorstroming kan ontstaan door een bloedvat vernauwing en zodanig ernstig zijn dat er klinische symptomen ontstaan. Een bekend voorbeeld hiervan is pijn op de borst bij zuurstoftekort in de hartspier. Een vernauwing van aanvoerende vaten naar de darmen kan leiden tot chronische mesenteriale (darm) ischemie (CMI). Om het tekort aan zuurstoftoevoer naar de darmen te bepalen wordt nu “visible light spectroscopy (VLS)” gebruikt, zichtbaar wit licht spectroscopie. Dit meet het percentage dat gebonden is aan zuurstof aan rode bloedcellen. VLS is erg gevoelig voor verstoringen en er wordt gezocht naar een betere techniek om zuurstof te meten in de darmen voor het diagnostische proces omtrent CMI.

Hoofdstuk 7 beschrijft een studie waarbij VLS wordt vergeleken met een gekalibreerde techniek (gebaseerd op zuurstofafhankelijke uitdoving van palladium porfyrine fosforescentie) om zuurstof te meten in de microcirculatie van de binnenwand van de darmen van een varken. Het resultaat was dat de VLS na 25 minuten hartstilstand van het varken nog steeds een redelijke rode cellen zuurstof saturatie liet zien, in tegenstelling tot de palladium porfyrine techniek. Daarnaast werd een omgekeerde relatie gezien tussen de VLS en de percentage zuurstof waarmee werd beademd. Hiermee hebben we laten zien dat er weinig correlatie is tussen de VLS-waarden en een tekort aan zuurstof. Het laat zien dat de VLS met name afvoerende aders meet, in plaats van de kleinste bloedvaatjes in het weefsel. Het blijft nu de vraag of saturatie in afvoerende vaten een goede meettechniek is om een tekort aan zuurstof te bepalen.

Voor het diagnosticeren van langdurig tekort aan zuurstof in de darmen is er dus een vraag naar een betrouwbare, gebruiksvriendelijke en functionele test. Omdat mitoPO$_2$ zuurstof meet op niveau van de mitochondriën waar de zuurstof ook gebruikt wordt, zou mitoPO$_2$ wellicht een goede kandidaat zijn om zuurstoftekort in de darmen te diagnosticeren. Echter, met de standaard huid sensor bij de COMET is dit niet mogelijk. In **hoofdstuk 8** beschrijven we de ontwikkeling van een opstelling waarmee door het werkkanaal van een endoscoop mitoPO$_2$ gemeten kan worden. Met een endoscoop wordt in de maag of darmen gekeken. Er is vervolgens een kleine studie gedaan waarmee we laten zien dat mitoPO$_2$ te meten is en dat de techniek veilig toepasbaar is tijdens een endoscopie procedure. Er is vervolgonderzoek nodig om te bepalen of dit gebruikt kan worden om CMI te diagnosticeren.

Als laatste is de mitoPO$_2$ gemeten tijdens een operatie waarbij gebruik is gemaakt van de hartlongmachine (HLM). Het gebruik van een HLM heeft een sterk effect op het menselijk lichaam, omdat de bloeddoorstroming, beademing, bloedstolling en temperatuur regulatie wordt overgenomen of verandert. Het is essentieel dat er tijdens de overname met de HLM er voldoende zuurstof naar de weefsels gaat en alle orgaanfuncties behouden blijven. Helaas komt acuut nierfalen (AKI) nog regelmatig voor na hartchirurgie, hoofdzakelijk omdat de nieren vatbaar zijn voor zuurstoftekort en tegelijkertijd een hoge vraag naar zuurstof hebben. Nabij-infrarood spectroscopie, "near-infrared spectroscopy (NIRS)" is een veel gebruikte techniek om in (hersen)weefsel zuurstof saturatie (StO$_2$) te meten tijdens het gebruik van de HLM. In **hoofdstuk 9** geven we de resultaten van de vergelijking tussen StO$_2$ en mitoPO$_2$ tijdens het gebruik van de HLM. Er is verder gekeken naar de invloed van bloeddruk variatie op de mitoPO$_2$. Daarnaast is er gekeken of lage mitoPO$_2$ waarden correleren met het ontstaan van AKI.

In totaal zijn er 41 patiënten gemeten waarbij een afname in mitoPO$_2$ is gemeten ten opzichte van het begin van de operatie, in tegenstelling tot de saturatie meting waarbij er geen verschil is gezien. Er is ook gekeken naar de invloed van bloeddruk variatie (pulsaties) voor en na het dicht klemmen van de aorta (grootste slagader in ons lichaam). Na het wegvallen van de bloeddruk variatie nam de mitoPO$_2$ significant af. De mitoPO$_2$ bleek gevoelig te zijn voor bloeddruk veranderingen. Meten van mitoPO$_2$ kan hierdoor een belangrijke toevoeging zijn ten opzichte van de huidige meettechnieken tijdens dergelijke grote ingrepen.

Conclusie:

Het meten van mitochondriale zuurstof spanning, mitoPO$_2$, komt in een nieuwe fase door de ontwikkeling van de COMET monitor die in de kliniek bij de patiënt gebruikt kan worden. Hierdoor kan het in verschillende velden en situaties toegepast worden. Dit proefschrift beschrijft de toepassing van mitoPO$_2$ bij de anesthesiologie, dermatologie, hematologie, gastro-enterologie en thoraxchirurgie.

Zuurstof is een fundamenteel en essentieel element voor adequate energiehuishouding van de cel. Hoeveel zuurstof een cel onder bepaalde omstandigheden (nodig) heeft en gebruikt is echter ook een veld waarin er nog vele onbeantwoorde vragen zijn. Verschillende toepassingen van het meten van zuurstof zijn beschreven in dit proefschrift, echter leidt dit momenteel nog tot meer vragen dan antwoorden. Tot op heden laat het ons zien dat hoe meer we ontdekken van mitochondriaal zuurstof en verbruik, hoe meer we beseffen wat we eigenlijk niet weten.

Meer vervolgonderzoek is dan ook nodig om het volledige potentieel van zuurstof meten op mitochondriaal niveau te ontdekken.

Chapter 13

Abbreviations

Abbreviations

ABG	arterial blood gas
ADP	adenosine diphosphate
AK	actinic keratosis
AKI	acute kidney injury
ALA	5-aminolevulinic acid
ALP	alkaline phosphatase
ALT	alanine aminotransferase
AST	aspertate aminotransferase
ATP	adenosine triphosphate
BCC	basal cell carcinoma
CA	celiac artery
CABG	coronary artery bypass graft
CMI	chronic mesenteric ischemia
CO_2	carbon dioxide
CPIII	coproporphyrinogen III
CPB	cardiopulmonary bypass
ECC	extracorporeal circulation
ECG	electrocardiogram
eGFR	estimated glomerular filtration rate
2,3 DPG	2,3- disphosphoglycerate
FU	flow units
GI	gastrointestinal
GGT	gamma-glutamyltransferase
HR	heart rate
ICU	intensive care unit
IMA	inferior mesenteric artery
IQR	interquartile range
MALS	median arcuate ligament syndrome
MAP	mean arterial blood pressure
$MitoPO_2$	mitochondrial oxygen tension
$MitoVO_2$	mitochondrial oxygen consumption
NA	numerical aperture
NIRS	near-infrared spectroscopy
NOMI	non-occlusive mesenteric ischemia
NS	non significant

ODR	oxygen disappearance rate
PaO_2	arterial oxygen partial pressure
Pd	palladium
PDT	photodynamic therapy
PMT	photo multiplier tube
PO_2	oxygen tension
μPO_2	microvascular oxygen tension
PpIX	protoporphyrin IX
PpIX-TSLT	protoporphyrin IX-triplet state lifetime technique
RBCT	red blood cell transfusion
ROS	reactive oxygen species
SD	standard deviation
SDF	sidestream Dark Field Imaging
SO_2	(hemoglobin) oxygen saturation
StO_2	tissue oxygenation (hemoglobin saturaion)
SNR	signal to noise ratio
SMA	superior mesenteric artery
TRALI	transfusion-related Acute Lung Injury
UI	user interface
VAS	visual analog scale
VLS	visible light spectroscopy
VU	velocity units

Chapter 14

Contributing authors

Contributing authors

List in alphabetical order

Peter A.W. te	Boekhorst
Marco J.	Bruno
Louisa J.D.	van Dijk
Floor A.	Harms
Rineke	Janse
Tanja	Johannes
Max P.	Ligtenberg
Egbert. G.	Mik
F. Michael	Münker
Desirée	van Noord
Errol P.	Prens
Patricia A.C.	Specht
Nicolaas J.H.	Raat
Robert. J.	Stolker
Luke G.	Terlouw
Mark A.	Wefers Bettink
Willem	van Weteringen
Calvin J.	de Wijs
Maarten	Ter Horst

Chapter 15

List of publications

List of publications

In this thesis

Harms F.A, **Ubbink R.**, C.J. de Wijs, M.P. Ligtenberg, M.P. ter Horst, Mik EG. Mitochondrial oxygenation during cardiopulmonary bypass: a pilot study. Front. Med. - Intensive Care Medicine and Anesthesiology, Submitted on: 29 Sep 2021 (2022)

Ubbink R, Prens E.P., and Mik E.G., Quantitative intracellular oxygen availability before and after 5-aminolevulinic acid skin photodynamic therapy. Photodiagnosis Photodyn Ther. 2021 Dec;36:102599.

Ubbink R, Wefers Bettink MA, van Weteringen W, and Mik EG. Mitochondrial oxygen monitoring with COMET: verification of calibration in man and comparison with vascular occlusion tests in healthy volunteers. J Clin Monit Comput. 2020 Oct 21.

Ubbink R[*], van Dijk LJD*, Terlouw LG., van Noord D, Mik EG, and Bruno MJ. Mitochondrial Oxygen Measurements of the Stomach and Duodenum during Upper Gastrointestinal Endoscopy. J Biophotonics. 2019 Oct;12(10):e201900025.

Ubbink R[*], van Dijk LJD*, van Noord D, Johannes T, Specht PAC, and Mik EG. Evaluation of visible light spectroscopy: comparison with microvascular oxygen tension measurements in a porcine model. *J Transl Med*. 2019 Feb 28;17(1):65

Ubbink R, Wefers Bettink MAW, Janse R, Harms FA, Johannes T, Münker FM, and Mik EG. A monitor for Cellular Oxygen METabolism (COMET): monitoring tissue oxygenation at the mitochondrial level *Journal of clinical monitoring and computing*. (2016).

** Both authors contributed equally to this manuscript.*

Book chapters:

Diemen MPJ, **Ubbink R,** Münker FM, and Mik EG, Groeneveld GJ. Measurement of Oxygen Metabolism In Vivo. Mitochondrial Dysfunction Caused by Drugs and Environmental Toxicants. 1-22018. p. 315-21.

Ubbink R, and Mik EG. Probing Tissue Oxygenation by Delayed Fluorescence of Protoporphyrin IX RSC Detection Science. 2018;2018-January(11):259-77.

Other publications

Bodewes SB, van Leeuwen OB, Thorne AM, Lascaris B, **Ubbink R**, Lisman T, Monbaliu D, De Meijer VE, Nijsten MWN, Porte RJ. Oxygen Transport during Ex Situ Machine Perfusion of Donor Livers Using Red Blood Cells or Artificial Oxygen Carriers. Int J Mol Sci. 2020 Dec 28;22(1):235.

Thorne AM, **Ubbink R**, Brüggenwirth IMA, Nijsten MW, Porte RJ, de Meijer VE. Hyperthermia-induced changes in liver physiology and metabolism: a rationale for hyperthermic machine perfusion. Am J Physiol Gastrointest Liver Physiol. 2020 Jul 1;319(1):G43-G50.

van Leeuwen OB, de Vries Y, Fujiyoshi M, Nijsten MWN, **Ubbink R**, Pelgrim GJ, Werner MJM, Reyntjens KMEM, van den Berg AP, de Boer MT, de Kleine RHJ, Lisman T, de Meijer VE, and Porte RJ. Transplantation of High-risk Donor Livers After Ex Situ Resuscitation and Assessment Using Combined Hypo- and Normothermic Machine Perfusion: A Prospective Clinical Trial. Ann Surg. 2019 Nov;270(5):906-914.

van Leeuwen OB, Fujiyoshi M, **Ubbink R**, Werner MJM, Brüggenwirth IMA, Porte RJ, and de Meijer VE. Ex Situ Machine Perfusion of Human Donor Livers via the Surgically Reopened Umbilical Vein: A Proof of Concept. Transplantation. 2019 Oct;103(10):2130-2135.

van Leeuwen OB, **Ubbink R**, de Meijer VE, and Porte RJ. The first case of ischemia-free organ transplantation in humans: A proof of concept. Am J Transplant. 2018 Aug;18(8):2091.

Eijsvogel MM, **Ubbink R**, Dekker J, Oppersma E, de Jongh FH, van der Palen J, and Brusse-Keizer MG. Sleep position trainer versus tennis ball technique in positional obstructive sleep apnea syndrome. J Clin Sleep Med. 2015 Jan 15;11(2):139-47.

Chapter 16

Portfolio

Portfolio

Rinse Ubbink

Cursus	
BROK 2015	1.0
Laser Safety 2015	0.3
Confocal microscopy 2016	0.2
Open Clinica database 2016	0.3
Donation and Transplantation 2017	0.3
Medical Science Transplantation Summer School 2016, 2017	2.0
NIHES:	
Research Integrity 2016	0.7
Opleiding en ondersteuning	
Internship guidance Technical Medicine	2.0
Internship guidance Medicine	2.0
A&I Praktijkgerichte nascholing over perioperatieve geneeskunde paper	2.0
Software and hardware development Anesthesiology Department	3.0
NVvTG Post Graduation Education Committee	3.0
Presentaties	
Scientific day Anesthesiology EMC, Rotterdam 2015, 2017	2.0
NVvTG congress, Amsterdam (major presentation) 2016	2.0
Symposium Sanquin Rotterdam (major presentation) 2017	2.0
ISICEM Milan (short presentation) 2016	1.0
ESICM Paris (short presentation) 2018	1.0
Anesthesiology congress, Lisbon (major presentation) 2018	1.0
NeSECC Zwolle 2018	1.0
Bezoekcongres	
Dutch School for Mitochondrial Medicine 2016	0.3
eHealthweek 2016	1.0
Experimental Centre for Technical Medicine congress 2016	0.3
ESA London 2016	1.0
ISICEM Milan 2017, 2018	2.0
ESICM Paris 2018	1.0
NVT Zeist 2017	0.3
GTC congress 2018	0.3
NeSECC Maastricht 2019	0.3

Chapter 17

Dankwoord

Dankwoord

En dan nu het best gelezen deel van dit boek, na lange tijd mag ik dan het dankwoord schrijven.

Prof dr. R.J. Stolker, beste Robert Jan, bedankt voor je begeleiding van dit promotieonderzoek. Erg bedankt voor de vrijheid en de mogelijkheid die ik heb gekregen. Bedankt voor het kritisch lezen van de stukken. De verhalen rondom de promotie en de zaken waarop je moet letten heb ik als zeer prettig ervaren.

Technische geneeskunde is de studie die ik heb gedaan om techniek en geneeskunde te combineren, echt een prachtige combinatie. Deze studie bestond toen jij studeerde nog niet, als iemand een autodidact technisch geneeskundige is dan ben jij het wel co-promotor dr. E.G. Mik. Beste Bert, heel erg bedankt dat ik dit promotie traject heb mogen doen. Ik heb me op mijn plek gevoeld op jouw afdeling experimentele anesthesiologie. Op wetenschappelijk gebied heb ik kunnen groeien, maar naast het wetenschappelijke gedeelte heb ik zo veel geleerd over hardware aansturing, laser en data-acquisitie. Dit heeft mij nieuwsgierig gemaakt hoe systemen werken, maar ook de omzetting van idee tot innovatie. Hier ben ik je zeer dankbaar voor. Je bent echt de enige dokter die ik ken die zelf even een signaalfilter in elkaar soldeert met een weerstandje en condensator, prachtig! Bedankt voor je altijd motiverende, hartelijke woorden en scherpzinnigheid. Bovenal het oog voor detail, waarbij ik zelf nog wel eens de Ï mis.

Geachte leden van de leescommissie: Prof. dr I.K.M. Reiss, Prof. dr. M.J. Bruno en Prof. dr. N.P. Juffermans. Bedankt voor jullie interesse en beoordeling van dit proefschrift.

Dr. M.A. Wefers Bettink, Beste Mark, je was me voor om te promoveren, maar nu mag ik jou hier ook bedanken voor onze mooie tijd die we samen gehad hebben tijdens onze promotie. Jammer dat we nu zo ver bij elkaar vandaan wonen, om nieuwe avonturen te beleven. Het was echt leuk om met jou samen te werken, je ongeremde enthousiasme en positiviteit. Bedankt voor de potjes tafeltennis als ontspanning op hoog niveau. [1] Altijd goedlachs en met het beste beentje voor, je snelle geest, creativiteit en je organisatie skills. Ook toen ik op afstand mijn promotie heb afgemaakt was er altijd een warm welkom, bedankt daarvoor. [1] M.A. Wefers Bettink; 2021; Dankwoord, *Mind the mitochondria*.

Dr. L.J.D. van Dijk. Louisa, Een bijzonder mooie en gezellige, maar bovenal zeer productieve tijd hebben we op het lab en jouw afdeling gehad. We hebben echt in korte tijd twee mooie artikelen vormgegeven. Ik heb diep respect voor je organisatietalent en punctualiteit. Daarnaast je volle 100% enthousiaste inzet om het endoscopisch meten met mitoPO$_2$ te laten slagen.

Dr. F. A. Harms, mijn voorganger in het doen van mitochondriaal zuurstof onderzoek. Beste Floor, Jij hebt nog laser onderdelen moeten afstellen en was met een koelkast groot meetapparaat onderweg om onderzoek te doen. Met de komst van de COMET konden we de kliniek in. Bedankt voor de samenwerking en nadenken over studies om mitoPO$_2$ toe te passen in de kliniek.

Beste Patricia Specht, een onmisbare factor binnen de afdeling Experimentele Anesthesiologie. Je hebt ontzettend veel voor mij gedaan en meegeholpen met het onderzoek. Ik ben blij dat ik toch ook een heel klein stukje terug heb kunnen doen door een referentie meting te introduceren in het lab in de vorm van een steentje wat ook een constante factor als resultaat moet geven. Je bent een top collega, bedankt voor alle mooi gesprekken en ondersteuning, als ook de gezelligheid.

Dr. N.J.H. Raat. Beste Harrold, bedankt voor de samenwerking en het kritisch meedenken met de gemaakte plannen en het en lezen van mijn stukken. Mooie gesprekken hebben we gehad over de nuances en details. Je bent een kritische luisteraar, het collectief geheugen met oog voor detail. Bedankt voor de mooie samenwerking op het lab.

Drs. W. van Weteringen. Beste Willem, de duizendpoot die zelf aan het programmeren en solderen is. Uitzonderlijk als arts zijnde. Heel erg bedankt dat ik ook samen met jou onderzoek heb mogen doen.

Beste Lucia, je stelt de goede vragen en hebt een bijzonder oog voor detail. De samenwerking met jou heb ik als zeer prettig ervaren. Bedankt voor je volledige inzet en enthousiasme, ga zo door!

Ook wil ik graag alle andere coauteurs bedanken voor de prettige samenwerking met mooie artikelen als resultaat.

Drs, F.M. Munker. Een onmisbaar begin van mijn promotie traject is mijn tijd bij jouw als werkgever geweest Michael. Ik mocht dan lange tijd als enige werknemer, werknemer van de maand zijn, jij bent voor mij werkgever van de maand geweest! De persoonlijke ontwikkeling die ik door heb mogen maken binnen medical device ontwikkeling, ben ik jou zeer dankbaar voor. Het blijft voor mij bijzonder om samen van een idee en prototype een produceerbaar medisch product te maken. De samenwerking is enorm prettig geweest vanaf dag 1 tot op de laatste dag en verder. Heel erg bedankt voor de mogelijkheden. Het altijd hartelijke ontvangst, de discussies en intensieve potjes tafeltennis.

Paranimfen bedankt voor jullie inzet om mijn afronding werkelijkheid te maken.

Graag wil ik ook de afdeling medische techniek bedanken voor hun samenwerking in de ontwikkeling van zowel hardware en software. Jullie zijn goud waard voor de ontwikkeling van nieuwe ideeën. Het is jammer dat dit steeds verder afneemt.

Alle mensen waarmee ik samen heb gewerkt op afdelingen Dermatologie, Hematologie, Maag Darm Lever, Operatie centrum wil ik hartelijk bedanken.

Familie en vrienden zijn onmisbaar om dit af te ronden. Bedankt voor jullie steun en hulp tijdens mijn promotietraject. In het bijzonder wil ik mijn lieve *Heit* noemen. Hij zal op de dag van mijn promotie in een ander universum meekijken. Je lichaam heeft jou ten tijde van mijn afronding in de steek gelaten.

Ik ben bijzonder trots op mijn vader, hoe hij krachtig en ook op eigen wijze in het leven stond. De passie voor het zeilen en de zee. Je bent een zeer belangrijk kompas voor mij en zal je ook blijven. Letterlijk in het leren van navigatie om de weg op zee te vinden. Maar bovenal een stabiele koers vinden in het leven. Dat het belangrijk is dicht bij jezelf te blijven, waarin het niet uitmaakt wat anderen doen of ervan vinden. Of het gras nu groener is bij de buren maakt niet uit, je hebt je eigen weg. Toch was het wel zo dat als daar een bordje bij de weg staat, we net doen of deze er niet is. Wij varen rustig verder op onze tocht. Wij gaan over het wantij verder, waarbij de tijd en de tocht even tot stilstand zijn gekomen. Behouden vaart en bedankt voor alles.

Lieve Veronique, jouw steun tijdens mijn promotietraject was onmisbaar. Ondanks dat door jou mijn promotie in Groningen afgemaakt moest worden. Ik ben iedere dag blij dat we samen door het leven gaan. Bedankt voor je steun en wind in de zeilen, op naar de toekomst. Ik kijk uit naar de avonturen die we nog gaan beleven.

Chapter 18

About the Author

About the Author

Rinse Ubbink was born in Dongeradeel in the upper north of the Netherlands on the 20th of May 1986. He attended secondary school at 'Parcival College' in Groningen, where he graduated in 2005. Subsequently, he started with Technical medicine at the University of Twente in Enschede, specializing in Medical Sensing and Stimulation. During this period, he competed several times in the Tour de France à la Voile with an ocean regatta sailing team in the Farr 30. In 2008 he paused his study for one year to serve on the study association board of Technical Medicine 'S.V. Paradoks'. When he finished his study in 2013, he started at the medical start-up Photonics Healthcare BV, to build, develop, and CE certify the monitor to measure mitochondrial oxygen. End 2015, he started with the PhD trajectory described in this thesis at the Anesthesiology department of Erasmus University Medical Center based in Rotterdam under the supervision of Prof. dr. R.J. Stolker. Rinse moved to Groningen in 2017 and worked as an organ perfusionist for three years at the University Medical Center Groningen, followed by a clinical perfusion educational program from 2019 to 2022.